Weather Responsive Internal Roof Shading Systems for Existing Long-Span Glazed Roof over Large Naturally Ventilated and Air-Conditioned Pedestrian Concourses in the Tropics

Kittitach Pichatwatana

Submitted for the degree of Doctor of Philosophy

Heriot-Watt University

School of the Energy, Geoscience, Infrastructure and Society

January 2016

ABSTRACT

This research aims are to optimize weather responsive internal roof shading design systems and to recommend some design principles and guidelines for internal roof shading systems. Such systems would then provide a better building-centric thermal environment and energy performance, while maintaining adequate levels of natural lighting within the existing long-span glazed roofs over large naturally ventilated and air-conditioned pedestrian concourse in the tropics. Two shading configurations: low and high level shadings were tested both the physical indoor environment and energy performance using dynamic thermal and lighting models on the typical clear days and overcast day in summer and winter respectively.

The thermal performance of these test cases was assessed using internal surface temperatures, air temperatures, mean radiant temperatures and operative temperatures. The energy performance of the tested cases was examined using solar heat gain and cooling loads as well as the visual performance using illuminance and daylight factors. These remedial solutions were also assessed the financial benefits using standard economic analysis methods to provide recommendation on the cost and payback periods.

The predicted results of the large glazed naturally ventilated pedestrian concourse reveal that the internal roof shading device was very effective in reducing inner surface temperatures and consequently reducing radiant heat gain into the space. The low level shadings are more effective than the high level shadings in term of providing better energy, internal thermal and lighting performance. This configuration would reduce two third of the solar heat gain in the large glazed pedestrian concourse space.

The predicted results of the large glazed air-conditioned pedestrian concourse reveal that only the low level shading can improve physical environment in terms of thermal, energy and lighting conditions. This configuration would reduce the ground floor heat gain and also the inner surface temperatures significantly.

The buffer zone is a key reason that the low level shadings perform better than the high level shading. For the naturally ventilated case, creating a ventilated naturally thermal buffer space is critical to the design of an effective internal roof shading system. The large

void space between the glazed roof and the low level shadings allows the free movement of the hot air to dissipate to the outdoors at a high level before it can enter the spaces below. For the air-conditioned case, a larger volume of air over the low level shadings allow for more accumulation of heat as compared to a smaller volume of air over the high shadings. In addition, high solar reflective property of the fabric decreases the solar heat by reflect a portion of the solar heat back out through the transparent roof, while some solar energy is also trapped within the air gap.

According to the thermal environmental conditions required for comfort by the operative temperature recommended by ASHRAE (2004), the both shading options of the large glazed naturally ventilated case could only ease to some degree thermal discomfort. While the low level shading of the large glazed air-conditioned case also goes a long way to alleviating summer thermal discomfort. However the shadings could reduce the internal surface temperature significantly which are the main causes of the radiation heat gain in the large glazed naturally ventilated and air-conditioned pedestrian concourses.

The visual performance results in both case studies reveal that the internal roof shading significantly reduced and maintained daylighting levels at an appropriate quality of light according to the CIBSE's recommendation only on hot clear days. Therefore retractable shading devices are recommended to provide sun screening only when required such as on summer clear days when solar gain is likely to result in overheating.

Apart from the possible financial benefits with a present interest rate at 4.85% in China and 1.35% in Thailand over a life time of 30 years, the investment of the shading system could be financially beneficial due to the $NPV>0$ and the *IRR* was greater than interest rate in both forms of long-span glazed roofs over large pedestrian concourses; natural ventilation and air-condition.

For my parents, beloved wife and children.

ACKNOWLEDGEMENTS

Foremost, I would like to express my sincere thanks and gratitude to my supervisor Dr Fan Wang, for his support, encouragement, and patience in dealing with my frustrations throughout the course of this research. This thesis would not be a reality without his support to overcome all of my research difficulties. His support really motivated and helped me in catching up with the thesis time schedules. This is only a simple way to express my gratitude, yet it hopefully shows how very thankful I am of having him as my supervisors. Special appreciation is also extended to my second supervisor, Prof Sue Roaf, for teaming up with my first supervisor to provide guidance.

I acknowledge the assistance of students and staff at the Department of Architecture, South China University of Technology, Guangzhou for their willingness to cooperate on the field measurement and data preparation and Zhichao Zhu and Manutsawee Anunnathapong for their willingness to cooperate during data analysis.

I would like to address special thanks to Professor Stephen Ogunlana, Dr Elizabeth Ogunlana, Dr Kassim Adebambo and Maury Middleton for their support, assistance and encouragement. My gratitude also goes to all my office mates, colleagues and friends for the chats, discussion, time of sharing and encouragement.

My sincere thanks the IT service team, Alex Heron and Ian Mcdougall for their help in keeping my work in order, especially with software installation and any other computer problems. In addition, I would like to thank FLEDGE Funding and Alumni Funding office of Heriot Watt University for their support in administration and both for research and conference funding so that I was able to carry out this work without any problems.

I wish to thank the Electricity Generating Authority of Thailand (EGAT) for allowing me to study that enables me to do this research and also the Airports of Thailand for allowing me to use Suvarnabhumi Airport Terminal building as a case study in this research.

My honourable mention must go to my beloved parent for keeping to make prayer for me. Finally, my special thanks to my wife, Piyapond for the support, sacrifice and patience throughout the long period of this research and to my lovely children (Gundit and Gandit) for their understanding of not spending enough time with them. Without the help of the people mentioned above, I would have faced many difficulties during this project.

ACADEMIC REGISTRY

Research Thesis Submission

Name*:*	KITTITACH PICHATWATANA		
School/PGI:	School of the Energy, Geoscience, Infrastructure and Society		
Version: *(i.e. First, Resubmission, Final)*	Final	Degree Sought:	PhD

Declaration

In accordance with the appropriate regulations I hereby submit my thesis and I declare that:

1) the thesis embodies the results of my own work and has been composed by myself
2) where appropriate, I have made acknowledgement of the work of others and have made reference to work carried out in collaboration with other persons
3) the thesis is the correct version of the thesis for submission*.
4) my thesis for the award referred to, deposited in the Heriot-Watt University Library, should be made available for loan or photocopying, subject to such conditions as the Librarian may require
5) I understand that as a student of the University I am required to abide by the Regulations of the University and to conform to its discipline.

* *Please note that it is the responsibility of the candidate to ensure that the correct version of the thesis is submitted.*

Signature of Candidate*:*		Date:	

Submission

Submitted By *(name in capitals):*	KITTITACH PICHATWATANA
Signature of Individual Submitting:	
Date Submitted:	

For Completion in Academic Registry

Received in the Academic Registry by *(name in capitals):*			
Method of Submission *(Handed in to Academic Registry; posted through internal/external mail):*			
Signature:		Date:	

TABLE OF CONTENTS

Abstract. i

Dedication iii

Acknowledgements iv

Declaration statement v

Table of Contents vi

List of Tables xiii

List of Figures xv

Glossary of Symbols xx

Published Papers. xxv

Chapter 1 : Introduction 1

1.1 Background 1

1.1.1 Overview of China and Thailand Current and Future Energy Scenario. 3

1.1.2 Overview of Green House Gas Emission in China and Thailand 5

1.1.3 Energy Efficiency Policies in China and Thailand 6

1.2 Statement of Problem 8

1.3 Research Aims and Objectives 13

1.4 Research Scope 14

1.6 Beneficiaries 16

1.7 Content of the Thesis 16

Chapter 2 : Literature Review 20

2.1 Introduction 20

2.2 Atrium and Large Glazed Pedestrian Concourse Design Review 21

2.2.1 Historical Development of Atrium Buildings 21

2.2.2 The Evaluation of Atrium 22

2.2.3 The Modern Atrium 23

2.2.4 The Generic Atrium Forms 26

2.2.5 Atrium and Large Glazed Pedestrian Concourse in the Tropical Climates of Asia 27

2.3 Overview of Research Trend in Atrium and Large Glazed Pedestrian Concourse in Tropical Climates 28
2.3.1 Architectural and Economic Aspect Relate Research 28
2.3.2 Air Quality Related Research 28
2.3.3 Fire Safety Related Research 29
2.3.4 Energy Related Research 29
2.4 Shading Systems 35
2.4.1 Principle of Solar Overheating Control 36
2.4.2 Typology of Shading Systems 36
2.4.3 Thermal and Visual Factors relating to the Shading Fabrics 38
2.5 Building Ventilation Systems 39
2.5.1 Appropriate of Ventilation System Design 40
2.5.2 Types of Ventilation System 41
2.6 Theories of Light and Heat Energy 48
2.6.1 Principle of Sun Light and Day Lighting 48
2.6.2 Solar Geometry 50
2.6.3 The Earth and Sun Relations 51
2.6.4 Architectural Design in Tropical Climates for Daylighting 52
2.6.5 Principle of Heat Energy Flow in Building 54
2.7 Thermal Comfort 55
2.7.1 Factors Affecting Thermal Comfort 55
2.7.2 Psychometrics Chart 56
2.7.3 Define the Thermal Comfort 58
2.7.4 Thermal Comfort Criteria for Tropical Climates 62
2.8 Post-Occupancy Evaluation 64
2.9 Degree-Days 66
2.10 The Economic Evaluation of Investment Proposals 68
2.11 Overview of Dynamic Thermal and Lighting Simulation Programs 70
2.11.1 Overview of TAS Application 70
2.11.2 Overview of Lighting Simulation Application 85
2.12 Summary 91

Chapter 3 : Research Methodology 94
3.1 Introduction 94
3.2 Research Design 95
3.3 A Field Study 100
3.4 Creating Dynamic Thermal & Lighting Models 101
3.5 Develop Design the Shading System 102
3.6 Testing Shading Design Options 103
3.7 Conducting Cost Analysis 104
3.8 Recommending Design Guideline 104
3.9 Conclusion. 104

Chapter 4: A Field Study on Internal Thermal and Lighting Condition in Large Glazed Pedestrian Concourse in the Tropics 106
4.1 Introduction 106
4.2 Data Collection Method 107
4.3 Site Measurement and Monitoring of Indoor Environment Parameters Method 107
4.4 The Large Glazed Pedestrian Concourse with Natural Ventilation of the GITC 107
4.4.1 General Characteristics of Guangzhou Weather 108
4.4.2 Description of the GITC Building 109
4.4.3 Problems of the GITC by CTG Ltd. Report 112
4.4.4 The Variables Measured and Equipment Used 114
4.4.5 Field Monitoring Results and Discussions 117
4.5 The Large Glazed Pedestrian Concourse with Air-Conditioning of Suvarnabhumi Airport Terminal 121
4.5.1 General Characteristics of Samut Prakarn Weather 121
4.5.2 Building Description of Suvarnabhumi Airport Terminal 123
4.5.3 The Variables Measured and Equipment Used 126
4.5.4 Limitation of Experiment Equipment 127
4.5.5 Field Monitoring Results and Discussions 128
4.6 Conclusion 133

Chapter 5 : Post Occupancy Evaluation of Suvarnabhumi Airport Terminal 135
5.1 Introduction 135
5.2 Subjective Assessment –Questionnaire Survey 137
5.3 Respondent Demographics 140
5.4 The Level of Satisfaction and Overall Perception 142
5.5 The Thermal Sensation and Impressions of Comfort 143
5.6 Conclusion 147

Chapter 6 : Dynamic Thermal and Lighting Simulation Models 150
6.1 Introduction 150
6.2 Methods 151
6.2.1 Computer Simulation Modelling Tools 151
6.2.2 Model and Parameters Assignment 152
6.2.3 Calibration Method 153
6.2.4 Variables for Calibration of Dynamic Thermal and Lighting Models 153
6.3 The Large Glazed Naturally Ventilated Pedestrian Concourse 154
6.3.1 Dynamic Thermal and Lighting Method and Parameters Examined 154
6.3.2 Weather and Internal Conditions 157
6.3.3 Results and Discussions 161
6.3.3.1 Dynamic Thermal Model Calibration 161
6.3.3.2 Lighting Model Calibration 166
6.4 The Large Glazed Air-Conditioned Pedestrian Concourse 168
6.4.1 Dynamic Thermal and Lighting Method and Parameters Examined 169
6.4.2 Weather and Internal Conditions 171
6.4.3 Results and Discussions 174
6.4.3.1 Dynamic Thermal Model Calibration 175
6.4.3.2 Lighting Model Calibration 184
6.5 Limitations in the Dynamic Thermal and Lighting Simulation Model. 186

6.6 Conclusion 187

Chapter 7 : Optimizing Weather Responsive Shading Systems Designed for Large Glazed Pedestrian Concourses 190

7.1 Introduction 190

7.2 Method 191

7.3 Fabric Selection for the Shading Blinds 192

7.3.1 Lighting Transmittance Experiment 193

7.3.2 Lighting Transmittance Experimentation Results 195

7.4 Representative Models 196

7.5 Proposed Shading Position 197

7.6 Selected Weather Conditions for Assessment 198

7.6.1 Large Glazed Pedestrian Concourse with Natural Ventilation 198

7.6.2 Large Glazed Pedestrian Concourse with Air-Conditioning 200

7.7 Testing the Performance of the Proposed Internal Roof Shading 201

7.7.1 Large Glazed Pedestrian Concourse with Natural Ventilation 202

7.7.1.1 Thermal Environment Aspect 202

7.7.1.2 Visual Environment Aspect 208

7.7.1.3 Energy Efficiency Aspect 210

7.7.2 Large Glazed Pedestrian Concourse with Air-Conditioning 213

7.7.2.1 Thermal Environment Aspect 213

7.7.2.2 Visual Environment Aspect 222

7.7.2.3 Energy Efficiency Aspect 223

7.7 Conclusion 226

Chapter 8 : Economic Assessment 231

8.1 Introduction 231

8.2 Standard Economic Analysis Methods 232

8.3 The Long-Span Glazed Roof over Large Pedestrian Concourse with Natural Ventilation Economic Assessment 233

8.3.1 Costs of the Internal Shading System 233

8.3.2 Inflow of the Investment 213

8.3.3 Interest Rate in China 234

8.3.4 Economic Benefits 234
8.4 The Long-Span Glazed Roof over Large Pedestrian Concourse with Air-Conditioning Economic Assessment 236
8.4.1 Costs of the Internal Shading System 236
8.4.2 Inflow of the Investment 236
8.4.3 Interest Rate in Thailand 236
8.4.4 Economic Benefits 237
8.5 Conclusions 238

Chapter 9 : Design Principles and Recommendations 240
9.1 Introduction 240
9.2 Design Principles and Recommendations Concerning Internal Roof Shadings for Long-Span Glazed Roof over Large Natural Ventilation and Air-Conditioning in the Tropics 240
9.2.1 Internal Shading Fabrics 241
9.2.2 Internal Shading Form and Position 241
9.3 Conclusions 245

Chapter 10 : Conclusions 247
10.1 Introduction 247
10.2 Summary of Research Development 247
10.3 Summary of Finding 249
10.3.1 Objective 1: to investigate the existing conditions and overall indoor physical behaviours within the existing long-span glazed roof over large pedestrian concourse buildings in the tropics 250
10.3.2 Objective 2: to create dynamic thermal and lighting models of the existing long-span glazed roof over large pedestrian concourse buildings in the tropics with two cases: natural ventilation and air-conditioning for the purpose of comparison 251

10.3.3 Objective 3: to examine the internal roof shadings in the form of retractable internal fabric sheet shadings to reduce discomfort and high energy consumption for the existing long-span glazed roof over large pedestrian concourse buildings in the tropics with two cases; naturally ventilated case and air-conditioned case 255

10.3.4 Objective 4: to analyse the financial benefits from the remedial solutions of the existing long-span glazed roof over large pedestrian concourse buildings in the tropics with the two cases 259

10.3.5 Objective 5: to recommend internal roof shading design guidelines applicable to the existing long-span glazed roof over large pedestrian concourses with natural ventilation and air-conditioning to reduce discomfort and energy consumption in the tropics 260

10.4 Originality of the Proposed Solution and Contribution to Knowledge 260

10.5 Recommendations for Future Research 261

Appendix A : Guangzhou weather data from 30/08/2011 to 04/09/2011 263

Appendix B : Bangkok weather data from 11/09/2012 to 01/10/2012 266

Appendix C : Weather Responsive Internal Roof Shading System for Long-Span Glazed Roof over Large Pedestrian Concourse in the Tropics Questionnaire 277

Appendix D : Internal Conditions (Guangzhou International Textile City) 279

Appendix E : Internal Conditions (Suvarnabhumi Airport Terminal) 279

Appendix F : Suvarnabhumi Airport Terminal Artificial Lighting Lay-out 280

Appendix G : Simulated illuminance comparison (lux) (Suvarnabhumi Airport Terminal) 280

Appendix H : Discounted Cash Flow for Guangzhou International Textile City 283

Appendix I : Discounted Cash Flow for Suvarnabhumi Airport Terminal 284

Reference 285

LIST OF TABLES

Table 2.1	Approximate ventilation rate requirement	40
Table 2.2	Average illuminance required for different tasks	50
Table 2.3	Clothing insulation values for typical clothing groups	56
Table 2.4	Metabolic rate and heat generation per unit area for various activities	56
Table 2.5	Thermal sensation scale	59
Table 2.6	Acceptable thermal environment for general comfort	60
Table 2.7	Thermal comfort condition	63
Table 2.8	Performance indicators and their interpretation	91
Table 4.1	Properties of some key building elements used in the model	111
Table 4.2	Properties of some key building elements used in the model	125
Table 4.3	Total international and domestic passengers	126
Table 4.4	Amounts of chilled water to cooling coil of Suvarnabhumi Airport	131
Table 5.1	Percentage of positive, neutral and negative Rating	148
Table 6.1	Properties of some key building elements used in the model	161
Table 6.2	Comparison between measured and predicted temperatures by the naturally ventilated model	163
Table 6.3	Properties of some key building elements used in the air-conditioned model	171
Table 6.4	Average transparent roof surface temperatures comparison by date from 12th September to 1st October 2012	178
Table 6.5	Average transparent roof surface temperatures comparison by time from 12th September to 1st October 2012	178
Table 6.6	Amounts of chilled water to cooling coil of Suvarnabhumi Airport	181

Table 6.7	Thailand cooling degree days (Base $18^{o}C$)	181
Table 6.8	Calculated Chilled Water to Cooling Coil in 2012	182
Table 7.1	The manufacture data of fabric from Silent Gliss Manufacturer	193
Table 7.2	Comparison of lighting transmittance and manufacture data	196
Table 7.3	Selected for proposed shading properties	196
Table 7.4	The mean illuminance (lux) on the ground floor concourse and the first floor balconies	210
Table 7.5	The predicted average DF (%) in the concourse under overcast sky	210
Table 7.6	Illuminance within the pedestrian concourse	223
Table 7.7	The predicted average DF (%) in the pedestrian concourse	223
Table 8.1	Economic analysis of the shading solution	239

LIST OF FIGURES

Figure 1.1	Global final energy consumption by sector	1
Figure 1.2	Primary energy consumption in major countries	2
Figure 1.3	China's oil production and consumption, 1990-2013	3
Figure 1.4	Thailand's oil production and consumption, 1990-2014	4
Figure 1.5	Annual average maximum ambient temperatures in Thailand from 1951 to 2011	4
Figure 1.6	Greenhouse gases emissions in top five countries, 1990-2010	5
Figure 1.7	Greenhouse gases emissions of ASEAN Countries, 1990-2010	6
Figure 1.8	Gazetteers of notable atrium buildings	9
Figure1.9	Gazetteer of notable large commercial buildings with large glazed pedestrian concourses in the tropics	10
Figure 1.10	Direct sunlight from atrium glazed roof of the Sandra Day O'Connor Federal Courthouse	12
Figure 2.1	Plan and section of house of Ur, Mesopotamia	21
Figure 2.2	Plan and section of Persian house	22
Figure 2.3	Plan and interior of Pension Building, Washington DC	23
Figure 2.4	Atrium of Hyatt Regency Hotel, Atlanta	24
Figure 2.5	Typical Plan and section trough atrium, the Ford Foundation Headquarters	25
Figure 2.6	Generic form of atrium buildings	26
Figure 2.7	Direct, difuse and reflected radiation	36
Figure 2.8	External shading devices	37
Figure 2.9	Thermal factors relating to the fabrics	39
Figure 2.10	Wind velocity drives pressure field	41
Figure 2.11	Stack effect within the building to the air flow	42
Figure 2.12	Natural ventilation through two openings by thermal buoyancy	42
Figure 2.13	Mechanical ventilation systems	44
Figure 2.14	Lower-level displacement ventilation	45
Figure 2.15	Vapour compression cycle	46
Figure 2.16	Typical AHUs	46

Figure 2.17	Typical upward air-flow arrangement	48
Figure 2.18	Solar spectrum	49
Figure 2.19	Definitions of solar position angles	51
Figure 2.20	Definitions of hour angles	51
Figure 2.21	Section of the earth's orbit	52
Figure 2.22	Annual variation of declination (Mean of the Leap-Year Cycle)	52
Figure 2.23	Psychometric chart: Climate classifications	58
Figure 2.24	Predicted Percentage of Dissatisfied (PPD) as a function of Predicted Mean Vote (PMV)	59
Figure 2.25	Schematic representation of heat transfer mechanism in a building	72
Figure 2.26	A simple luminous system	87
Figure 2.27	Three possible paths of light entering the room	89
Figure 3.1	Dynamic interactions of sub-system in buildings	97
Figure 3.2	Methodology flow chart	99
Figure 4.1	Weather data for Guangzhou China	109
Figure 4.2	Guangzhou International Textile City Building (GITC)	111
Figure 4.3	Average indoor air temperatures within sample retail shops	113
Figure 4.4	Thermal imaging maps by infrared radiant heat sensitive camera (ModelTH9100MV/WV) and the corresponding real photos	114
Figure 4.5	Section of the central glazed pedestrian concourse with locations of hygrothermal sensors (dots)	115
Figure 4.6	Hot-bulb Anemometres ZRQF-F30 and the position of the sensors in the computer model (Air Flow Sensors X)	116
Figure 4.7	Measured air temperatures and wind speed	118
Figure 4.8	Measured DF distributions within the central pedestrian concourse	121
Figure 4.9	Climate data for 30 year average (1961-1990) - Bangkok Metropolis	123
Figure 4.10	Departure lounge of Suvarnabhumi Airport Terminal	125
Figure 4.11	Positions of the Sensors in the Airport Passenger Lounge	127
Figure 4.12	Measured air & transparent roof temperatures compared with solar irradiation and RH	130

Figure 4.13	Measured daylight factor on the passenger lounge floor at 13.00-14.00 on 28th Sep 2012	132
Figure 5.1	Respondents' demographics	142
Figure 5.2	Distribution of subjective response on thermal comfort and overall perception	143
Figure 5.3	Thermal Sensations and Impress of Comfort	144
Figure 5.4	Internal air qualities	145
Figure 5.5	Visual comforts and visual condition	146
Figure 5.6	Comment of airport environment	147
Figure 6.1	3D model by TAS	157
Figure 6.2	3-D Lighting model of GITC building by Ecotect	157
Figure 6.3	TAS centre glazed pedestrian concourse model and the corresponding real photos	161
Figure 6.4	Comparison between the measurement and model prediction	164
Figure 6.5	Predicted cooling load by TAS	165
Figure 6.6	Typical electricity consumption by end-use in the building sector in Singapore	166
Figure 6.7	Comparisons between the measured and simulated daylight factors	168
Figure 6.8	Comparison between the measured and predicted DF over 7 floors around the centre pedestrian concourse	168
Figure 6.9	Suvarnabhumi International Airport Terminal configuration model	170
Figure 6.10	3-D model of the Departure Lounge, Suvarnabhumi Airport by Dialux	171
Figure 6.11	Transparent roof surface predicted temperatures by TAS vs. measurement by date	176
Figure 6.12	Transparent roof surface predicted temperatures by TAS vs. measurement by time	176
Figure 6.13	Comparison between the measurement and model prediction	179
Figure 6.14	The Scatter Chart between energy consumption and degree days	182
Figure 6.15	Predicted annual cooling loads by TAS	183
Figure 6.16	Typical energy consumption at terminal building	184

Figure 6.17	Comparison between measurement and simulation daylight factors between check-in counters, Suvarnabhumi Airport Departure Lounge	185
Figure 6.18	Comparison of maximum, minimum, and average daylight factor between measurement and simulation	186
Figure 7.1	Scale model experiment	196
Figure 7.2	Detailed cross-sections showing the base models	197
Figure 7.3	Detailed across-section showing the roofs and shadings	198
Figure 7.4	Comparison of the internal surface temperature in the central concourse	203
Figure 7.5	Comparison of the mean radiant temperature in the central concourse	205
Figure 7.6	Comparison of the air temperature in the centre pedestrian concourse	206
Figure 7.7	Comparison of the operative temperature in the centre pedestrian concourse	208
Figure 7.8	The daily solar gain over the ground floor and balconies	211
Figure 7.9	Daily total cooling loads in the retail units due the two shading options compared against the base case	213
Figure 7.10	Comparison of the Internal surface temperature in the passenger lounge	215
Figure 7.11	Comparison of the MRT of the ground floor and the top floor ceiling	217
Figure 7.12	Comparison of the air temperatures of the seventh floor ceiling and under glazed roof	219
Figure 7.13	Comparison of the operative temperature of the ground floor concourse and seventh floor view point	222
Figure 7.14	The total solar gain over the large glazed pedestrian concourse with air-conditioning	225
Figure 7.15	The total cooling load due the two shading options compared against the base case	226
Figure 8.1	Average interest rate in China from 2005-2015 Figure 8.2	234
Figure 8.2	Cost analysis of the shading solution with UK and China price scenarios (p=4.8% and 6.85%)	235
Figure 8.3	Average interest rate in Thailand from 2005-Figure 8.5	237

Figure 8.4	Cost analysis of the shading solution with UK and Thailand price scenarios (p=4.8% and 1.35%)	237
Figure 9.1	Temperature stratification in the large glazed pedestrian concourse space	242
Figure 9.2	Free air movement of air dissipates to the external diagram in the large naturally ventilated glazed pedestrian concourse	244
Figure 9.3	Insulting layer of hot air diagram in the large air-conditioned glazed pedestrian concourse	245

GLOSSARY OF SYMBOLS

A : Effective component surface area (m^2)

A_i : The mean of the internal and external surface areas (m^2)

a : Air change rate (air changes per hour)

AZI : Solar Azimuth Angle

ALT : Solar Altitude Angle

ATUs : Air terminal Units

CAV : Constant air volume

CDD : Cooling degree-days

B_t : Benefit (inflows) for year *t*

C_o : Initial investment

C_t : Cost (outflows) for year *t*,

c_p : Specific heat capacity at constant pressure of the fluid (=1.012 kJ/kg.K)

DF : Daylight Factor

DPP : Discount payment period or depreciated payment period

dA : Area of the surface element

E : Illuminance

E_i : Internal illuminance

E_o : Simultaneous external illuminance

F_t : Net cash flow at year *t*

F_i : View factor (as yet undetermined) between surfaces *i* and the MRT node

g : Gravitational acceleration (=9.82 m/s^2)

G_i : Internal radiant exchange between room surfaces (W/K)

h_c : Surface heat transfer coefficients by convection ($W/m^{2o}K$)

h_r : Surface heat transfer coefficient by radiation (W/m^2K)

h^{int} : Internal convective heat transfer coefficient (W/m^2K)

h^{ext} : External convective heat transfer coefficient (W/m^2K)

$h^{rad,\text{ext}}$: External radiative heat transfer coefficient (W/m^2K)

$h^{rad,\text{int}}$: Internal radiative heat transfer coefficient (W/m^2K)

H : Vertical distance between the centre of inlet and the centre of outlet (m)

HRA : Hour angle

HDD : Heating degree-days

HVAC : Heating ventilation air-conditioning

I_{hor}^{glob} : Global radiation incident on the horizontal plan

IRR : Internal rate of return

K_{tot} : Total heat-transfer coefficient of the building (W/°C)

l : luminous intensity

L : Luminance

Tv : Lighting transmittance

M : Metabolic rate (W/m^2)

Msz : Mass flow rate from source zone s (with zone 0 representing the outside air) to zone z

m^{vent} : Ventilation air mass flow rate in (kg/s)

m^{inf} : Infiltration mass flow rate (kg/s)

NPV : Net present value

n : Number of years of the investment's lifetime

OF, Co: Openness factor

p : Radiant proportion

p : Static pressure (N/m^2)

p : Pressure at the opening (Pa)

p : Cost of capital,

p^{htg} : Radiant proportions for heating

p^{clg} : Radiant proportions for cooling

PMV : Predicted Mean Vote

PPD : Predicted Percentage Dissatisfied (%)

POE : Post-occupancy evaluation

$q^{cond,\text{int}}$: Internal surface conduction heat flux (Wm^{-2})

$q^{cond,\text{ext}}$: External surface conduction heat flux (Wm^{-2})

$q^{conv,\text{int}}$: Internal convective heat flux (Wm^{-2})

$q^{conv,\text{ext}}$: External convective heat flux (Wm^{-2})

q^{ext} : Long-wave radiant flux by the surface

q^{dir_beam} : Direct normal (beam) solar radian intensity (Wm^{-2})

$q_{hor}^{dir,\text{ext}}$: Direct solar radiation on the horizontal plane (Wm^{-2})

$q_i^{sol,ext}$: Solar radiation (Watts) absorbed on outside surface *i* of the zone

$q_i^{sol,int}$: Solar radiation (Watts) absorbed on inside surface *i* of the zone

q_{env} : Total long-wave incident on the surface from its environment (Wm^{-2})

q^{ext} : Long-wave radiant flux by the external surface (Wm^{-2})

q_{hor}^{glob} : The global radiation incident on the horizontal plane (Wm^{-2})

q_{sky} : Long-wave incident on the surface from the sky (Wm^{-2})

q_{gnd} : Long-wave incident on the surface from the ground (Wm^{-2})

Q_{h} : Annual heating requirements (kWh)

Q_{c} : Annual cooling requirements (kWh)

Q^{am} : Total sensible heat gain (Watts)

Q^{gnd} : Incident ground-reflected radiation (Watts)

$Q^{dir,\text{ext}}$: Direct solar radiation incident on the surface (Watts)

Q^{dif_sky} : Diffuse solar radiant power incident on a surface from a sky (Watts)

Q^{sol} : Zone solar gain inside the building (Watts)

$Q_i^{sol,\text{ext}}$: Solar radiation absorbed on the external surface (Watts)

$Q_i^{sol,\text{int}}$: Solar radiation absorbed on the internal surface (Watts)

$Q^{rad,\text{ext}}$: Net long-wave radiation gain on the external surface (Watts)

Q^{ref_gnd} : The ground reflected radiation incident on a surface (Watts)

Q^{inf} : Sensible heat gain due to infiltration

rh : Relative humidity (%)

r : Interest rate

R : Area-weighted average reflectance of interior surfaces, including windows

R : Thermal resistant

Rs : Solar reflectance

Rv : Lighting reflectance

t : Time period (year)

T : Diffuse transmittance of glazing material including effects of dirt

Ts : Solar transmittance (^{o}C)

$T\,dif$: Diffuse transmittance factor

T_a : Air temperature (ºC)

Tb : Base temperature (^{o}C)

Tc : Comfort temperature (^{o}C)

T_i : Indoor temperature (^{o}C)

T_m : Daily mean outdoor temperature

T_o^{air} : Outdoor temperature (^{o}C)

T_o : Operative temperature (ºC)

T_r : Mean radiant temperature (ºC)

T^{int} : Temperature on the internal surfaces (ºC)

T^{ext} : Temperature on the external surfaces (ºC)

$T_{(ref)}^{\text{ext}}$: Absolute temperature of the external surface (K)

$T^{mrt(c)}$: Mean radiant temperature in Carroll's method;

$T_k^{\,int}$: Temperature of internal surface *k*

U : Heat transfer

UVR : Ultraviolet radiation

UVA : Ultraviolet with wavelengths between 315 and 400 nanometres (nm.)

UVB : Ultraviolet with wavelengths between 280 and 315 nm.

UVC : Ultraviolet with wavelengths between 100 and 280 nm.

v : Relative air velocity (ms^{-1})

v_m : Air velocity measured at the meteorological station at 10m high (ms^{-1})

V_1 : Volume flow, ventilation capacity at inlet (m^3s^{-1})

V_2 : Volume flow, ventilation capacity at outlet (m^3s^{-1})

VAV : Variable air volume

V : Room volume (m^3)

W : External work (Wm^{-2})

$W^{cond,int}$ I: nternal surface conduction heat flux (W/m2)

$W^{cond,ext}$: External surface conduction heat flux (W/m2)

W : Net glazed area of window (m^2)

w_{am} : Moisture gain due to air movement (kg/s)

x : Humidity ratio

x_i, x_j : Coordinate variable

ZEN : Zenith angle

Δ : Time step

α_p^{ext} : Absorptance at a point at the external surface

α_p^{int} : Absorptance at a point at the internal surface

η : Efficiency of the heating or cooling system

ρ_i : Indoor air density (kgm^{-3})

ρ_o : Outdoor air density (kgm^{-3})

ρ^{gnd} : The ground reflectance

ρ^{air} : Density of air at standard atmospheric pressure and a temperature of 20C (1.210 Kg/m^3)

σ : Stefan-Boltzmann constant ($=5.6697\times10^{-8}\,Wm^{-2}K$)

γ : Angle between the inward-facing surface normal and the vertical

Θ : Angle in degrees subtended, in the vertical plane normal to the window, by sky visible from the centre of the window

Φ : luminous flux

$\Theta_{(ref)}^{zone}$: Reference absolute temperature which should be close to the mean

PUBLISHED PAPERS

The following papers have been published as a result of this research:

Wang F., Pichawatana K., Roaf S., Zhao L., Zhu Z. and Li J. (2014) 'Developing a Weather Responsive Internal Shading System for Atrium Spaces of a Commercial Building in Tropical Climate', *Built and Environment,* Volume 71, January 2014, p.259-274.

Pichawatana K. and Wang F. (2013) 'Impact of Internal Shading on Indoor Environment Condition in Atrium Building in Tropical Climates', *3rd International Conference on Ecological, Environment and Biological Science (ICEFB 2013),* April 29-30 2013, Singapore

Additional published journal:

Wang F., Pichatwatana K., Hendry R. and Galbraith R. (2014) 'Thermal Performance of Gallery and Refurbishment Solution Research', *Energy and Building*, 03/2014 71:38-52.

CHAPTER 1 – INTRODUCTION

1. 1 Background

Globally, the major growth in energy consumption is from the building sector, most noticeably in the commercial sector (Figure 1.1). Energy demand in the building sector accounted for 40 percent of total global energy consumption (IEA, 2010). Buildings also contribute one-third of the total global greenhouse gas emissions (UNEP SBCI, 2009). Energy use in the building sector mainly relates to electricity for heating, ventilation and air-conditioning systems (HVAC), which account for approximately 50 percent of total energy use (Pérez-Lombarda, Ortiz and Pou, 2008). Fossil fuels have been the basic source of the generation of electrical, including the building sector (IEA, 2009); thereby causing the emission of greenhouse gases: predominantly carbon dioxide. These emissions form a major contribution to global warming (Chow, 2009). However, energy demand will continue to grow in every user-sector (EIA, 2014; WEC, 2013), even if global energy resources are depleted in the near future (Roaf, Fuentes and Thomas, 2013).

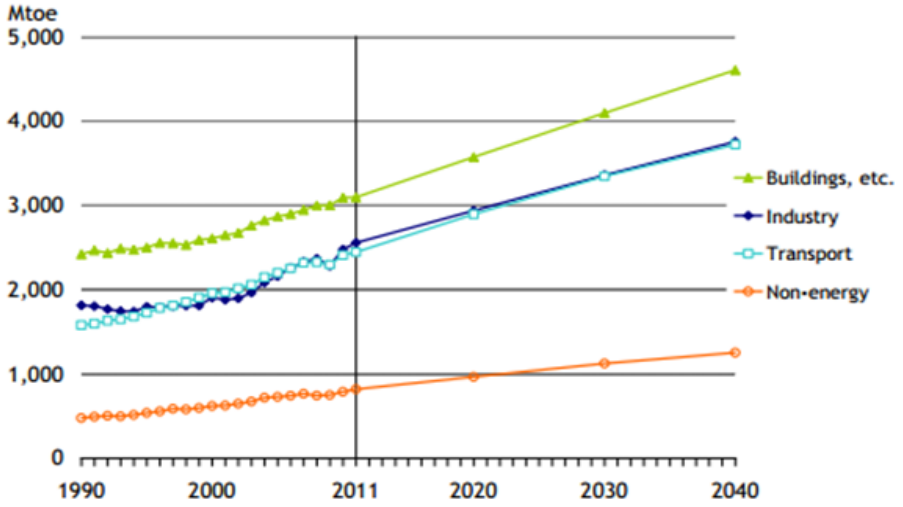

Figure 1.1 Global final energy consumption by sector (IEEJ, 2015)

As global primary energy consumption will rise at an annual rate of 1.4 percent through to 2040, Asia will become the biggest energy user (Figure 1.2). Asia will increase energy consumption; accounting for about 60 percent of global energy consumption growth (IEEJ, 2015).

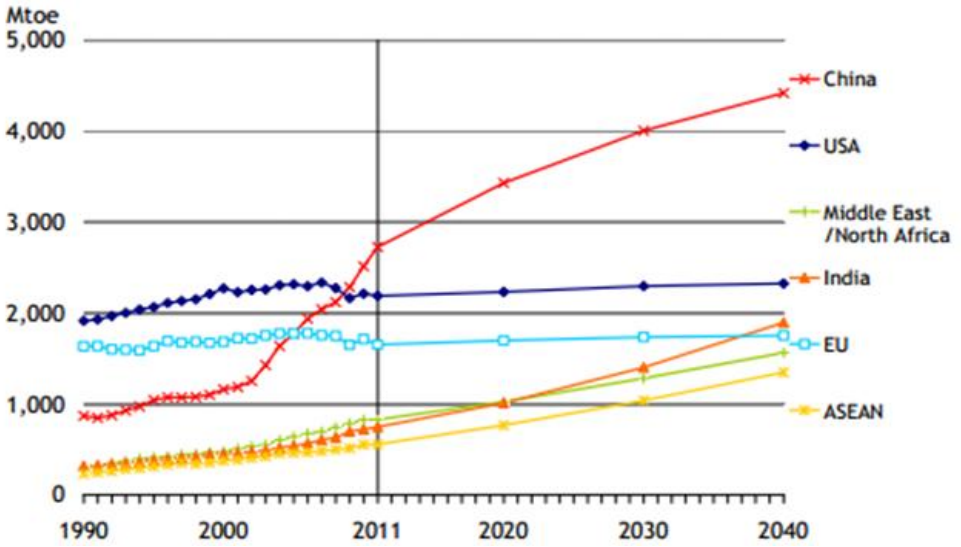

Figure 1.2 Primary energy consumption in major countries (IEEJ, 2015)

In addition, more than half of the world's new buildings are being constructed in Asia. China is the largest construction market of the world. It has 40 billion square meters in existing buildings and adds an additional 2 billion square meters of floor space each year. Most of the new buildings in Asia are both large commercial projects and mixed-use developments, which were the main cause of the increase of energy consumption (Laurenzi et al, 2007).

Energy consumption in the building sector has been growing rapidly in Asia. This consumption of energy occurs in each stage; from construction to operation and maintenance throughout each building's life cycle. Construction of buildings includes various activities, such as planning, execution, operation and maintenance. Therefore, the construction of buildings will not only impact on their operating costs, but will affect our global environmental quality and condition for many years to come (UNEP SBCI, 2009). The building sector in Asia has played a significant role in delivering energy demand. Just as much of Asia's economic growth exceeds the global average, China's energy consumption nearly tripled from 2000 to 2011. Specific attention is given to the building sector in China and Thailand which are in the midst of the growth of urbanization. The next section of this chapter reveals the energy scenario, carbon emissions and energy efficiency policies of both countries.

1.1.1 Overview of China's and Thailand's Current and Future Energy Scenario

(i) China

China is the most populous country and the largest consumer of energy in the world. As a result of China's rapid economic growth in 2009, the country increased its overall energy consumption and became the second largest net oil importer behind the United States (Figure 1.3).

In 2011, the country's oil consumption accounted for half of the global total. The country is also the largest coal producer in the world, and consumes around half of the world's coal production. China's net power generation in 2011 was 4,476 terawatt-hours (TWh), which were mainly used in the building sector; nearly 80 percent of the electricity is generated from fossil sources, primarily coal (US Department of Energy, 2012).

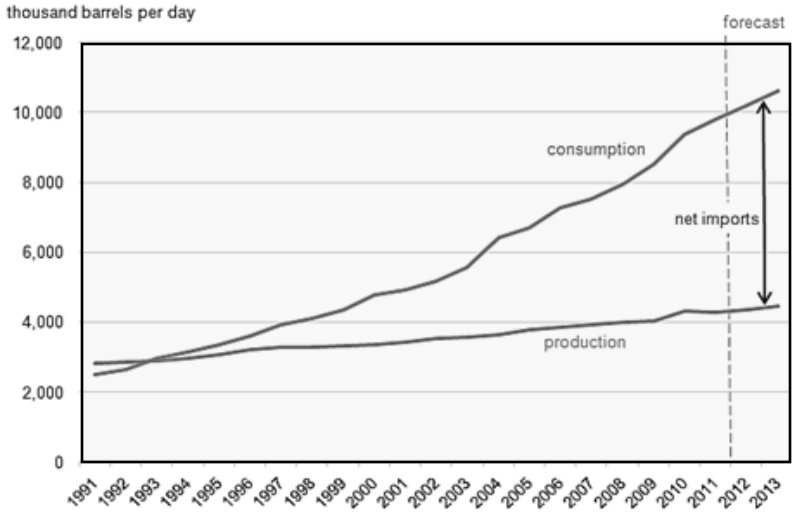

Figure 1.3 China's oil production and consumption, 1990-2013
(US Department of Energy, 2012)

Energy demand growth for HVAC and lighting was driven mostly by the building sector in China. As most of the industrial energy consumption outputs peak, and reach a plateau; the building sector, especially in commercial buildings, could potentially account for the largest future reduction in energy demand (Zhou et al., 2011).

(ii) Thailand

Thailand is considered as a newly industrialized economy. The country is not only highly dependent on energy imports, but also has one of the highest electrification rates in Southeast Asia. Thailand has limited domestic oil production and reserves. Over the last

few years, the country has been shown to hold large proven reserves of natural gas. However, the country still remains dependent on imports of fuel to meet growing demands for energy (APEC, 2012), as shown in Figure 1.4.

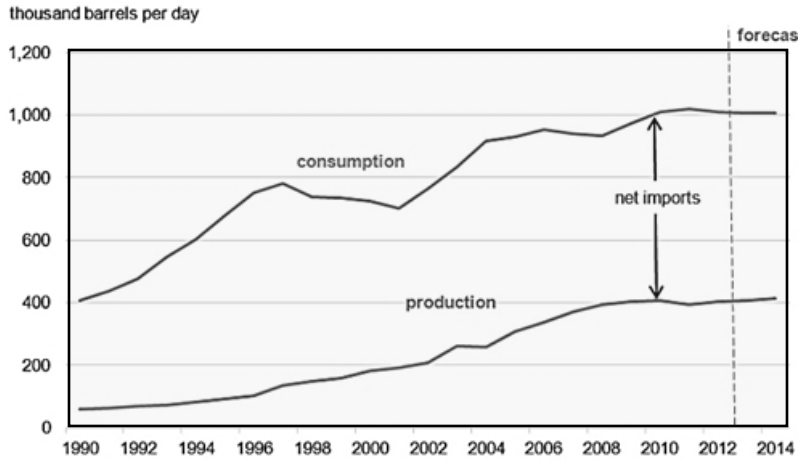

Figure 1.4 Thailand's oil production and consumption, 1990-2014
(U.S. Department of Energy, 2013)

The electricity generating process is one of the biggest sources of CO_2 emissions in Thailand. Electricity generated in Thailand rose from around 90 terawatt-hours (TWh) in 2000, to be higher than 152 TWh in 2011. The building sector accounts for approximately 26 percent of the total energy use, particularly in commercial buildings (U.S. Department of Energy, 2013).

Electricity demand grew considerably due to a rise in the maximum average ambient temperature. The maximum temperature in Thailand slightly increased by 2.50 percent, or around 0.8°C, from 1951 to 2011; this trend seems set to continue in the future (Figure 1.5) (TMD, 2013).

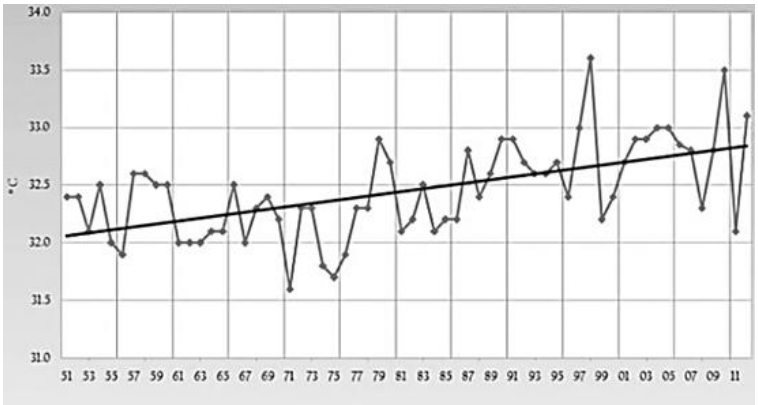

Figure 1.5 Annual average maximum ambient temperatures in Thailand from 1951 to 2011
(TMD, 2013)

Although Thailand is a growing producer of natural gas, the country is still a net importer of oil and natural gas. Thus, as the economy grows, the amount of energy used to fuel the economic growth will increase (AP Energy Business Publications PTE. Ltd, 2013).

The building sector constitutes one of the biggest energy consumers in Thailand, which is the main cause of the country's climate change. Not only could energy efficiency in buildings reduce their operating cost, but it can also deliver a range of benefits to our global environment, particularly a reduction of greenhouse gas emissions.

1.1.2 Overview of Green House Gas Emissions in China and Thailand

(i) China

Energy consumption is the major source of greenhouse gas (GHG) emissions. The building sector is a major energy consumer from which carbon dioxide (CO_2) emissions exceed those of both the industry and transport sectors (Architecture 2030, 2012).

The top CO_2 emitter in the world is China, followed by the United States of America. CO_2 emissions in China increased very rapidly from 2.10-7.40 percent in recent years with an average of 7,666 $MtCO_2$, putting great pressure on environmental sustainability in the world (SEPO, 2013).

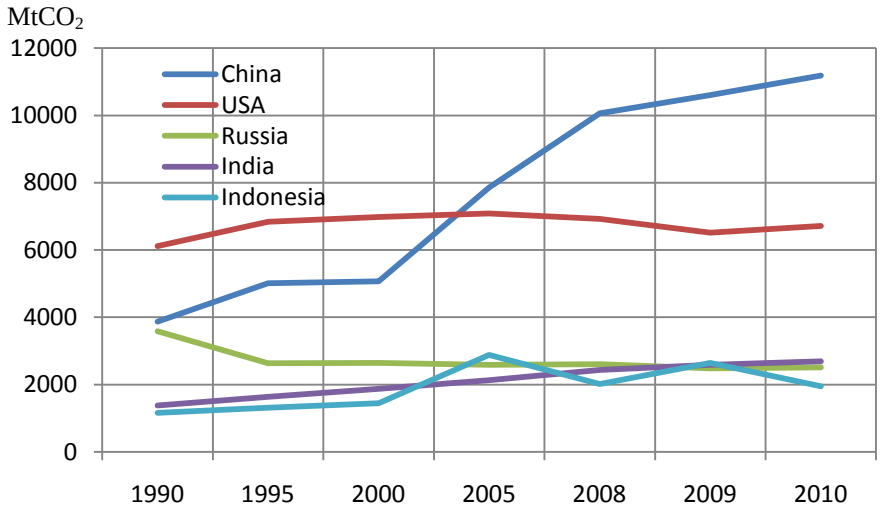

Figure 1.6 Greenhouse gases emissions in top five countries, 1990-2010 (SEPO, 2013)

(ii) Thailand

Developing Asia alone would emit CO_2 more than 22 billion ton by 2035 (ADB, 2014). Myanmar as a net emitter of GHG was ranked 1st in Southeast Asia from 1990-2008. Most importantly, Thailand increased annual GHG emissions and was ranked 1st in the region from 2008 to 2010. Thailand rose at an average annual rate of 8.0 percent (SEPO, 2013).

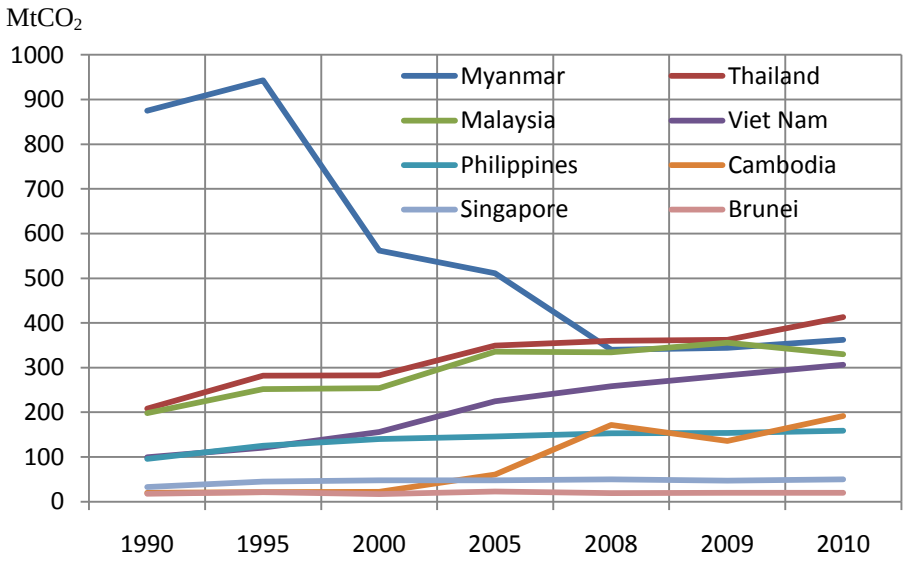

Figure 1.7 Greenhouse gases emissions of ASEAN Countries, 1990-2010 (SEPO, 2013)

The way that buildings are designed and constructed would not only have an impact on their operating costs, but would also affect the world's environment. One key way to reduce, and ultimately phase out, carbon dioxide emissions would be by the creation and use of well-designed energy efficient buildings (Eteghad et al., 2014). Governments thus have a role to play in mandating regulations that will drive forces in this positive environmental change.

1.1.3 Energy Efficiency Policies in China and Thailand

(i) China

Due to China's rapid economic growth, the increase in energy demand outran energy supply. China's government adopted building energy standards set by the Ministry of Construction (MOC) in 1986. Building energy efficiency programmes in China remain

focused on the enforcement of building energy codes. Recently, the MOC, through demonstration buildings, has developed building performance ratings and green building rating systems. The MOC authorized a building standard for buildings in central China in 2001 and other parts of China in 2003 (Chmutina, 2010).

In 2002, the MOC developed the national energy efficiency design standard for public buildings, which was completed and adopted in 2005. Although the MOC had established this standard, the enforcing of these buildings standards is only during design and construction. Also the issue of non-compliance to this standard remains a problem; particularly as the purpose of this standard was to reduce building energy consumption by 50 percent, compared to pre-existing buildings (Huang and Deringer, 2007).

Energy consumption of existing buildings in China is a very big problem. There are more than 30 percent (approximately 13 billion square meters) of the current 40 billion square meters of existing buildings that require retrofitting to meet the average energy consumption from the National Energy Efficiency Design Standard (Asia Green Building Congress, 2014). The annual electricity consumption of existing large-scale public buildings accounted for 22 percent of China's total electricity consumption, which was 10-20 times higher than that of ordinary residential buildings. In order to promote building efficiency in these buildings, the Central Government provided financial support for retrofitting existing buildings (Bin and Jun, 2012).

(ii) Thailand

Thailand has incited the need for more electricity for the building sector due to the nation's rapid economic growth over the past 20 years. Even though the economic recession and extensive flooding in 2011 caused gross domestic product (GDP) to grow by only 0.1 percent, the economy is now expected to increase by 5.5 percent and energy consumption is anticipated to continue to increase (U.S. Department of Energy, 2013).

In 1995, the Building Energy Code Ministerial Regulation for large and complex buildings developed by private sectors, with over 1MW energy consumption, was endorsed by the Thai Government. In 1997, the Energy Conservation Act was made effective, by the Ministry of Energy, for new buildings. The Act includes mandatory regulations and incentives to facilitate the implementation of required energy efficiency measures which

consist of maximum allowable lighting loads and maximum allowable overall thermal transfer values (OTTV), as well as roof thermal transfer values (RTTV) of the building envelope. In 2008, the Ministerial Order presented a new draft of regulations for existing buildings. When this Ministerial Regulation comes into effect, it will enforce the owners of these buildings especially to audit their own buildings' performance. For the designated buildings under the code requirement, they will have to improve their energy efficiency to achieve the prescribed standard.

The awareness of environmentally efficient buildings in public sectors is rising; there is an increase in the collaboration framework of energy efficiency, such as a voluntary green labelling by Electricity Generating of Thailand (Huang and Deringer, 2007). While green building awareness in private sectors is still low, most entrepreneurs of designated buildings only concern themselves with energy efficiency and energy management in buildings (Chotichanathawewong and Thongplew, 2012).

Thailand's Eleventh National Economic and Social Development Plan (NESDP) for 2012-2016 indicated that energy efficiency is the key to achieving energy security and reducing greenhouse emissions (UNDP, 2012). In order to reduce energy consumption, the Thai Government has recently launched a 20 year Energy Efficiency Development Plan (EFDP) which aims to reduce energy consumption by 20 percent by 2030, targeting mainly the industrial and building sectors (Polycarp, Brown and Fu-Bertuax, 2013).

China and Thailand are energy importers. As energy consumption has risen rapidly, the governments of these two countries are increasingly considering the issue of energy efficiency, particularly in the building sector. While the Central Government of China provided financial support for retrofitting energy efficiency in existing buildings, the Thai Government has also launched an Energy Efficiency Development Plan (EFDP), with the main aim to reduce energy consumption in the industrial and building sectors, particularly energy being consumed in existing buildings. The next section moves on to look more specifically at a statement of the problems investigated in this thesis.

1.2 Statement of the Problems

In recent years, environmental concerns about the greenhouse gas emissions by the building sector have driven architects to adopt the design concept of energy conservation.

The potential for passive solar performance to contribute significantly to and by natural lighting is demonstrated by atrium design (Saxon, 1994).

Highly glazed spaces have proliferated in various forms, making a remarkable architectural statement (Saxon, 1986). The advance of steel construction and the technology of glass contribute to this new era of large glazed pedestrian concourses. Various forms of atria and glazed pedestrian concourses are widely used in buildings, especially commercial buildings, shopping malls and transport hubs, in order to take advantage of natural day light regardless of cultural and climatic conditions (Calcagni and Paroncini, 2004; Saxon, 1994).

In modern architecture, an atrium is a large open space within a building, often several stories high, or galleries with glazed roofs and/or large windows. A pedestrian concourse is a large space for pedestrian gathering which may include passageways, hallways, arcades and plazas.

Figure 1.8 shows the growing of atrium buildings in many countries in America, Europe, Australia and Asia. Atria are included in new buildings due to their attractive appearances and daylight benefit.

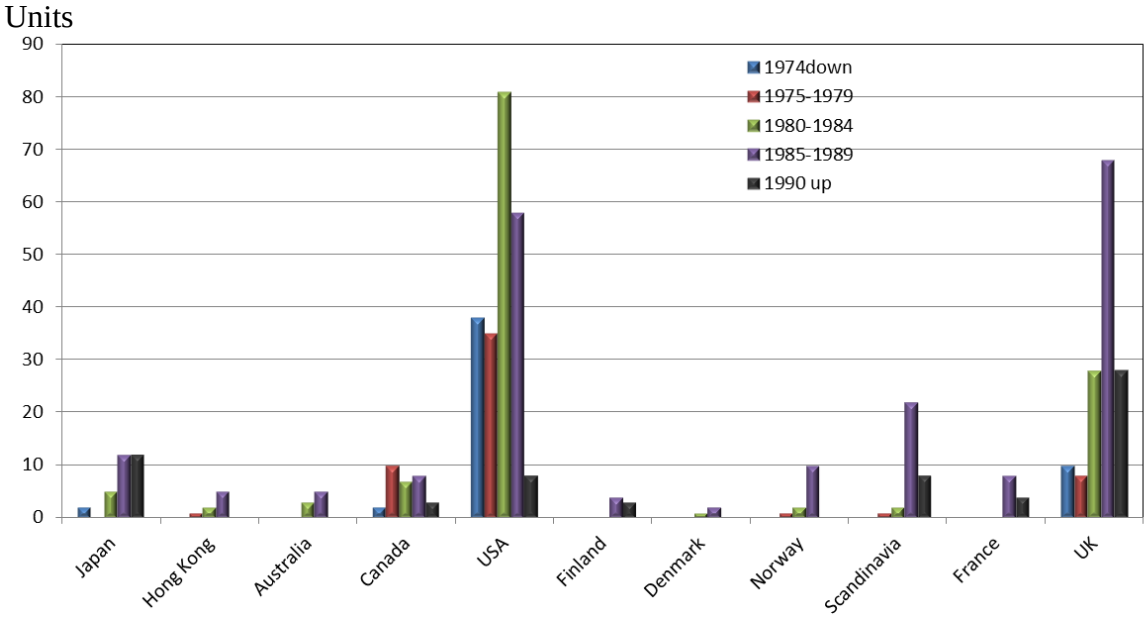

Figure 1.8 Gazetteers of notable atrium buildings (Saxon, 1994)

The use of large glazed pedestrian concourses has become popular in every global region, including the hot countries in Asia. According to Figure 1.9, rapid growth in large commercial constructions with glazed pedestrian concourses continued in Asia from 2001

to 2012. There were 229 new projects in Dubai, 76 in Guangzhou and 30 in Bangkok (Emporis GMBH., 2000-2013).

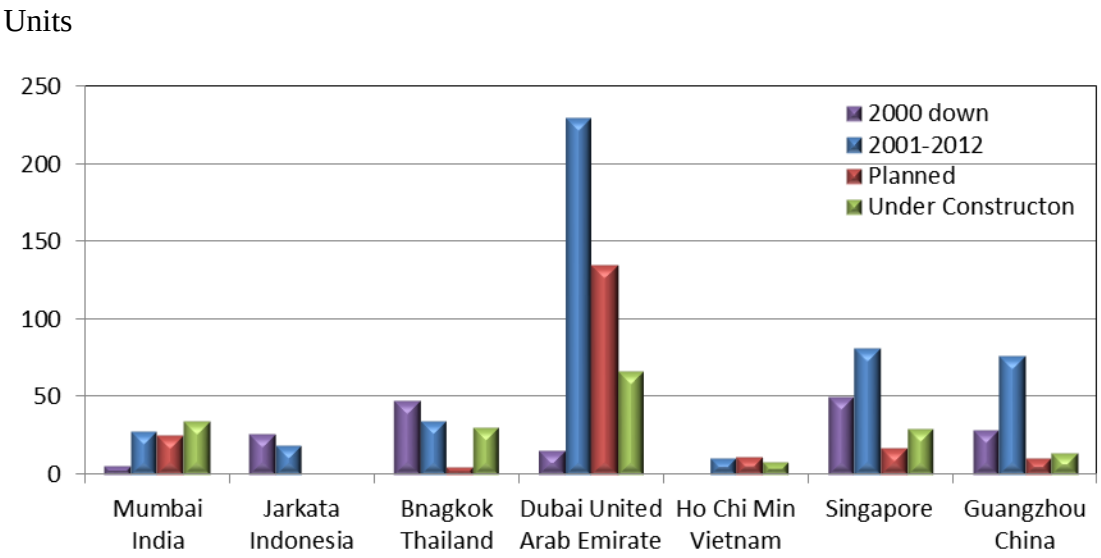

Figure1.9 Gazetteer of notable large commercial buildings with large glazed pedestrian concourses in the tropics (Emporis GMBH., 2000-2013)

A large glazed space, either an atrium or pedestrian concourse design, allows natural light to enter into the centre space of a building in order to take advantage of day lighting to make the space bright, open and attractive. Abundant daylight admitted into the glazed indoor space is impressive. Thermal effects, such as over-heating risks and the extensive cost of operating their cooling systems are harder to visualise and foresee. These problems are exacerbated by the tropical equatorial climate due to the heat radiation via the high altitude of the afternoon sun, which can result in severe over-heating in this space, and that in turn affects occupants' comfort. Additional air-conditioning systems would be needed to cool down the internal temperature to a comfortable level (Ahmad and Rasdi, 2000).

Large glazed pedestrian concourse buildings not only need excessive energy to run the HVAC system at a rapid rate, but such buildings also make it complex for HVAC systems to maintain an acceptable level of thermal comfort. Such problems emerge only after the building is occupied and bills are required to be paid. High heat gains through the glass result in expensive and maintenance intensive mechanical systems. The poor thermal performance in these buildings may also necessitate remedial improvements to increase comfort and lower operating costs after a couple year of occupancy (ASHRAE, 2009).

A large glazed roof allows the nature light to flood in and also results in excessive solar heat gained in summer, together with heat loss in winter. Although the heat gathered under such a roof could enhance the thermal buoyancy and encourage natural ventilation (Lomas, 2007), it also leads to discomfort on higher level floors and overheating in adjacent occupied areas (Moosavi et al., 2014). These problems are exacerbated in tropical climates due to high solar attitude and ambient temperatures. The internal temperatures can exceed external ambient temperatures in such buildings, which is clearly problematic. The stratification within the upper floors of this space is not only intensified, but the mean radiant temperatures of the internal surfaces in the space also increase due to solar radiation and convection. As a result, the operating temperature in this space leads to thermal discomfort and overheating, particularly in the upper areas (Atif, 1994; Pan et al., 2010). Besides, the stratification impacts of the building can also result in complications and expense for the HVAC system to keep the space thermally comfortable. These are some of the problems experienced in high profile buildings in tropical countries (Datta, 2001; Gocer, Tavil and Ozken, 2006).

The Sandra Day O'Connor Federal Courthouse is a typical example. The courthouse is built with a sleek steel and glass structure of impressive dimensions, thereby making impressive use of light. It is located in Phoenix, Arizona where the desert climate results in temperatures of up to 48^{o}C and 1,810 Btu/sq.ft./day solar radiation intensity (web.utk.edu).

There are courtrooms and offices along the south side of the building on each floor; all are air-conditioned with no windows. The building has been plagued with climate-control problems which challenge its advance air-conditioning system, including evaporative-cooling system. The air temperature in the building has been known to reach 38^{o}C in the summer; people who have spent much time in the courthouse have been reported to feel uncomfortable as a result of both the heat and humidity (Santos, 2012).

Cooling the atrium with a conventional HVAC system would be too costly. The General Services Administration's estimates put the price at approximately $800,000 per year with a traditional HVAC system; it costs approximately $51,000 with the adiabatic cooling system in place now (Rice, 2012).

Figure 1.10 Direct sunlight from atrium glazed roof of the Sandra Day O'Connor Federal Courthouse (Santos, 2012)

The Sandra Day O'Connor Federal Courthouse glass box is a perfect example showing that the overheating problems in large glazed spaces in the hot climates. Internal thermal and remedial solutions, after the building's occupancy, are very difficult and expensive to come up with. To resolve these problems, the proposed solution for large glazed pedestrian concourses is to provide suitable sunshade (Prowler, Prowler and Associates, 2014; Steemers and Yannas, 2000). Shading devices are the most applicable and flexible methods in all climates; as they may be located at the external or internal face of the façade (Stack, Goulding and Lewis, 2002).

External shading devices are the most effective at preventing the build-up of solar heat inside, by intercepting solar radiation before it reaches the building. Hence it is often preferred and considered at the early design stage for better integration into new building (Tzempelikos and Atheienitis, 2005). Other concerns relating to external shading included the increased construction cost to achieve structural durability, especially for long-span roof structures (Wang et al., 2014). Rosencrantz (2005) investigated the performance of various internal and external shading devices, combined with a specific window in an office and concluded that external shading devices cut the annual cooling load in half, while highly reflective internal shading devices decreased it by one third.

Even though external shading devices are more effective than internal shading devices, because they block the solar penetration before it enters through windows or roofs, the

proposed remedial solution for existing long-span glazed roof over large pedestrian concourses is an internal roof shading system. Easy installation is considered crucial to minimise disruption to the already very busy occupants in the spaces below. Most importantly, the light weight is considered vital as the existing large glazed atria pedestrian concourses spanning over 40 meters in both directions (Wang et al., 2014). The following are also seen as the advantages of internal shades compared to external shades (Umaru, 2009):

- The deterioration rate is slower, as they are protected from external conditions;
- They are lighter, thereby affecting fewer loads on the existing structure;
- They are less expensive, compared with the external ones;
- They are easier to install and operate;
- They have less impact on the outdoor appearance of the building;
- They can be designed to integrate with the interior design to provide and enhance aesthetic effects.

To resolve the identified problems of blocking solar penetration from any existing transparent roof, reducing solar gain across the whole long-span glazed roof over large pedestrian concourse and lowering the internal temperatures, the proposed solution for these problems was an internal roof shading system. Thus, this leads to the following research aims and objectives.

1.3 Research Aims and Objectives

In considering the impact of an internal solar shading device on the energy efficiency of the building, the central research question is:

"Which configuration of internal roof shading system is the most appropriate for use with existing long-span glazed roofs over large naturally ventilated and air conditioned pedestrian concourses in the tropics?"

Thus the ultimate aims of this research are to optimize weather responsive internal roof shading design systems and to recommend some design principles and guidelines for internal roof shading systems. Such systems would then provide a better building-centric thermal environment and energy performance, while maintaining adequate levels of natural lighting within the existing long-span glazed roofs over large naturally ventilated and air-

conditioned pedestrian concourse in the tropics. In order to achieve the aims of this thesis, the following objectives have been set:

1. To investigate the existing conditions and overall indoor physical behaviour within existing long-span glazed roofs over large pedestrian concourse buildings in the tropics;
2. To create dynamic thermal and lighting models of existing long-span glazed roofs over large pedestrian concourse buildings in the tropics with two cases: natural ventilation and air-conditioning for the purpose of comparison;
3. To examine the internal roof shading arrangements: high and low level blinds in the form of retractable internal fabric sheet blinds to reduce temperature and high energy consumption, while maintaining adequate levels of natural lighting for existing long-span glazed roofs over large pedestrian concourse buildings in the tropics with two cases in (2);
4. To analyse the financial benefits from the remedial solutions of existing long-span glazed roofs over large pedestrian concourse buildings in the tropics with the two cases;
5. To recommend internal roof shading design guidelines applicable to existing long-span glazed roofs over large naturally ventilated and air-conditioned pedestrian concourses to reduce temperature and high energy consumption, while maintaining adequate levels of natural lighting for existing long-span glazed roofs over large pedestrian concourse buildings in the tropics.

1.4 Research Scope

This thesis focuses on buildings with existing long-span glazed roofs over large pedestrian concourses in the tropics; thus two case studies were selected:

- Guangzhou International Textile City (GITC) represented a large naturally ventilated glazed pedestrian concourse building. The existing large glazed pedestrian concourse of GITC building is naturally ventilated while the surrounding retail units are air-conditioned. Even though, the total cooling load was designed at 180 Wm^{-2} , according to the national standard for retail units in China, but many complains also came from the tenants after the first year of operation regarding the overheating, due to solar heat gain and high cooling bills (CBTG Ltd., 2010);

- Suvarnabhumi Airport Terminal represented a large glazed air-conditioned pedestrian concourse building. The interest towards the energy consumption has been shown particularly for cooling systems, which have caused and created serious concerns at many other airports. The measured cooling load over the whole Suvarnabhumi airport in 2010 was very high at 553.41 $kWhm^{-2}$, as compared to the energy intensity benchmark for cooling systems in large airports is 393.1– 467.7 $kWhm^{-2}$ (EarthCheck, 2013; Costa et al., 2012).

The selection of the case studies was mainly based on the size of the project (in excess of 100,000 m^2) and designed with long-span glazed roofs over large pedestrian concourses, with mainly external glazed walls and transparent roofs in the tropics. GITC has a total floor area of approximately 140,000 m^2 with a total top-glazed roof area covering nearly 10,000 m^2. The long-span glazed roof over large pedestrian spaces is intended to be airy to suit the tropical climate and open to maximise natural lighting. Suvarnabhumi Airport Terminal has a total floor area of nearly 140,000 m^2 with a total top-glazed roof area covering nearly 25,000 m^2. The long-span glazed roof, over large spaces, provides an operating air-conditioned departure lounge that is also open to maximize natural light. The construction of the outside façade of both case studies is mainly 12 mm. thick laminated glasses with a *U*-value of 5.5 W/m^2K. Hence these two buildings are applicable to many other long-span glazed roofs over large pedestrian concourse buildings with the similar construction.

The effectiveness of internal shading devices to block out solar radiated heat depends on the position with respect to the glazed components, geometry, material properties (solar reflection, solar transmittance and light transmittance), control option and colour (Unterpertinger, 2005). Thus this thesis focuses mainly on internal roof shading systems in the form of retractable internal fabric sheet blinds with light colours.

Fabric samples and properties were provided by Silent Gliss manufacturers (Silentgliss, 2011). Five reflective shade fabric samples were selected and examined their realistic light transmission by scale model experiment tested in the artificial sky dome at Heriot-Watt University and also in open-field context, under an over cast sky. The highest lighting transmission and lowest solar transmission material was selected for proposed shades in

this thesis. Two screening positions were simulated: the horizontal level shade and the beneath glazed roof shade.

Shade control systems are required for retractable internal fabric sheet blinds, for these long-span glazed roofs over large spaces. The choice of electric motor or automatic control should be considered. However the shade control systems themselves were not a focal point in this thesis. Therefore, the cost analysis for installation of the shade control system was directly calculated from the manufacturer's recommended price list.

1.6 Beneficiaries

This research has benefit to proposed design principles and guidelines for consultants, architects, facility managers and owners to make wise decisions on energy use for the installation of internal roof shading within existing long-span glazed roofs over large pedestrian concourses.

1.7 Content of the Thesis

This thesis is divided into ten chapters. Chapter one presents a brief introduction to the whole research project and provides an outline of the structure with the major contents and purpose in the thesis for each of the following chapters.

Chapter two reviews the related literature which directly informs the general understanding of this study. It begins with the worldwide design of long-span glazed roofs over large pedestrian concourses in the form of atrium buildings, a specific review of its development in the tropics in an Asian context and an overview of research trends in atria. This chapter reviews shading systems. The fundamental concept of internal physical comfort and a brief discussion of the internal comfort criteria for countries with hot-humid climates are also presented. The general review of mechanical ventilation systems, and the basis for natural ventilation by thermal buoyancy in long-span glazed roofs over large spaces, is presented. Next, the post occupancy evaluation is discussed. Degree days used in the assessment and analysis of weather related energy consumption in buildings are discussed. The economic evaluation of investment proposals is also presented. The purpose of this chapter is to provide basic knowledge, to justify the need to carry out the research and to establish a reliable research methodology, which is documented in Chapter 3

Chapter three presents the methodology used for this study. This research deals with dynamic interaction of sub-systems in buildings: building, environment, equipment, people, natural ventilation and mechanical ventilation. The research methodology using in this thesis consists of six stages; the first stage involve the field study which was carried out by using data collection, filed measurement and questionnaire survey. The collected data were in two groups. These data were used to create the dynamic thermal and lighting model in the second stage. In order to increase the accuracy of the thermal and lighting models, it is necessary to calibrate these models by comparisons with the measures results for two critical variables, the indoor temperatures, the average cooling load and daylight factors. At the third stage the shading blind fabric was selected. To find such a material, five samples were collected from Silent Gliss manufacturer and examined their realistic light transmission by scale model experiment tested in the artificial sky dome at Heriot-Watt University and also in open-field context, under an over cast sky. The highest lighting transmission and lowest solar transmission material was selected for proposed shadings. In the fourth stage, two shading configurations were proposed and tested with the simulation under various conditions to compare their environmental and energy performance against the standard thermal, the cooling loads and the lighting variables within the large pedestrian concourse buildings. According to the most practical installation, two screening positions were simulated: the horizontal screen (Low level shading) and the beneath glazed roof screen (High level shading). In the fifth stage, a cost analysis was carried out taking into consideration both the installation and the running cost of the shading options using standard economic analysis methods. The final stage, the design principles and guidelines for internal roof shading systems in order to provide a better building-centric thermal environment and energy performance, while maintaining adequate levels of natural lighting within the existing long-span glazed roofs over large naturally ventilated and air-conditioned pedestrian concourse in the tropics was recommended.

Chapter four provides details of two field studies carried out in two large pedestrian concourse buildings with long-span glazed roofs. The one in China is the Guangzhou International Textile Building, which is a naturally ventilated circulation area with air-conditioned individual retail units. In Thailand the researcher will investigate the air-conditioned long-span glazed roof over the pedestrian concourse of Suvarnabhumi International Airport Terminal. This field study is to gain more understanding of the

internal physical environment and to obtain measured data for the calibration of dynamic thermal and lighting based models to propose the retractable internal fabric shadings to reduce discomfort and high energy consumption for these spaces. The building data collected during the field study is also included and analysed.

Chapter five presents the post-occupancy evaluation (POE) of thermal and lighting comfort in Suvarnabhumi Airport Terminal building. This chapter explains the questionnaire survey in order to evaluate the actual performance of the case study in term of energy and internal environment performance. The factors which influence the condition of thermal comfort are also explored including external physical and organic parameters. The overall occupancy satisfaction is also presented as the closing analysis.

Chapter six discusses the thermal and lighting computer simulation to model the measured conditions of the case study buildings; Guangzhou International Textiles Centre (GITC) and Suvarnabhumi Airport Terminal. It describes the modelling calibration by a comparison between thermal performance results from the measurement and the prediction by computer simulation to evaluate the capability and accuracy of the computer modelling. A summary of the procedure to modal thermal and lighting performance within the long-span glazed roof over a large naturally ventilated and air-conditioned pedestrian concourse is also concluded.

Chapter seven describes the development of a shading system, designed for both case studies, as a remedial solution to reduce temperatures while maintaining adequate levels of natural lighting from the long-span glazed roofs over large naturally ventilated and air-conditioned pedestrian concourses. Five types of fabric used for the blinds were tested under the artificial sky dome and in a ‘real sky’ experiment. The effects of the shading system on both thermal and lighting environments of the two shading arrangements – low and high level shadings over models on typical overcast days and clear days in summer and winter - are also discussed. An important component in this chapter is the discussion on the results of proposed shading systems designed with regards to improving indoor physical environments and energy performance.

Chapter eight discusses the economic implications by using results from the computer models. The calculated annual energy cost saving from the reduction of cooling loads, as

predicted by the modelling, is also presented. The methods used for the economic profits of energy saving project alternatives are: the net present value method (*NPV*), the internal rate of return method (*IRR*) and depreciated payback period (*DPP*).

Chapter nine presents the design principles and guidelines for internal roof shading systems in order to provide a better building-centric thermal environment and energy performance, while maintaining adequate levels of natural lighting within the existing long-span glazed roofs over large naturally ventilated and air-conditioned pedestrian concourse in the tropics was recommended. The design principles and guidelines will be based on the results of the work presented in the previous chapter; it will also suggest the good practices of internal shading to improve the thermal environment and maintain adequate levels of natural lighting within the long-span glazed roofs over large naturally ventilated and air-conditioned pedestrian concourses in the tropics.

The overall research is summarised in the last chapter of the thesis; based on the research objectives. Recommendations for future research regarding long-span glazed roofs over large naturally ventilated and air-conditioned pedestrian concourses in the tropics are also presented.

Chapter 2 Literature Review

2.1 Introduction

As has been explained in the statement of problems presented in chapter 1, large glazed pedestrian concourses have seen a significant increase in large buildings; they appear in various forms making a remarkable architectural statement (Saxon, 1983), particularly for commercial and office buildings (Calcagni and Paroncini, 2004). This popularity apparently is due to the natural light penetration deep into the building and the provision a central communal space. This building form was widely found in cold regions for its role as a buffer zone at night time and sun space during the daytime. The use of this form has been expanding to other regions, including the hot climate countries in Asia.

The reasons for using large glazed pedestrian concourses in the majority of these buildings are for its bright, spatial and aesthetic nature, which is obvious and easy to see at the design stage. Thermal effects, overheating risks and consequently expensive cooling system and high cooling bills are less easy to foresee and therefore are secondary concerns, or may not even be considered (Ahmad and Rasdi, 2000). Such problems only emerge after the building is occupied. High heat gains through the glass result in large, expensive and maintenance intensive mechanical systems and high running costs to correct the poor thermal performance in these glazed buildings (ASHRAE, 2009).

This chapter presents the literature that directly influences the general area of the study by addressing concerns about the physical environment and energy performance within large glazed pedestrian concourses in the tropics. The literature review also provides the fundamental science related to the internal shading systems designed to provide a better thermal and visual environment.

This chapter is composed of ten main sections. Firstly, it begins with the overall development and design of atriums and large glazed pedestrian concourse spaces, with a specific review of their development in the tropics. The second section reviews the research trend into atriums and large glazed pedestrian concourses. The third section discusses shading systems. The fourth section also discusses building ventilation systems for natural and mechanical ventilation and the theoretical basis for natural ventilation by thermal

buoyancy. The fifth section shows relevant theories relating to daylight and heat energy. Sixth, the fundamental concept of thermal comfort and the internal comfort criteria in the tropical climates in both China and Thailand are reviewed. The seventh section discusses the overview of post occupancy evaluation. Degree days used in the assessment and analysis of weather related energy consumption in buildings are presented in the eighth section. The ninth section of this chapter briefly reviews the economic evaluation of investment appraisals. The final section of this chapter presents the introduction of the computer software utilized in this thesis.

2.2 Atrium and Large Glazed Pedestrian Concourse Design Review

This section initially reviews the historical, development and design perspectives of atrium buildings and glazed spaces in the tropical climates and researches trend in atrium and large glazed pedestrian concourses.

2.2.1 Historical Development of Atrium Buildings

Back to 3000 BC, the traditional atrium has been traced in the archaeological remains of a courtyard house in Ur, Mesopotamia (Bednar, 1986) as shown in Figure 2.1. The term "atrium" was first used in the Roman architecture. It was composed of a central courtyard, a semi-public shelter area and a grand entrance (Kent, 1989).

A Persian courtyard house was found later as a covered courtyard in warm and hot climates as shown in Figure 2.2. They were designed for commercial activity on the ground floor and accommodation on the upper floor(s). The courtyard of the house allows natural ventilation and light into the centre of the buildings (Noor, 1986).

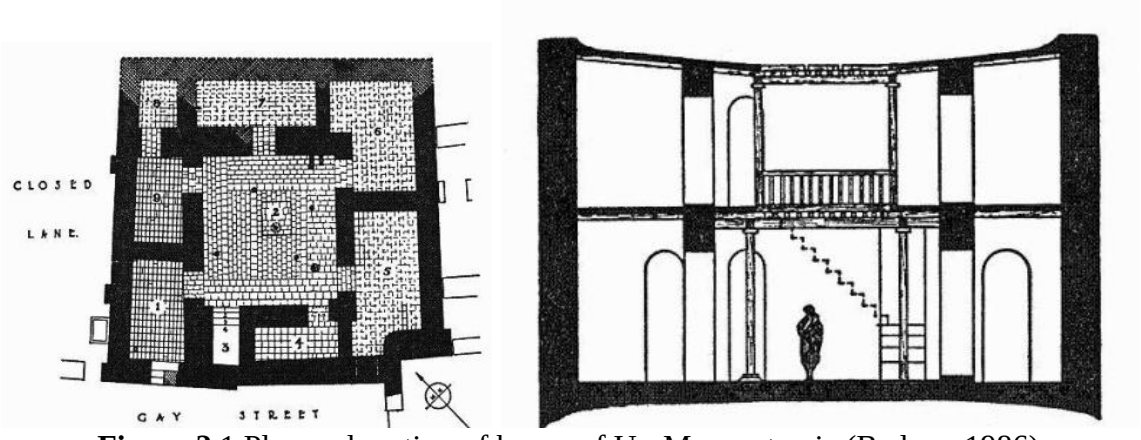

Figure 2.1 Plan and section of house of Ur, Mesopotamia (Bednar, 1986)

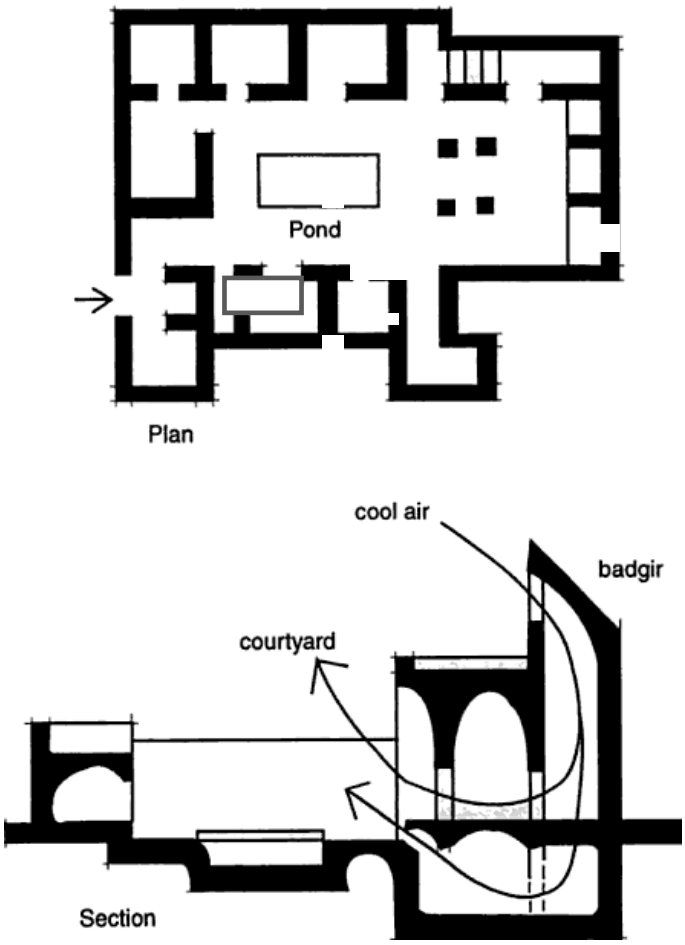

Figure 2.2 Plan and section of Persian House (Noor, 1986)

2.2.2 The Evolution of the Atrium

The development of iron construction and the possibilities of glass created a new era for the atrium buildings during the Industrial Revolution in Europe between 1820 and1870. The Crystal Palace was designed by Joseph Paxton with the grand scale of enclosed space and the innovative of prefabrication techniques and glass architecture (Bednar, 1986).

The Pension Building by General Montgomery Meigs illustrated the use of the atrium in the United States. This building was designed in a civic square, a social space for staff and the public. Its large central linear space was purposely designed to maximize daylight and natural ventilation. It is a very good example of an atrium building from the late Nineteenth Century (Bednar, 1986) (Figure 2.3).

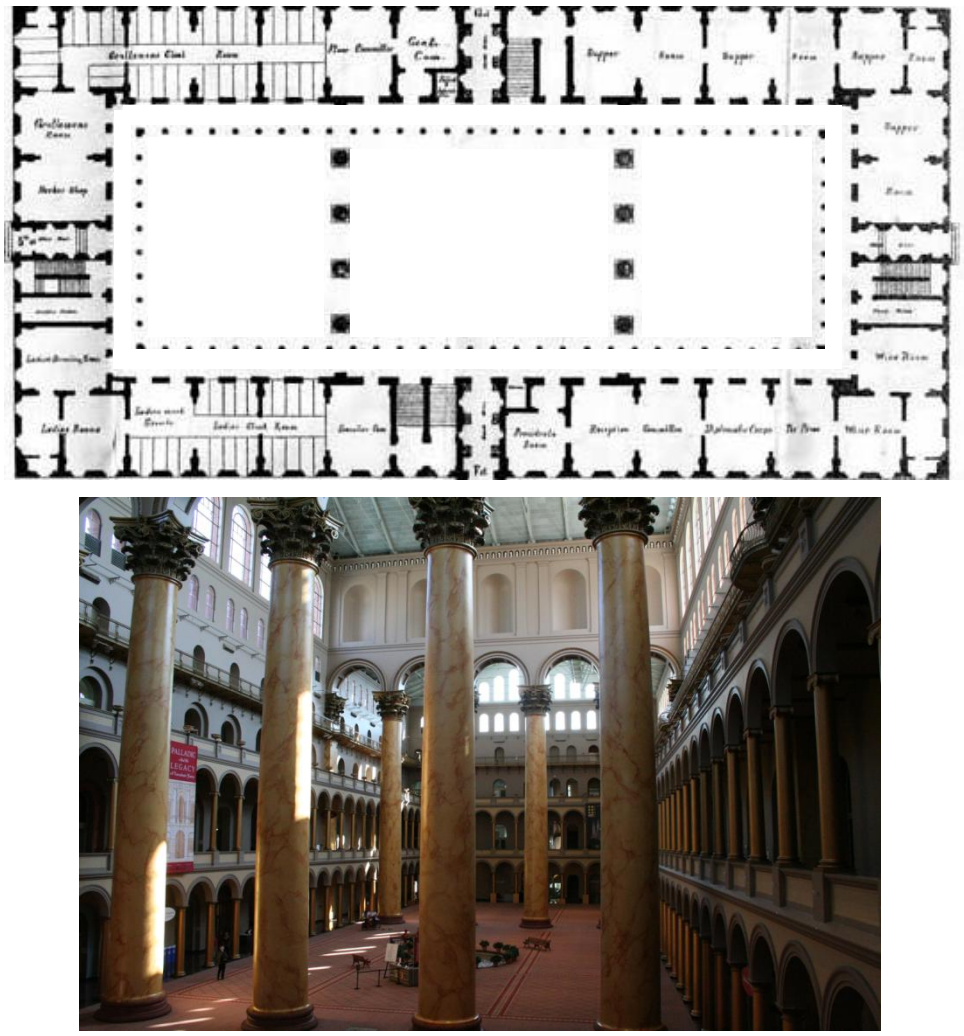

Figure 2.3 Plan and interior of Pension Building, Washington DC (Bednar, 1986)

2.2.3 The Modern Atrium

A new concept of atrium design emerged in America. The atrium was transformed into an ordinary light well to make better use of natural light (Hong and Chow, 2001).

The Hyatt Regency Hotel, Atlanta by John Portman in 1968 and the Ford Foundation Headquarters, New York by Kevin Roche, John Dinkeloo and Association in 1967 were the early influential buildings in this modern period of atrium buildings (Saxon, 1983). The Hyatt Regency Hotel has a full high internal atrium lit by a skylight and clearstory glazing. The atrium area uses extensive water features and planting, reflecting the natural space. It revolutionized and influenced later hotel designs (Bednar, 1986).

Figure 2.4 Atrium of Hyatt Regency Hotel, Atlanta
(https://en.wikipedia.org/wiki/Hyatt_Regency_Atlanta)

The Ford Foundation was an example of the function of the atrium in office buildings. It has an atrium at the corner of the floor plan, acting as a transition between the private space of the building and the urban public space.

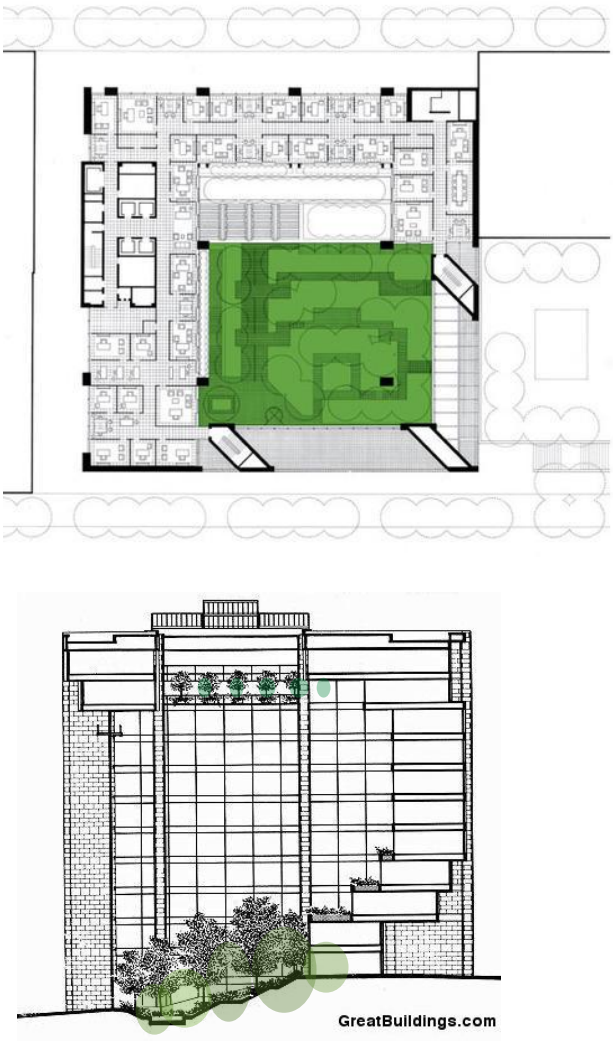

Figure 2.5 Typical plan and section trough atrium, the Ford Foundation Headquarters, New York (http://www.greatbuildings.com)

The definition of the new atrium by Bednar (1986) was an enclosed, daylit, centroidal space which represented only a grand entrance space, a focal courtyard or a sheltered semi-public area. The early atrium buildings would be designed for the main purpose of offering an impressive architectural space. The environmental benefit of the atrium was considered after a post-oil-crisis response to high energy use in these buildings (Abdullah, 2007).

Designers afterwards were inspired by Portman and developed the atrium space atmosphere to their commercial space design (Kent, 1989). The openness of the atrium was designed to allow occupants' visibility, enabling them to look around in the atrium and the adjacent spaces. In order to anchor attractions, not only spatial spaces or relaxing atmosphere are used as the attractions, but thermal comfort and daylighting are also the most influential factors for these spaces (Hong and Chow, 2001).

2.2.4 The Generic Atrium Forms

There are nine basic configurations of atrium space. The simplest atrium forms are open-sided (one-sided, two-sided, three sided), core (four sided) and linear atria (Figure 2.6). The bridging, podium, multilateral and multi vertical atria are appropriate for large scale and high-density development (Gritch and Eason, 2010).

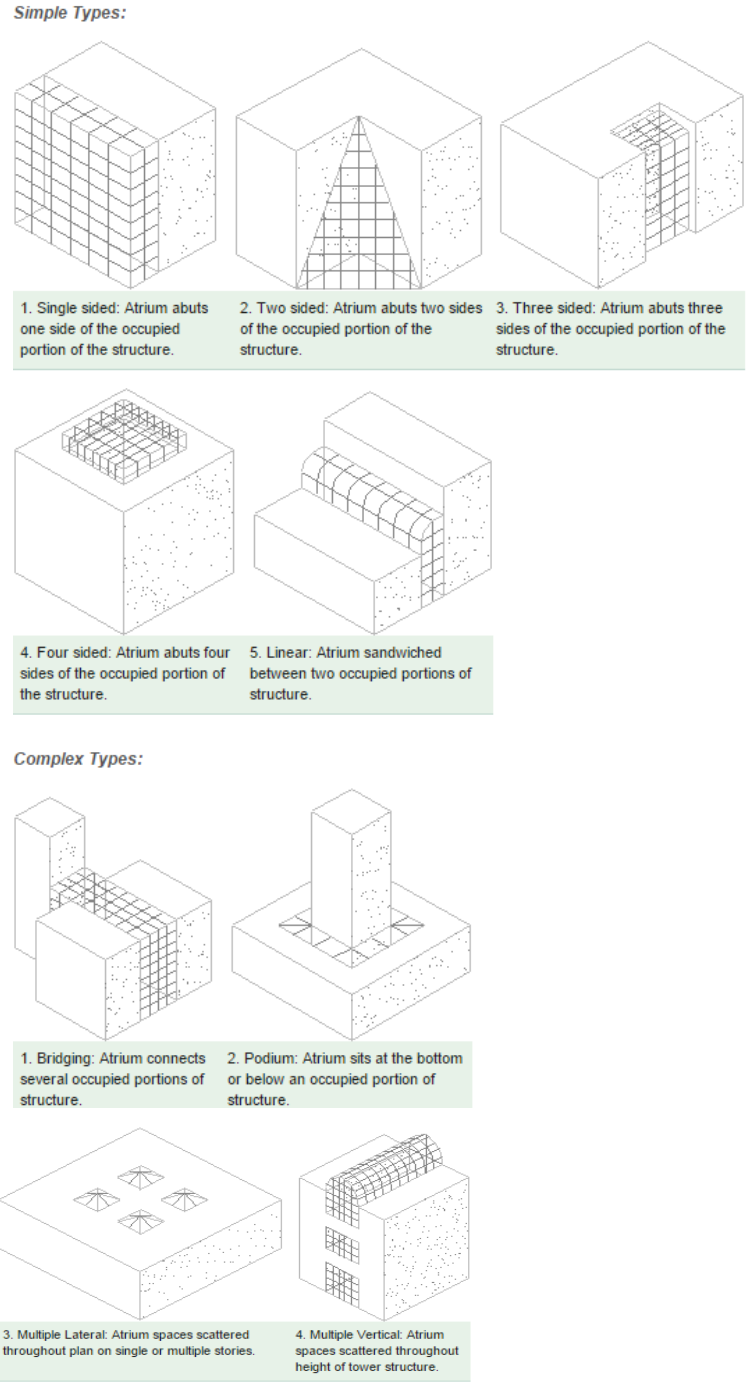

Figure 2.6 Generic forms of atrium buildings (Gritch and Eason, 2010)

These different configurations can be developed into various designs informed by the function of buildings and purposes of the atrium and adjoining spaces.

2.2.5 Atrium and Large Glazed Pedestrian Concourses in the Hot Climates of Asia

Western architects are concerned with the conservation of energy, so the potential of natural light and heat gains were demonstrated by atrium building design (Saxon, 1994). An atrium can be a source of daylight as it transmits from glazed material into the internal space. In winter, the total heat loss through the external glazing is higher than solar heat gain, leading to an increase in internal temperature without providing thermal radiation to the glazing. Therefore a glazed space has become a popular feature in temperate climates (Hong and Chow, 2001).

The use of the atrium form has now become popular in other regions, including the hot regions of Asia. The atrium in a hot climate would be in a heat surplus condition, due to a large glazed atrium allowing solar heat gain gathering and finally leading to conditions of discomfort in this space. Therefore, mechanical air-conditioning systems are required to cool down the high air temperature throughout the year (Quek, 1989).

The evaluation of atrium form in the tropical areas of Asia started with an open courtyard which was glazed over. The glazing not only maintains the daylight but also traps heat and reduces the flow of natural ventilation. So additional mechanical cooling would be needed to cool down the internal temperature to comfortable levels (Al-Obaidi et al., 2013).

The development of atria in Asia was mostly used in large commercial buildings. The atrium form was incorporated in various building types, particularly in office buildings and hotels; large glazed pedestrian concourses are widely used in shopping malls and airports (Calcagni and Paroncini, 2004).

The main purpose of having an atrium in a building is for its visual impact, brightness and openness. While a large glazed roof allows natural light to the centre of a deep plan building, it also results in excessive solar heat gain in summer, leading to discomfort in its occupied zone. These problems are exacerbated by Asia's tropical equatorial climates; due

to the high solar altitude and ambient temperatures, internal temperatures can exceed outdoor ambient temperatures in such buildings (Wang et al., 2014).

2.3 Overview of Research Trend in Atrium and Large Glazed Pedestrian Concourses in Tropical Climates

The key reasons for using glazed roofs over public concourses are not only their visual impacts but also a strong return on investment, raising value and occupancy rate (Saxon, 1994). Furthermore, cost comparisons from some studies show that construction cost of atrium buildings are cheaper than the ordinary buildings of the same size (Schittich, 2007).

However, operating costs connected to the thermal effect only emerge after the building is occupied. High heat gains result in large, expensive and maintenance intensive mechanical systems, with high running costs; they also lead to thermal discomfort in hot climates (Ahmed and Rasdi, 2000).

These misconceptions of the environmental and energy benefits drove many researchers to find out the effects of incorporating atriums into any type of building. Research on atria and large glazed pedestrian concourses can be classified into four main categories: architectural and economic aspects related, air quality related, fire safety related and energy related.

2.3.1 Architectural and Economic Aspects Related Research

The architectural research relates to the atrium design concept for spatial expression and aesthetic value, such as “Those Proliferating Atria” by Harney A. (1979) and “A Review on Architectural Aspects of Atrium Buildings” by Hong W.Y. and Chow W.K. (2001). The economic related research contributes data about the investment returns on the part of owners or developers, such as “The Architect as Developer” by Portman and Barnett (1976).

2.3.2 Air Quality Related Research

The research on internal air quality within atria is concerned with the efficiency of the ventilation systems in the removal of pollutants and excessive heat from this space. Some the of common causes of air quality problems are the presence of indoor pollution sources; as well as poorly maintained or operated mechanical ventilation systems (Abdullah, 2007).

Natural ventilation in large glazed pedestrian concourse buildings can be achieved with solar driven by buoyancy-induced airflows through the space. Good design would maximize the natural environment to minimize energy consumption (Hussain and Oosthuizen, 2012). The effectiveness of the mechanical ventilation systems placed on the top of the roof can significantly improve internal environment; a benefit that has been investigated by Kato, Murakami and Shoya (1995).

In general, the study of the efficiency of the ventilation systems within large glazed pedestrian concourses can also be associated with energy-related research.

2.3.3 Fire Safety Related Research

The openness of the atrium design through many levels can cause fire and smoke to spread rapidly in the large glazed pedestrian concourse spaces and adjacent levels. Fire safety management is of the greatest concern among researchers. The use of different functions in these spaces would have different evacuation patterns. Therefore, various methods were examined for smoke and fire movement patterns in atriums, such as 'Scale Modelling Studies on Atrium Smoke Movement and Smoke Filling Process" by Chow W.K. and Henry H.W. (2008); "Numerical Simulation Study of Smoke Exhaust Efficiency in an Atrium" by Zhan et al. (1997); and "Experiment Data and Numerical Modelling of 1,3 and 2,3 MW Fire in 20 M Cubic Atrium" by Gulierrez-Montes and Sammigual-Rojas (2009).

Other relevant areas of concern include sprinkle or smoke control system designs for this space, such as "Atrium Sprinkle Performance Analysis" by Chow W.K. and Fong W.K. (1988) and "Smoke Control in Mall with Atria and Restaurants" by Clark J. (2004).

2.3.4 Energy Related Research

Obviously the main concern of energy-related research in atriums is to study the internal physical environment. The major problems with physical environments within the atrium space are overheating, thermal stratification and visual discomfort from glare.

- **Overheating and Day Lighting Problems in Large glazed Pedestrian Concourses in Tropical Climates**

The large glazed pedestrian concourse design allows the benefit of deep penetration of the natural light into the centre communal spaces of a building. Abundant daylight being admitted in the large gazed concourse make it appear impressive, but this can also cause excessive solar heat gain and glare, especially in hot climates (Ahmad and Rasdi, 2000). Beyond a certain level of daylight penetration, a large glazed space may in fact generate far more problems than benefits. The radiation of the high altitude of the afternoon sun can result in severe overheating and that can negatively affect occupants' comfort.

Numerous studies of atrium buildings and large glazed pedestrian concourse spaces in hot climate countries have been conducted, in order to assess the performance of energy, user comfort, luminous impact, thermal environment, solar heat gain and computational fluid dynamic (CFD) in atrium buildings.

Pan et al., (2010) showed that the air temperature in the atrium space rises gradually along with the height. The temperature gradient becomes moderately large in the area near the top of the atrium because the solar radiation passes through the glazed roof and heats the internal surfaces to higher temperatures and then influences the air temperature through long-wave radiation between internal surfaces and room air. There is a rapid increase of the air temperatures in the region from roof down to 10 meters below the roof; a prognosis supported by using CFD simulation.

In addition, there is a popular misconception that glass technology has become so advanced that unshaded glass walls will reduce cooling loads. Modern low e-coated glass may be slightly better than older glass in thermal conductivity, but it still conducts over five times more solar heat than a well-insulated solid wall. The designers of new projects may not be aware of the negative effects of unshaded glass on thermal comfort. In hot-humid climates, unshaded glass buildings not only consume the mechanical budget for HVAC system at a rapid rate but make it difficult for HVAC system to maintain a thermally comfortable environment (ASHRAE, 2009).

The reasons to use an atrium in the majority of these buildings are spatial and aesthetic. Energy advantage has become secondary or may not even be considered (Ahmad and Rasdi, 2000). Located in hot climates, glass box building was notoriously uncomfortable, regardless of a very large, expensive and maintenance-intensive mechanical temperature control system. High thermal heat loads through the glass required the retrofitting of another cooling system under the floor in their space (ASHRAE, 2009).

The light coming into the atrium is impacted by several factors such as the average brightness of the local sky, the type of glazing, whether transparent or translucent, the orientation of the glazing and reflectivity of wall surfaces facing the atrium. These issues must be balanced in order to provide an adequate amount of light at the occupied area of the atrium (Gritch and Eason. 2010). However, daylight from the large glazed surface of the atrium causes excessive solar heat gain in summer and heat loss in winter and also air stratification, especially in summer (Gocer et al., 2006). The complex thermal phenomena occur at the atrium buildings because of their large size and high solar gains through the fenestration. The cooling load is responsible for the biggest part of the energy consumption. This result reveals the requirement of solar shading devices and proper glazing system design to prevent high excessive solar heat gain. User comfort was analysed considering hydro thermal and vision comfort conditions.

The integration of daylight and controlled lighting strategy is a key component of a sustainable approaching to atrium buildings. The atrium space might need luminance of 50-200 lux and office space in atria require illumination levels of 200-1000 lux, while the major source of daylight has an intensity that varies from 1,000 to 30,000 lux, depending on the degree of overcast and solar attitude. The configuration of interior balconies in atrium space would affect daylighting performance in atrium space. Well index and the depth of balcony are the most significant factors in the performance of daylighting in atrium spaces with interior balconies. In the case of a deep balcony in a deep atrium building, intensive supplementary artificial lighting systems should be carefully installed with reference to the amount of light attenuation, because of the balcony configuration and the geometric characteristics of the atrium (Kim and Kim, 2010).

The glazed pedestrian spaces in tropical equatorial climates are likely to become over heated due to high solar attitude and high ambient temperature. The indoor temperature can be above the external temperature; the high proportion of solar radiation heat absorbed by the atrium envelope will increase the mean radiated temperatures of the internal surfaces. These conditions lead to the increase in the resultant temperature inside the atrium, creating a great risk of thermal discomfort and overheating problems as well. In addition, due to the large glazed wall and roof, the air in the atrium generated by solar heat can lead to thermal stratification, which is difficult to control (Abdullah et al., 2009).

- **Replication of Large Glazed Pedestrian Concourse Buildings**

Many studies have suggested the way to reduce heat gain through the building roof. One method is by evaporative spray cooling, which can prevent the overheating of the roof and interior of the building. The study on the effect of solar gain control by water spray with high–level blind clearly concluded that water spray helped to significantly reduce the thermal stratification at the higher level. On the other hand, the study on the effect of solar gain control using the solar blinds indicated that as the blinds absorbed solar energy from the top, its radiant temperature would rise due to the increase in surface temperature. With the contribution of radiant energy from other internal surfaces, the mean radiant temperature and the air temperature at high level would also increase and lead to greater stratification in the atrium. As a result, the comfort conditions at the higher levels would be greatly reduced (Abdullah et al, 2009).

Moreover, Abdullah and Wang (2005) utilised dynamic thermal simulation and reviewed that side-lit form atrium performs better than lit form atrium in term of the total solar heat gain and resultant temperature in the occupied levels in the atrium spaces. The amount of solar gain for the lit form is double that from the side-lit form because the larger glazed area for lit form allowed the higher transmittance characteristics for both solar and heat of the glass material. It is less possible to use full natural ventilation to ventilate the atrium space in atrium building because the hot-humid climate has almost stable hot external air temperature, with generally low wind speed throughout the year.

It can be clearly seen that, the critical design of large glazed spaces in tropical climates directly influences energy performance and user comfort. Thermal comfort is important to the design of buildings for three reasons. Firstly, comfort is an important aspect of occupants' satisfaction. Secondly, the temperature which people try to achieve in that building is a significant factor in deciding the energy it will use. Lastly, if a building fails to be comfortable, then the occupants will make themselves comfortable by the use of mechanical equipment which involves the use of extra energy (Roaf, Crichton and Nicol, 2009).

Atria with glazed spaces may be designed to provide sufficient light to this common space. However, direct sunlight admitted to the atrium can cause glare or undesirable strong patterns of shadow. Sunlight can be intercepted at a window wall facing the atrium or at the atrium roof. Solar shading can diffuse the direct sunlight by filtering and reflecting. (Brown and Dekay, 2014) The primary reason for sunshading is to provide thermal comfort by reducing unnecessary solar gain. Design parameters, which include orientation, sun path, sun angle, daylight transmission, ventilation, user control, maintenance and cost, vary according to the climatic characteristics and the function of the space. The reason for using either of the shading options in atrium building is unlikely to be based on solar gain and daylight factors alone. It may also be for aesthetic reasons. Arguably, the most effective way to reduce heat gain in an atrium is to provide sunshade to the large glazed pedestrian concourse roof (Steemers and Yennas, 2000).

Although numerous studies have also examined the indoor physical and energy performance within atria and large glazed pedestrian concourses, there is no study available on remedial solutions by internal roof shading. Such shading is designed to provide a better thermal environment and energy performance, while maintaining adequate levels of natural lighting within the existing long-span glazed roof over large naturally ventilated and air-conditioned pedestrian concourses in the tropics.

- **Shading Devices**

Shading devices play a major role in limiting the heat gain of buildings and on their energy performance. It is thus useful to understand the potential to control daylight,

overheating risk and visual comfort by the use of shading devices (Haldi and Robinson, 2010).

Cheng et al. (2007) studied external shading devices and provided evidence that a proper setting for shading devices could promote the room's lighting performance. Kim and Kim (2009) illustrated that an external shading device is much more effective than an internal shading device, as the former provides better illumination and energy consumption. Rosencrantz (2005) used the dynamic energy simulation software to investigate the performance of various internal and external shading devices in offices and also insisted that external shading devices were more efficient than internal solar shading devices. External sunshades halved the cooling peak energy consumption load, while internal sunshades with solar reflecting coatings reduced it by one third.

The study of external shading devices and daylight quality by Dubois (2003) identified that grey screen external shading provided poor uniformity and unacceptable low illuminance for working, while overhanging and horizontal Venetian external blinds provided adequate work plane illuminance. Furthermore, this study also identified that not all types of external blinds can provide quality daylight during winter. The better results should thus consider moveable shading devices.

Recent studies have shown that appropriate internal shading design and control could significantly reduce peak cooling load and energy consumption for both lighting and HVAC. Gratia and Herde (2007) applied dynamic thermal simulation software to investigate optimal blind location, size and colour in a double skin façade. The researchers concluded that shading devices possible reduce cooling consumption by up to 14% during summer season. Moreover, Tzempelikos and Athienitis (2007) suggested that shading should be considered as an integral part of fenestration system design for commercial buildings, not only to balance daylighting requirements, but also to reduce solar heat gain.

What is clear from the previous studies is that correctly designed solar shading devices can improve building energy consumption and provide daylight quality. A proviso is that an external shading device is preferred as it blocks most of the heat from solar radiation before it reaches the building's surface. However, external shading device

needs should be properly addressed at the early design stage due to its construction loads. The widespread preference for large glazed pedestrian concourses in commercial building has created an 'artificial' need for sophisticated shading devices. Over-glazed buildings are often subject to intense solar heat build-up and visual discomfort. The proper solution to these critical issues is an internal shading system which would be easy to install, light weight, effective to operate and economic to run over its life time (Wang et al., 2014).

The indoor thermal and lighting environments of large glazed pedestrian concourses are influenced significantly by the transparent part of a roof and facade. To prevent these buildings from overheating and causing visual discomfort in their internal environments, retractable shading devices are recommended (Wienold et al., 2011). The number of shading systems available today on the market is huge and it is therefore not always easy to choose the best solution for a building. Many parameters influence the choice of the system and of the control strategy itself. The building's energy performance using different shading designs (Simmler and Binder, 2008) and internal shadings have been studied already (Florides et al., 2000). But none of these studies investigated how thermal and lighting environments are affected by the internal roof shading systems.

2.4 Shading Systems

Protection of the building from unwanted solar gain is the first and most important consideration in the design of a shading system. Correctly designed shading systems can effectively control the sun's radiation by blocking diffuse radiation as well as reflecting it. Direct radiation emanates straight from the sum to buildings in parallel beams. Diffuse radiation emanates from the entire area of the sky, while reflected radiation comprises both direct and diffuse radiation reflected from the ground and surroundings (Stack, Goulding and Lewis, 2002).

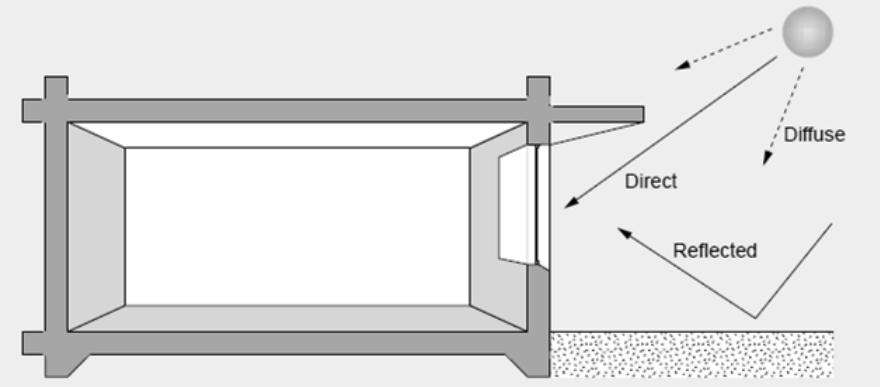

Figure 2.7 Direct, Difuse and Reflected Radiation
(Stack, Goulding and Lewis, 2002)

2.4.1 Principles of Solar Overheating Control

Solar overheating can be reduced by the following techniques (CIBSE, 2006):

- Planning the building to maximise the benefit of sunlight and minimise the disadvantages of heat gain;
- Limited window areas: this is the main source of solar heat gain;
- Thermal mass with heavyweight structure will absorb heat with a long response time;
- Good ventilation: this can be achieved by cross ventilation, stack ventilation or mechanical ventilation;
- Reduce internal heat gain: specifying energy efficient equipment with small power loads;
- Mechanical cooling;
- Solar shading, which may include external, internal or mid-pane shading devices.

2.4.2 Typology of Shading Systems

As indicated above, shading devices may be internal or external and fixed or moveable. Sunshade strategy is determined by building location, orientation and solar radiation. Shading devices can be an integral part of the building's envelope influencing thermal and daylighting issues. Selecting the correct form of shading device is therefore extremely important (Stack, Goulding and Lewis, 2002).

Shading devices can be particularly effective as a part of a cost effective way to control overheating. Thermal comfort could be achieved with a combination of glazed windows and shading devices. Selecting the proper shading devices is considered vital as the solar control system blocks incoming solar energy (CIBSE, 2006). A variety of shading devices are available as follows:

- **External Devices** are the most effective in reducing heat gains. They intercept most of the solar heat before it reaches the building. However, they tend to have a greater impact on the character of the building and tend to be more expensive to install and maintain. A variety of external blinds are available such as horizontal overhangs, vertical fins or moveable louvers (Figure 2.8).

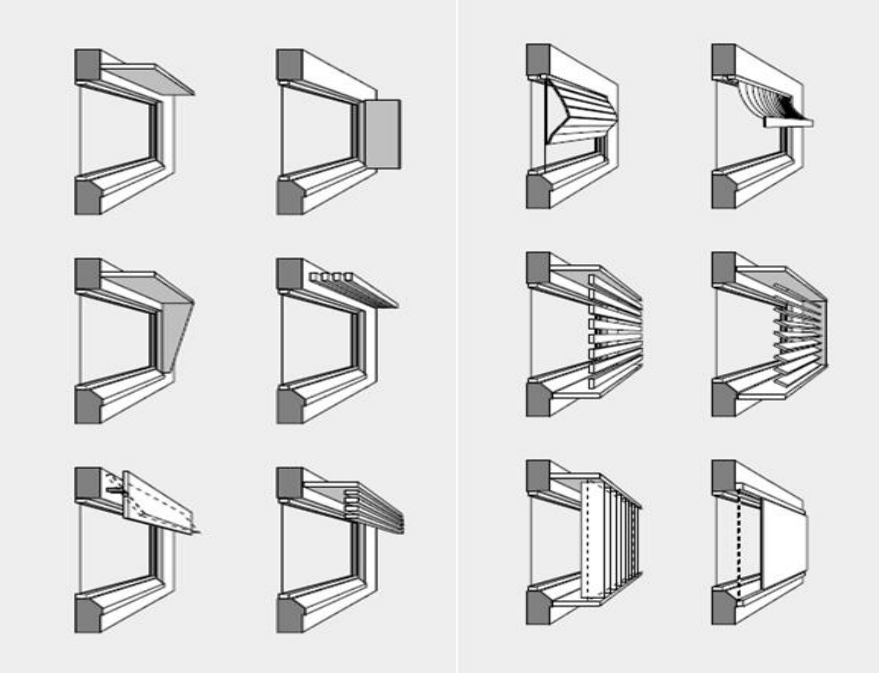

Figure 2.8 External Shading Devices (Stack, Goulding and Lewis,2002)

- **Internal Devices** are almost always adjustable or retractable. They are easily adjusted and maintained and also are generally cheaper. Internal shading devices can be curtains, blinds or louvers. However, internal shading devices allow direct sunlight to pass through the glazing. Fabrics with a solar reflecting coating can help reflect this solar heat and offer improved thermal performance (CIBSE, 2006).
- **Mid-Pane Blinds** will be intermediate between double glazed units. Various options are available to allow mid-pane blinds to be controlled from the inside of the building (CIBSE, 2006).

External shading devices are more effective than internal shading devices because they block the solar penetration before it enters through windows or roofs, but the proposed remedial solution for existing long-span glazed roof over large pedestrian concourses is an internal roof shading system. Easy installation is considered crucial to minimise disruption to the already very busy occupants in the spaces. Most importantly, the light weight is considered vital as the large glazed atria pedestrian concourses span is often over 40 meters in both directions (Wang et al., 2014).

2.4.3 Thermal and Visual Factors relating to the Shading Fabrics

Thermal and visual factors are defined by the European Standard EN 14501 as the major properties for the solar protection performance of the fabrics covering the following characteristics (http://www.sunscreen-mermet.com):

- Thermal factors relating to the fabrics:
    - Solar transmittance (*Ts*) is the proportion of the energy transmitted through the fabric. A low percentage means the fabric performs well at reducing solar energy;
    - Solar reflectance (*Rs*) is the proportion of solar radiation reflected by the fabric. A large percentage means the fabric performs well at reflecting solar energy;
    - Solar absorptance is the proportion of solar radiation absorbed by the fabric. A low percentage means the fabric absorbs little solar energy;
    - G-value is the coefficient to measure the solar energy transmittance of glass or fabric. A low percentage represents a material with low solar energy transmittance.

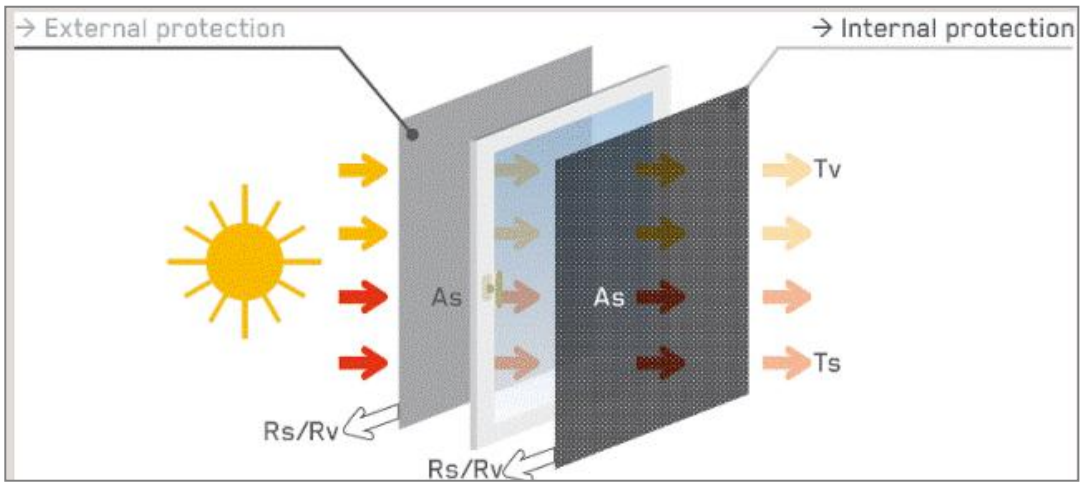

Figure 2.9 Thermal factors relating to the fabrics
(http://www.sunscreen-mermet.com)

- Visual factors relating to the fabrics:
    - Openness factor (*OF*, *Co*) is relative area of the openings in the fabric (hole) which is considered as dependent of the colour;
    - Lighting transmittance (*Tv*) is the total percentage of lighting radiated through the fabric over the wavelength of 380 to 780 nanometres. Lighting transmittance of the window components including glazing, frame, gap and shading device is an important factor in the calculation of interior daylight illuminance from the window;
    - Lighting reflectance (*Rv*) is the proportion of light reflected by the fabric;
    - Diffuse transmittance factor (*T dif*) is obtained by correlation the two factors of lighting transmittance and openness factor: *T dif = Tv –OF*.

      T dif indicates the aspects of glare, outward visibility and night privacy. It shows better visual comfort.

2.5 Building Ventilation Systems

This section looks at the objectives and requirements for building ventilation and the criteria for the effective ventilation.

2.5.1 Appropriate Ventilation System Design

Appropriate ventilation system design can provide acceptable air quality and meet thermal comfort requirement throughout the full range of climatic conditions.

Ventilation in buildings can be mechanical or natural. The purpose of ventilation is to remove heat, moisture, and contaminants or to reduce the concentrations of contaminants. This is extremely important for the designer needs to know where pollutants will be generated or where they will occur naturally; keeping such areas negatively pressurized relative to the adjacent areas is important to avoid unwanted distribution of the contaminants from one area to another. Locations of activities or equipment that will be strong sources of contaminants should be provided with exhaust ventilation or surrounded by areas that are positively pressurized relative to the source location. Sensitive areas should always be isolated by air pressure and fixed barriers where feasible. (Watson, Crobie and Callender, 1997)

Ventilation is the act of supplying clean air to satisfy the need for fresh air. Ventilation rate is one of the important parameters to be considered. The ventilation rate can be measured in air-changes per hour. It depends on the volume of the space of floor area per person and activities of the occupants (Yeang, 1996). The approximate values for the ventilation rates need for each function shows in Table 2.1.

Requirement	ACH	I/S sq.m.
Health	0.5 to 1.0	0.4 to 0.8
Comfort	1.0 to 5.0	0.8 to 4.0
Cooling	5.0 to 30.0	4.0 to 25.0

Table 2.1 Approximate ventilation rate requirement (BRESCU, 1995)

ASHRAE Standard 62 (1999) “Ventilation for Acceptable Indoor Air Quality” is the basis for most building code ventilation requirements. Minimum rate in Standard 62-1999 includes 20 cfm/p in open space office area, educational laboratories, and commercial dining rooms. For many typical spaces such as office, schools, and public assembly space a standard of 15 cfm/p is required.

2.5.2 Type of Ventilation System

The method of ventilation chosen for a building should be based on concern about likely gain and the admittance. Some of the basic ventilation systems available for the control of interior space are discussed below.

(i) **Natural Ventilation**

Natural ventilation can be used effectively for cooling buildings that are properly shaded and otherwise designed to suit local climatic conditions. In many locations and building types, the climatic design elements can provide the principal source of cooling comfort in buildings (Watson, Crobie and Callender, 1997).

Natural ventilation depends on three climatic conditions as follow (Abdullah, 2007):

- Wind Velocity: The direction of the wind and its velocity over the building drive a pressure field around the building. As air piles up in front of the building, its pressure rises until forced over and around the solid building, creating a lower-pressure area behind the building. Air in this lower-pressure area on the downwind side is eddying and moving slowly back upwind toward the solid building.

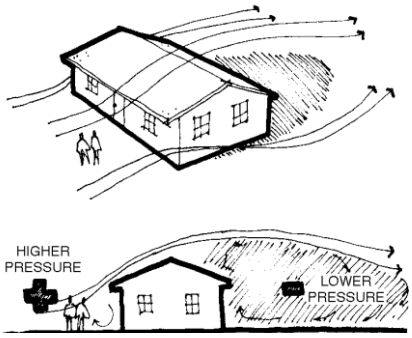

Figure 2.10 Wind velocity drives pressure field (Watson, Crobie and Callender, 1997)

- Wind Direction: As the wind moves over the building, it creates a varying higher and lower pressure field. Air will then flow from the higher pressure zone(s) to the lower pressure zone(s) as shown in Figure 2.10.
- Temperature difference: When solar radiation heats the air in a space, reducing its pressure and causing it to rise, air will act like a fluid; the lower temperature and higher pressure air flow into that space. This principle is known as 'stack ventilation' as shown in Figure 2.11.

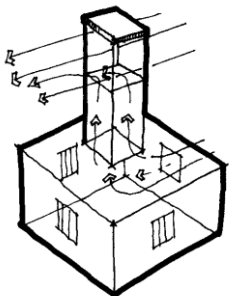

Figure 2.11 Stack effect within the building to the air flow
(Watson, Crobie and Callender, 1997)

(ii) Natural Ventilation by Thermal Buoyancy in an Atrium

Natural ventilation in an atrium or large glazed pedestrian concourse is based on thermal buoyancy driven force, which occurs when the internal temperature is hotter than the external temperature. Warm internal air will rise through outlet openings and being replaced by cooler air (Khan et al., 2008).

The vertical air movement equation can be expressed as following (Terpager, 2003):

$$p_{i1} - p_{i2} = \rho_i g H \quad (2.1)$$

$$p_{o1} - p_{o2} = \rho_o g H \quad (2.2)$$

Subtracting Equation 1 from 2 results in

$$(p_{o1} - p_{i1}) + (p_{i1} - p_{i2}) = (\rho_o - \rho_i) g H \quad (2.3)$$

$$\Delta p_1 + \Delta p_2 = \Delta \rho g H \quad (2.4)$$

Where ρ_i and ρ_o = indoor and outdoor air densities (kg/m^3)

g gravitational acceleration (m/s^2)

p pressure at the opening (Pa)

H vertical distance between the centre of inlet and outlet.

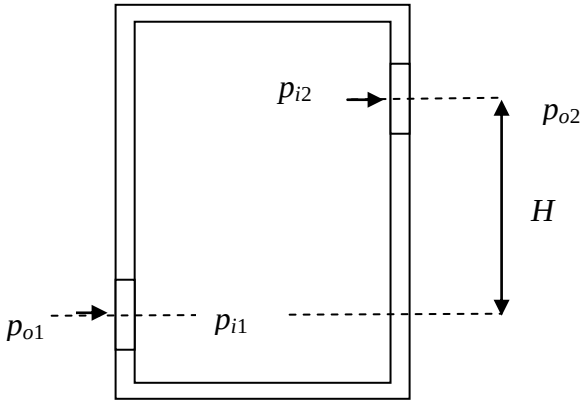

Figure 2.12 Natural ventilation through two openings by thermal buoyancy
(Terpager, 2003)

Figure 2.12 shows pressure differences between the indoor and outdoor at height *H* due to the heated air inside the building which has lower density than the air outside the building. Hence, the outdoor air enters via a lower inlet and indoor air exits at the higher outlet. $\Delta \rho gH$ is known as the quantity or the stack effect which creates the air movement between two openings (Terpager, 2003).

Designing such a ventilation system needs more attention due to the complicated thermal phenomena in these spaces. In hot-humid climates, using thermal buoyancy ventilation alone has an insignificant effect on the atrium space's thermal condition (Moosavi et al., 2014).

(iii) Mechanical Ventilation System

Mechanical Ventilation can change the airflow through the building by affecting the internal pressure. This system involves promoting air ventilation by using fans and air supply and extractor ducts. A well-designed and operated system will provide the thermal comfort and ventilation necessary for healthy and productive environments. The designer's understanding of this system is essential for effective mechanical system integration. The design criteria for mechanical ventilation systems are as follows (Chadderton, 2013):

1. Correct fresh air quality, minimum normally 10 l/s per person;
2. Avoidance of hot or cold draughts by design of the air inlet system;
3. Some manual control over air movement;
4. Mechanical ventilation to provide a minimum of air changes/h to ensure adequate flushing of all parts of rooms;
5. Air change rates that can be increased to remove solar and other heat gains;
6. Air cleanliness achieved by filtration of fresh air intake and re-circulated room air.

There are three basic sub-categories of mechanical ventilation systems (Chow, 2009):

- **Supply Mechanical Ventilation**: This system is supplied fresh air to the occupied space without extraction. The space is slightly pressurized and excess air flow through openings of the building's envelope. This kind of system maintains a positive pressure within the ventilation space. It can prevent infiltration and ingress

of extraneous materials thanks to an adequate oxygen supply, as shown in Figure 2.13.

- **Extract Mechanical Ventilation**: This system is the removal of contaminants, regardless of whether solid or thermal. The air in this system is extracted from the occupied area and replaced by outside fresh air. The space is not only kept at negative pressure, but helps in preventing the contaminants from spreading to adjoining spaces. Inlet and outlet openings in this system must not to be too close to each other, so as to avoid creating a short circuit.
- **Balanced Mechanical Ventilation**: This system is a combination use of supply and exhaust fans, which is more costly than the other two options. Large openings in the building envelope are not required for a close control of the environment. This system can be designed by two concepts:

  -A surplus of supplied air over extracted air, so as to maintain positive pressure within the building at a slightly higher level in order to minimize natural infiltration of untreated air into the area.

  -A deficiency of supply air with respect to air extraction to maintain a lower pressure of air than outside. So that any contaminant generated inside the space will not spread to the adjoining area.

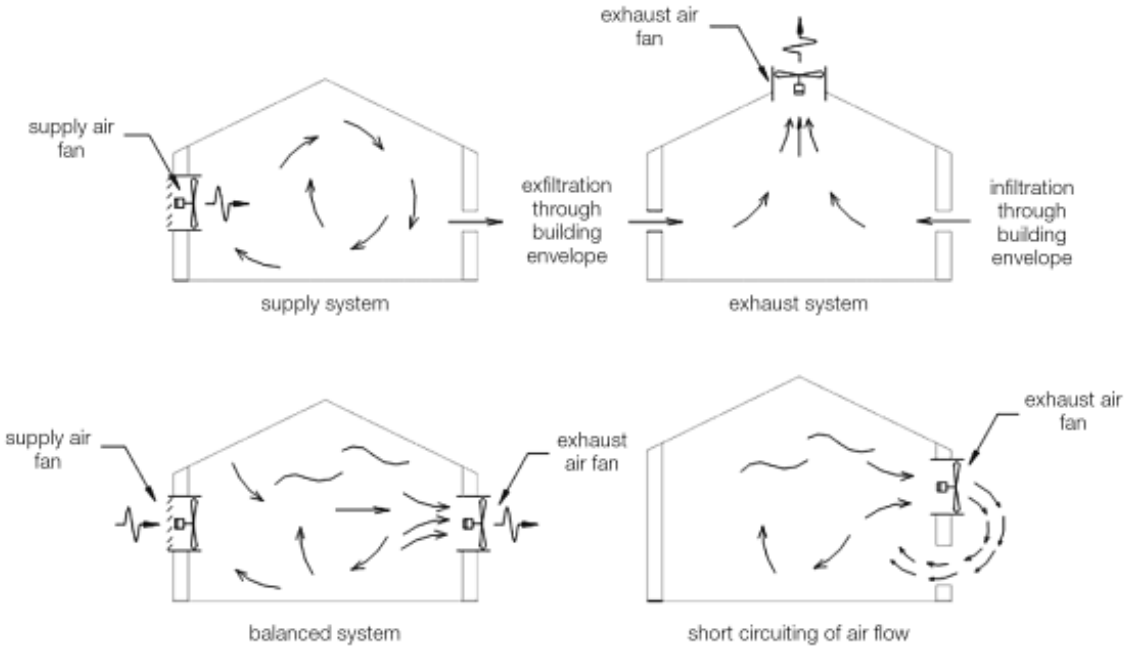

Figure 2.13 Mechanical ventilation systems (Chow, 2009)

The mechanical strategy can be used for a low-level displacement ventilation system required to supply natural ventilation (Chow,2009), as shown in Figure 2.14.

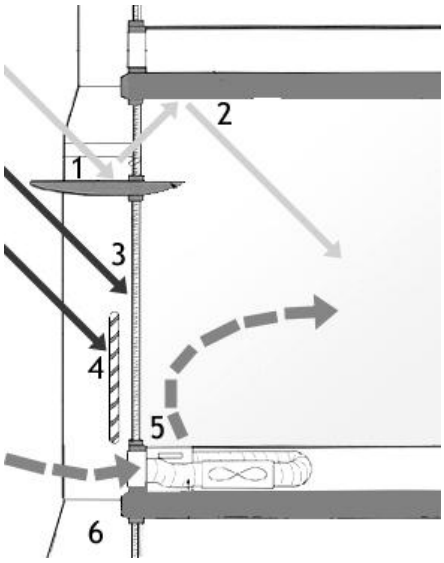

Figure 2.14 Lower-level displacement ventilation (CIBSE, 1997)

(iv) **Air-Conditioning Systems for Large Buildings in Hot-Humid Climates**

In tropical countries, air-conditioning systems are required primarily to cope with the high ambient temperatures to make working and living environmental conditions more tolerable. All air-conditioning systems involve the handing unit of air for cooling and dehumidifying. Ventilation air for occupancy has to be included in the design for maximum economy of cooling. This quality is usually kept to a minimum, depending on the numbers of occupants to be served. Thus, the circulated air in an air-conditioning system mostly exceeds the amount of external air brought in and exhausted (Oughton and Hodkinson, 2011).

Air-conditioning systems in large buildings are different from those used in typical smaller buildings due to larger buildings having a greater density of people, lighting and equipment. The major components for an air-conditioning system include chillers, air-handing units (AHUs), air terminal units (ATUs) and variable air volume equipment (VAV) (Sinopoli, 2010).

- **Chillers** utilize heat exchanges and circulate fluid or gas to cool the air that is passed through the air-conditioning unit. Chillers cool air by removing heat using a

vapour-compression cycle which is comprised of condensation, expansion, evaporation and compression (Figure 2.15).

Chillers' condensers remove heat from the system by evaporation, cooling water and cooling air. The water-cooled systems are used for large buildings, whereas air-cooled systems are more suited for cooling typical small buildings. Water is used to extract heat and then pumped to a cooling tower where the heat is rejected into the atmosphere and the water is then pumped back to the condenser.

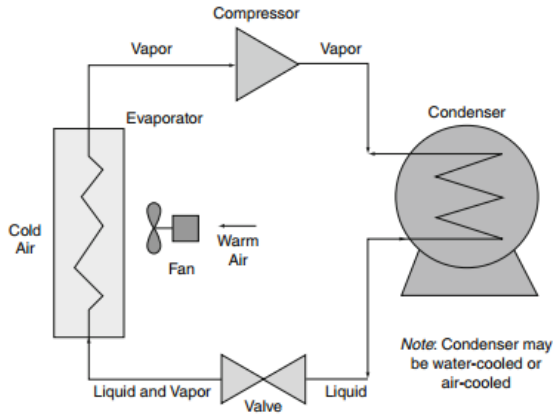

Figure 2.15 Vapour Compression Cycle (Sinopoli, 2010)

- **Air-Handing Units (AHUs)** provide cool air to different parts of a building, using chilled water to cool the air. The AHUs draw air in, pass the air over heating and cooling coils and then force it through air ducts. The AHUs have many of the networked points of the cooling comfort system (Figure 2. 16).

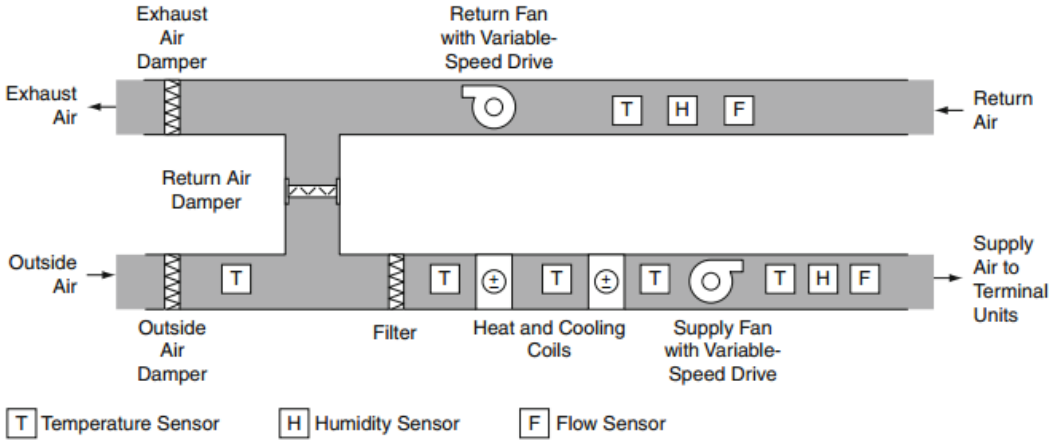

Figure 2.16 Typical AHUs (Sinopoli, 2010)

- **Air Terminal Units (*ATUs*)** address specific air-conditioned zones. Thermal loads in a space can be composed of external loads caused by outside air temperatures increasing or decreasing and internal loads from people, lighting and equipment. Defining air-conditioned zones in a building reduces the amount of air-conditioning subsystems needed. *ATUs* compensate for these thermal loads by varying the air temperature or varying the air volume; while constant air volume (*CAV*) systems provide air at a variable temperature and constant flow rate. Variable air volume (*VAV*) systems provide air at a constant temperature by changing the flow rate of the air into the room.

(v) Air-Conditioning System for Atria in Hot-Humid Climates

Using thermal buoyancy ventilation alone has an insignificant effect on the thermal condition of the atrium space (Moosavi et al., 2014), so additional air-conditioning systems would need to cool down the internal temperature to a comfortable level.

A development of the upward air distribution principle is an arrangement where both the supply and the extract positions are at the floor level. With this arrangement no false ceiling is necessary since all services may be from low level which is widely used in an atrium building. This system uses fan-assisted conditioning modules to filter, cool, and humidify re-circulated air; the units being either free-standing in the space served or incorporated into service zones. In most cases, they will be supplied with chilled and main water piping and with a power supply. A typical arrangement of such a system is illustrated in Figure 2.17 (Oughton and Hodkinson, 2011).

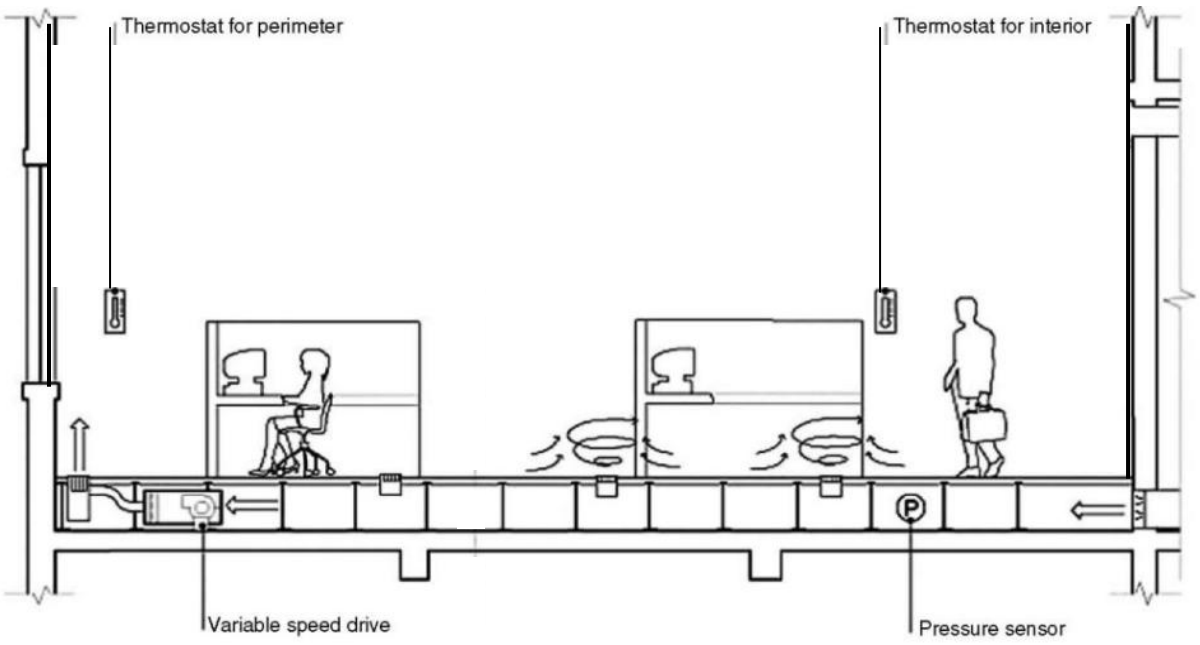

Figure 2.17 Typical upward air-flow arrangement (Oughton and Hodkinson, 2011)

2.6 Theories of Light and Heat Energy

Solar radiation penetrates through atria or large glazed pedestrian concourses not only providing daylight but also creating thermal stratification, which is the most significant factor of discomfort in these buildings in the tropics.

2.6.1 Principle of Sun Light and Day Lighting

Sun light is one kind of energy. Electromagnetic radiation emitted by sun is composed of parts of the spectrum (Figure 2.18). They include ultraviolet radiation (*UVR*), gamma rays, X-rays, visible light, infra-red radiation and radio waves. Gamma rays, X-rays and very short wavelength *UVR* are absorbed by gases in the upper atmosphere. Infra-red radiation can be felt as heat; visible light can be seen as light (Ashley, 2001).

The different parts of the spectrum are referred to as energy bands and are characterized by varying wavelengths. *UVR* comprises the following different wavelength ranges (Greenwood, Soulos and Thomas, 2013):

- *UVA* ultraviolet with wavelengths between 315 and 400 nanometres (nm.);
- *UVB* ultraviolet with wavelengths between 280 and 315 nm. ;
- *UVC* ultraviolet with wavelengths between 100 and 280 nm. ;

- Visible spectrum (light) with wavelengths between 400 and 760 nm. ;

- Infrared (heat) with wavelengths between 760 and 900 nm.

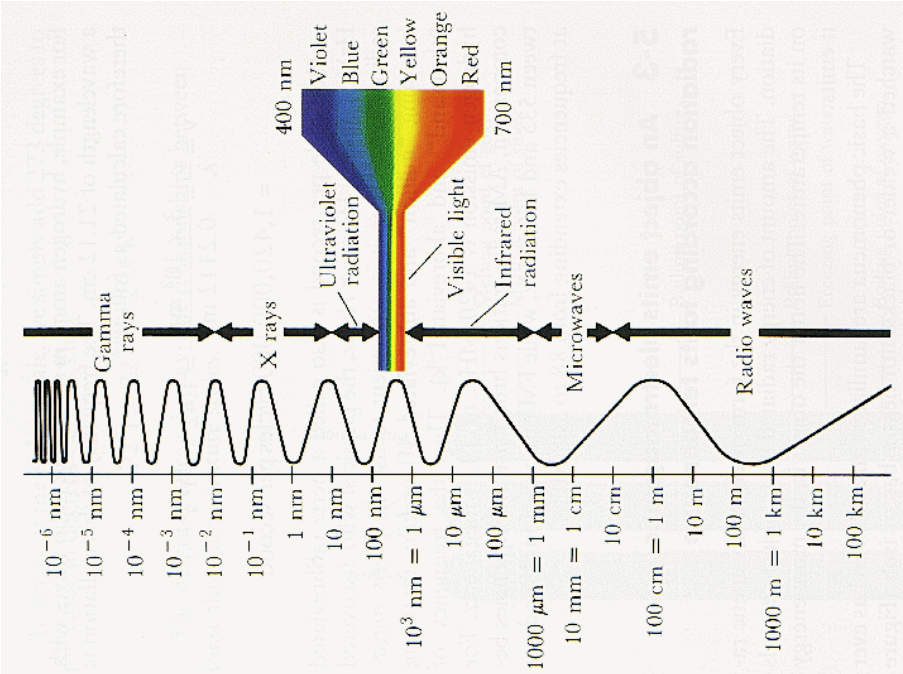

Figure 2.18 Solar spectrums (Ashley, 2001)

Luminance is the amount of light coming from a light source with a given direction per unit area. Luminance unit is cd/m^2. The sun has luminance at noon around 1.6x10^9 cd/m^2 (Pode and Diouf, 2011).

Illuminance is the amount of light incident per unit surface area. Illuminance can be calculated as follows:

$$E = d\Phi / dA \qquad (2.5)$$

Where E = Illuminance

$d\Phi$ = Luminance flux incident on a given surface element,

dA = Area of the surface element.

The unit is the lumen/m^2 or lux. The minimum recommendations of illuminance levels for specific tasks and interiors are stated in the CIBSE Lighting Guide (CIBSE, 1999).

Activity	Illumination (lux)
Walkways	20–50
Corridors	100–150
Warehouses	150
Basic office work	250
Continuous reading	500
Supermarkets	750
Mechanical workshop	1,000
Detailed drawing work	1,500–2,000
Short time small size detailed work	2,000–5,000
High detailed task on long periods	5,000–10,000

Table 2.2 Average illuminance required for different tasks (CIBSE, 1999)

2.6.2 Solar Geometry

The sun's apparent position over this celestial dome is defined by these two angles, as shown in Figure 2.19. For effective shading device design, a designer needs to know the solar azimuth angle and the solar altitude angle for admitting or blocking the sun (Greenwood, Soulos and Thomas, 2013).

(i) **Solar Azimuth Angle (*AZI*)**

The azimuth determines the direction of shadow which will fall on the ground. It is the horizontal plane angle between the direction of the sun and true north, measured clockwise from 0^o to 360^o from true north. The azimuth at solar noon in the southern hemisphere is always 0^o.

(ii) **Solar Altitude Angle (*ALT*)**

The solar altitude is the angle between the sun and the horizon of a solid object on the ground. It determines the length of the shadow cast by that object. It varies according to the time of the day and season.

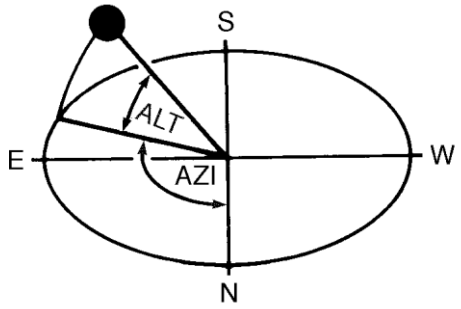

Figure 2.19 Definitions of solar position angles (PLEA, 2007)

The zenith angle (*ZEN*) is measured between the sun's direction and the vertical and it is a supplementary angle of the altitude:

$$ZEN = 90^{o} - ALT \qquad (2.6)$$

The hour angle (*HRA*) expresses the time of day with respect to the solar noon: it is the angular distance, measured within the plane of the sun's apparent path, as shown in Figure 2.20.

$$HRA = 15 * (h-12) \qquad (2.7)$$

h = the hour considered (24 hour clock)

e.g: for 9 am: $HRA = 15*(9-12) = -45^{o}$

but: for 2 pm: $HRA = 15*(14-12) = +30^{o}$

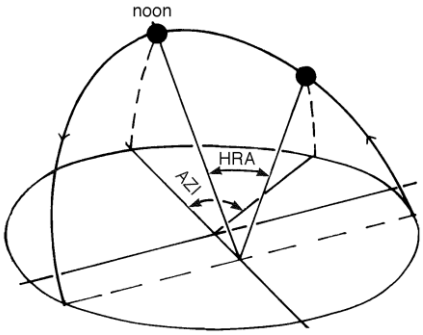

Figure 2.20 Definitions of hour angles (HRA) (PLEA, 2007)

2.6.3 The Earth and Sun Relations

Watson, Crobie and Callender (1997) stated that the earth's revolution is referred to as the ecliptic. The earth's axis of rotation is tilted 23.45^{o} from the normal to the plane of the ecliptic. The angle between the earth's equator and the ecliptic (the earth - sun line) is the declination (DEC) and it varies between+23.45° on June 22 (northern solstice) and -23.45°

on December 22 (southern solstice), as shown in Figure 2.21. On equinox days (approximately March 22 and September 22) the earth—sun line is within the plane of the equator, thus DEC = 0°. The variation of this declination is shown by a sinusoidal curve as shown in Figure 2.22.

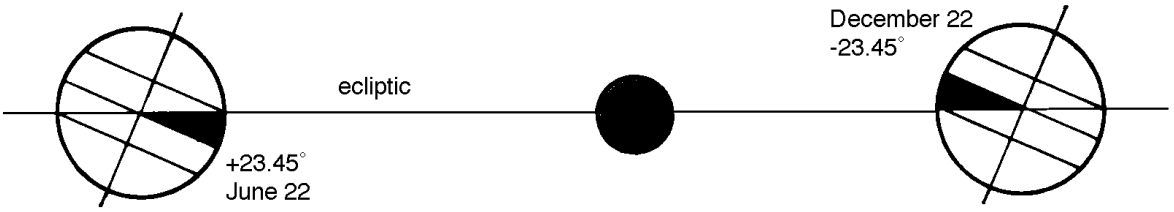

Figure 2.21 Section of the earth's orbit (Watson, Crobie and Callender, 1997)

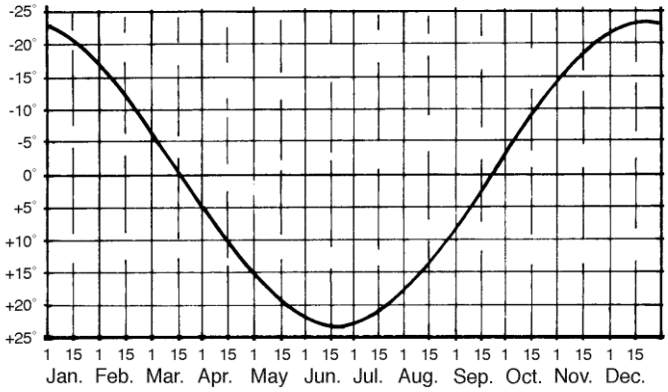

Figure 2.22 Annual variation of declination (Mean of the Leap-Year Cycle) (Watson, Crobie and Callender, 1997)

The longitude of the site affects the solar time, while the latitude affects the position of the sun in the sky and the time of sun rise and sun set. The lower latitude countries in the tropics do not want excessive heating from the sun while the higher latitude countries in a temperate climate welcome the sun's warmth during the winter months. Both of these points are the first factors that designers have to be concerned about (You et al., 1993).

2.6.4 Architectural Design in Tropical Climates for Daylighting

The sun contributes about 8,000 to 10,000 foot-candles of light on a clear and bright day. There is almost always adequate light available from the sun and sky to provide illumination for most human vision. Due to constantly changing cloud cover, the amount of illumination varies from time to time. Nevertheless, a designer should be aware of a range

of expected daylight conditions based on the sun's behaviour at particular area or time (Philip, 2010).

In hot-humid climates, designers must imagine buildings that not only collect energy from the sun to provide lighting, but also prevent heat energy build-up which can lead to overheating of the building. Sunlight can be used as a complementary source to light interior space. On the other hand, too much sunlight will lead to excessive solar heating (Fosdick, 2012).

For effective daylighting, designers should consider (Ander, 2014):

- Taking benefit of daylight as much as possible;
- Maintaining a uniform distribution of daylight in the whole area;
- Avoiding visual discomfort and glare.

Atria or large glazed pedestrian concourses are designed with large glass facades to allow maximum sunlight penetration into the buildings. Sunlight can be used as a complement to artificial lighting depending on the function of the buildings. The amount of daylighting in building can be controlled through the actual design structure of the building itself. The main methods of designers to control the effect of the sun on the building are by the orientation of the building and the overall design structure layout (LANL, 2002).

As mentioned earlier, natural lighting is variable and for design purposes, the design measure used is the Daylight Factor. This is the percentage of the horizontal diffused external illuminance from sky which is received at an internal point. The Average Daylight Factor (DF) can be calculated from the following formula (DfEE, 1999):

$$Average\ DF = \frac{W}{A}\ \frac{T\theta}{(1-R^2)} \qquad (2.8)$$

Where: W is the area of the windows (m^2)

A is the total area of the internal surfaces (m^2)

T is the glass transmittance corrected for dirt

θ is visible sky angle in degrees from the centre of the window

R is the average reflectance of area A.

Interiors with an average daylight factor of 5% or more are considered to be a day-lit room and not requiring artificial lighting. Interiors with an average daylight factor of between 2% and 5% will require some artificial lighting; whereas interiors where the average daylight factor is below 2% will need frequent use of artificial lighting (DfEE, 1999).

2.6.5 Principle of Heat Energy Flows in Buildings

Heat is a form of energy, which can be converted into other forms of energy such as electricity. Heat energy also can be stored in building materials with a high thermal capacity. There are 2 types of heat energy as follows (Tang and Chin, 2013):

- **Sensible heat** is heat energy which a substance absorbs. In building science, any object that causes a temperature rise is sensible heat such as occupants, lighting, solar radiation through building envelopes, etc.
- **Latent heat** is heat energy which causes the change of phase of a substance from one stage to another stage. In building science, latent heat occurs when moisture is added to the space from internal sources such as vapour emitted by occupants and from external sources such as air infiltration.

Heat energy can be transferred from one body to another by conduction, convection and radiation. Heat gain or heat loss by a building refers to the transfer of heat from the outside through all surfaces of the building into its inside. Heat transfer is classified into 3 mechanisms (Straube, 2006):

- **Conduction** is the heat flow through a solid material, such as buildings' walls and window frames. In building science, conduction heat transfer is represented by the U-value of building materials. While thermal resistance is represented by the R-value (Vassigh, Ozer and Spiegelhater, 2013).

$$R = 1/U \qquad (2.9)$$

- **Convection** is heat transfer from one place to another place by air movement.
- **Radiation** is heat transfer by the emission of electromagnetic waves through space.

Thermal stratification was initially investigated in environmental areas such as the indoor air volume of buildings with high ceilings. Stratification in atria or large glazed pedestrian concourse occurs when solar energy transfers into an enclosed building causing hot air to

rise, and the stratification of the medium results in the hotter, lighter fluid overlaying the colder, heavier fluid. The fluid flow that results from the heat loss from the heated body rises above it as a buoyant flow (Ashley, 2001).

2.7 Thermal Comfort

Human thermal comfort is the main purpose of dealing with thermal comfort. There is heat transfer between a human body's heat generation and the release of body heat into its surrounding environment. A thermal balance between them is simplified as the condition of thermal comfort. Thermal comfort is an important requirement in architectural design, as it can improve the health and mental performance of occupants of buildings (Roaf, Chrichton and Nicol, 2009).

2.7.1 Factors Affecting Thermal Comfort

The factors affecting thermal comfort according to CIBSE (2008) are as follows:

- **Temperatures** are composed of the room air temperature and mean radiant temperature which can be combined as the operative temperature.
- **Air Movement** is the net mean air speed across the body. Where air speeds in a room are greater than 0.15 $m \cdot s^{-1}$ the operative temperature should be increased from its 'still air' value to compensate for the cooling effect of the air movement.
- **Humidity is** the amount of water vapor in the air. Humidity has little effect on feelings of warmth unless the skin is damp with sweat. So the influence of humidity on warmth in moderate thermal environments may be ignored for most practical purposes. Humidity in the range 40–70 % RH is generally acceptable.
- **Metabolic heat production** is largely dependent on activity and the unit used to express this activity is the met, where 1 met = 58.2 $W \cdot m^{-2}$. Table 2.3 shows metabolic rates for specific activities.

Activities	Metabolic (M) rate/met	Heat generation /W· m^2
Resting:		
— sleeping	0.7	41
— reclining	0.8	46
— seated, quiet	1.0	58
— standing, relaxed	1.2	70
Walking (on level):		
— 0.9 m·s^{-1}	2.0	116
— 1.3 m·s^{-1}	2.6	151
— 1.8 m·s^{-1}	3.8	221
Office work:		
— reading, seated	1.0	58
— writing	1.0	58
— typing	1.1	64
— filing, seated	1.2	70
— filing, standing	1.4	81
— lifting/packing	2.1	122
Occupational:		
— cooking	1.4–2.	81–134
— house cleaning	1.7–3.	99–198
— seated, heavy limb movement	2.2	128
— machine sawing	1.8	105
— light machine work	1.6–2.0	93–116
— heavy machine work	3.0	175
— handling 50 kg bags	4.0	233
Leisure:		
— dancing (social)	1.4–4.4	82–256
— calisthenics/exercise	3.0–4.0 1	175–233
— tennis (singles)	3.6–4.0 2	210–233
— basketball	5.0–7.6	291–442
— wrestling (competitive)	7.0–8.7	407–506

Table 2.3 Metabolic rate and heat generation per unit area for various activities (CIBSE, 2008)

- **Clothing** is the unit for thermal insulation of clothing, where 1 clo = 0.15m^2·K·W^{-1}. Clothing insulation values for typical clothing groups are shown in Table 2.4.

Clothing combination	*Icl* (clo)*	*Fcl*
Nude	0	1.0
Shorts	0.1	1.0
Light summer clothing	0.5	1.1
Light working ensemble	0.6	1.1
Typical business suit	1.0	1.15
Typical business suit and cotton coat	1.5	1.15
Light outdoor sport wear	0.9	1.15
Heavy traditional European suit	1.5	1.15-1.2
Heavy wool pile ensemble	3-4	1.3-1.5

Table 2.4 Clothing insulation values for typical clothing groups (CIBSE, 2006)

2.7.2 Psychometrics Chart

A psychometric chart illustrates physical and thermal properties of moist air in a graphical form. Psychometric properties are dependent on the atmospheric pressure, so their determination at different elevations is filled with errors that may be considerable at higher

altitudes. Psychometric charts developed for specific atmospheric conditions eliminate errors but lack general applicability. Psychometric charts are printed mostly for sea level atmospheric pressure. Since virtually all psychometric air processes involving HVAC design occur within a 0^{o}C and 50^{o}C range, most psychometric charts only show this range as a practical measure. Psychometric properties are also available as data tables, equations, and slide rulers.

The psychometric chart that pertains to those conditions of dry bulb temperature, wet-bulb temperature, relative humidity etc. in which most people wearing specified cloths and involved in specific activity will feel comfortable, i.e., neither too cold nor too warm. Figure 2.23 present the range of operative temperature for 80% occupant acceptability used in computer model method. It is permissible to apply to spaces where the occupants have activity levels that result in average metabolic rates between 1.0 and 2.0 met. Thermal insulation of clothing is provided 1.5 clo or less of thermal insulation. The comfort zone is defined by the combinations of the five key factors; the air temperature and mean radiant temperature, applicable metabolic rate, clothing insulation, air speed, and humidity. Use of the PMV model in this standard is limited to air speeds below 0.20 m/s (40 fpm). It is acceptable to use air speeds greater than this to increase the upper temperature limits of the comfort zone in certain circumstances (ASHRAE, 2010).

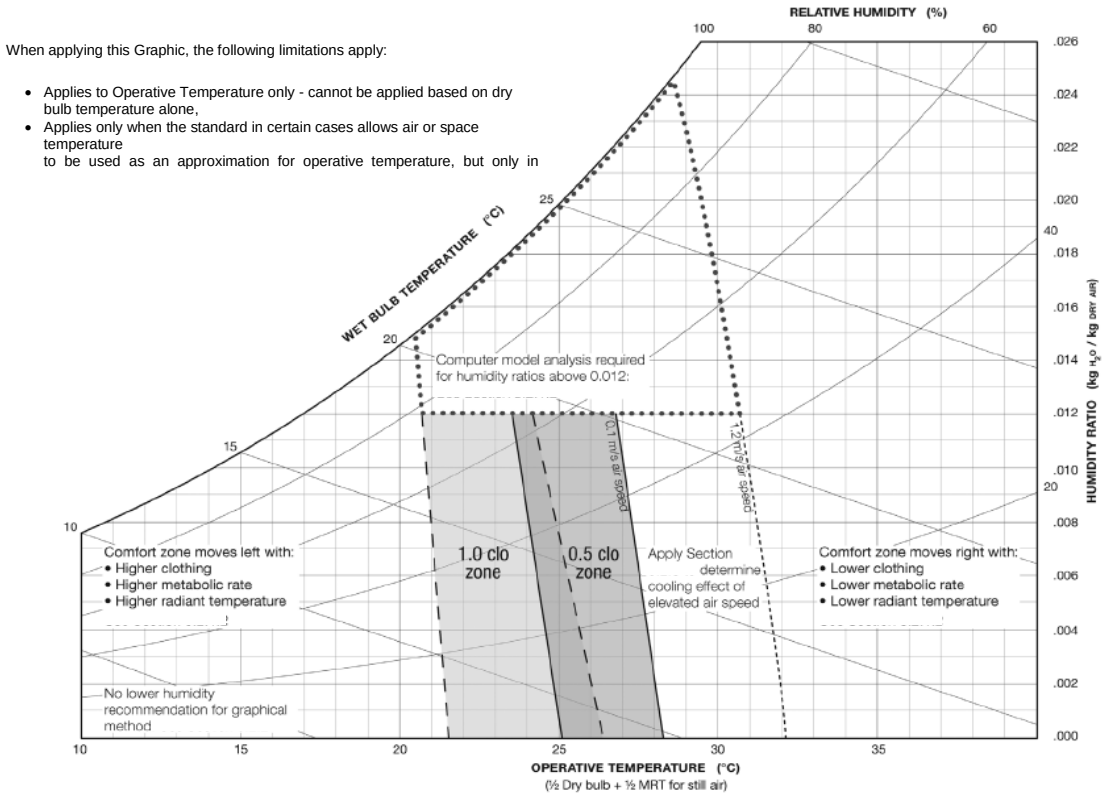

Figure 2.23 Psychometric chart: Acceptable range of operative temperature and humidity (ASHRAE, 2010)

2.7.3 Define Thermal Comfort

Thermal comfort standards are required to help building designers provide an internal building climate that occupants can find thermally comfortable (Nicol and Humphreys, 2002). Although there are several thermal comfort models for qualitatively investigating thermal comfort conditions, the following 3 basic thermal comfort models are internationally recognized by ASHRAE and ISO Standards (Tang and Chin, 2013).

- **Fanger's (1970) PMV Comfort Model**: Theory of Predicted Mean Vote (PMV) and the index of Predicted Percent of Dissatisfied by Fanger are the most popular (Santamouris and Asimakopolous, 1996).

Thermal sensation	Index value
Hot	+3
Warm	+2
Slightly warm	+1
Neutral	0
Slightly cool	–1
Cool	–2
Cold	–3

Table 2.5 Thermal sensation scale (CIBSE, 2008)

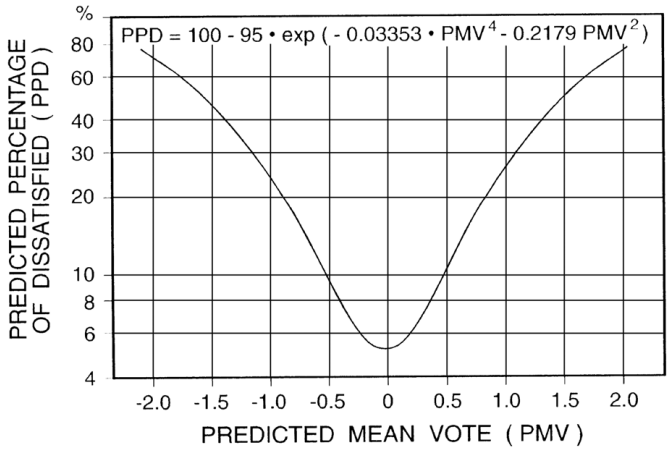

Figure 2.24 Predicted Percentage of Dissatisfied (PPD) as a function of Predicted Mean Vote (PMV) (ASHRAE, 2004)

The percentage of people dissatisfied (i.e. voting -3,-2, +2, or +3) can be estimated by the thermal environment at various temperature conditions. Results of various research initiatives led to a relationship between PMV and PPD as shown in Table 2.6.

The PMV model is derived from the air temperature and mean radiant temperature in question along with the applicable humidity, air speed, metabolic rate and clothing insulation. If the resulting PMV value generated by the model is within the recommended range, the conditions are within the comfort zone (ASHRAE, 2004).

PPD	PMV Range
<10	-0.5 <PMV< +0.5

Table 2.6 Acceptable Thermal Environment for General Comfort (ASHRAE, 2004)

- **Thermal Adaptive Comfort Model**: Recently international standards, such as ASHRAE 55-2004 and the European Standard EN 15251, have recognized the possibility that the thermal comfort temperature can vary with changing external conditions. The theory of adaptive comfort is based on the adaptive principle which stated that 'people in general are naturally adaptable'. If a change occurs to produce discomfort, people always react in the way which tends to restore their comfort (Nicol, and Humphry, 1972).

  A number of equations of comfort temperature have been developed by researchers based on field studies in free running buildings in warm climates as follows:

  Humphreys has found that the comfort temperature can be obtained from the mean outdoor temperature with Equation 2.10 (Feriadi and Wong 2004).

$$Tc = 0.53\ To + 11.9 \qquad (2.10)$$

  Auliciems revised Humphreys equation by deleting some fields studies, such those with children as the subjects, and adding more information from other studies not included by Humphreys. These revisions increased the database to 53 separate field studies in various climatic zones covering more countries and more climates. After combining the data for naturally ventilated buildings and air-conditioned buildings, the analysis led to an equation involving the outdoors air temperature (*To*) and the indoor air temperature (*Ti*), this resulting equation is Equation 2.11:

$$Tc = 0.48Ti + 0.14To + 9.22 \qquad (2.11)$$

  Auliciems has also proposed a single line for all buildings, which covered the naturally ventilated buildings and air-conditioned buildings. This relationship is given by Equation 2.12

$$Tc = 0.31To + 17.6 \qquad (2.12)$$

Nicol has conducted several surveys under different climatic conditions. In a first survey by Nicol in Pakistan, he established a relation between comfort temperature and outdoor temperature given by Equation 2.13 (Bouden and Ghrab, 2005).

$$Tc = 0.38To + 17.0 \qquad (2.13)$$

In a second survey by Nicol in Pakistan, he found a second regression given by Equation 2.14.

$$T_c = 0.36T_O + 18.5 \qquad (2.14)$$

- **Operative Temperature Model**: The operative temperature combines the simply air temperature and the mean temperature, which is the average surface temperature of the surrounding walls, into a single value to express their effect. CIBSE Guide A (2006) gives general guidance and recommendations on suitable summer and winter temperature ranges (Appendix A).

  Operative temperature (T_o) combines the air temperature (T_a) and the mean radiant temperature (T_r) into a single value. It is a weighted average of the heat transfer coefficients by convection (h_c) and by radiation (h_r) at the cloth surface of the occupant (ASHRAE, 1992).

  The operative temperature is defined as:

$$T_o = \frac{(h_c T_i + h_r T_r)}{(h_c + h_r)} \qquad (2.15)$$

  where T_o is the operative temperature (^oC);

  T_i is the indoor air temperature (^oC);

  T_r is the mean radiant temperature (^oC);

  h_c is the surface heat transfer coefficients by convection ($W \cdot m^{-2} \cdot K^{-1}$);

  h_r is the surface heat transfer coefficient by radiation ($W \cdot m^{-2} \cdot K^{-1}$).

  Researchers have differed in their estimates of the values of these heat transfer coefficients. In this method the value of $\sqrt{10v}$, where v is the air speed ($m \cdot s^{-1}$) is retained for the ratio of h_c to h_r and so:

$$T_o = \frac{(T_r + (T_a \times \sqrt{10v}))}{1+\sqrt{10v}} \quad (2.16)$$

Indoor air speed is assumed to be equivalent to v =0.10 $m \cdot s^{-1}$ and equation 2.16 becomes:

$$T_o = \frac{T_a + T_r}{2} \quad (2.17)$$

Roaf et al., (2009) state that one method has been widely used to express the condition of 'comfortable'; this takes a group of subjects who are going about their normal everyday lives and asks them how hot they feel on a scale. The thermal sensation is classified in a seven-point scale as the subjects' rating responses for environmental thermal comfort. This will be explained further in chapter 5.

2.7.4 Thermal Comfort Criteria for Tropical Climates

There are some thermal comfort studies done in hot-humid climate countries, which have been conducted in the area of energy conservation to find means to provide comfortable interior environments.

The ASHRAE Standard 55 (1992) gave the purposed natural temperature of thermal comfort as 23-26^{o}C (Table 2.7), while, the CIBSE Guide A (2006) recommended comfort criteria for air conditioned passenger lounge in any airport terminals between 22-24^{o}C. However, many studies have concluded that the comfort temperature is higher in a hot-humid climate.

Season	Optimum Temperature [a]	Acceptable Temperature Range [a]	Assumption for other PMV Input [b]
winter	22°C	20-23°C	-relative humidity: 50% -mean relative velocity:<0.15m/s -mean radiant temperature: equal to air temperature -metabolic rate: 1.2 met -clothing insulation: 9.9 clo
summer	24.5°C	23-26°C	-relative humidity: 50% -mean relative velocity:<0.15m/s -mean radiant temperature: equal to air temperature -metabolic rate: 1.2 met -clothing insulation: 9.9 clo

a: refer to operative temperature, defined as *"the uniform temperature of an imaginary black enclosure in which an occupant would exchange the same amount of heat by radiation plus convection as in the actual non-uniform environment."*
b: if the value of these assumptions differ, refer to the comfort zone diagrams and tables given in ASHRAE standard 55, for appropriate temperature ranges.

Table 2.7 Thermal comfort condition (ASHRAE, 1992)

In Thailand, Busch (1992) has reviewed thermal comfort with over 1100 office workers in both air-conditioned and naturally ventilated offices in Bangkok. From the field study, it found that the upper temperature boundary for a Thai comfort standard, instead of being the currently accepted level of 26.1°C for those accustomed to air-conditioning and naturally ventilated interior spaces, was as high as 28°C for those accustomed to air-conditioning, and 31°C in naturally ventilated buildings.

Moreover, a large thermal comfort survey, using 1520 Thai volunteers in different types of air-conditioned buildings from private and public sectors, pointed out that the highest thermal acceptability of comfort condition for Thais was 27.4°C for Bangkok (Yamtraipat, Khedari and Hirunlabh, 2005). In addition, another field study by Rangsiraksa (2006) showed that the comfort temperatures for Thai people in residential building are 25°C, with the range of 22.°C to 27.5°C, for air-conditioned buildings and 28°C, with the range 25.5°C to 30.5°C, for naturally ventilated buildings during the summer season.

In China, Yang and Zhang (2008) conducted a thermal comfort field study in the humid subtropical climates in China with 229 occupants from 111 buildings. The assessment reveals that people tended to be more tolerant of hot temperatures than another people from

temperate climates. Preferred temperatures were 27.9^{o}C in natural ventilation and 27.3^{o}C in air-conditioned buildings. Han et al., (2007) revealed that the operative temperature denoting the thermal environment accepted by 90% of occupants is 22.0^{o}C~25.9^{o}C for residences in hot-climates in China. Zhang et al. (2010) reviewed thermal comfort in naturally ventilated buildings, concluding the 90% acceptable range was from 23.5 ~ 27.4^{o}C.

Results of the studies indicate that people in hot-humid climates are acclimatized to much higher temperature levels than the thermal comfort range proposed by ASHRAE Standard 55 (Tantasavasdi, Srebric and Chen, 2001). Therefore adopting the ASHRAE standard for indoor comfort conditions may lead to overcooling and energy waste for hot-humid climates.

A large glazed pedestrian concourse is normally use as a transitional space. Interaction between the large glazed enclosure and unfavourable outdoor environment is the primary contribution to interior thermal discomfort in atrium buildings. Therefore, in order to provide thermal comfort in the atrium spaces, a higher thermal comfort range for the tropical climate countries compared to the thermal comfort range proposed by international standards at 22.0~27.5^{o}C as defined by Rangsiraksa (2006).

The operative temperature is the most useful indicator of thermal comfort in buildings. As mentioned on scope of study in chapter 1, the Guangzhou International Textile City design is intended to facilitate international commercial activities related to the textile industry, while Suvarnabhumi Airport Terminal serves both domestic and international passenger. In order to assess thermal comfort in those spaces, thus the recommended operative temperatures for international thermal comfort criteria of The ASHRAE Standard 55 (1992) and the CIBSE (2006) were chosen in this research. Even though, there were arguments from previous researches that these conditions may lead to overcooling and energy waste for hot-humid climates.

2.8 Post-Occupancy Evaluation

Historically, post-occupancy evaluation (POE) was developed to evaluate actual building performance, providing feedback for a building's manager and designer to improve the quality and operation of the building by gathering information based on user satisfaction

(Deuble and John De Dear, 2014). Presently, a range of POE methods have been developed which has demonstrated a huge potential not only to improve the comfort and productivity of a building's occupants, but also to reduce the financial and environment costs and impacts of buildings. The POE typically includes a survey of user satisfaction with the chosen building, an analysis of the energy consumption and information about physical operating circumstances (Nicol and Roaf, 2005). POEs are usually carried out after the completed project for a period of at least 12 months and can include both objective and subjective techniques such as questionnaires, interviews, focus groups, observation, documentation audits and technical monitoring. Ideally, stakeholders should be involved in order to provide a holistic picture of the successes and shortcoming of the project (Morrison, 2008).

The POE process model was developed in three complementary versions as follows (Preiser, 1995):

- **Indicative POEs** are quick, walk through evaluations. They involve interviews with key personnel with both positive and negative aspects of building performance.
- **Investigative POEs** are more in-depth. They utilize interviews and questionnaires, in addition to photographic evidence and physical measurements.
- **Diagnostic POEs** are focused, longitudinal and cross-sectional evaluation studies of such performance aspects as physical environment, lighting, etc.

POE techniques are available worldwide with their effectiveness dependent upon the following (Preiser, 2002):

- Giving results which can be comparable with previous studies;
- The time and patience of respondents are not encroached too much;
- It offers value in terms of quality and content;
- It is relevant in a given situation;
- It is reliable by giving similar results when used by different people within similar circumstances;
- It addresses factors related to the needs, activities and goals of the building users.

A generally common set of problems in building performance is outlined as follow (Preiser, 1995):

- Health and safety problems;
- Security problems;
- Leakage;
- Poor signage and way finding problems;
- Poor air circulation and temperature control;
- Handicapped accessibility problems;
- Lack of storage;
- Maintainability of glass surfaces such as skywalks or inaccessible skylights.

The value of POE can be seen from a number of different perspectives, particularly those of architectural professionals and facilities managers (Riley, Moody and Pitt, 2009). POE is a way of providing feedback throughout a building's lifecycle from initial concept through to occupation; the data from which can be used for informing future projects. The benefits of POE for designer and facility manager are as follows (Barlex, 2006):

- **Short term benefits of POE**
  These include user feedback and identification of appropriate solutions to problems in buildings;
- **Medium term benefits of POE**
  These include built-in capacity for building adaptation to organizational change and growth;
- **Longer term benefits of POE**
  These are aimed at the creation of databases for long-term improvements in building performance and in design quality.

2.9 Degree-Days

Degree days are tools that can be used in the assessment and analysis of weather related energy consumption in buildings. Degree-days are essentially the summation of temperature differences over time, and hence they capture both extremity and duration of external temperatures. The temperature difference is between a reference temperature (base temperature) and the outdoor air temperature. The reference temperature is known as the base temperature which, for buildings, is a balance point temperature, i.e. the external

temperature at which the heating (or cooling) systems do not need to run in order to maintain comfortable conditions (CIBSE, 2006).

A key issue is heating and cooling energy consumption tends to depend on the external air temperature around the building. There are 2 types of degree-days: heating degree-days (*HDD*) are used for calculations that relate to the heating of building and cooling degree-days (CDD) are used for calculations energy used for air-conditioning. Calculation methods are simple and accurate. Equation 2.16 shows the general formula for this process for heating degree-days (ASHRAE, 2001):

$$HDD = (1 \text{ day}) \sum_{\text{days}} (T_b - T_m)^+ \qquad (2.16)$$

For cooling degree-days this simply becomes:

$$CDD = (1 \text{ day}) \sum_{\text{days}} (T_m - T_b)^+ \qquad (2.17)$$

Where T_b = the base temperature,

T_m = the daily mean outdoor temperature,

The annual heating or cooling requirements can be calculated using HDD and CDD, respectively as:

$$Q_h = \frac{K_{tot}}{\eta} \text{ HDD } \frac{24}{1000} \qquad (2.18)$$

$$Q_c = \frac{K_{tot}}{\eta} \text{ CDD } \frac{24}{1000} \qquad (2.19)$$

where Q_h = the annual heating requirements (kWh),

Q_c = the annual cooling requirements (kWh),

K_{tot} = the total heat-transfer coefficient of the building in W/°C,

η = the efficiency of the heating or cooling system.

Traditionally, cooling degree-days are calculated at a base temperature of 18°C for a typical building (Kreider and Rabl, 1994).

2.10 The Economic Evaluation of Investment Proposals

Economic evaluation is vital in investment decisions which take time to mature, and have to be based on the returns which that investment will make. If the investment is unprofitable in the long run, it is unwise to invest in that project unless it is for social reasons only (Carter et al., 1997).

Economic evaluation is needed to allow comparisons to be made between competing project alternatives. Three common methods of comparison are currently in widespread use: the depreciated payback period method (*DPP*), the net present value method (*NPV*) and the internal rate of return method (*IRR*) (Nikolaidis et al., 2009).

(i) The Discounted Payback Period (*DPP*)

The payback period (*PP*) is often used as the first screening method; it was noted that a variation called the discounted payback period (*DPP*) improved this approach. *DPP* recognizes the time value of money. *DPP* means 'the time it takes the cash inflows from the initial investment project to recover the cash outflows in years'. When deciding between two or more competing projects, the decision is normally to accept the one with the shortest payback. The formula used to calculate the *DPP* is:

$$DPP = \frac{-\ln\left(1-\frac{p'C_o}{F_t}\right)}{\ln(1+p)} \qquad (2.18)$$

Where: C_o = the initial investment, startup cost

p = the cost of capital

F_t = the net cash flow which is assumed to be constant for every t.

(ii) The Net Present Value (*NPV*)

The NPV method is used for evaluating the desirability of investments or projects. This method is based upon the concept that money today is worth more than money in the future. The discount rate, as with interest rates, is the mechanism that equates today's dollar with its value in the future.

For an investment to be cost beneficial, it must return more income in the future than the amount of investment in the present. The formula for *NPV* is:

$$NPV = -C_0 + \sum_{t=1}^{n} \frac{F_t}{(1+p)^t} \quad \text{and} \quad F_t = B_t + C_t \qquad (2.19)$$

Where; t = the time period (year),

F_t = the net cash flow at year t,

B_t = the benefit (inflows) for year t,

C_t = the cost (outflows) for year t,

C_o = the initial investment,

p = the cost of capital,

n = the number of years of the investment's lifetime

A project is deemed profitable if its net present value is greater than zero. In case alternative investments are compared, the best of them would be the one with the higher *NPV*. When *NPV* is greater than zero a project is sufficient to:

- pay of the initial start-up cost;
- pay off interest payment to creditors who lent the company money to pay for the start-up cost;
- provide the required return to shareholders or to meet a company's financial requirements;
- increase economic value in the company.

The *NPV* is a very useful method since it is a direct project's profitability measurement and most directly related to a company's monetary value. Traditionally, *NPV* is one of the strongest economic evaluation indicators, because it has few limitations and can be used in all type of analyses (Alkaraan and Northcott, 2006).

(iii) Internal Rate of Return (*IRR*)

The Internal Rate of Return (*IRR*) method is another evaluation technique used in decision making. The purpose of this method is to determine the interest rate (r) at which *NPV* is

equal to zero. If that rate exceeds the hurdle rate (defined as the minimum acceptable rate of return on a project), this project is deemed worthy of funding. The formula for *IRR* is:

$$NPV = -C_0 + \sum_{t=1}^{n} \frac{F_t}{(1+p)^t} = 0 \qquad (2.20)$$

IRR is usually calculated through trial and error; where different interest rates are tried until the *IRR* is found. A given project might have a lower *NPV* but a higher *IRR* than an alternative project. The problem arises because the *IRR* is the implied reinvestment rate for cash flows under the *IRR* method. The discount rate used in the *NPV* method is a cost of capital. In case the *IRR* for a project is very different from the actual situation, reinvestment of cash flows at a rate close to the cost of capital is more realistic. Therefore, utilization of the *NPV* technique is generally superior (U.S. Environmental Protection Agency, 2001).

2.11 Overview of Dynamic Thermal and Lighting Simulation Programmes

Nowadays there are many thermal and lighting simulation programmes available. There are some difference approaches in each programme. TAS, Radiance and Dialux are employed for the prediction of the thermal and lighting environment performance within a large glazed pedestrian concourse with natural ventilation in China (GITC) and air-conditioning in Thailand (Suvarnabhumi Airport Terminal). Therefore, it is important to carefully consider how these programmes simulate the heat and lighting within the buildings.

2.11.1 Overview of TAS Application

Thermodynamics is the science of heat flow and of its relationship to mechanical work (Szokolay, 2004). The dynamic thermal simulation software (TAS) was selected to assess the thermal environment and energy performance of large glazed pedestrian concourses in this thesis, because this software has been used widely in building research as follows:

- Wang et al., (2014) used TAS to examine the thermal performance of gallery and refurbishment solutions of the Scottish Art Gallery;
- Schuss et al., (2010) utilised TAS to present the method allowing for control of multiple devices in holistic and predictive way to optimize the building's energy and environment performance;
- Fisher (2008) used TAS to examine the wind tunnel testing of Ashburton Court;

- Zakaria, Woods and Ramly (2008) utilised TAS to generate the thermal and energy performance of roof insulation for residential buildings in Malaysia;
- Abdullah (2007) utilised TAS to model thermal stratification within a three-storey atrium in Malaysia;
- Gratia and Herde (2007) used TAS to study the effective position of shading devices in a double-skin façade;
- Carbon trust (2005) utilised TAS to model the thermal performance, ventilation and daylight in Great Glen House, Scottish Natural Heritage's new headquarters in Inverness.

Dynamic thermal simulation software: TAS is a complete solution for the thermal simulation of a building, and a powerful design tool in the optimisation of a building's environmental, energy and comfort performance (Jones, 2010). It utilises proven and accurate empirical methods for estimating convective heat transfer from internal surfaces (Alamdari, 1984). Therefore, the TAS simulation software is chosen because it provides an effective, realistic and comprehensive virtual environment in which the thermal and energy responses of any building may be accurately modelled.

TAS is computer software which simulates the thermal performance of buildings. The main applications of the software are in assessment of environmental performance, prediction of energy consumption, plant sizing and analysis of energy conservation. The movement of heat in various forms is conveyed into, out of and around the building by heat transfer.

- **Conduction** is treated dynamically using a method derived from the ASHRAE *response factor* technique. This efficient computational procedure calculates conductive heat flows at the building elements and surface of wall as functions of the temperature histories at those surfaces.
- **Convection** is treated using a combination of empirical and theoretical relationships relating convective heat flow to temperature difference, surface orientation and, in the case of external convection, wind speed.
- **Radiation** exchange is modelled using the Stefan-Boltzmann law, using surface emissivity from the materials database. Long-wave radiation from the sky and the ground is treated using empirical relationships. Solar radiation absorbed, reflected and transmitted by each element of the building is calculated from solar data on the

weather file. The calculation entails resolving the radiation into direct and diffuse components and calculating the incident fluxes using knowledge of sun position and empirical models of sky radiation. Solar absorption, reflection and transmission are all calculated from the thermo physical properties of the building elements. External shading and the tracking of sun patches around room surfaces may be included at the user's option.

- **Air movement** is taken account for each zone by latent gains, moisture transfer and the operation of humidification and dehumidification plant.

This following discussion is an adaptation from the TAS Theory Reference Manual (EDSL, 2011). It outlines the main environmental parameters considered and applied by the TAS software during the simulation process. TAS simulates the thermal state of the building by accumulating a variety of heat transfer mechanisms (Figure 2.25).

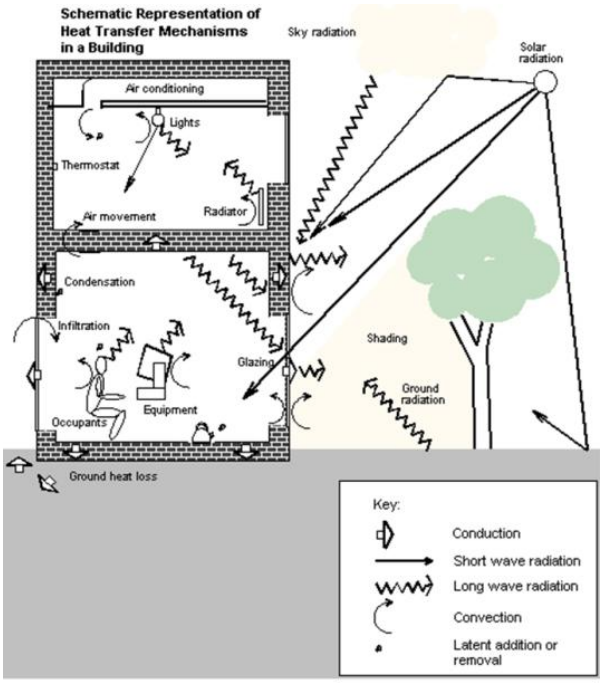

Figure 2.25 Schematic representation of heat transfer mechanism in a building (EDSL, 2011)

(i) Conduction

Conduction in the envelope of the building is treated dynamically using a method derived from ASHRAE response factor technique. The simulation procedure calculates conductive

heat flows at the surfaces of walls and other building elements as functions of the temperature histories at those surfaces.

The main quantities of conduction transfer function are the heat fluxes at the two surfaces of the component. The following equations are calculated from recent surface temperatures and a set of normal co-ordinate variables:

Internal surface condition heat flux:

$$W^{cond,int} = X^0 T^{int} + X^1 (T^{int}) - Y^0 T^{ext} - Y^1 (T^{ext}) + \sum_{n=1}^{N} V_n^{int} v_n \quad (2.21)$$

External surface condition heat flux:

$$W^{cond,ext} = Z^0 T^{ext} + Z^1 (T^{ext}) - Y^0 T^{int} - Y^1 (T^{ext}) + \sum_{n=1}^{N} V_n^{ext} v_n \quad (2.22)$$

where: $W^{cond,int}$ is the internal surface conduction heat flux (W/m^2);

$W^{cond,ext}$ is the external surface conduction heat flux (W/m^2);

T^{int} is the internal surface temperature (C);

T^{ext} is the external surface temperature (C);

(X) (where X is any variable) denotes the value of x at the previous time step;

$X^0, X^1, Y^0, Y^1, Z^0, Z^1$ are response factors ($Wm^{-2}K$) – constants which characterise the wall's response to recent surface temperature history;

v_n ($n = 1, 2....N$) are a set of normal co-ordinate variables (with the dimensions of heat flux (Wm^{-2}) which describe the thermal state of the wall at time-step t in relation to a set of functions;

V_n^{int} V_n^{ext} ($n = 1, 2....N$) are dimensionless constants which characterize the relationship between the surface fluxes and the normal co-ordinate variables.

Surface temperature histories and the normal coordinate variables are initialised to a steady state condition at the first stage of simulation. The process of preconditioning ensures that

the initial condition does not have a significant influence on simulation results. As the simulation proceeds, equations 2.27 and 2.28 are used at each time-step to establish linear relationships between the current temperatures and heat fluxes at the component's surfaces, and these relationships are incorporated in the matrix equations representing the overall heat balance for each zone.

$$q^{cond,int} = AW^{cond,int} = AX^0 T^{int} - AY^0 T^{ext} + q^{hist\_cond,int} \qquad (2.23)$$

and

$$q^{cond,ext} = AW^{cond,ext} = AZ^0 T^{ext} - AY^0 T^{int} + q^{hist\_cond,ext} \qquad (2.24)$$

where: $q^{cond,\text{int}}$ is the internal surface conduction heat flux (Wm^{-2}),

$q^{cond,\text{ext}}$ is the external surface conduction heat flux (Wm^{-2}),

$q^{hist\_cond,\text{int}}$ is the sum of all the *historical* terms which are related to the results from previous time-steps.

(ii) Convection

Building surface convection is treated using a combination of empirical and theoretical relationships relating convective heat flow to temperature difference surface orientation and in the case of external convection, wind speed.

(a) External Convection

The convection coefficient at external building surfaces, h^{ext}, is calculated from hourly values of the wind speed provided on the weather file, which is computed via the following expression provided by CIBSE.

$$h^{ext} = 5.8 + 4.1\, v_m \qquad (2.25)$$

where: h^{ext} is the external convection coefficient (W/m^2);

v_m is the wind speed measured at the meteorological station at a height of 10m.

Therefore, external convection heat flow is given by the following equation:

$$q^{conv,ext} = AW^{conv,ext} = Ah^{ext} (T_o^{air} - T^{ext}) \qquad (2.26)$$

where: $q^{conv,ext}$ is the external convective heat flow (Watts);

A is the effective component surface area (the mean of the internal and external surface areas provided by 3D-TAS);

h^{ext} is external convective heat transfer coefficient (W/m^{2}K).

T_o^{air} is the outdoor air temperature

T^{ext} is the external surface temperature

(b) Internal Convection

Convection at internal zone surfaces: the calculation of internal convection coefficients in TAS; the procedures set out by Alamdari and Hammond (1983) for the calculation of free convection heat transfer in rooms with the exception of zone divides.

For vertical surfaces, when the heat flow is in the upward direction, the following formula is recommended to use for calculated.

$$h^{int} = \left(\left\{ a \left[\frac{\Delta T}{L} \right]^{1/4} \right\}^6 + \left\{ b(\Delta T)^{1/3} \right\}^6 \right)^{1/6} \qquad (2.27)$$

where; h^{int} is the convection heat transfer coefficient (W/m^{2}K) applying between a surface and the room air;

$\Delta T = [T^{air} - T^{int})$ is the absolute temperature difference (K) between the room air (temperature T^{air}) and the surface (temperature T^{int});

L is a characteristic length (m) of the heat transfer surface (height of wall or hydraulic diameter of floor or ceiling);

a and b are taken from following table;

Vertical surface (horizontal beat flow):	a =1.50 and	b =1.23
Horizontal surface (upward beat flow):	a =1.40 and	b =1.63

Equation 2.28 is used in TAS for windows, with L set to the window height as defined in 3D-TAS.

For walls, TAS used the following simpler formulae:

Vertical surface (horizontal heat flow):

$$h^{int} = h^{hor} = h^{H} + 1.239\,(\Delta T)^{1/3} \qquad (2.28)$$

Horizontal surface (upward heat flow):

$$h^{int} = h^{up} = 1.63\,(\Delta T)^{1/3} \qquad (2.29)$$

Where the height-dependent term in equation 2.30 is computed from the zone height, H, using

$$h^{H} = \frac{1}{(670.656\,H^{6} + 120.43\,H^{8.7})^{1/6}} \qquad (2.30)$$

Horizontal surface (downward heat flow):

$$h^{int} = h^{down} = 0.6 \left[\frac{\Delta T}{L^{2}}\right]^{1/5} \qquad (2.31)$$

Sloping wall (upward heat flow):

$$h^{int} = h^{up} + (h^{hor} - h^{up})(\sin\gamma)^{1/4} \qquad (2.32)$$

where: γ is the angle between the inward-facing surface normal and the vertical.

The dependence of h^{int} on the temperature difference, ΔT, means that the internal convection varies from hour to hour.

(c) Infiltration

Infiltration is used in TAS to describe the user-specified exchange of air between a building zone and the exterior by natural ventilation. Infiltration carries both sensible and latent heat into or out of the zone.

$$Q^{inf} = m^{inf} c_p (T_o^{air} - T^{air}) = ((\rho^{air} a V)/3600)\, c_p (T_o^{air} - T^{air}), \qquad (2.33)$$

where: Q^{inf} is the sensible heat gain due to infiltration;

m^{inf} is the infiltration air mass flow rate (kg/s);

c_p: the specific heat capacity of air at constant pressure, for which the value

1.012 kJ/kg K;

J/kgK is taken (corresponding to a humidity ratio of about 0.003 kg/kg);

T_o^{air} is the outside air temperature

ρ^{air} is 1.210 Kg/m3(the density of air at standard atmospheric pressure and a temperature of 20C);

a: the air change rate (air changes per hour);

V: the volume of air in the zone.

(d) Air movement

Air moving between zones in a building carries with it sensible heat and water vapour, and thus affects the thermal balance in the zones concerned. Air movement may represent either natural or mechanical ventilation. The total sensible heat gain, Q^{am} (Watts), into zone z due to air movement is given by:

$$Q^{am} = \sum_{s=1}^{z} M_{sz}\, c_p\, (T_s^{ext} - T^{air}) \qquad (2.34)$$

where: *Z*: the number of zones in the model

Msz: the mass flow rate from source zone s (with zone 0 representing the outside air) to zone z

T_s^{air}: the air temperature in source zone s (or the outside temperature in the case);

(iii) Radiation Heat Exchange

Radiation heat exchange involves direct high frequency solar radiation (short-wave) and diffused or reflected low frequency radiation (long-wave) at the external and internal building surfaces. For long-wave radiation, the Stefen-Bolzmann law and the surface emissivity (in the material data base) are recommended to calculate radiation exchange.

(a) Long-Wave Radiation

The long-wave radiant heat exchanges on the external and internal zones are calculated separately by TAS. The long-wave radiation balance at the external building surfaces takes into account both long-wave radiations from the sky and from the ground.

$$q_{env} = q_{sky}(\gamma) + q_{gnd}(\gamma) \quad (2.35)$$

where: $q_{sky}(\gamma)$ = is irradiance on a surface with outward-facing normal making and angle γ with the zenith;

$q_{gnd}(\gamma)$ is ground long-wave irradiance on a surface.

The net long-wave radiation gain on the external building surface, $Q^{rad,ext}$, is calculated in TAS using the following equation:

$$Q^{rad,ext} = \varepsilon^{ext} A q_{env} - A q^{ext} \quad (2.36)$$

where: q_{envi} is the total long-wave flux incident on an external building surface from its environment;

$q^{ext} = q^{(raf)} + h^{rad,ext} T^{ext}$ is a long-wave radiant flux by the surface;

$q^{(raf)} = 273.15\, h^{rad,ext} - 3\, \varepsilon^{ext} T^{4}_{ext\,(ref)}$;

$h^{rad,extn} = 4\, \varepsilon^{ext} T^{ext\,3}$;

ε^{ext} is the emissivity of the surface;

$T_{ext\,(ref)}$ is the absolute of the surface;

A is the component areas (the mean of the internal and external surface areas provide by TAS)

T^{ext} is the external surface temperature.

Internal long-wave radiation exchange in zones is modelled in TAS using Carroll's MRT method. In Carroll's method, the surfaces are first treated as black body radiators. The i'th surface is assumed to be coupled to the MRT node with a coupling coefficient

$$G_i = h^{rad,int} A_i F_i \quad (2.37)$$

where: G_i Internal radiant exchange between room surfaces (W/K)

A_i is the component area of surface i (the mean of the internal and external surface areas provided by 3D-Tas);

F_i is the view factor (as yet undetermined) between surfaces *i* and the MRT node;

$h^{rad,int}$ is a linealised radiative heat transfer coefficient derived by differentiating the Stefan-Boltzmann radiation equation:

$$h^{rad,int} = 4 \sigma \Theta^{3}_{(ref)}{}^{zone} \qquad (2.38)$$

where: $\sigma = 5.6697 \times 10{-}8 W/m^2K^4$ is the Stefan-Boltzmann constant;

$\Theta^{zone}_{(ref)}$ is a reference absolute temperature which should be close to the mean temperature of the surfaces $\Theta^{zone}_{(ref)}$ = 288.15 K (or 15 C).

The temperature of the MRT node is

$$T^{mrt(c)} = \frac{\sum (G_k T_k{}^{int})}{\sum G_k} \qquad (2.39)$$

where: $T^{mrt(c)}$ is the mean radiant temperature in Carroll's method;

$T_k{}^{int}$ is the temperature of internal surface *k* ,

and the radiant heat transfer (Watts) from surface *i* to the MRT node is

$$- q_1{}^{rad,int} = G_i (T_i^{int} - T^{mrt(c)}) = G_i \ T_i - \sum \left(\frac{G_k T_k}{\sum G_k} \right) \qquad (2.40)$$

(b) Short-Wave Radiation

Short-wave radiation absorbed, reflected and transmitted by each building elements is calculated from solar data on the weather file. The direct and diffuse radiation is assessed using knowledge of sun position and an empirical model of sky radiation. External shading and the tracking of sun patches around building envelope may be included as the user's option.

Solar Radiation on the building exterior: Solar radiation incident on the building external surface ($Q^{dir,ext}$) is calculated as follows:

$$Q^{dir,ext} = p (q_{hor}^{dir\_beam} \text{ x } u \text{ x} A_1) \qquad (2.41)$$

where:

$$p(x) = \begin{cases} x \ (x > 0) \\ \\ 0 \ (x \le 0) \end{cases} \quad ; \qquad (2.42)$$

$q^{dir\_beam} = \dfrac{q_{hor}^{dir,ext}}{u_3}$ is the direction normal (beam) solar intensity

$\boldsymbol{q}_{hor}^{dir,ext}$ is the direction on the horizontal plane;

$u = (u_1, u_2, u_3)$: the unit vector pointing towards the sun which express the sun's position;

A_1) : the mean of the internal and external surface areas provided by 3D-TAS.

Diffuse and ground-reflected solar radiation incident on the surface is assumed to be isotropically distributed over solid angles. The diffuse solar radiant power incident on a surface from a sky, Q^{sky} (Watts) is consequently the following function of the surface tilt;

$$Q^{sky} = A_1 I_{hof}^{dif} \cos^2\left(\frac{\gamma}{2}\right) \qquad (2.43)$$

where: γ is the tilt angle from the horizontal.

The ground-reflected radiation is also assumed to be isotropic:

$$Q^{gnd} = A_1 \rho^{gnd} I_{hor}^{glob} \sin^2\left(\frac{\gamma}{2}\right) \qquad (2.44)$$

where: Q^{gnd} is the incident ground-reflected radiation;

A_1 is the global radiation incident radiation on the horizontal plane;

ρ^{gnd} (which the user may set) is an angle factor arising from integration over solid angle;

I_{hor}^{glob} is the global radiation incident on the horizontal plan;

TAS does not account for diffuse radiation shading.

Solar Transmission and Absorption: To calculate the characteristics of a glazing construction a normal ray is beamed into the construction from each side in turn. Reflections and absorptions are calculated and successive reflected rays are traced until residuals become small. This computation yields an overall transmittance, and (for rays from each side) a reflectance and a distribution of absorptance through the construction, all applying at normal incidence. Using the assumed linearity of heat transfer in the glazing construction, the absorptance distributions are then reduced to equivalent absorptances on the external and internal surfaces. Absorptance α_p can be shown to be equivalent as follow:

$$\alpha_p^{ext} = \frac{\alpha_p \gamma_p^{int}}{\gamma_p^{int} + \gamma_p^{int}} \quad (2.45)$$

and

$$\alpha_p^{int} = \frac{\alpha_p \gamma_p^{ext}}{\gamma_p^{ext} + \gamma_p^{int}} \quad (2.46)$$

where: α_p^{ext} : the absorptance at the external surface within a construction;

α_p^{int} : the absorptance at the internal surface within a construction;

γ_p^{ext} and γ_p^{int} : the external and internal surfaces, respectively.

Solar radiation entering the building through windows and other transparent building components is distributed over the building surfaces. The radiation absorbed by the building surfaces of each zone is totally stored in the quantities $q_i^{sol,ext}$ and $q_i^{sol,int}$,

where: $q_i^{sol,ext}$ is the solar radiation (Watts) absorbed on outside surface *i* of the zone;

$q_i^{sol,int}$ is the solar radiation (Watts) absorbed on inside surface *i* of the zone;

In the case of transparent components the *internal* and *external* labels on these quantities refer to the effective absorption on the two surfaces in the venin equivalent circuit theory.

Whilst the external surfaces of opaque building components, which are exposed to the outside environment, $q_i^{sol,ext}$ can be calculated as follow:

$$q_i^{sol,ext} = \alpha_i^{ext}(Q_i^{dir,ext} + Q_i^{dif\_sky} + Q_i^{ref\_gnd}) \quad (2.47)$$

where: α_i^{ext} is the external solar absorptance of the component

$Q_i^{dir,ext}$, $Q_i^{dif\_sky}$, $Q_{i\,r}^{ref\_gnd}$ are the incident solar powers appearing to external direct solar radiation, the diffuse component of solar radiation and the ground-reflected radiation , respectively.

$q_i^{sol,ext}$ will have a contribution of the same form, but it will also have a contribution from radiation returning from the zone through the component.

Solar Radiation Distribution inside the Building through transparent surface is determined in a series of radiation distributions. The surface solar gain ($q_i^{sol,int}$, $q_i^{sol,ext}$), computed for an inside and outside zone surface, is the total solar radiation (kW) absorbed by the surface in the course of the solar distributions.

Radiation is actually absorbed within the transparent construction, rather than at its surface, and in this case the surface solar gains are computed on the basis of the equivalent surface absorptances.

Zone solar gain is the total of the surface solar gains for all the surfaces facing into the zone;

$$Q^{sol} = \sum q_i^{sol,int} \quad (2.48)$$

(iv) The Transfer of Heat by Air Movement

Air movement between zones in a building carries with it sensible heat and moisture content which affects the thermal balance in the zone concerned. TAS represents air movement either by natural ventilation (Aperture Air Flow) given data on the characteristics of apertures in the building fabric or mechanical ventilation. The air movements are calculated as mass flow rates (kg/s).

The total sensible heat gain, Q^{am} (Watts), into zone z due to the air movement is modelled as follow:

$$Q^{am} = \sum_{s=0}^{z} m_{sz}\, c_p\, (T_s^{air} - T^{air}) \qquad (2.49)$$

where: m_{sz} is the mass flow rate from source zones s (with zone 0 representing the outside air) to zone z;

Z is the number of zone in the model;

T_s^{air} is the air temperature in source zone s (or the outside temperature in the case s = 0);

T^{air} is the air temperature in source zone z.

The total moisture gain for the zone due to inter-zone air movement, w^{am} (kg/s) is calculated as:

$$w^{am} = \sum_{s=0}^{z} m_{ss}\,(x_s - x) \qquad (2.50)$$

where: x_s is the humidity ratio in source zone s (or the exterior humidity ratio in the case s = 0);

x is the humidity ratio in zone z.

In addition, the zone air heat balance can be calculated by the following equation. The total heat gain is added from infiltration, ventilation, air movement, casual gains, plant and surface convection:

$$Q^{air} = Q^{inf} + Q^{vent} + Q^{am} + Q^{gains,conv} + Q^{plant,conv} - \sum q_i^{conv,int} \qquad (2.51)$$

The term in the above equation are defined as follows:

$$Q^{air} = \frac{(p^{air} V c_p)\,(T^{air} - \langle T^{air} \rangle)}{\Delta} \qquad (2.52)$$

where; p^{air} is the density of air (= 1.21 kg/m^3);

V is the zone volume;

c_p is the specific heat capacity of air at constant pressure (= 1,021 J/kg K);

Δ is the time-step (1 hour or 3,600 seconds in TAS);

$\langle \chi \rangle$ (where χ is any variable) denote the value of χ at the previous time step.

$$Q^{air} = m^{inf} c_p (T_0^{air} - T^{air}) \quad (2.53)$$

where; m^{inf} is the information air mass flow rate in kg/s, $(= \frac{p^{ai} NV}{3600})$;

c_p is the air rate (air change per hour)

T_0^{air} is the outside air temperature;

T^{air} is the zone air temperature.

$$Q^{vent} = m^{vent} c_p (T_0^{air} - T^{air}) \quad (2.54)$$

where; m^{vent} is the ventilation air mass flow rate in kg/s.

$$Q^{am} = \sum_{s=0}^{z} m_{sz} c_p (T_s^{air} - T^{air}) \quad (2.55)$$

where; m_{sz} is the mass flow rate from source zones s (with zone 0 representing the outside air)

to zone z;

T_s^{air} is the air temperature in source zone s (or the outside temperature in the case s = 0);

T^{air} is the air temperature in source zone z.

$$Q^{plant,conv} = (1 - p) Q^{plants} \quad (2.56)$$

where;

p is the radiant proportion where, $p = \begin{cases} p^{htg} & (Q^{plantS} > 0) \\ p^{clg} & (Q^{plantS} \leq 0) \end{cases}$

p^{htg} and p^{clg} are the radiant proportions for heating and cooling, respectively;

Q^{plants} denotes the sensible power input (Watts) to a zone from the plant.

$$Q^{conv,int} = Ah_1^{int} (T_{ai} - T_i^{int}) \quad (2.57)$$

where; A is the effective component surface area;

h_1^{int} is the convective heat transfer coefficient (W/m^2K) applying between a surface and the zone i ;

T_i^{int} is the internal surface temperature of zone i.

2.11.2 Overview of Lighting Simulated Applications

A number of lighting software programmes such as Lightscape, Radiance, Ecotect and Dialux are available, each of which requires different input characteristics and provides various outputs. Acosta et al., (2011) examined five light simulation software programmes and established that the illuminance levels reached with the Ecotect and Dialux are acceptable results. Therefore, they were selected to assess the visual performance of large glazed pedestrian concourses in this thesis, because these software programmes have been used widely in building research as follows:

- Abdulsalam et al., (2014) used Ecotect and Dialux to simulate daylighting characteristics under the same sky condition (overcast sky) in the cavity of double glazed facade;
- Sibilio, Rosato and Scorio (2014) investigated a scale model under artificial sky and compared the results with those obtained by Ecotect to determine the interior distribution of illuminance in terms of Daylight Factor;
- Sherma (2014) analysed insufficient lighting in a substation using Dailux software.
- Uyan and Sener (2010) utilised Ecotect and Dialux to simulate daylighting in a high rise residential building through a real case in Istanbul.

In order to simulate lighting performance, the model was required with geometrics and parameters. It has been found that when constructing a model in Ecotect it is easy to change geometry and add material to the model correctly. (Ibarra & Reinhart, 2009). So Ecotect software was used in the daylighting simulation of Guangzhou International Textile City (GITC).

Dialux is available as free software and is currently used by many designers and light planner worldwide. It is simple, effective and professional; also providing the latest

luminaire data from the world's leading manufacturers. Dialux relies on CAD data and can be exported easily. Dialux was employed for the daylighting simulation of Suvarnabhumi Airport Terminal.

Lighting fundamentals

Light is electromagnetic radiation, which becomes visible to the human eye by falling on the retina. Electromagnetic phenomena occur when an atom receives energy by either collision or heat; it will then release this energy via its electrons.

(i) Human visual response

Human eyes have two separate functions. The first is to act as a receiver of light, which focuses on the back of the eye (the retina). If compared to the camera, the retina acts as a film (Steffy, 2002). The second function of the eye is to act as the converter at the nerve ending of the retina, which converts the received image into an electrical signal and then transmits it to the brain. The factors that affect the visual ability of humans can be separated into two main categories: first, human factors such as optical performance, colour perception and the general condition of the eye; secondly, environmental factors such as relative brightness, glare from surroundings and movement in the task.

Good lighting conditions depend not only on the quantity of light. As the lighting level is increased, background luminance is also increased; however, this is not applied to the task. A loss in visual performance usually occurs if the background luminance is increased because of the contrast between task and background luminance. The ability to recognise the task in contrast with background luminance is known as *contrast sensitivity*.

Glare is very bright light, which has a negative effect on human visual ability. There are two types of glare: discomfort glare and disability glare. Discomfort glare refers to the situation where background light is too bright and visually uncomfortable. Bad planning of electric lighting can be the simplest source of discomfort glare (Chadderton, 2013). The difficulty of seeing the task is defined as disability glare, which normally occurs from a direct light source, such as sunlight through windows or any reflection of room elements. In some situations, glare is more troubling than lack of lighting level.

(ii) Theory of Photometry

The luminous system consists of a light source (a lamp), a surface illuminated and eyes perceiving from the source of light and reflected by the surface (Figure 2.26).

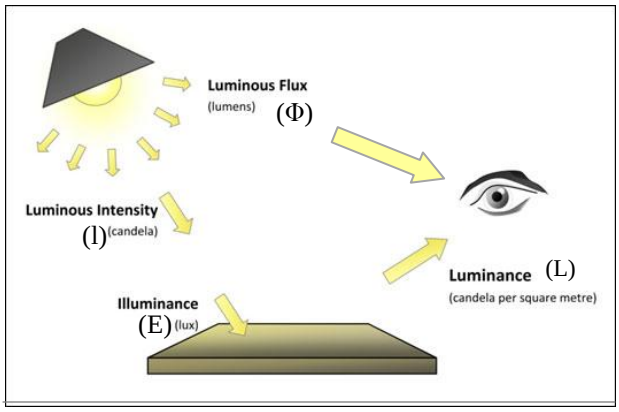

Figure 2.26 Simple luminous system (Jacob and Solomon, 2002)

The four measureable photometric quantities consist of (Szokolay, 2004):

- The luminous intensity (*I*) of a source is a measure of the wavelength-weight power in units of candela (cd);
- The luminous flux (Φ) of light is the measure of the perceived power of the light, measured in units of lumen (lm);
- The illuminance (*E*) is the total luminous flux incident on a surface, per unit area, measured in lux (lx) which is lumens per square meter (lm/m^2);
- The luminance (*L*) is the measure of the luminous intensity per unit area of light from a given direction which is emitted or reflected from a particular area.

Light incident on the surface can be distributed three ways: reflected, transmitted and absorbed.

(iii) Lamp and Luminaire

A lamp is an instrument that can produce light. It is a technical device that converts electric energy into radiation – and to light. Currently, there are many type of lamps, such as filament lamps, the general lighting service lamp (GLS), tungsten-halogen lamps, low-voltage display lamps, discharge lamps, compact fluorescent lamps, low-pressure sodium vapour lamps, high-pressure mercury lamps (MBF), metal halide lamps (MBI) and high-

pressure sodium lamps (SON, SON-L). These lamps can be characterized according to their assembly, operation and technical data (Steffy, 2002).

Luminaire is the electrical equipment that is used to create artificial light, which is contained within the lamp. Luminaire has four main functions: connecting to the electricity supply: controlling the light emitted by the lamp, protecting the lamp from a hostile environment and providing a fixture of satisfactory appearance. The importance of each factor depends on the use. The shape and material of the luminaire depends on the shape of the lamp. There are four basic materials for luminaires: steel, aluminium, plastics and glass. The luminaire can also be used to control the light distribution by reflection, refraction or diffusion. The way in which it controls distribution of light depends on the material property of the luminaire.

(iv) Daylight Factor

The use of daylight has become one of the most popular strategies in sustainable building design. However, it is very difficult to evaluate daylight quality and quantity in non-standard spaces, and this is where daylight factors become useful. Daylight factor (DF) is usually one of the first measurements to stimulate newcomer calculation of daylight performance (Ibarra et al., 2009). Daylight factor is the proportion of internal illuminance at a particular point on the work plane and the external illuminance on a horizontal plane, which is usually shown as a percentage. Daylight factor is typically evaluated under overcast sky conditions, in which there are few or no direct solar beams (Ananthakrishnan and De Caestecker, 2006).

The daylight factor is defined as:

$$DF = (E_i / E_o) \text{ x } 100\% \qquad (2.58)$$

Where, E_i = internal illuminance at a particular point on the work plane (lux)

E_o = simultaneous external illuminance on a horizontal plane (lux)

To calculate internal illuminance (Ei), the amount of external light received inside of the building is required: the summation of sky component (SC), externally reflected component (ERC) and internally reflected component (IRC). Daylight can reach the work plane in the room through three possible paths: direct light from the sky at the particular point in the room (SC), light reflected from a surface outside the room that then reaches the

point (ERC) and light that enters the window and then is reflected from the internal surfaces before reaching the point (IRC).

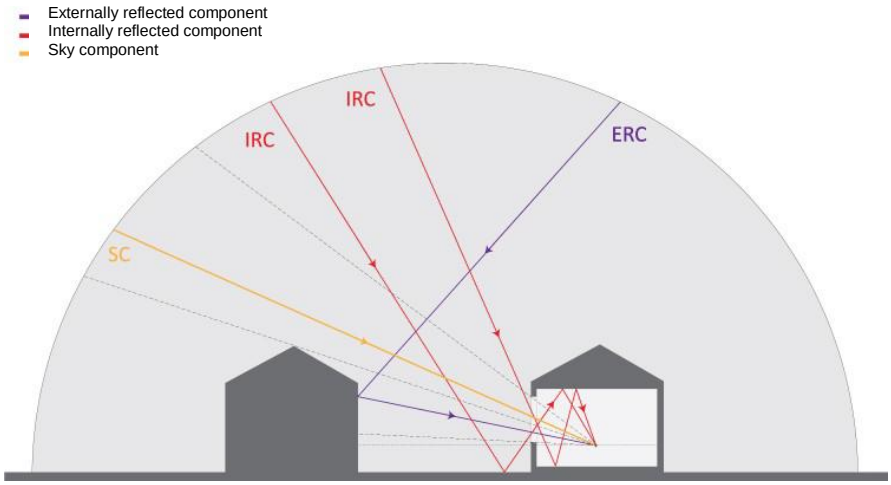

Figure 2.27 Three possible paths of light entering the room
(Iversen et al., 2013)

The average daylight factor is the outcome of calculation of luminous flux falling on a surface, and finding the fraction of the transmission on the other surface. The amount of illuminance can be obtained by dividing the flux received by the surface area. This gives the average value, but not the lighting distribution across the surface. The daylight factor on the outer face of the window can be calculated by using the amount of illuminance on the window surface divided by the simultaneous illuminance on unobstructed ground (Tregenza, 2011).

(v) Lighting Computer Simulation Model

In building design, the lighting simulation model has become more popular. This programme helps designers to make an appropriate decision on choosing the best solution for the building to achieve the building comfort requirement, as well as minimizing energy consumption (Maamari et al., 2006).

Reinhart and Fitz (2006) presented the finding from a web-based survey on the current use of daylight simulation in building design. The lighting simulation technique has been used as a substitute for the traditional verification techniques in building science; 77% of the participants used both computers and physical models for their professional practice, while the number of participants using daylight prediction software had increased by 21% in 2004.

Lighting simulation has two main advantages: photorealistic rendering and predictive rendering. Photorealistic rendering is associated with the artistic projection of images, while predictive rendering provides accurate presentation and prediction of reality under the given conditions. The lighting simulation system can be divided into three parts: direct calculations, view-dependent and scene-dependent algorithms. However, all three have their own specific applications and limitations as follows:

- Direct calculations are appropriate for artificial lighting, as the formulas and the simplifications are usually based on national standards. Therefore, they cover most general illumination situations;
- View-dependent algorithms are appropriate for lighting calculation and rendering. The calculation is based on the direction of tracing ray. There are three types of tracing ray: forward tracing (ray from light source), backward tracing (ray from observer's eyes) and bidirectional ray tracing (the ray from both light source and observer);
- Scene-dependent algorithms, due to their complex formulation, are usually used for calculation rather than rendering. A scene can be divided into two –surface elements or meshes. Radiometric values are given for each surface and viewed independently. The best example would be radiosity that changed from heat transfer to lighting simulation.

Contemporary models have enabled the use of one, or a combination, of these three applications, but in the case where diffusing and reflecting of light are involved, the supporting calculations are essential.

The most common technique for calculation is the statistical sampling method or Monte Carlo method. This method assumes that the expected value of the sample is correct, where the estimated value will complete the solution. The algorithm must run several times in order to produce enough values (Dutre et al., 2006). This technique has several accuracy limitations due to the value assumption. However, this is sometimes the best technique to solve certain physical problems.

The standard assessment of daylight quality is based on an interpretation of the measured data as presented in Table 2.8.

	Performance Indicator	Interpretation
1	**DAYLIGHTFACTOR**	
	< 1%	Unacceptable
	1-2%	Acceptable
	2-5%	Preferable
	> 5%	Ideal for paper work/ too bright for computer work
2	**WORK PLANE ILLUMINANCE**	
	<100 lx	Too dark for paper and computer work
	100-300 lx	Too dark for paper work/ acceptable for computer work
	300-500 lx	Acceptable for paper work/ acceptable for computer work
	>500 lx	Ideal for paper work/ too bright for computer work

Table 2.8 Performance Indicators and Their Interpretation

(Dubois, 2003)

2.12 Summary

Firstly, historical and design development of the atrium and large glazed pedestrian concourse buildings in international and hot-humid regional contexts were discussed in this section. Highly glazed spaces originated in colder regions where their roles were as a sun space during the daytime and a buffer zone in the night-time. The use of this form of building has become popular worldwide, including the hotter countries of Asia where glazed atria are less climatically appropriate. Overheating and unwanted thermal stratification resulting from excessive solar gain were identified as the two major causes of discomfort within large glazed pedestrian concourse in the tropical climate. Highly stable thermal stratification at upper levels would cause the stratified hot air to flow into top occupied levels adjacent to the central atrium, thus causing great discomfort to the users surrounding the area. High heat gain through the glass not only causes discomfort to the user surrounded by this area, but also results in the need for large intensive air-conditioning systems with high running costs.

Then, the overview of research trends focusing on atriums and large glazed pedestrian concourses and suggested solutions were also presented. What is clear from the previous studies is that correctly designed solar shading devices can improve building energy consumption and provide daylight quality. A proviso is that an external shading device is preferred as it blocks most of the heat from solar radiation before it reaches the building's surface. However, external shading device needs should be properly addressed at the early design stage due to its construction loads. The widespread preference for large glazed

pedestrian concourses in commercial building has created an 'artificial' need for sophisticated shading devices. Over-glazed buildings are often subject to intense solar heat build-up and visual discomfort. The proper solution to these critical issues is an internal shading system which would be easy to install, light weight, effective to operate and economic to run over its life time.

The number of shading systems available today on the market is huge and it is therefore not always easy to choose the best solution for a building. Many parameters influence the choice of the system and of the control strategy itself. The building's energy performance using different shading designs and internal shadings have been studied already. But none of these studies investigated how thermal and lighting environments are affected by the internal roof shading systems. Thus the research attempted to examine the effectiveness of internal roof shading device in blocking out the solar radiate heat with the form and position of the shading device as a remedial solution to reduce temperatures while maintaining adequate levels of natural lighting in the large glazed pedestrian concourse buildings.

Following that, theories relating to daylight and heat energy were discussed particularly in hot-humid climates. Solar radiation penetrates through atria or large glazed pedestrian concourses not only providing daylight but also creating thermal stratification, which is the most significant factor of discomfort in these buildings in the tropics. So designers must design buildings not only to collect energy from the sun to provide lighting, but must also control heat energy, which if not limited can lead to overheating of the building.

Additionally, the criteria relating to the fundamental concept of thermal and internal comfort in China and Thailand were reviewed. Since the Guangzhou International Textile City design is intended to facilitate international commercial activities related to the textile industry, while Suvarnabhumi Airport Terminal serves both domestic and international passenger. In order to assess thermal comfort in those spaces, thus international thermal comfort criteria of the ASHRAE Standard 55 (1992) and the CIBSE (2006) were chosen in this research. Even though, there were arguments from previous researches that these conditions may lead to overcooling and energy waste for hot-humid climates.

A general review of building ventilation systems for both natural and mechanical ventilation, as well as a theoretical basis for natural ventilation by thermal buoyancy was presented later. In hot-regions, using thermal buoyancy ventilation alone has an insignificant effect on the atrium space's thermal condition, so mechanical conditioning systems are required to cool down the internal temperature to the comfort level.

The overview of post occupancy evaluation (POE) and theoretical basis for degree-days analysis of related buildings' energy consumption was also reviewed. Then POE will be used to evaluate actual building performance by gathering information based on user satisfaction. This will be explained further in chapter 5. While degree-days will be used to analyse weather related energy consumption in buildings which will be assessed; specifically the energy consumption of Suvarnabhumi Airport terminal will be examined further in chapter 6.

The standard economic analysis methods were also presented, which will be used to assess the proposed internal shading solutions on their costs and payback periods. This will be presented further in chapter 8.

Finally, the section reviews dynamic thermal and daylighting software used in this thesis: TAS, Ecotect and Dialux. They were selected to assess the thermal and visual performance of large glazed pedestrian concourses in this thesis, because these software programmes have been used widely in building research.

In the next chapter, research methodology for this thesis will be discussed.

CHAPTER 3 – RESEARCH METHODOLOGY

3.1 Introduction

Chapter 2 deals primarily with overheating in atriums and glazed pedestrian concourses due to solar radiation, especially in the upper levels. The stratification impact in the building can result in the need for complicated and expensive cooling systems (Datta, 2001; Gocer, Tavil and Ozkan, 2006). In the tropics, these problems will be greater than the other more temperate regions because of the year round requirements of air-conditioning systems. Moreover, high heat gains through the glass results in large power demands, expensive equipment and maintenance intensive mechanical systems. The poor thermal performance in these buildings may also necessitate remedial improvements to increase comfort and lower operating costs after a couple year of occupancy (ASHRAE, 2009). To resolve these problems, the remedial solution for long-span glazed roofs over large pedestrian concourses is to provide suitable sun shading (Prowler et al., 2014; Steemers and Yennas, 2000).

The ultimate aims of the thesis are to propose design principles and guidelines for internal roof shading systems created to provide a better thermal environment and energy performance; while maintaining adequate levels of natural lighting within existing long-span glazed roofs over large naturally ventilated and air-conditioned pedestrian concourses in the tropics. This chapter discusses the methodology applied to achieve the aims and objectives of the study.

The chapter is structured into eight sections. It starts with a discussion on the research design and also focuses on the research method of inquiry in section 3.2. Section 3.3 provides a brief discussion on the data collection and site measurement. Section 3.4 describes the created dynamic thermal and lighting models used in this research as a testing tool to examine the design options. Sections 3.5 and 3.6 explain the developing design of the shading system method and the testing of shading design options, respectively. Section 3.7 presents a discussion on the cost analysis, while 3.8 provides the recommended design principles and guidelines. The last section presents a conclusion to the chapter.

3.2 Research Design

Asia's increased energy consumption accounts for about 60 percent of the growth in global energy consumption (IEEJ, 2015). A combination of global higher energy prices and rapid growth of energy consumption has pushed Asia to a target with regard to energy efficiency in buildings (WEC, 2013). Furthermore, more than half of the world's new buildings are constructed in Asia (Schwarz-Herion and Oman, 2015). Specific attention is given to the building sector in China and Thailand, since China is in the midst of its huge growth in urbanization, which is happening on a smaller scale in Thailand and throughout the rest of developing Asia (Laurenzi et al., 2007).

This thesis focuses on the existing buildings with atrium and long-span glazed roofs over large pedestrian concourses in the tropics; thus the two case studies were selected from Southern China and Thailand where local climate is hot and humid: Guangzhou International Textile City (GITC) represented a large existing naturally ventilated glazed pedestrian circulation area and Suvarnabhumi Airport Terminal represented a large existing air-conditioned glazed pedestrian concourse. The two case studies are approximately of the same size, categorised as mega buildings. GITC has a total floor area of approximately 140,000 m^2 with total top-glazed roof area covering nearly 10,000 m^2. The existing long-span glazed roof over large pedestrian concourse of the GITC building was naturally ventilated, while the surrounding retail units were air-conditioned. The long-span glazed roof over a large pedestrian space is intended to be airy to suit the tropical climate and open to maximise natural lighting. Even though the total cooling load was designed at180 Wm^{-2} according to National Standard for retail unit in China, many complaints also came from the tenants after the first year of operation. These complaints focused on serious overheating due to solar gain and the corresponding high cooling bills (CBTG Ltd., 2010);

Suvarnabhumi Airport Terminal has a total floor area of nearly 140,000 m^2 with total top-glazed roof area covering nearly 25,000 m^2. The long-span glazed roof over a large pedestrian concourse is provided as an existing air-conditioned departure lounge and also opens to maximise natural light. The interest towards the energy consumption relates to energy needed for the cooling system; a serious concern at many other airports. The measured cooling load over the whole Suvarnabhumi airport in 2010 was very high at

553.41 $kWhm^{-2}$, as compared to an energy intensity benchmark for large airports of 393.1 – 467.7 $kWhm^{-2}$ (EarthCheck, 2013; Costa et al., 2012).

The construction of the outside façade of both case studies is mainly 12 mm laminated clear glasses with a *U*-value of 5.5 W/m^2K. Hence these two building are applicable to many other long-span glazed roofs over large pedestrian concourse buildings with the similar construction. More details are explained in chapter 4.

Case studies were carried out to gain a better understanding of the thermal and lighting conditions within the existing long-span glazed roofs over large pedestrian concourse buildings in the tropics, and to obtain measured data for calibrating the capacity of dynamic thermal and lighting model in order to propose internal roof shadings.

This research deals with the dynamic interaction of sub-systems in buildings: building, environment, equipment, people, natural ventilation and mechanical ventilation (Figure 3.1). In order to achieve the aims of this thesis, integrated research methods were applied. General methodologies were assessed using the following methods:

- Data collection was undertaken to provide the buildings' geometric and occupancy data to create dynamic thermal and lighting models to test the various shading options. Annual weather data was used to test the performance of the various shading options and predict the annual energy consumption;
- Site measurements were conducted by mechanical instruments to gain more understanding of the internal physical environment. The measured data was also used to calibrate the computer models;
- Questionnaire survey was undertaken to explore the occupancy satisfaction and the existing indoor environment qualities;
- Scale model experiments were used to obtain realistic light transmittance of fabric for propose shadings;
- Dynamic thermal and lighting simulation modelling was carried out to build the models without shading, representing the Base Case, and was also used to propose the internal roof shading arrangements: low level shading (horizontal screen) and high level shading (curved/ sloped screen);

- Standard economic analysis methods were used to assess the costs, benefits and payback periods to provide recommendation for installation of the internal roof shading system.

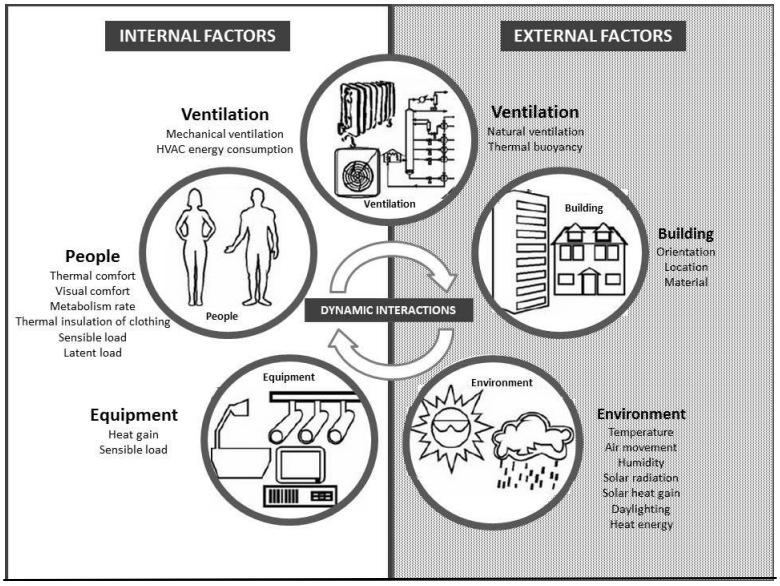

Figure 3.1 Dynamic interactions of sub-system in buildings (Hensen and Lambert, 2011)

Therefore, the research methodology in this thesis consists of six stages (Figure 3.2); the first stage involves the field study which was carried out by using data collection, filed measurements and a questionnaire survey. The collected data were in two groups. The first was a set of full year's weather data consisting hourly values of seven weather variables: the direct and diffuse solar radiation, cloudiness, air temperatures, relative humidity, wind speed and direction. The second data group relates to the building, including dimensional data, indoor conditions, occupancy, building materials and construction details. These data were used to create the dynamic thermal and lighting model in the second stage. In order to increase the accuracy of the thermal and lighting models, it was necessary to calibrate these models by comparisons with the measures resulting from two critical variables: the indoor temperatures, and the average cooling load and daylight factors. At the third stage the shading blind fabric was selected. Ideally the selected material for the shading blinds should have the highest possible lighting transmittance and lowest solar transmittance in order to maximise light transmission and minimise solar penetration into the atrium. To find such a material, five samples were collected from the manufacturers Silent Gliss. The researcher examined their realistic light transmission by a scale model experiment carried

out in the artificial sky dome at Heriot-Watt University and also in an open-field context, under an over-cast sky. The highest lighting transmission and lowest solar transmission material was selected for proposed shadings. In the fourth stage, two shading configurations were proposed and tested with the simulation under various conditions to compare their environmental and energy performance against the standard thermal cooling loads and the lighting variables within the large pedestrian concourse buildings. Two screening positions were simulated: the low level shading (horizontal blind) and the high level shading (curved/ slopped blind). In the fifth stage, a cost analysis was carried out, taking into consideration both the installation and the running costs of the shading options. Standard economic analysis methods employed addressed: the net present value, the internal rate of return and depreciated payback period were assessed. In the final stage, the design principles and guidelines for internal roof shading systems in order to provide a better building-centric thermal environment and energy performance were presented. The systems were designed to maintain adequate levels of natural lighting within the existing long-span glazed roofs over large naturally ventilated and air-conditioned pedestrian concourses in the tropics.

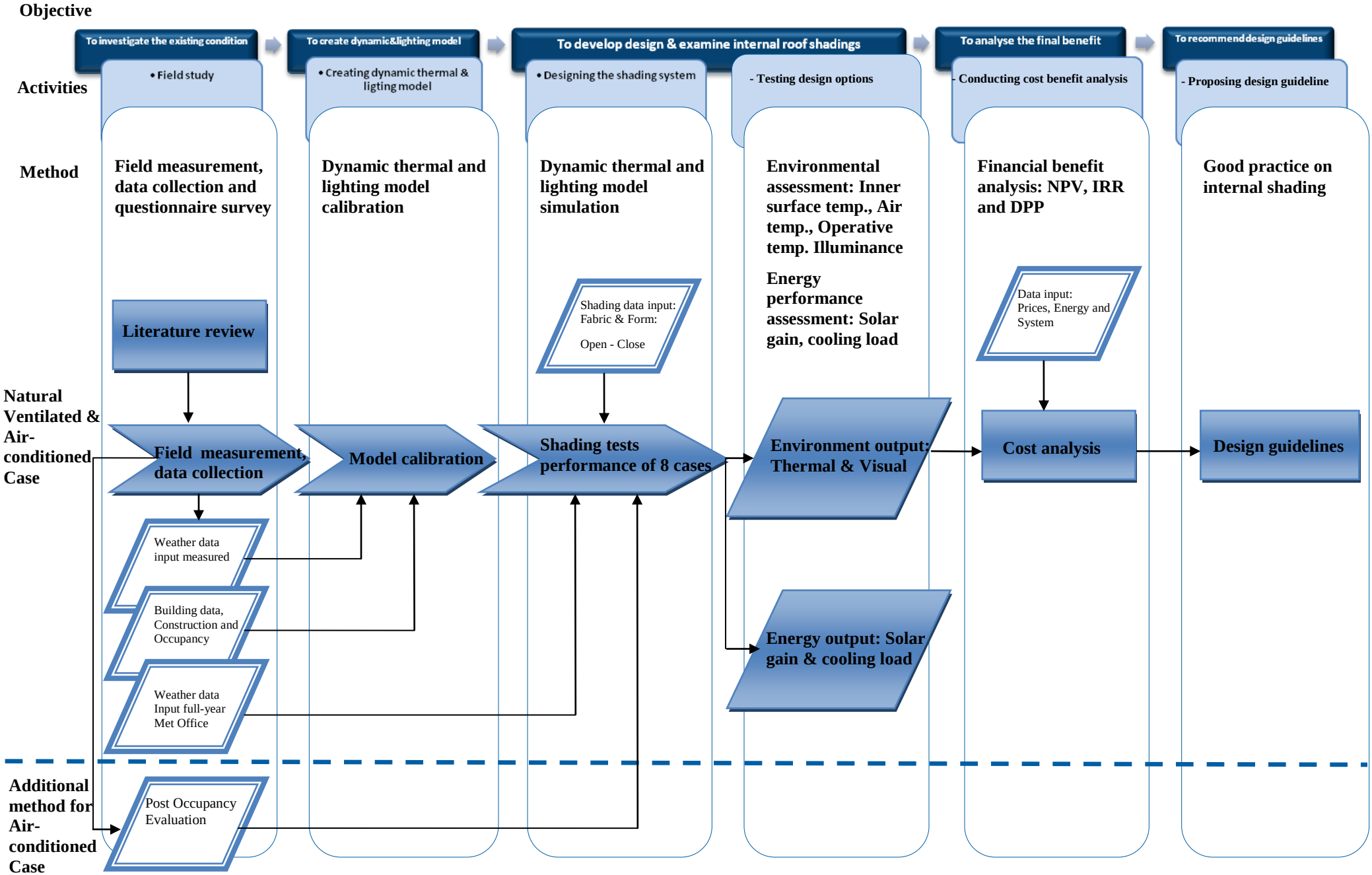

Figure 3.2 Methodology flow chart

3.3 A Field Study

To investigate the existing conditions and overall indoor physical behaviour within existing long-span glazed roofs over large pedestrian concourse buildings in the tropics with two cases: natural ventilation and air-conditioning is carried out by the filed study.

The method of field study used in this thesis combines the two common sources, namely primary and secondary sources.

- The primary sources include site measurement using mechanical equipment and data collection within Suvarnabhumi Airport terminal for the purpose of the calibration of the two models: the dynamic thermal and the lighting models, questionnaire survey, and also building simulation using the dynamic thermal and lighting software.
- The secondary sources are obtained from field measurement data from a colleague team in South China University of Technology, publications and earlier researches which were used to build models, support and strengthen the overall research process, which is finally to achieve the main goal of the study.

  In China, there were two preliminary studies carried out over 35 selected air conditioned retail shops in GITC building by China Building Technology Group Ltd (CBTG Ltd., 2010). A parallel survey of commercial units by students and staff at the Department of Architecture, South China University of Technology, Guangzhou (Jingyan, 2012) was carried out by using mechanical equipment which mapped four environmental variables over the main glazed pedestrian concourse and corridors: the daylight factor, air temperatures, relative humidity and air movement.

The data collections in these studies are divided into two groups:

- Annual weather data

  It consisted of hourly values of seven weather variables collected from the local meteorological station: the direct and indirect solar radiation, cloudiness, air temperature, relative humidity and wind speed and direction. This set of weather data was used in dynamic thermal modelling to predict the annual energy consumption for the Base Case and the Shading Case.

- The geometric data

  These were based on the construction drawings. The materials' data and construction details were collected from the architectural firm as well as contractors though a painstaking process. The occupancy data came from the building management team and they included lighting loads, number of occupants, cooling loads and so on. The data was used to build the computer models to test the various shading options in this thesis;

The measured data, included key indoor variables such as air temperatures, cooling loads and illuminance, was gathered from inside both case studies with mechanical instruments from a group of selected locations within the long-span glazed roofs over large pedestrian concourses. The data was used to calibrate the computer models. For the naturally ventilation case study in China, the air flow speed was further monitored at the entrances and opening of the roofs. This will be discussed in detail in chapter 4.

In addition, the questionnaire survey was used to evaluate building performance and occupants' experience of Suvarnabhumi Airport Terminal. This will be discussed further in chapter 5.

3.4 Creating Dynamic Thermal & Lighting Models

Computer modelling simulation has been playing a significant role in design, diagnostics and evaluation of buildings. It can also help designers and researchers to evaluate the physical and energy performance of buildings. Due to the complexity of long-span glazed roofs over large pedestrian concourse buildings' geometry, and the limited measurement period of the two case studies, dynamic thermal models and lighting models are thus used. The models enable the researcher to carry out an overall assessment of the annual indoor physical environment and energy consumption of the long-span glazed roofs over large pedestrian concourses. Creating representative dynamic thermal and lighting models is crucial to the achievement of the objectives of this study.

In order to achieve the objective to create dynamic thermal and lighting models of the existing long-span glazed roofs over large pedestrian concourse buildings in the tropics with two cases: natural ventilation and air-conditioning, the whole case study buildings were created in both thermal and lighting models and run under the weather data files

from the local meteorological stations over the same selected periods as the field measurements. These were facilitated by dynamic thermal and lighting software tools known as TAS, Ecotect and Dialux.

In order to increase the accuracy of the thermal and lighting simulations, it is necessary to calibrate these models. Calibration of the thermal models was by comparison with the measured results for two critical variables, the indoor temperatures and the total average cooling loads within the long-span glazed roofs over large pedestrian concourses on the hottest clear and overcast days. Calibration of the lighting models was by comparison with the daylight factors (DF) within the long-span glazed roofs over large pedestrian concourses on the selected overcast days. This will be presented further in chapter 6. The representative models were also used to predict the physical environment with differing designed shading configurations which were assessed by dynamic thermal and lighting simulation software in the next step.

3.5 Develop and Design the Shading System

In order to achieve the objective to examine the internal roof shading as remedial solutions relating to two cases of existing long-span glazed roofs over large pedestrian concourse buildings in the tropics with two cases: natural ventilation and air-conditioning, the shading blind fabric was selected and examined. Their realistic light transmission was tested by scale model experiment in the artificial sky dome at Heriot-Watt University and also in an open-field context, under clear and overcast sky.

The effectiveness of internal shading devices to block out the solar radiated heat depends on their position with respect to glazed components, geometry, material properties (solar reflectance, solar transmittance and light transmittance), control options and colour (Unterpertinger, 2005). Easy installation is considered crucial to minimise disruption to the already very busy occupants in the adjacent businesses. Most importantly, light weight is considered vital as the pedestrian concourses are enclosed beneath large glazed roofs spanning over 40 meters in both directions (Wang et al., 2014). Thus, in this thesis, internal shading was proposed in the form of retractable internal fabric sheet blinds of light colours, as a shading solution.

Ideally, properties for the shading fabrics should have the highest possible lighting transmittance and lowest solar transmittance in order to maximise light transmittance

and minimise solar penetration into the atrium. In addition, fabrics with a solar reflecting coating can help reflect this solar heat and offer improved thermal performance (CIBSE, 2006).

Fabric samples and properties in this thesis were provided by Silent Gliss Ltd. (Silentgliss, 2011). Five reflective shade fabric samples were selected and examined for their realistic light transmittance. To obtain realistic light transmittance of these fabrics, a scaled model box was made and each of the collected fabric samples was tested in the artificial sky at Heriot-Watt University and also in open field conditions under an overcast sky. This will be discussed further in chapter 7.

3.6 Testing Shading Design Options

In order to achieve the objective to examine the internal roof shading as remedial solutions of the existing long-span glazed roofs over large pedestrian concourse buildings in the tropics with two cases: natural ventilation and air-conditioning, the shading blind fabric was proposed and tested with the simulation under various conditions.

The best fabrics from previous stage, which have the highest transmittance, can be chosen for further dynamic thermal and lighting simulation measurements, which will serve to identify the appropriate internal shadings for large glazed concourse spaces. According to the most practical installation, two shading arrangements were proposed: the low level shading (horizontal screen) and the high level shading (curved/sloped screen). The effects of the shading options were quantified and assessed using the defined environmental variables to judge environmental and energy performance improvement. These assessments were based on comparisons between the Shading Cases and the Base Case on both summer clear and overcast days and winter clear and overcast days.

The environmental variables examined to assess the thermal conditions in the case studies were the inner surface temperature of the ceiling, the mean radiant, air and operative temperatures over the existing long-span glazed roofs over large pedestrian concourses. The operative temperature was also used as an indicator of thermal comfort in buildings in this study. The visual condition of these tested cases was assessed for illuminance and daylight factors. Then solar heat gain and cooling load variables were

examined to assess the energy performance. This will also be discussed further in chapter 7.

3.7 Conducting Cost Analysis

To analyse the financial benefits from the remedial solutions of the existing long span glazed roofs over large pedestrian concourse buildings in the tropics with two cases (natural ventilation and air-conditioning), standard economic analysis methods were employed to provide recommendations on the solutions' costs and payback periods.

A cost analysis was carried out taking into consideration both the installation and the running costs of the shading options. There is a need for studies to evaluate the relative, long term performance of common capital budgeting decision procedures, when used in practice.

As mentioned in the scope of this thesis, micro details of the recommended shade control systems were not focused on. Therefore, the cost analysis for installation of the shade control system was directly calculated from the manufacturer's recommended price list.

The shading devices that have the greatest potential for reducing energy consumption and achieve better physical environment will be assessed financially by using the following concepts: Internal Rate of Return (*IRR*), Net Present Value (*NPV*) and Discount Payback Period (*DPP*); all of which will be discussed in detail in chapter 8.

3.8 Recommending Design Principles and Guidelines

The recommended internal shading design principles and guideline objectives are addressed by summarizing the data analysis of both the site measurements and computer simulation; the recommendations are also supported by a literature survey, which will be addressed further in chapter 9.

3.9 Conclusion

This research deals with the dynamic interaction of sub-systems in buildings: building, environment, equipment, people, natural ventilation and mechanical ventilation. In order to achieve the aims of this thesis, integrated research methods were employed include data collection and field measurement to provide the buildings' geometric and

occupancy data to create dynamic thermal and lighting models and calibration; questionnaire survey to explore the occupancy satisfaction and the existing indoor environment qualities; scale model experiments to obtain realistic light transmittance of fabric for propose shadings; standard economic analysis methods to assess the costs, benefits and payback periods and proposing design guidelines.

The following chapter, Field Studies, will discuss in detail the site measurement and monitoring.

CHAPTER 4 – A FIELD STUDY of INTERNAL THERMAL and LIGHTING CONDITIONS in LARGE PEDESTRIAN CONCOURSES in THE TROPICS

4.1 Introduction

In order to investigate the existing conditions and overall indoor physical behaviours within two cases of long-span glazed roofs over large pedestrian concourse buildings in the tropics a field study was carried out by using data collection and field measurement. One of the two cases involved natural ventilation and the other air-conditioning.

The aim of collecting detailed measurements and other information was to prepare data to build the dynamic thermal and lighting models; while the aim of the measured data was to enable the researcher to calibrate the capacity of the dynamic thermal and lighting models. In addition, the Post Occupancy Evaluation (POE) questionnaire-based survey was further used to evaluate building performance and occupants' experience of Suvarnabhumi Airport Terminal. The aim of questionnaire survey was to explore occupancy satisfaction levels and the existing indoor environment qualities, which will be explained further in chapter 5.

This current chapter (four) is structured into five sections. Firstly, the data collection method is presented. Secondly, this chapter sets out what is involved with the site measurement and monitoring of indoor environmental parameters. Third, the field study involving data collection, field measurement using mechanical instruments and site monitoring in the long-span glazed roof over a large naturally ventilated pedestrian concourse case study in Guangzhou, China is presented. The field study was carried out in the central glazed pedestrian concourse of Guangzhou International Textile City (GITC) for seven consecutive days from 30th July to 5th August 2011 by a colleague team from the South China University of Technology. Fourth, this chapter then presents the field study which took place in the long-span glazed roof over the large air-conditioned pedestrian concourse case study in Samut Prakarn, Thailand. The field study was carried out in the departure lounge of Suvarnabhumi Airport Terminal for twenty consecutive days from 12th September to 1st October 2012; involving data collection and field measurements. These site tests were done during hot and humid days, when the outdoor air temperature average 30±4^{o}C and relative humidity in the

afternoon was generally above 60%. Finally, a conclusion is presented at the end of this chapter.

4.2 Data Collection Methods

The data collections consisted of 2 categories: annual weather data and geometric data.

- Annual weather data consisted of hourly values of seven weather variables collected from the local meteorological station. The variables are direct and indirect solar radiation, cloudiness, air temperature, relative humidity and wind speed and direction;
- The geometric data was based on the construction drawings. The materials' data and construction details were collected from the architect's firm, as well as contractors, though a painstaking process. The occupancy data came from the building management team and included lighting loads, number of occupants, and cooling loads amongst other variables.

4.3 Site Measurement and Monitoring of Indoor Environment Parameters Method

The survey method involved site measurement and the monitoring of indoor environmental parameters. The measured data included the key indoor variables of air temperatures; surface temperatures and illuminance for both case studies. Measurements were conducted with mechanical instruments over a group of selected locations within the atria, while cooling loads were derived from the statistics from the building manager and agent. The recorded data represented the existing internal conditions in the atriums. This data was used to calibrate the computer models. Calibration of the thermal models was by comparison with the measured results for two critical variables; the indoor temperature and the total average cooling load, on the hottest clear and overcast days. Calibration of lighting models was by comparison with the daylight factors within the long-span glazed roof on the selected overcast days. For the natural ventilation case study in China, the air flow speed was further monitored at the building's entrances and the roof openings.

4.4 The Large Glazed Pedestrian Concourse with Natural Ventilation of the GITC

Guangzhou International Textile City Building (GITC) located at Guangzhou, China, was built in 2005 as a centre for the textile industry and commerce. It claims proudly to be the largest modern textile wholesale building in Asia. Characterised by its

"openness", its design is intended to facilitate all commercial activities related to the textile industry under one roof from logistic arrangements, easy flow of goods and people, display of material samples and products, offices, catering, and even one-stop shopping.

4.41 General Characteristics of Guangzhou Weather

The city of Guangzhou is located in Southern China at latitude of 23.13^{o}north and longitude of 113.23^{o}east. The weather is generally hot and humid, with occasional showers. The average maximum air temperature is 26.2^{o}C, whilst the average relative humidity is 77.3%. Meteorological statistics show that the hottest month in Guangzhou City is July. The country has a long summer with a peak between August and October with the average highest daily temperatures ranging between 32.6°C and 32.7°C; January is the coolest month with daily minimum temperatures averaging 9.8^{o}C (Figure 4.1). In the summer months between June and December, the monsoon blows from the south and southeast directions (Du et al., 2013).

Annual weather data for 2011 was collected from the local meteorological office as the representative yearly data. The data set included the hourly figures of seven recorded variables: global and diffused solar radiation, air temperature, relative humidity, cloudiness, wind speed and direction (Appendix A). This set of weather data was used in dynamic thermal modelling to predict the annual energy consumption for the base case; the model being created to compare the performance of the shading cases. This would allow energy savings to be assessed for the shading options.

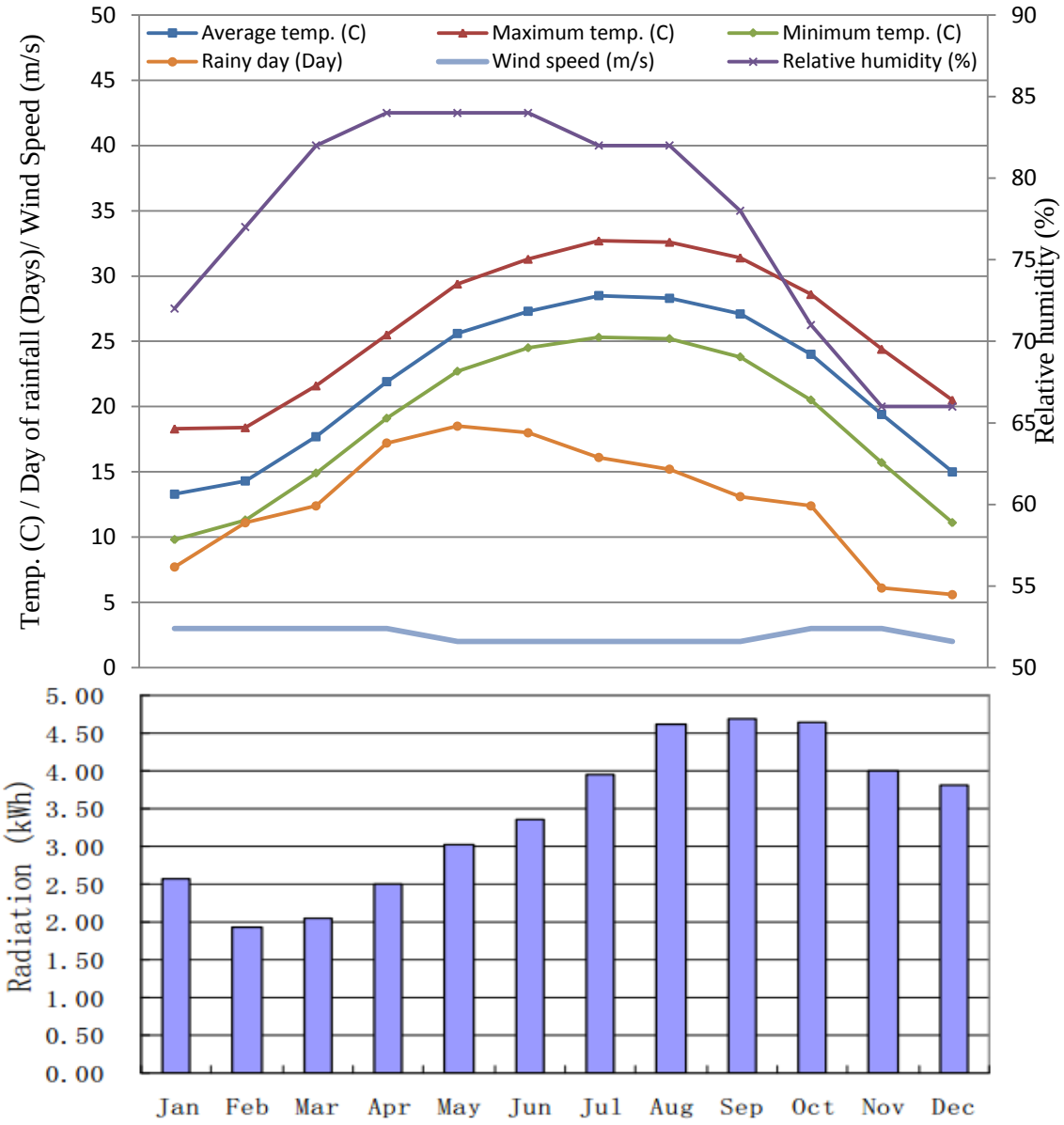

Figure 4.1 Weather data for Guangzhou China
(http://www.climate-charts.com, Zuo, Hu and Meng, 2006)

4.4.2 Building Description of the GITC Building

The GITC building is a seven storey block designs with a total floor area of nearly 140,000 square metres for all floors above the ground level (Figure 4.2). Retail units are located on the lower four floors and offices on the top three. Each floor is surrounded by long corridors providing easy access to the retail shops which are occupied by over 4,000 brands of textile traders.

There are four main east-west streets and two main north-south' streets, which are from 12 to 15 metres wide. All are linked and fully open to the outside on the ground level for access of people and commercial vehicles. The streets, together with the junctions,

are all covered above their top levels by raised transparent glass canopies forming large glazed pedestrian concourses. The sides of the transparent roofs are fully opened and covered by louvers that are angled to admit light, air but to keep out rain. All these spaces are naturally ventilated to suit the tropical climate and are open in order to maximise natural lighting, while the surrounding retail units and offices are air-conditioned daily from 0800h to 2000h. The central glazed pedestrian concourse is the largest space with a floor area of 1,500 square metres and height of 35 metres. These were used by approximately 30,000-50,000 people a day in GITC during the busy season in August to November.

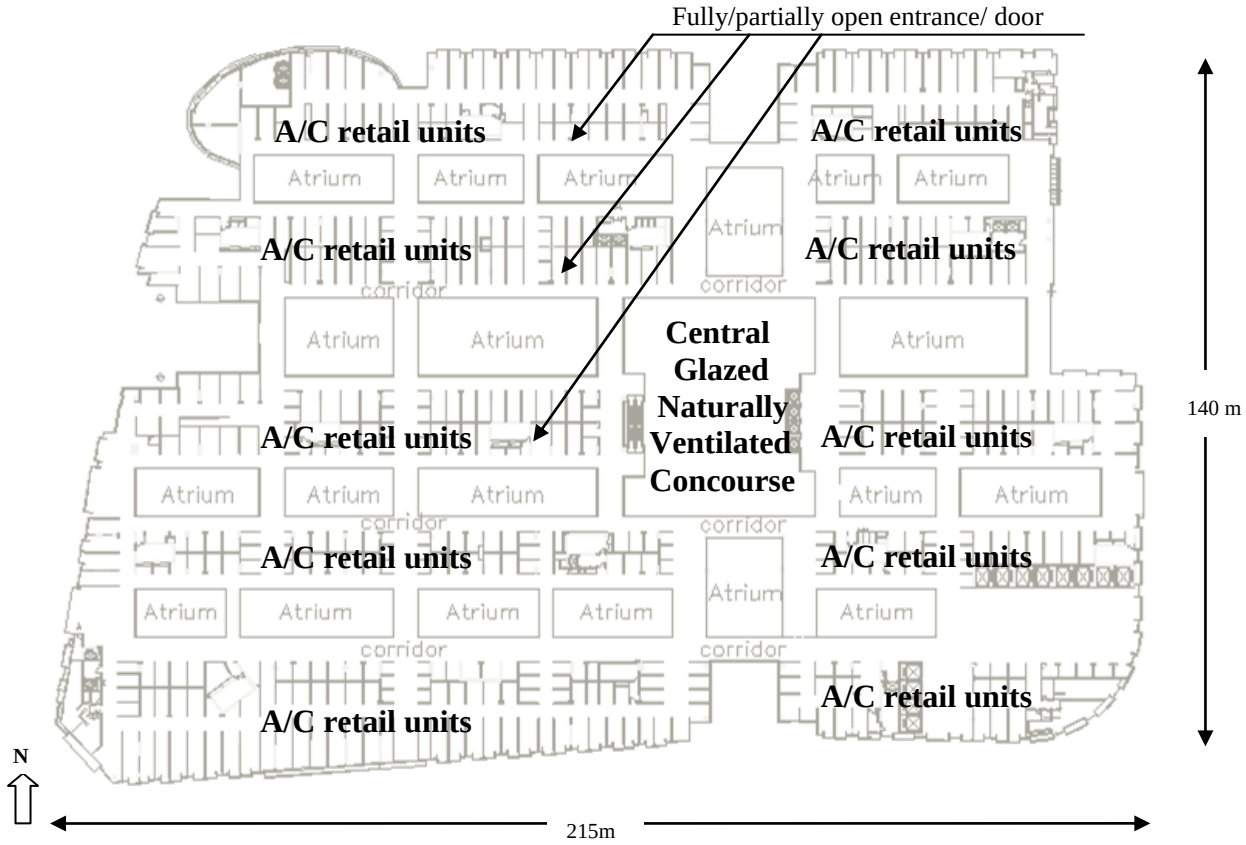

a) Typical floor plan

b) Exterior and Central Glazed Pedestrian Concourse of Guangzhou International Textile City Building (GITC)

Figure 4.2 Guangzhou International Textile City Building (GITC)

The construction of the outside facades are mainly 12 mm. thick tempered glass with aluminium frames, while the curved glazed roofs are 12 mm. thick laminated glass with steel frames. The ground floor and intermediate floors are of reinforced concrete with vinyl tiles. The slab roofs are made of 120 mm thick reinforced concrete with 2.5 mm thick waterproof coating.

The dimensional construction data were collected from the designer and contractor through a painstaking process. Table 4.1 presents some key variables from the TAS construction database used to create the computer models to test the various shading options investigated in this thesis.

Specification	Material	Width (mm)	Solar Absoptance	Solar Reflectance	Conductivity (W/m^oC)	Specific Heat (J/kg^oC)	Density (Kg/m^3)	Vapor Diffusion Factor g/(m.h.pal)	Transmittance
Floor	Vinyl	2	0.48	0.5	N/A	N/A	N/A	N/A	-
	Concrete	120	0.65	0.2	1.74	0.92	2500	$1.58x10^{-5}$	-
Ceiling	Aluminum	4	N/A	N/A	N/A	N/A	N/A	N/A	-
Transparent Roof	Glass	6	0.08	0.08	0.76	0.84	2500	0	N/A
	Laminate	0.76/1.52	0.08	0.08	N/A	N/A	N/A	N/A	N/A
	Glass	6	0.08	0.08	0.76	0.84	2500	0	N/A
External wall	Glass	12	0.14	0.60	1.00	N/A	N/A	99999	0.84
Internal wall	Lightweight Plaster	150	0.40	N/A	1.05	N/A	1840	36.8	-
Slab Roof	Concrete	10	0.60	0.35	0.93	1.05	1800	$2.1x10^{-5}$	-
	Water Proof Coat	2.5	N/A	N/A	N/A	N/A	N/A	N/A	-
	Poly Styrene	10	N/A	N/A	N/A	N/A	N/A	N/A	-
	Concrete	120	0.65	0.2	1.74	0.92	2500	$1.58x10^{-5}$	-

Table 4.1 Properties of some key building elements used in the model

4.4.3 Problems of the GITC by CBTG Ltd. Report

Many tenants complained about the overheating and the high cooling bills after the first year of operation. The building fails to maintain an acceptable temperature of about 26^{o}C in this space. There were thus two preliminary studies carried out during the summer of 2010. The preliminary study by the China Building Technology Group Ltd (CBTG Ltd., 2010) was carried out with 35 selected air conditioned retail shops to represent the whole building during summer. The randomly selected retail shops are located on the fourth floor. The cooling output was also measured in these units and against the designed capacity; an actual ratio of 0.87 was calculated for each of these units. It revealed that more than 75 percent of the tenants are not satisfied due to excessive heat in the building, particularly in the corridors. In over one quarter of the examined shops, the indoor temperatures were higher than 28°C in the afternoon, even when the cooling system had been running at full capacity for over 12 hours (Figure 4.3). The high levels of solar gain in the space were the major cause of the overheating in the atrium spaces and lack of the air curtains were a direct cause of the heavy cooling loads.

The GITC building, ground floor and corridors were all naturally ventilated while the surrounding retail units were air-conditioned daily from 0800h-2000h. The total cooling capacity of the plant was 21,837 kW over the total air-conditioned area of 120,000 m^2, so the average cooling load index was 180 Wm^{-2} which was designed according to the National Standard for retail units (CBTG Ltd., 2010). Almost all the doors of these retail shops were kept fully open by tenants to attract potential clients passing by and to extend their trading area to their own corridor. Most of these doors were unequipped with air curtains, so the air conditioning in each retail shops ran improperly by failing to separate the air conditioned space and the naturally ventilated corridor; an anomaly resulting in heavy electricity bills.

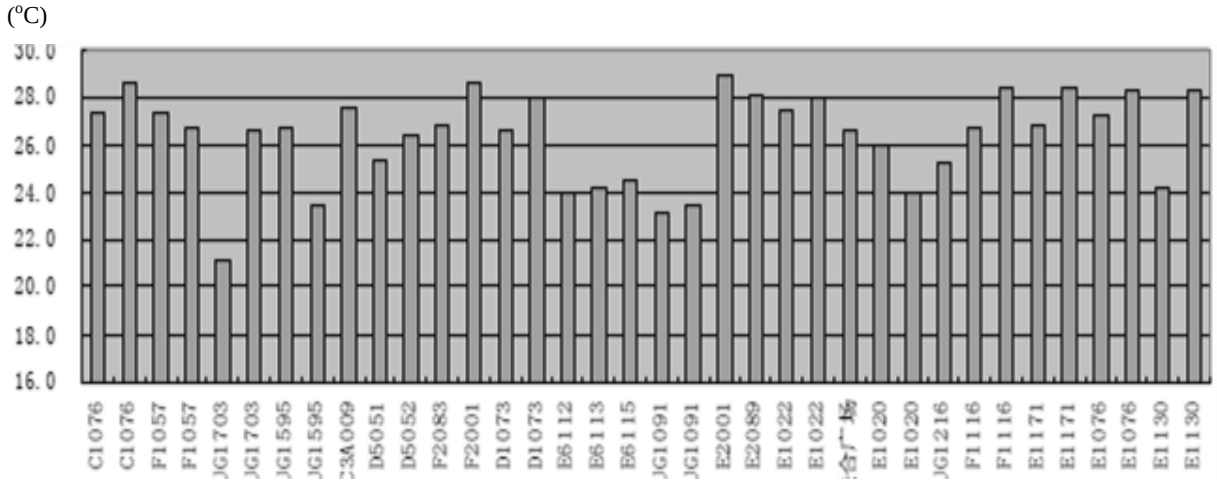

Figure 4.3 Average indoor air temperatures within sample retail shops (CBTG Ltd, 2010)

A parallel survey of commercial units was carried out by using mechanical equipment which mapped four environment variables over the main glazed pedestrian concourse and corridors: the daylight factor, air temperatures, relative humidity and air movement (Jingyan, 2012). This survey also highlighted that the high surface temperatures mainly occurred on the ground floors, internal surfaces of the roof glazing and the walls exposed to the direct sunlight (Figure 4.4).

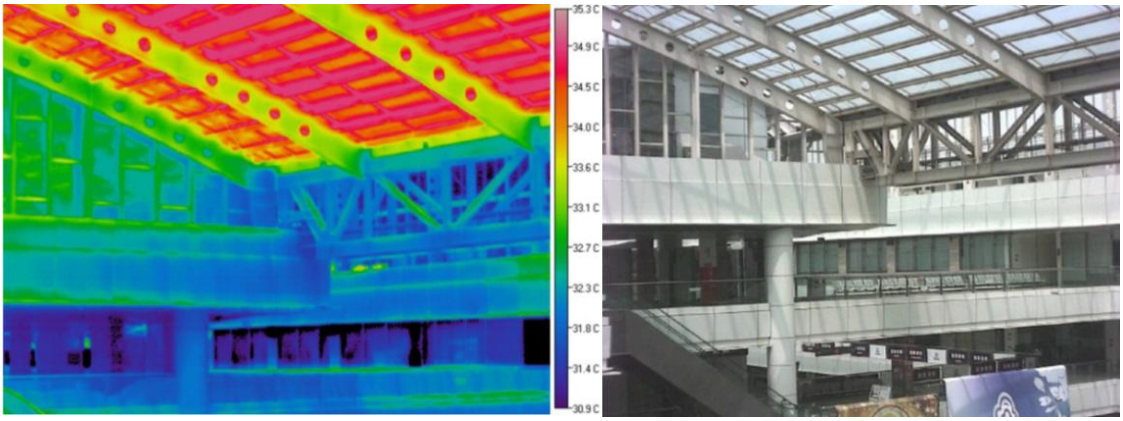

a) Central transparent roof and air-conditioned offices on the top floor

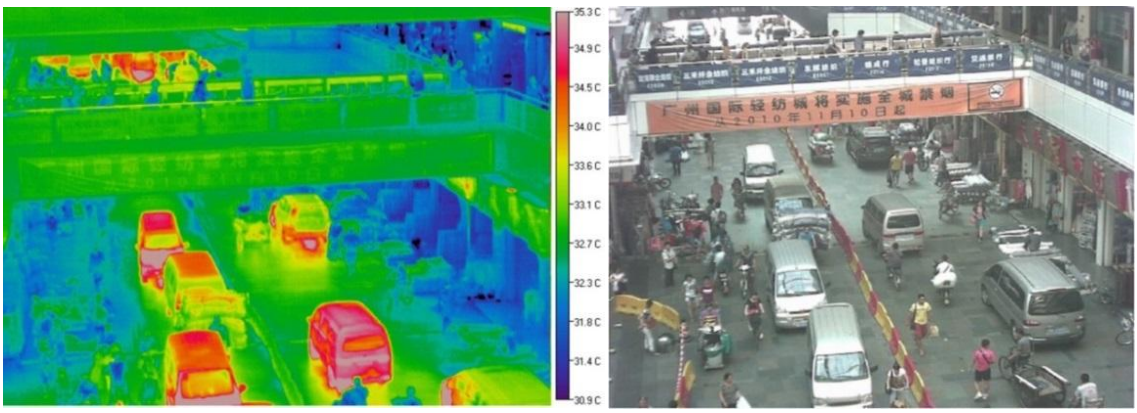

b) Air-conditioned retails around main the ground floor glazed pedestrian concourse

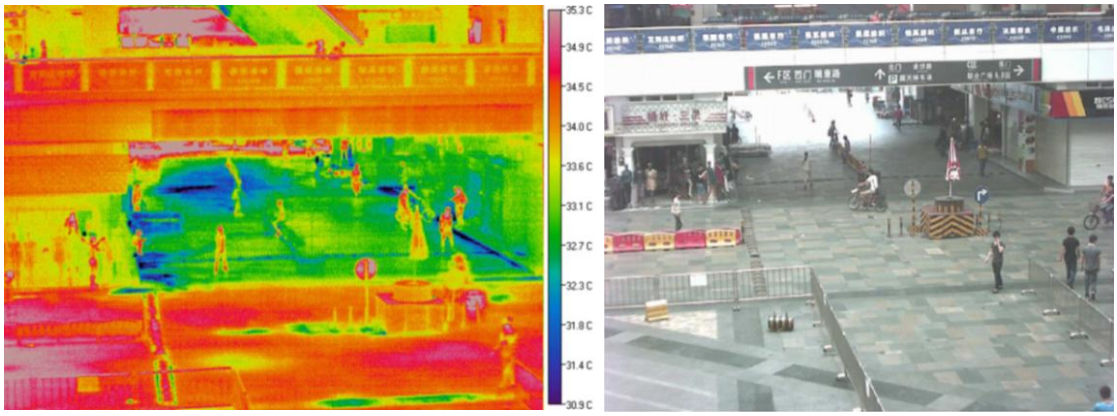

c) Ground floor central glazed pedestrian concourse

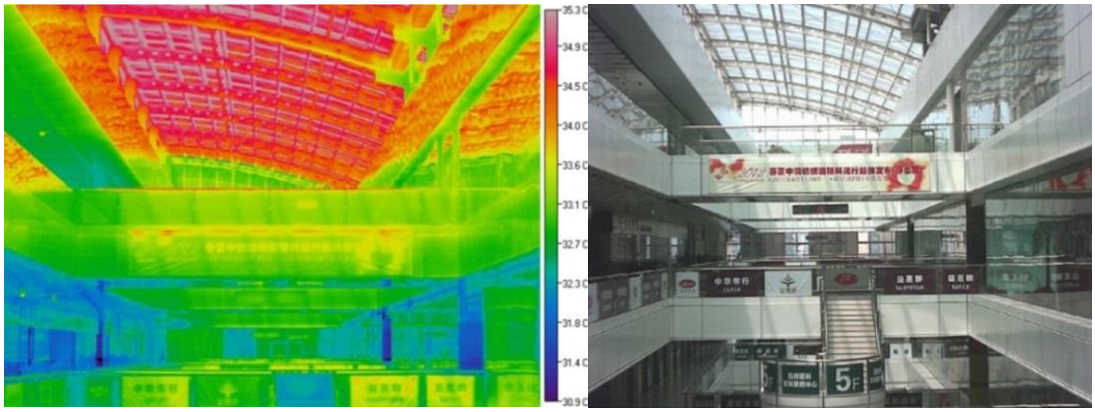

d) Transparent roof and air-conditioned offices on the top floor

Figure 4.4 Thermal imaging maps by infrared radiant heat sensitive camera (ModelTH9100MV/WV) and the corresponding real photos (Jingyan, 2012)

4.4.4 The Variables Measured and Equipment Used

Additional data was collected from field measurements carried out for seven consecutive days from 30th July to 5th August 2011 for the purpose of the calibration of the two models: the dynamic thermal model and the daylighting model.

- The air temperature and relative humidity were measured over eight locations: one outdoors on the roof, and one for each corridor of the seven floors in the main glazed pedestrian concourse; all measurements were taken from 1.50 m above the floor (Figure 4.5). The hygrothermal conditions were recorded by simple HOBO U23-001 data loggers wrapped with alumina foil and synchronised before the monitoring.

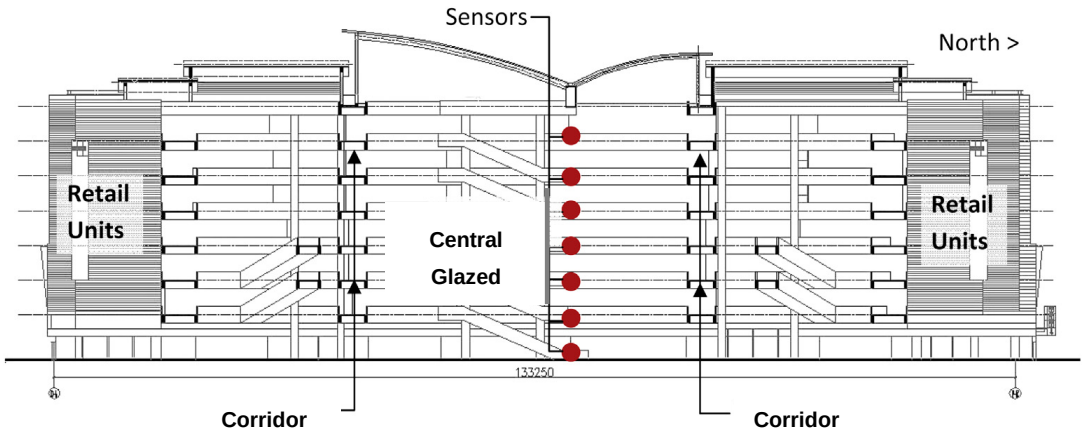

Figure 4.5 Section of the central glazed pedestrian concourse with locations of hygrothermal sensors (dots)

- The airflow speed was measured by hot-bulb anemometers ZRQF-F30 at the 12 entrances of the streets, from 3m above the ground and at the centres of the 15 openings of the roof canopies (Figure 4.6a and 4.6c). ZRQFs monitored the speed but not velocity as it accounted all directions of the airflow over the heated sphere sensors. Although hot-bulb anemometers have a high 3% accuracy, the actual accuracy would be 10-20 percent, due to the instability of the wind during the measurement.

a) A ground floor plan of the building showing the central glazed spaces, indoor streets and model zoning i = location1, 2,…, 22 and j = floor1, 2,…,7

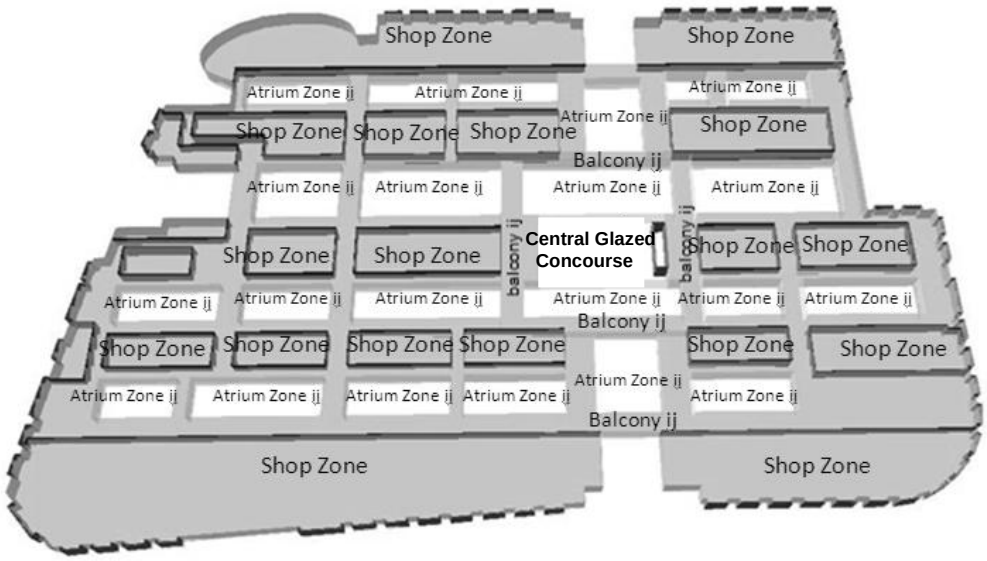

b) A typical floor plan showing zoning of the central glazed spaces, corridors, and units (i=2 – 7)

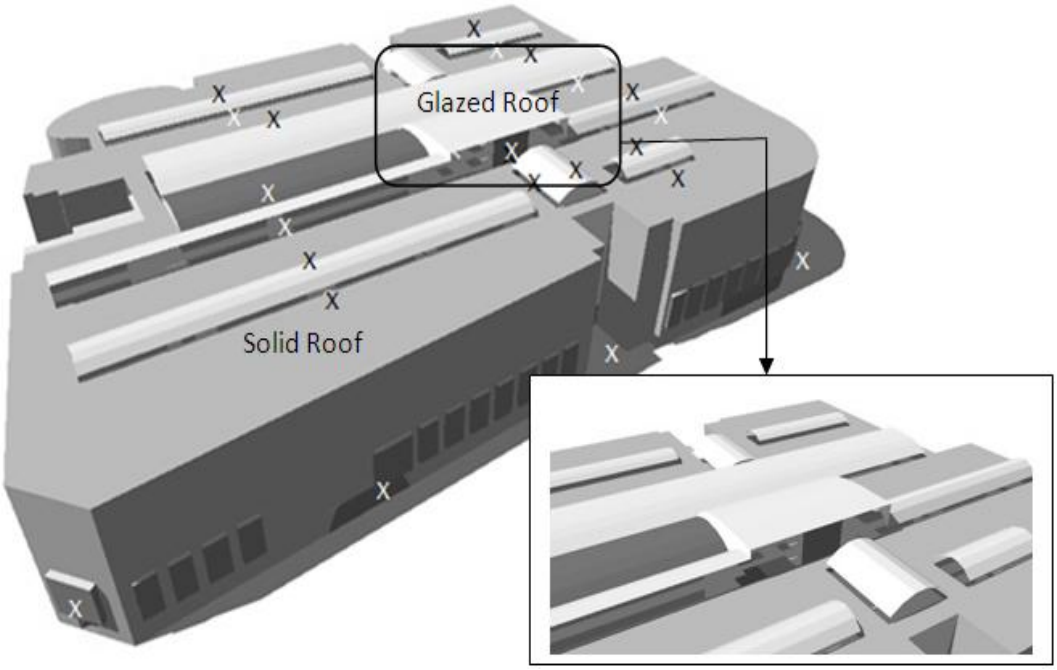

c) Top view of the computer model and the details, showing the central glazed concourse, side openings

Figure 4.6 Hot-bulb Anemometres ZRQF-F30 and the position of the sensors in the computer model (Air Flow Sensors X)

- The illuminance was also measured. Then the daylight factor was calculated over selected locations on the overcast day of the 1st September 2011. The locations included two at roof level to get a reference baseline, an array of 2m × 2m covering the whole ground floor of the central pedestrian concourse and every 2m on the walkways on the upper floors. This was done using Lux metre TES-1334A with accuracy ±3percent. In order to derive daylight factors, each pair of the illuminance metres (the indoor metre and a roof one for outdoor reference) was calibrated and synchronised.
- The 35 randomly selected retail units on the lower four floors and offices on the upper floors had their room temperatures measured together with air-conditioning operational data during the afternoon. The cooling output was also measured in these units and against the design capacity and then an actual ratio of 0.87 was estimated for each of these units.
- Out of the seven days measuring period, the measured result on the 31st August 2011 represented a clear summer day; the 1st September 2011 represented an overcast summer day. Both days were used in the calibration of the thermal model.

4.4.5 Field Monitoring Results and Discussions

There were various meteorological conditions during the monitoring session: clear hot days, overcast hot days and mixed with intermittent showers. A week from 30th August to 5th September 2011 was selected to be examined. Results from 30th to 31st August 2011 and 5th September 2011 represented three hot clear days and results from 1st to 4th September 2011 then represented three consecutive hot overcast days.

(i) The Air Temperature and the Airflow Speed

Figure 4.7 presents the air temperatures on the ground floor, third floor and seventh floor of the central pedestrian concourse including outdoor air temperatures.

During the clear summer days, the external air temperatures were between internal 25°C and 38°C. It is very interesting to note that the monitored results show that the internal air temperatures at the top floor of the glazed pedestrian concourse were very close to the external air temperatures during the clear summer day, (30th-31st August and 5th September), and these days were all fairly windy, particularly during the daytimes when

the wind speed went beyond 4.0 $m \cdot s^{-1}$.The measured airflow speeds recorded during day time were all around 1.0 $m \cdot s^{-1}$for all the points on both the street and roof levels throughout the day.

During the cloudy summer days, the external air temperatures were between 25^{o}C and 36^{o}C, the internal air temperature was around two degrees higher than the external air temperatures and the wind was remarkably weaker (1st and 3rd September). There was no measurement of airflow speed on these days, but the wind data from the weather station showed the wind being low.

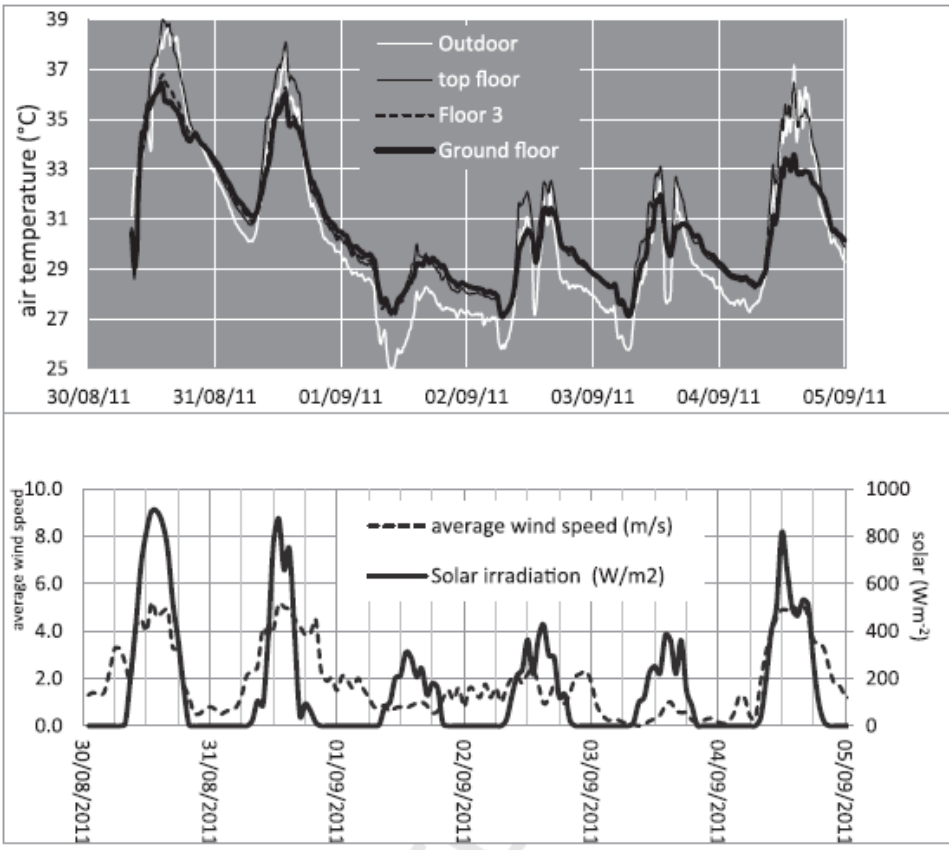

Figure 4.7 Measured air temperatures and wind speed

In general, during both hot/clear days and hot/overcast days, particularly in the afternoon, the measured results clearly show that the temperature stratification would occur at high level inside the glazed pedestrian concourse, as the internal air temperatures considerably exceeded the external air temperatures, thereby causing the thermal condition to be extremely hot, especially on the top floor.

(ii) Cooling Loads

The total cooling load of the whole existing building was 28,000 kW over the seven floors of 120,000 square metres, giving the average cooling power of 180 Wm^{-2} (CBTG Ltd,2010). It was reported that the indoor air temperature was over 28°C in most of 35 selected air conditioned retail units and this resulted in many of them replace their own cooling units and increase the cooling capacity doubled for extra cooling which cause the entire building' electricity supply shortage in some regions.

(iii) Daylight Factors

Figure 4.8 shows the measured results over the selected floors: the ground floor central pedestrian concourse, the first floor corridor and the second floor corridor. The outdoor lighting standard was based on the critical illumination 5,000 Lux specified.

The range of Daylight Factors from the ground floor concourse space to the third floor corridor was between 0.1 - 8.8 percent. There were 58.3 percent of measured areas which had good lighting conditions (daylight factors over 1.5percent). Hence, although the natural light benefits most of the circulating areas within the large glazed pedestrian concourse space, the penetration of the daylight through the skylight roof leads to too much lighting effect on the higher circulating areas and too little lighting effect within the perimeter area, especially on the ground floor and the balconies on the lower floors.

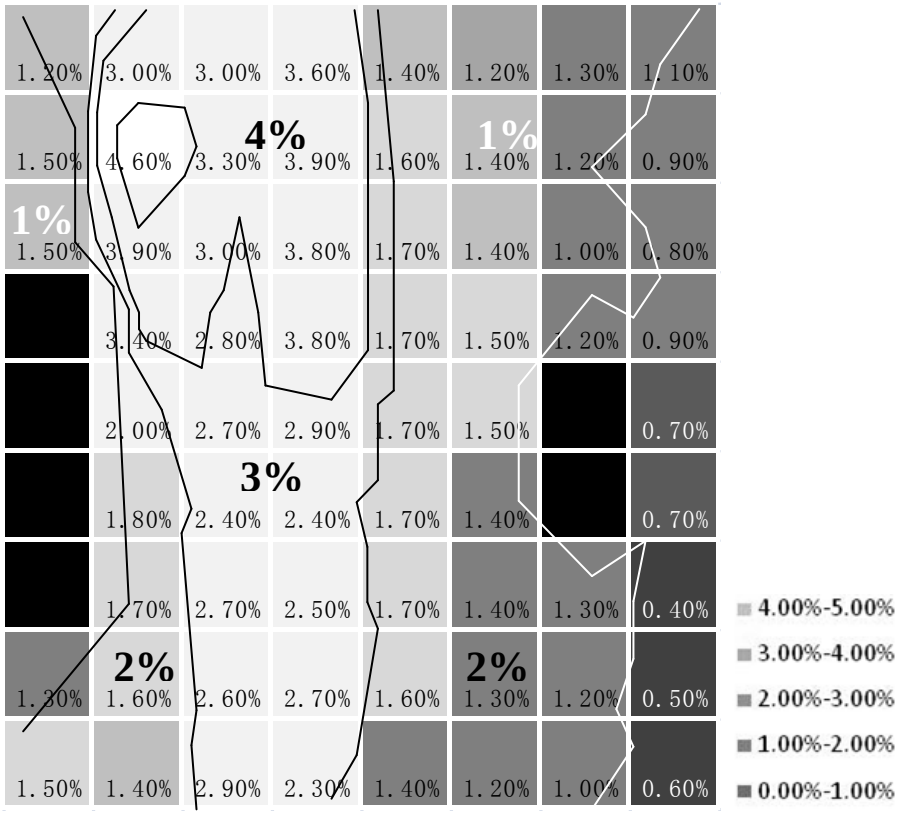

(a) The ground floor central pedestrian concourse

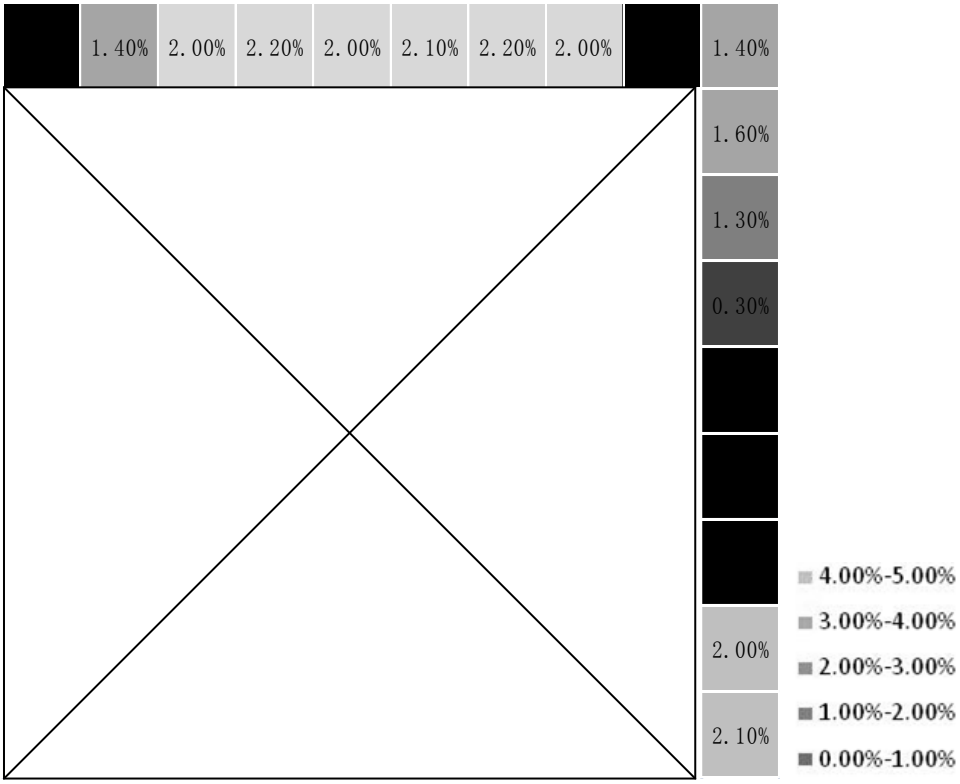

(b) The first floor corridor

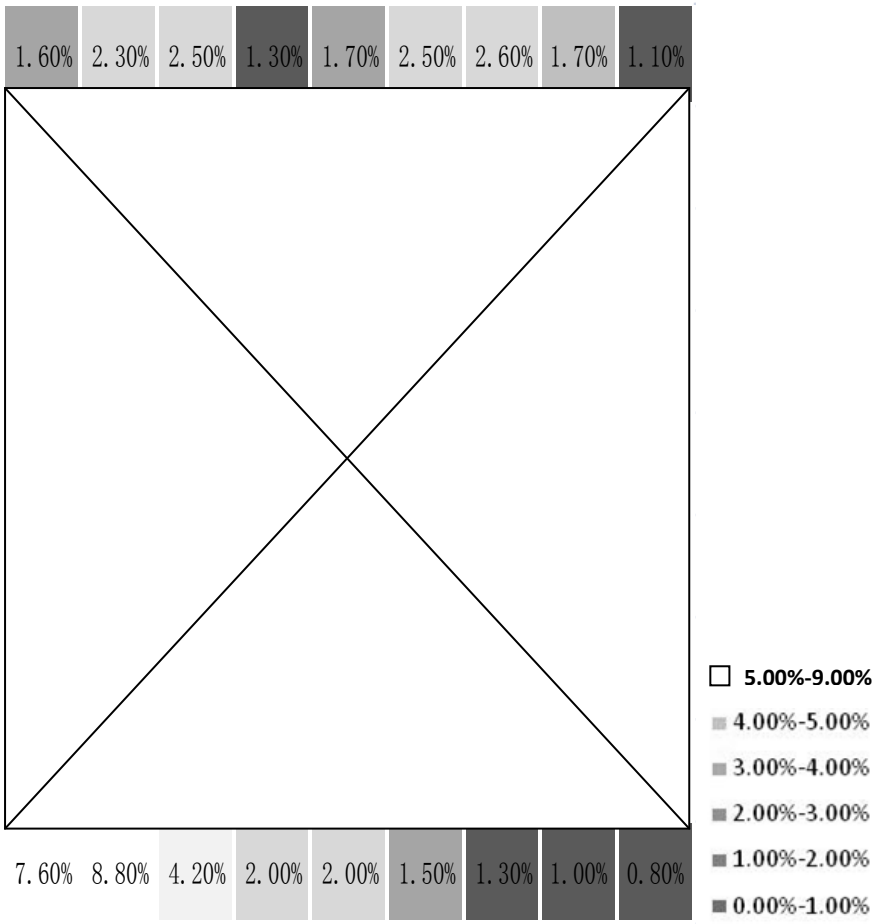

(c) The second floor corridor

Figure 4.8 Measured DF distributions within the central pedestrian concourse

4.5 The Large Glazed Pedestrian Concourse with Air-Conditioning of Suvarnabhumi Airport Terminal

Suvarnabhumi is located in Samut Prakarn about 25 kilometres east of downtown Bangkok, Thailand; it was officially opened in 2006. The airport serves as regional gateway and connecting point for various foreign carriers. The building was designed by Helmut Jahn. This airport is the sixteenth busiest in the world and the sixth busiest airport in Asia (Lamprecht, 2013).

4.5.1 General Characteristics of Samut Prakarn's Weather

Samut Prakarn is located at latitude of 15.00^{o} north and longitude of 100.00^{o} east. It is considered to have a tropical climate, with high temperatures and high humidity levels throughout the year. Samut Prakan is one of the central provinces of Thailand. It is settled to the east and south of Bangkok. This province is a part of the Bangkok Metropolis.

Meteorological statistics show that summer is between March and June, while the hottest month in Thailand is April and May with the highest daily maximum temperature at 38.5^{o}C. Average maximum air temperature is 30.0^{o}C (Figure 4.9). Winter is between November and February with daily minimum temperature at 20.0^{o}C. The daily minimum is reached between 0500h-0700h and the maximum 1200h-1600h. The time of daily maximum and minimum seldom varies by more than an hour throughout the year. A fairly rapid rise in temperature take place during the first six or seven hours of daylight and after reaching the maximum the temperature falls gradually in late afternoon and slowly throughout the night.

The average annual mean relative humidity is 71.9 percent. The 24 hours mean relative humidity varies significantly in the range of from 42~94 percent.

The highest radiation received is in the month of March when most places experience a dry season and the sky is generally clear during the day and at night. The average daily range for March is 7.0 kWh$\cdot$m^{-2}.

Annual weather data for 2012 was collected from the local meteorological office as the representative yearly data. The data set included the hourly figures of seven recorded variables: global and diffused solar radiation, air temperature, relative humidity, cloudiness, wind speed and direction (Appendix B). This set of weather data was used in dynamic thermal modelling to predict the annual energy consumption for the base case; the model being created to compare the performance of the shading cases. This would allow energy savings to be assessed for the shading options.

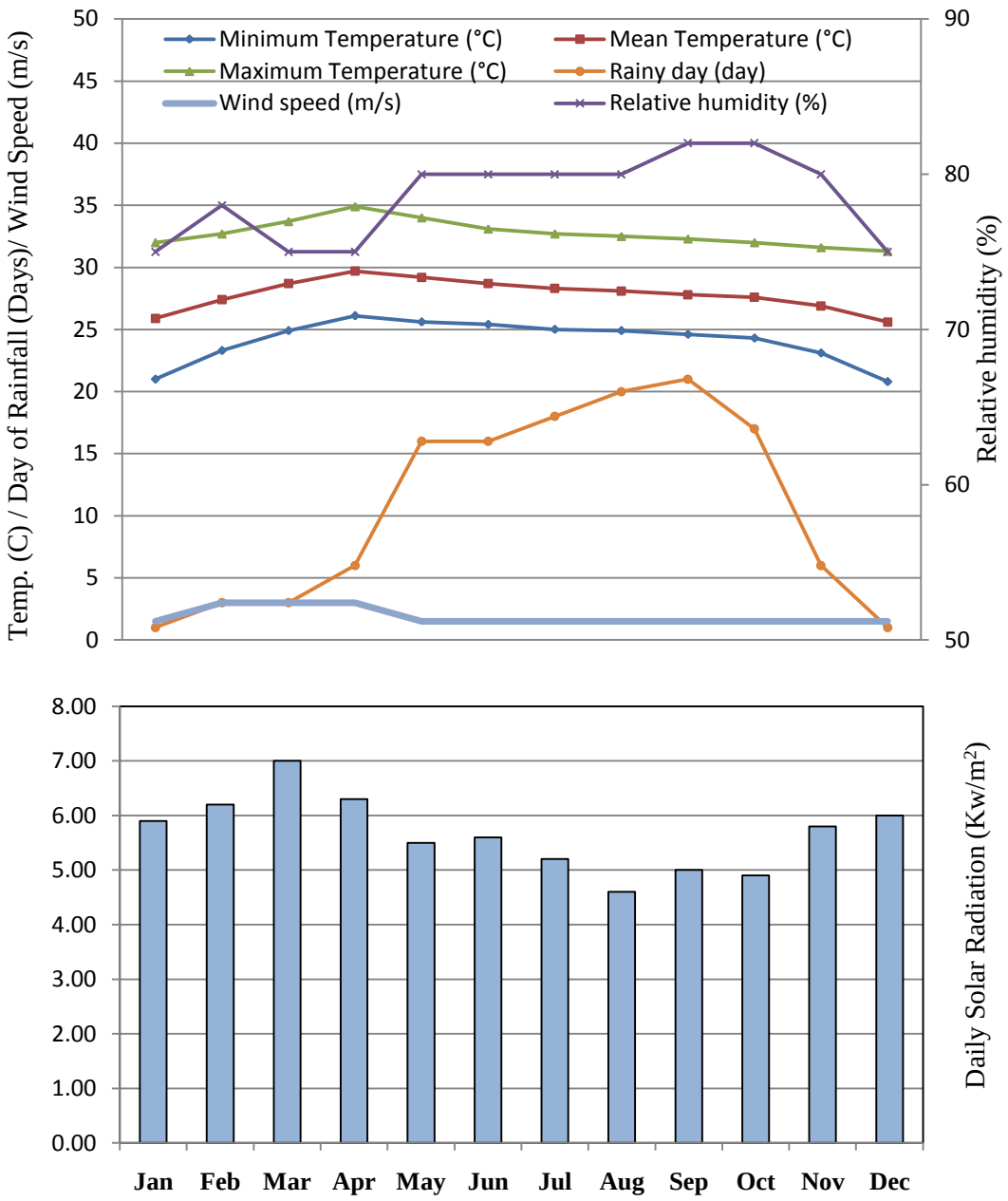

Figure 4.9 Climate data for 30 year average (1961-1990) - Bangkok Metropolis (http://www.tmd.go.th)

4.5.2 Building Description of Suvarnabhumi Airport Terminal

Suvarnabhumi Airport is situated in the Bang Phli district of Samut Prakan province. This airport is located at 13°40'52" north latitude and 100°44'50" east longitude. Suvarnabhumi airport serves both domestic and international passengers, with a useable area of around 563,000 square metres (6,060,081 sq ft). The single passenger terminal building is 111 metres in width, 444 metres in length, 6 floors and 2 basements and faces north, with a useable area of around 140,000 square metres (1,506,960 sq ft) (Figure 4.10).

1st Floor - Bus and Taxi Service

2nd Floor- Domestic and International Arrivals

3rd Floor - Shops, Restaurants and CIP rooms

4th Floor - Domestic and International Departures comprises of Thai Airway International Premium Passenger Service, immigration, customs, airline check-in counters and Airport International Counters.

5th Floor - Thai Airways International Public Co., Ltd. & Star Alliance Offices

6th Floor - View Point

a) Viewing the departure lounge from the 6th floor view point

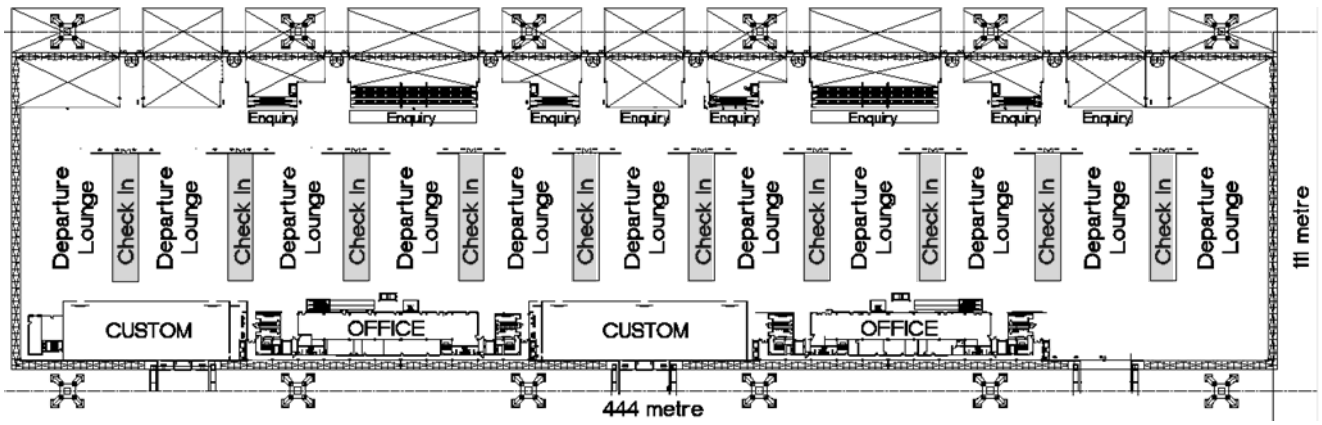

b) Departure lounge floor plan

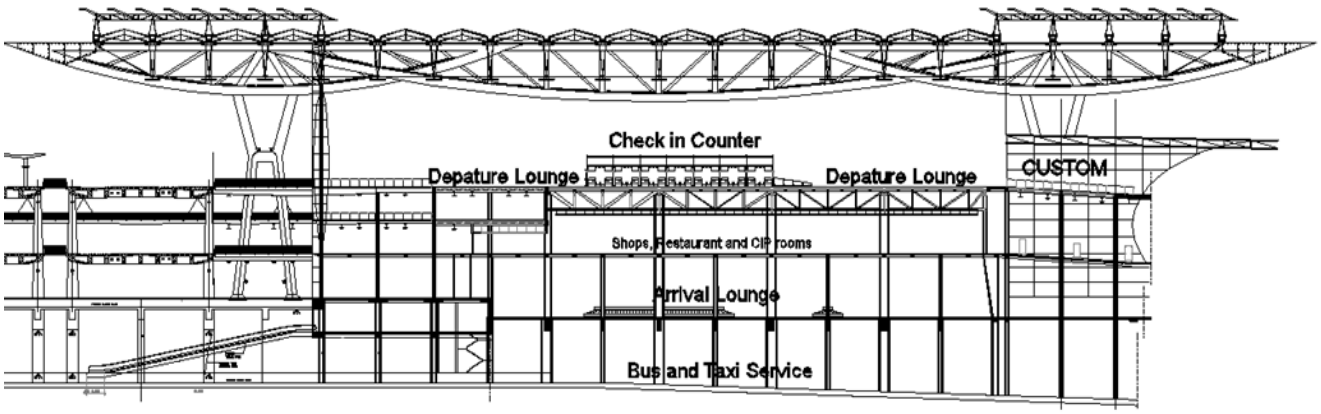

c) Terminal Building Section

Figure 4.10 Departure lounge of Suvarnabhumi Airport Terminal

The construction of the terminal facades is mainly 12 mm. thick laminated tempered glass with supported steel trusses, while the terminal roof consists of insulated metal sandwich panel facing south and low-e coated hard coating glass facing north are 12 mm. thick laminate glasses with steel frames. The ground floor and intermediate floors are of 23 cm. thick precast concrete.

The dimensional construction data were collected from the architect's firm. Table 4.2 presents some key variables from the TAS construction database, used to create the computer models to test the various shading options in this thesis.

Specification	Material	Width (mm)	Solar Reflection	Daylight Transmittance	Inner Daylight Reflection	Outer Daylight Reflection	Shading Coefficient	U-Value	R-Value
Floor	Terrazzo tiles Concrete	3 200	N/A	N/A	N/A	N/A	N/A	N/A	13.4
External wall	Laminated glass	12	0.22	0.30	0.16	0.20	0.45	5.6	0.182
Internal wall	Aluminium cladding	10	N/A	N/A	N/A	N/A	N/A	N/A	2.045
Metal sheet roof	Insulated metal sandwich	100	N/A	N/A	N/A	N/A	N/A	0.375	2.67
Transparent roof	Low E coated glass	12	0.2	0.02	0.12	0.16	0.15	4.5	0.194

Table 4.2 Properties of some key building elements used in the model

Table 4.3 presents the passenger statistics, the occupancy was 145,211 people over a 24 hour period, based on the passenger statistics of Airports of Thailand (AOT, 2012).

Year	Embarked	Disembarked	Total	Direct Transit	Grand Total
2006	5,523,477	5,670,336	11,193,813	458,856	**11,652,669**
2007	19,691,507	19,849,426	39,540,933	1,669,149	**41,210,081**
2008	18,501,099	18,595,694	37,096,793	1,506,697	**38,603,490**
2009	19,435,337	19,609,567	39,044,904	1,455,320	**40,500,224**
2010	20,566,476	20,687,417	41,253,893	1,531,074	**42,784,967**
2011	23,104,464	23,209,373	46,313,837	1,597,067	**47,910,904**
2012	25,672,146	25,970,442	51,642,588	1,359,740	**53,002,228**

Table 4.3 Total international and domestic passengers
(AOT, 2012)

4.5.3 The Variables Measured and Equipment Used

Additional data was gathered by using field measurement carried out for twenty consecutive days from 12th September to 1st October 2012 for the purpose of calibrating the two models: a) the thermal model including the air temperatures and glazed roof surface temperatures and b) the daylighting model including illuminance and daylight factor.

- Temperature and humidity measurement was done by Squirrel Grant (SQ2010) data loggers. The accuracy of the data logger is 1%. The measured data can be recorded and transferred to a PC by Squirrel View software. The air temperatures were measured simultaneously over six locations from the 4th, 5th and 6th floors in the departure lounge, all from 2.0 metres above the floor. The other temperatures were recorded in the 6th floor ceiling, underneath the transparent roof and the transparent roof surface (Figure 4.11a and 4.11b). The humidity was also measured in the 6th floor.
- Lux metre TES 1330 (±3percent) was used to measure illuminance and converted to daylight factor which will be analysed and compared with predicted results from lighting simulation results. Lighting measurement was carried on an overcast sky day, the 28th September 2012. The illuminance was measured every 2.0 metres between check in counters at the walkways; between counter check in on the passenger lounge floor; and outdoor at one single moment.
- The cooling loads output was derived from the main supplier District Cooling System and Power Plant Ltd. (DCAP, 2011).

- Out of the twenty day measuring period, the measured result on the 12th September 2012 represented a clear summer clear day; the 28th September 2012 represented an overcast summer day. The data from these two days were used in the calibration of the thermal model.

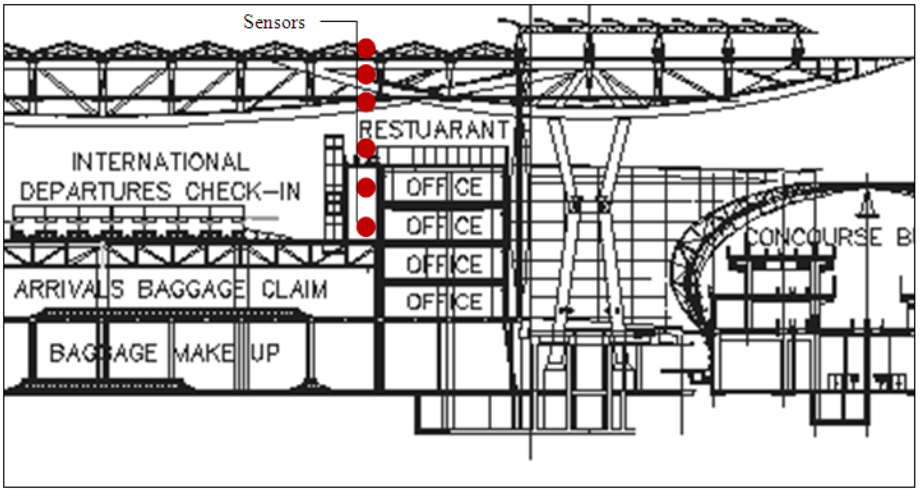

(a) Section of the Airport Terminal building with location of thermal sensors

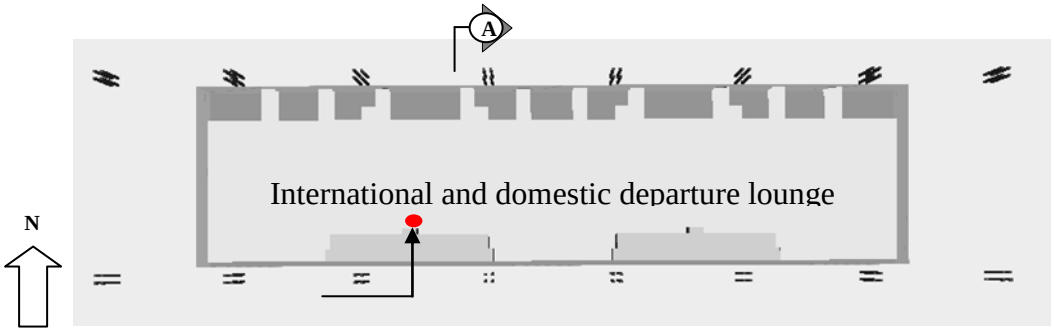

(b) Plan of the Airport Terminal Building with Location of Thermal Sensors

Figure 4.11 Positions of the Sensors in the Airport Passenger Lounge

4.5.4 Limitation of Experimental Equipment

The data logger types Squirrel Grant (SQ2010) and lux metre (TES 1330) have been calibrated during manufacture and no provision is made for the user to make nay adjustment. However, before being used in this field experiment, the instrument had been checked to ensure that it would perform correctly by following the procedure prescribed by the manufacturer. The thermocouple sensors of the data logger were wrapped with alumina foil and synchronised before the monitoring in order to reduce the number variable under consideration which would affect the accurate results of the measurement.

4.5.5 Field Monitoring Results and Discussions

There were various meteorological conditions during the monitoring sessions: clear hot days and overcast hot days mixed with intermittent showers. Results from 15th to 16th September 2011 and 28th September 2011 represented three overcast hot days and the rest were clear hot days.

(i) The Air Temperature and Relative Humidity

It can be seen that the internal thermal environment on the departure lounge floor was not significantly affected by the external weather conditions, since this area is air-conditioned.

During both hot clear and cloudy days, the external air temperatures were between 24°C and 35°C, while the internal air temperature over the twenty days remained stable and marginally swung between 21.8°C and 26.9°C within the departure lounge floor. Slightly higher indoor air temperatures normally occurred between 1200h to about 1700h, when the outdoor temperature gradually started to rise. The internal air temperatures considerably exceeded the CIBSE (2006) standard at 24°C, which occurred almost every day (Figure 4.12).

The internal thermal environment over the 6th floor ceiling was affected by the outside conditions. The daily air temperature was in a range of between 24.6°C to 35.4°C, even though it was cooled down by air-conditioning. Solar radiation greatly influenced the glazed roof surface temperature. The air temperatures gradually started to rise during the afternoon. Then the highest glazed roof surface temperature recorded was 66.9°C, which occurred on 23rd September at 1300h. These surface temperatures fluctuated between 25.5~66.9°C. Around midday for 4~5 hours, the temperature was over 40°C. The high glazed roof surface temperatures are enhanced by direct radiation and convection from the heated air. As a result, the operative temperature within the large glazed pedestrian concourse leads to overheating and thermal discomfort, particularly in the upper floor (Pan et al., 2010).

In general, during both hot/clear days and hot/overcast days particularly in the afternoon from 1200h to 1700h, the graph clearly shows that the temperature stratification would occur at high level in the long-span glazed roof over a large pedestrian concourse, as the internal top floor ceiling temperatures considerably exceeded the external air

temperatures causing the thermal condition on the top floor to be extremely hot, especially from early afternoon to late afternoon.

Even though measurements revealed that the internal air temperature in the occupied zones was not affected by the external weather conditions, the temperatures also exceeded the standard between 22.0^{o}C and 24.0^{o}C for the departure lounge in the airport terminal, during summer conditions (CIBSE, 2006).

Humidity has a significant effect on thermal comfort, especially in hot climates. In normal circumstances, humidity in the range 40~70 percent RH is acceptable. Average relative humidity on the passenger lounge floor was within 43.7 percent and 63.0 percent. The mean relative humidity was 55.0 percent. The mean values of relative humidity were within the CIBSE (2006) standard.

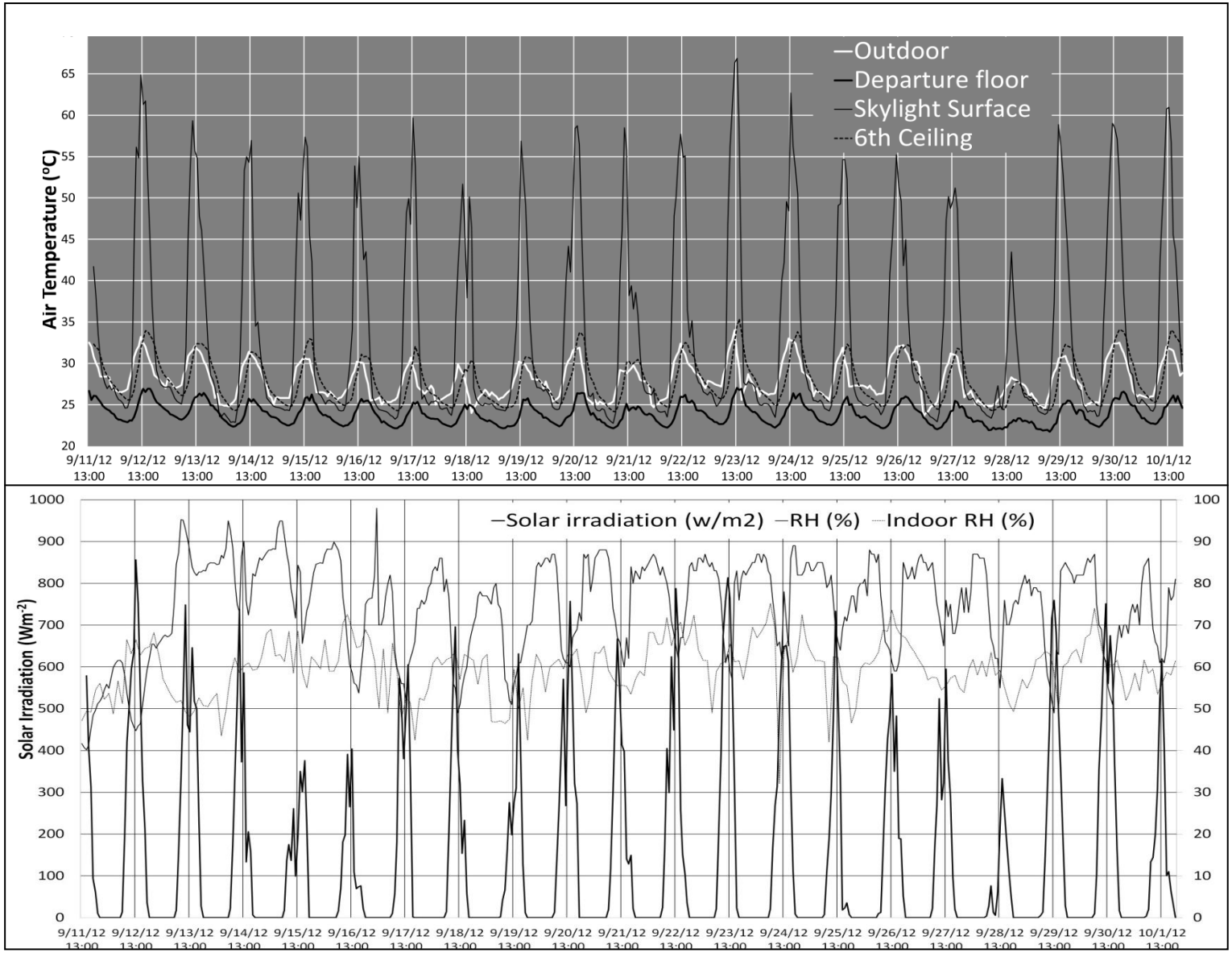

Figure 4.12 Measured air & transparent roof temperatures compared with solar irradiation and RH

(ii) Energy Consumption in the Airport

Energy use for cooling in a tropical climate is the largest area of use on a national level. The best way to determine energy consumption is to analyse utility bills over a period of time, as part of the energy assessment of a building (Patrick et al., 1993).

Air-conditioning at Suvarnabhumi Airport Terminal building is based on a chilled water cooling system. The amounts of chilled water to cooling coil for air-conditioning system in the airport are summarized in Table 4.4.

YEAR	2006	2007	2008	2009	2010
Jan	-	7.43×10^7	8.00×10^7	6.73×10^7	8.12×10^7
Feb	-	7.78×10^7	7.84×10^7	7.88×10^7	8.23×10^7
Mar	2.91×10^7	1.01×10^8	9.34×10^7	9.47×10^7	9.35×10^7
Apr	1.99×10^7	9.71×10^7	9.69×10^7	9.49×10^7	9.70×10^7
May	2.09×10^7	9.73×10^7	9.67×10^7	9.32×10^7	9.89×10^7
Jun	2.40×10^7	9.76×10^7	9.33×10^7	9.25×10^7	9.12×10^7
Jul	5.68×10^7	9.63×10^7	9.30×10^7	9.04×10^7	9.36×10^7
Aug	5.82×10^7	9.60×10^7	9.33×10^7	9.05×10^7	9.09×10^7
Sep	6.85×10^7	9.05×10^7	8.53×10^7	8.29×10^7	8.84×10^7
Oct	9.57×10^7	8.87×10^7	9.06×10^7	8.54×10^7	8.73×10^7
Nov	9.01×10^7	7.56×10^7	7.22×10^7	7.90×10^7	7.73×10^7
Dec	7.73×10^7	8.21×10^7	6.56×10^7	7.83×10^7	8.16×10^7
MBTU/h	**5.40×10^8**	**1.07×10^9**	**1.04×10^9**	**1.03×10^9**	**1.06×10^9**
MBTU/h sq ft	**89.21**	**177.23**	**171.40**	**169.63**	**175.43**
MJ/ h sq m	**1,031.12**	**2,012.72**	**1,946.51**	**1,926.41**	**1,992.28**
kWhm^{-2}	**281.42**	**559.10**	**540.70**	**535.11**	**553.41**

Table 4.4 Amounts of chilled water to cooling coil of Suvarnabhumi Airport (DCAP, 2011)

(iii) Internal Lighting Condition

Figure 4.13 shows the measured daylight factor results over the passenger lounge floor. The outdoor lighting standard was based on the critical illumination 5,000 Lux specified. Throughout the measurements, the range of daylight Factors from the ground floor departure lounge was between 0.63 – 2.75 percent. Only 18.8 percent could be shown to have an adequate level of daylight as recommended by CIBSE (2009). Since Suvarnabhumi Airport Terminal roof was designed in a saw tooth form with metal sheet roofs facing south and glazed roofs facing north, a large quantity of daylight can enter from the northern aspect of the transparent roofs. The natural light then only benefits some areas underneath the airport's transparent long-span glazed roof. In fact, the

passenger lounge of Suvarnabhumi Airport Terminal building was not able to receive an adequate quality of natural light into the building interior.

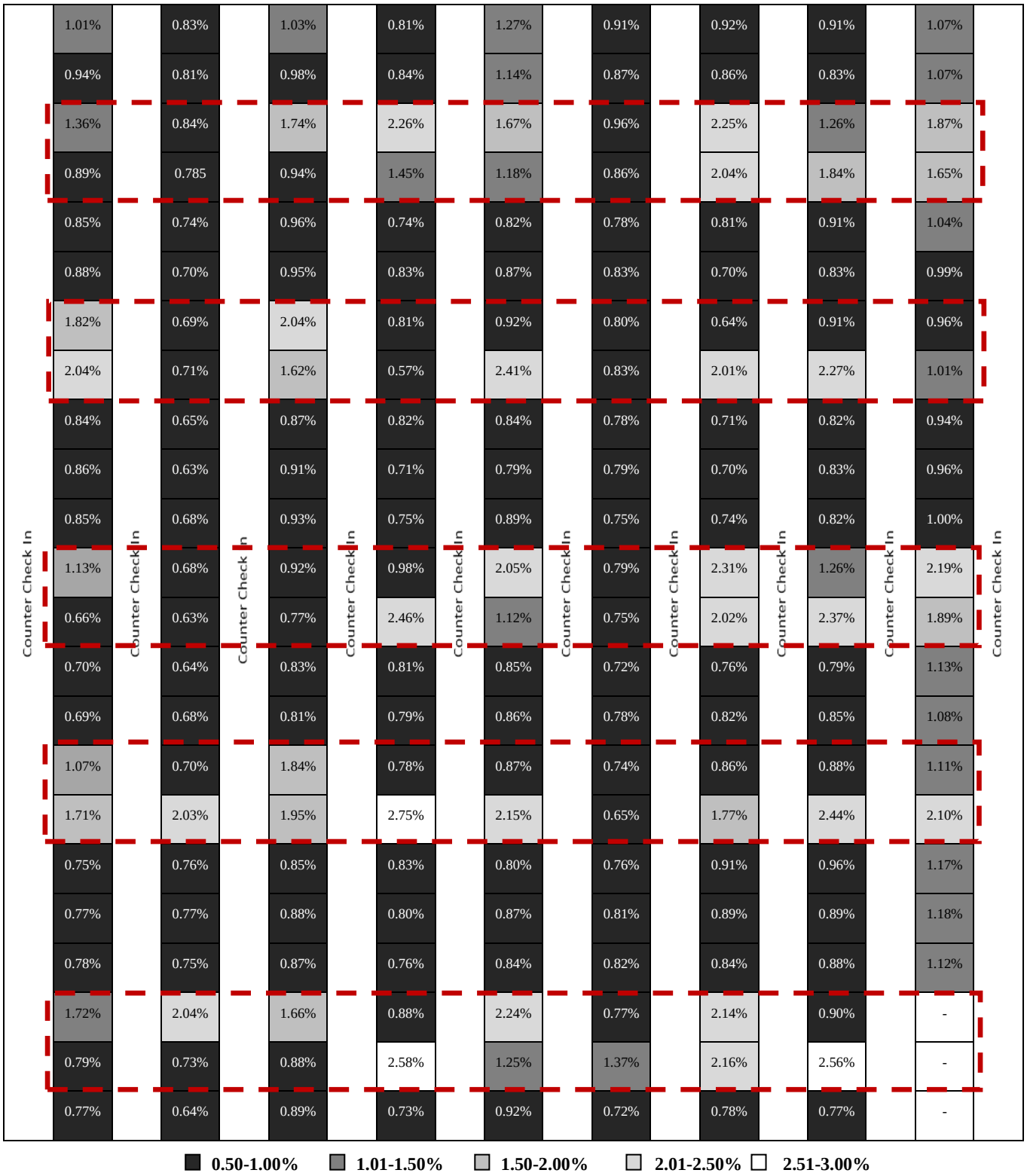

Figure 4.13 Measured daylight factor on the passenger lounge floor at 13.00-14.00 on 28th September 2012

4.6 Conclusion

The field studies were done through site measurement and data collection work. The measured data included key indoor variables such as air temperatures, surface temperatures and illuminance inside both case studies conducted with mechanical instruments over a group of selected locations. Cooling loads were derived from statistics gathered from the building manager and agent. The data was used to calibrate the computer models which will be explained future in chapter 6. For the naturally ventilation case study in China, the air flow speed was further monitored at the entrances and opening of the roof.

According to the measurements for the long-span glazed roof over large pedestrian concourses with natural ventilation in the GITC results indicated that the external air temperatures were between 25^{o}C and 38^{o}C. The measured internal ground floor air temperatures were between 28^{o}C and 36^{o}C. The top floor temperature can reach up to 39^{o}C which were far more common to keep the ambient temperature around 21~25^{o}C with the CIBSE (2006) standard.

The internal temperature at the top floor balcony of the large glazed pedestrian concourse followed very closely the external readings during the clear days, when the wind speed went beyond 4 ms^{-1}. These spaces were fairly well ventilated during these days. The internal temperature at the top floor balcony was around two degrees higher than the external reading during the cloudy days, while the wind data from the weather station was low. Hence it is believed that the ventilation was weak during these days and the heat inside the atria was not dissipated effectively to the outside and this led to higher internal than external temperature.

Although the natural light benefits most of the circulating areas within the large glazed pedestrian concourse space, the penetration of the daylight through the skylight roof leads to an excessive lighting effect on the higher circulating areas and a too low lighting effect within the perimeter area, especially on the ground floor and the balconies on lower floors.

For the long-span glazed roof over large pedestrian concourse with air-conditioning, results indicated that the internal air temperature at the passenger lounge floor remained stable and was not affected by the external conditions. Whereas, the external air

temperatures were between 24^{o}C and 35^{o}C, while the internal air temperature over the twenty days remained stable and marginally swung between 21.8^{o}C and 26.9^{o}C within the departure lounge floor. Slightly high indoor air temperatures normally occurred between 1200h to about 1700h, during which time the outdoor temperatures gradually started to rise. The internal air temperatures considerably exceeded the same standard at 24^{o}C, which occurred almost every day.

The internal temperature at the top floor ceiling was affected by the external conditions, even though it was cooled down by air-conditioning. Interestingly, the glazed roof surface temperatures were over 40^{o}C around midday for 4~5 hours almost every day. As a result, the operative temperature within the space led to overheating and thermal discomfort, particularly on the upper floors.

Throughout the measurements, the natural light only benefits some areas underneath transparent roofs within the large glazed air-conditioned concourse space. It was noted that the passenger lounge on the ground floor was also lacking in natural light in some areas.

These measurements revealed that the two case-study buildings with long-span glazed roof over large pedestrian concourses, one with natural ventilation and one with air-conditioning in the tropics, would suffer high-temperature stratification on the top floors causing great discomfort to the occupants. In addition, it can be seen that daylighting tended not to be uniform within these buildings' interiors.

Due to the complexity of the geometry of long-span glazed roofs over large pedestrian concourses and the limited measurement period of the two case studies, dynamic thermal and lighting models were therefore used for overall assessment of the annual indoor physical environment and energy consumption of the two atria in question. The results from these physical measurements were used to analyse and compare with the predicted results from the dynamic thermal and lighting simulation modelling in order to calibrate the capability and accuracy of the software to model and simulate thermal and lighting environments within the large pedestrian concourse space, as demonstrated in chapter 6.

The next chapter discusses the post-occupancy evaluation data in order to obtain the airport officers and staff groups' qualitative feedback on their experience with the

existing internal environment. This feedback was gained by the use of a standardised questionnaire.

CHAPTER 5 – POST OCCUPANCY EVALUATION of SUVARNABHUMI AIRPORT TERMINAL

5.1 Introduction

Suvarnabhumi Airport is located in Samut Prakarn about 25 kilometres east of downtown Bangkok, Thailand and was completed in 2006. The airport serves both domestic and international passengers, with a useable area of around 563,000 square metres (6,060,081 sq ft). A single passenger terminal building is 111 metres in width, 444 metres in length, with a useable area of around 140,000 square metres (1,506,960 sq ft). This airport is the sixteenth busiest airport in the world and the sixth busiest airport in Asia (Lamprecht, 2013). In 2012, it is recorded that 145,000 passengers visited Suvarnbhumi Airport Terminal on a daily basis. The construction of the outside façade of the airport is mainly 12 mm. thick laminated glasses with a *U*-value of 5.5 W/m^2K.

Energy use for cooling in a tropical climate is the largest area of use on a national level. The best way to determine energy consumption is to analyse utility bills over a period of time, as part of the energy assessment of a building (Patrick et al, 1993). In a comparison of the energy consumption of an airport and typical domestics, an airport can consume more energy than typical domestics. For instance, the total energy used by Heathrow Airport was as high as 687 GWh, while the average of energy used by UK's dwellings was 20 MWh in 2008 (Heathrow, 2012; OFGEM, 2011). Thus any improving energy efficiency in airports can result in huge energy savings (Membo, 2013).

According to ASHRAE (2009), glazed buildings are notoriously uncomfortable, regardless of their huge, complicated, high running costs and high maintenance cooling systems; a perception that is especially relevant in tropical climates. There is also the high probability of encountering significant thermal discomfort in these glazed buildings.

There is increasing concern over the quality of buildings' internal environments, particularly in hot climates where air-conditioning of the internal environment is necessary. (Cheong et al., 2003). The post-occupancy evaluation (POE) is a prominent tool which can be used to indicate satisfaction and comfort level needs by building occupants to identify problems in indoor environment (Khalil and Husin, 2009).

Although numerous studies have also examined the occupants' feedback on the existing internal environment in many airports, there is no study available based on the airport officers' and staff groups' qualitative feedback regarding their experience with the existing internal environment in Suvarnabhumi Airport Terminal. Thus this POE was initialized to quantitatively investigate, through the use of a questionnaire, the airport officers' and staff groups' satisfaction with the existing environment; particular focus being directed towards temperature, daylight and ventilation.

The POE technique depends upon the level of information available to support the evaluation and the level of detail required in the study. One of the most accurate assessments can be obtained from survey questionnaires among a focus group to examine any major problems, in addition to photographic records and physical measurements (Preiser, 1995). Therefore, this chapter uses the post-occupancy evaluation (POE) in order to obtain feedback on the existing internal environment (thermal, visual and internal air quality) by using a questionnaire survey of a representative sample of the airport's personnel.

This chapter is organised into five sections. Section 5.2 discusses the concept of subjective assessment. Section 5.3 then discusses the respondents' demographics results. The level of satisfaction in each season and the respondents' perceptions of the thermal sensation and impressions of comfort are discussed in sections 5.4 and 5.5, respectively. Section 5.6 provides a conclusion to the chapter.

5.2 Subjective Assessment – Questionnaire Survey

Airport terminals are buildings in airports which provide passengers with access from ground transportation to board aircraft, as well as processing passengers after they disembark from their aircraft. Terminals are characterised by their large open spaces and high ceilings. Also, for aesthetic reasons, glazed panels are used extensively for the construction of transparent roofs and walls in most of airport terminals (Piechowski and Rowe, 2007). Physical environments like this experience rapid deterioration due to solar heat radiation and external thermal conditions, particularly relating to comfort quality (Kim et al., 2001).

Mambo (2013) stated that the occupants are a major factor in comfort definition within airports. They are the passengers, the airport officers, the airline operators, the security

personnel and the shop attendants. Airport passengers and their escorts occupy spaces for a short time, so drift in temperature might not have any noticeable effect on them. On the other hand, the airport officers and staff groups work for long periods within the terminals, and so the building is expected to provide the necessary indoor environments that will ensure, rather than detract from, those individuals' efficiency and productivity.

The survey was conducted simultaneously with the environment parameter measurements and data collection for twenty days from 12th September to 1st October 2012 in the passenger lounge of Suvarnabhumi Airport Terminal.

The measured data included the key indoor variables of air temperatures; surface temperatures and illuminance. Measurements were conducted with mechanical instruments over a group of selected locations within the passenger lounge and cooling loads data were derived from the statistics from the airport facility team; an exercise discussed in detail in chapter 4. These measured results and collected data were used to create and calibrate the computer models, which is discussed further in the next chapter.

The questionnaire used in this thesis was a modified version of the one used in the 'Thermal Comfort Study of an Air-conditioned Lecture Theatre in the Tropics' (Cheong et al., 2003); the modifications designed to make it more applicable to the airport passenger lounge environment. Thermal comfort for a person, according to the American Society of Heating, Refrigerating and Air-conditioning Engineers (ASHRAE) Standard 55 (1992) is defined as: 'that condition of mind which expresses satisfaction with the thermal environment'. The factors affecting thermal comfort, which are assessed in the questionnaire, are as follows:

- Temperature is the most important factor affecting thermal comfort;
- Humidity in the range 40-70% is generally acceptable;
- Air movement is the net mean air speed across the body;
- Metabolic heat production is dependent on activity level;
- Clothing is the unit for thermal insulation of clothing.

Visual conditions for working are also included for the visual comfort assessment in the questionnaire.

Thus the questionnaire survey consisted of three categories: respondent demographics, the level of satisfaction in each season and the respondents' perceptions of the thermal sensation and impressions of comfort (Appendix C).

- The respondents' demographics were collected including gender, age, nationality, occupation, working period, activity levels (metabolism) and type of clothing (Santamouris and Asimakopolous, 1996);
- Respondents were asked to rate the level of satisfaction in each season and score their perception within a four-point preference scale;
- The seven-point ASHRAE sensation scale was used to evaluate thermal sensation and impressions of comfort with regard to thermal comfort, visual comfort and indoor air quality.

The questionnaire also included an open-ended section designed to encourage the respondents to comment on the issues not covered in the questions.

The dominant population sampled comprised the airport officers and staff groups. In 2011, Suvarnabhumi Airport had a total of 7,626 personnel. 2568 permanent employees and 5058 outsourced workers (AOT, 2011). Suvarnabhumi Airport accommodated 100 scheduled airlines, 88 of which were mixed passenger-cargo airlines, and 12 of which were pure cargo airlines (AOT, 2012). Assuming that each airline provides 10 employees for 24 hours service, the airlines would have an approximate total number of 1,000 personnel. In addition, there are other agencies' employees such as the Customs Department, Police and the Thailand Post Company, making up around 200 personnel.

The process used to select the sample was random sampling. The sample size for the members of staff in the airport departure lounge was calculated, based on Yamane's equation as follows (Yamane, 1965 cited in Kasunic, 2005).

$$n = \frac{N}{1 + Ne^2}. \qquad (5.1)$$

where: n is the sampling number;

N is the statistic population;

e is allowable error ratio.

With a confidence coefficient of 95%, and with an error of 5%., the calculation from a population of the sample size would need to be 383. After gathering the questionnaires,

the survey data will be keyed into an Excel file before transferring to the Statistical Package for the Social Sciences program (SPSS) for analysis of the occupants' responses. The analysis addressed the calculation of mean values, frequency distributions and correlation between independent factors.

The questionnaire was presented to the 700 airport officers and staff groups working in the passenger lounge (300 airline operators, 300 airport officers and 100 other agency and shop attendants). 383 responses (54%) were obtained.

5.3 Respondent Demographics

383 responses were obtained from the airport employees in the main terminal building. The beginning of the questionnaire detailed the background of the respondent including gender, age, nationality, occupation, working period, activity levels (metabolism) and type of clothing.

There were 188 women (49.1%) and 195 men (50.9%) who filled the questionnaire survey. The majority of the subjects were under 30 years of age (40.99%). The dominant working period distribution sampled was day shift for 6-12 hours (54.05%) and night shift for 6-12 hours (16.45%) who work as Thai Airway employees (28.72%) and Airports of Thailand (AOT) employees (26.37%), respectively.

The clo value and metabolic rate were calculated from the CIBSE (2006) standards. It was revealed that the clothing ensemble consisted of typical business suit (61.88%) which was expressed in 1 (clo) units or 0.155 $m^2 \cdot K \cdot W^{-1}$. In addition, their major responsibilities related to customer service (35.51%) and check in (38.12%) respectively; which were classified as light activities (1.2 met) (Figure 5.1 a- 5.1e).

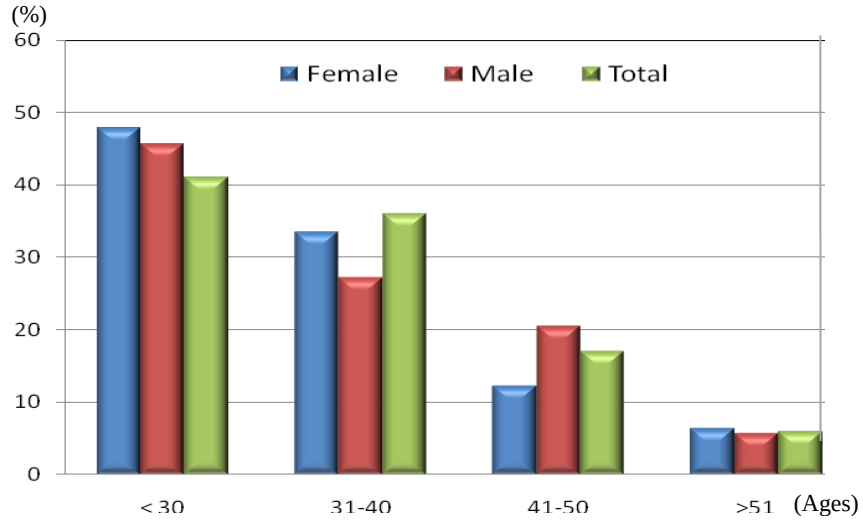

a) Age distribution of the sample

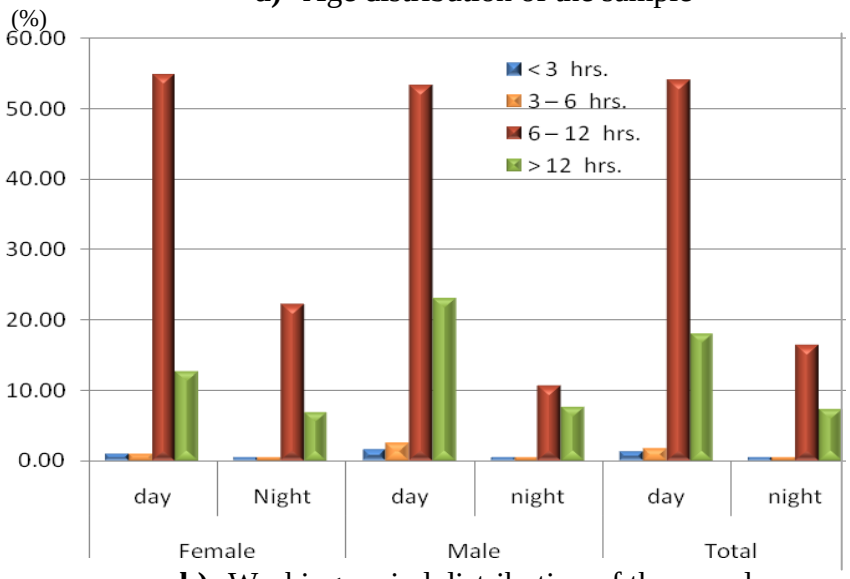

b) Working period distribution of the sample

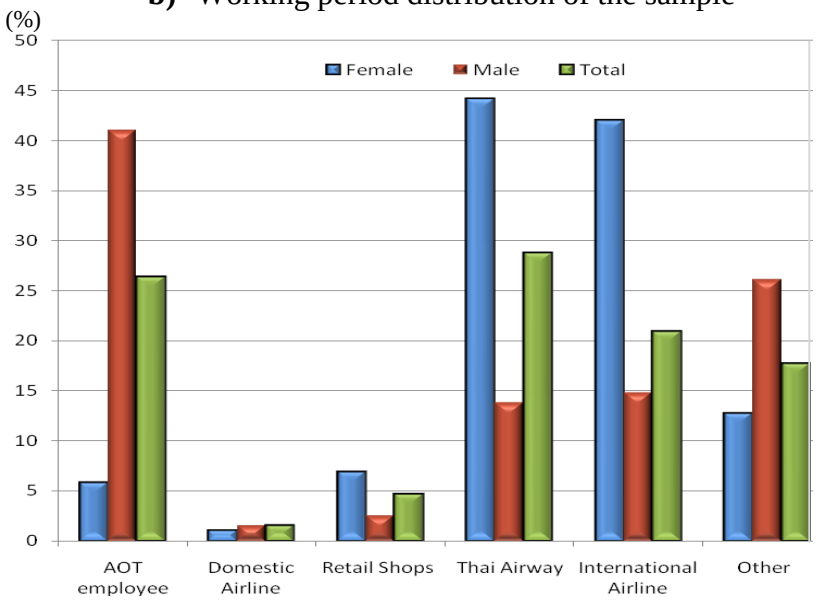

c) Occupation status distribution of the sample

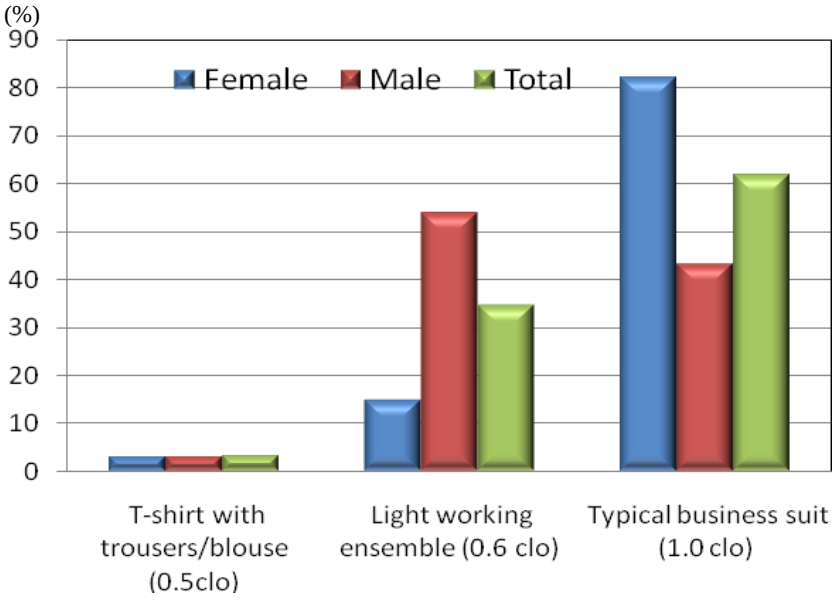

d) Clothing distribution of the sample

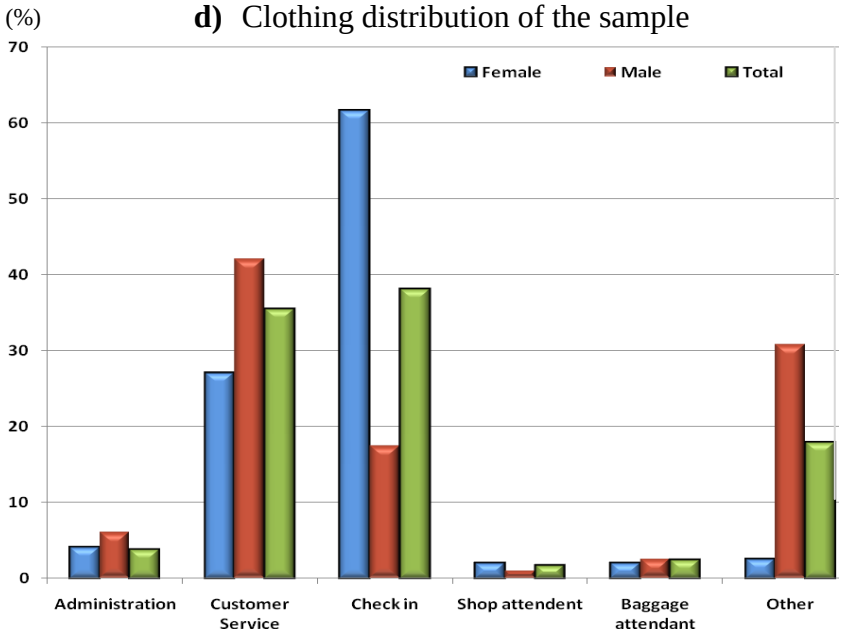

e) Responsibilities distribution of the sample

Figure 5.1 Respondents' demographics

5.4 The Level of Satisfaction and Overall Perception

The POE focused on assessment of the airport officers' and staff groups' satisfaction with the thermal comfort within the passenger lounge space. The distribution of the subjective response on the level of satisfaction and overall perception is presented in Figures 5.2(a) and 5.2(b).

Questions on the level of satisfaction and overall perception used a four-point preference scale with variable end anchors. Regarding the level of satisfaction, the majority of respondents voted 'dissatisfied' at 54.05% in summer, 39.95% in winter and 46.21% in rainy weather. It was also observed that 32.9% of the respondents were

'strongly dissatisfied' in summer. The responses regarding the overall perception of indoor condition were negative; 'unacceptability' registering close to 45.0%.

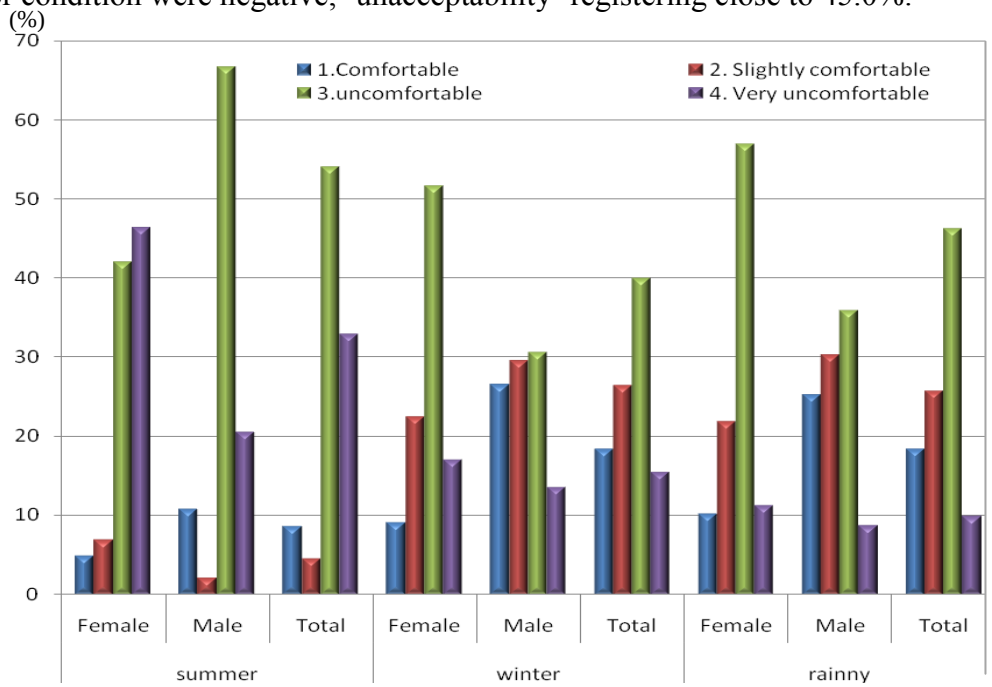

a) Level of satisfation on thermal comfort

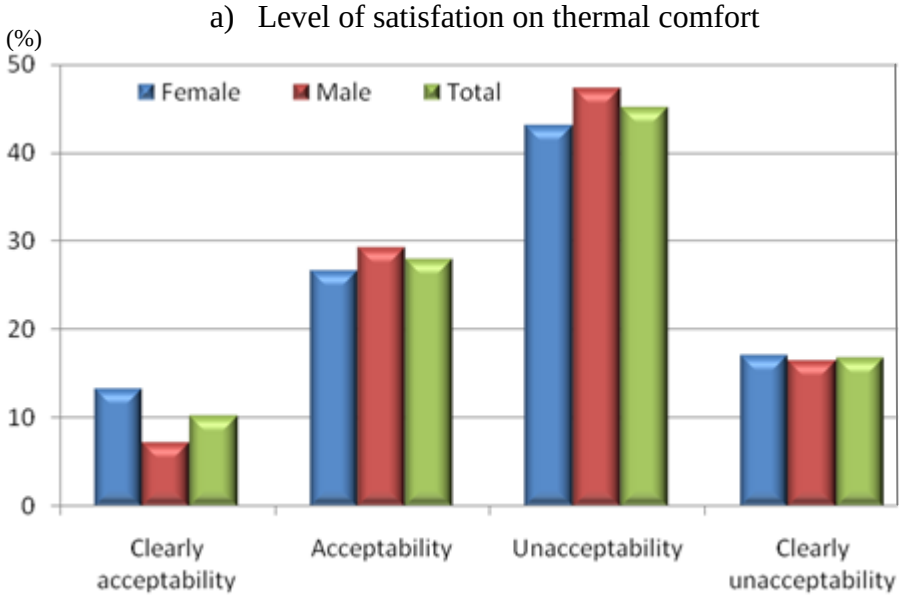

b) Overall perception

Figure 5.2 Distribution of subjective response on thermal comfort and overall perception

5.5 The Thermal Sensation and Impressions of Comfort

This thesis has carried out a post-occupancy survey to examine building performance, particularly from the viewpoints of the building's occupants. Additionally, a seven-point ASHRAE sensation scale was used to evaluate thermal sensation and impressions of comfort with regard to thermal comfort, visual comfort and indoor air quality.

Figures 5.3(a) and 5.3(b) display the thermal sensation and impressions of comfort with temperature and humidity. Only 12.62% of respondents indicated 'neutral'. The majority of temperature sensation responses were concentrated in the 'slightly warm' category at 40.62%. The humidity sensation responses were concentrated in the 'slightly humid' category at 29.77%.

Interestingly, 23.16% of respondents indicated 'slightly cool' which their dominant working period was the night shift occupants. It was observed that the day shift responses claimed that the air temperatures were 'slightly warm' while the night shift responses claimed that the air temperatures were 'slightly cool'.

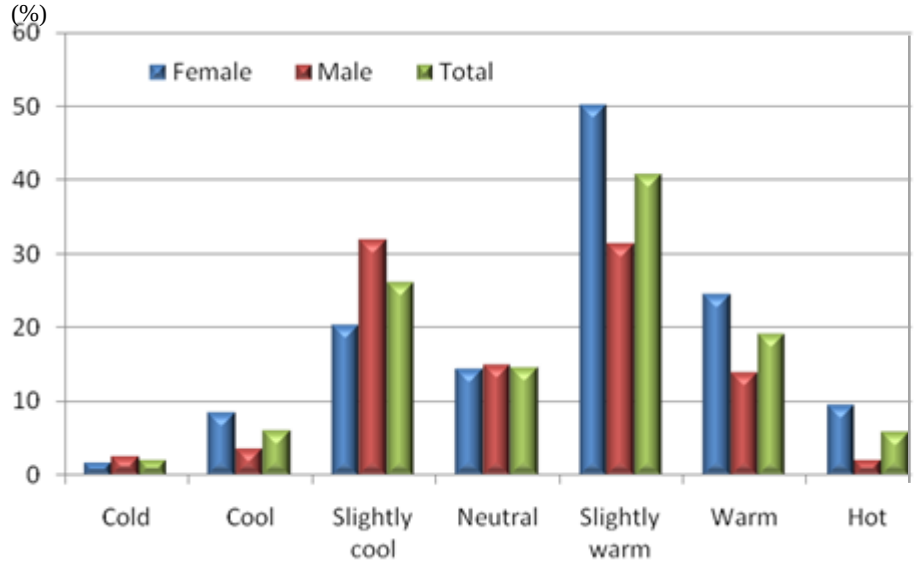

a) Temperature

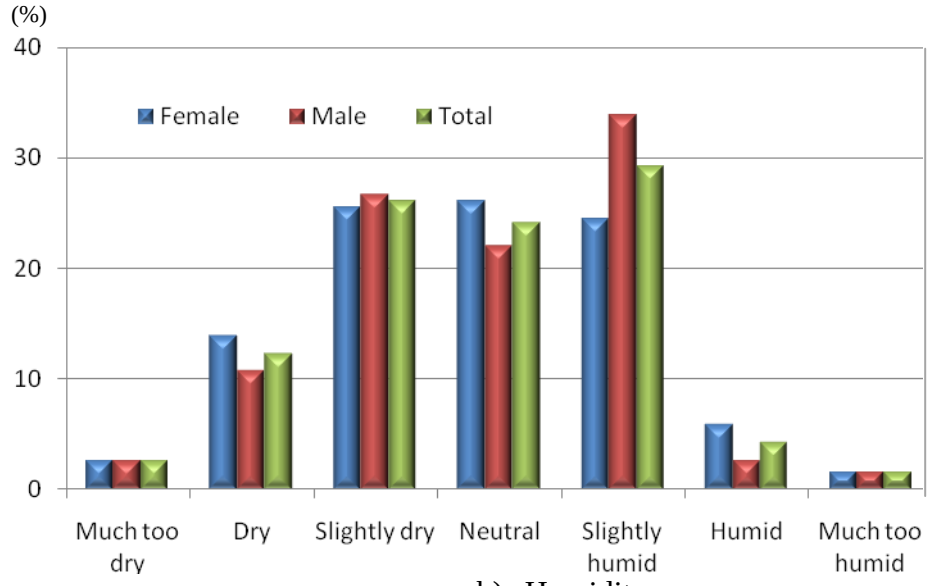

b) Humidity

Figure 5.3 Thermal Sensations and Impress of Comfort

Figures 5.4(a), 5.4(b) and 4.3(c) reveal that the majority distribution of subjective responses on ‘air movement’ was under the category of ‘slightly still’ (22.13%) and ‘air freshness’ was under the category of ‘neutral’ (33.68%), respectively. The responses from the total occupants on ’air quality satisfactory’ were biased towards the ‘neutral’ category (26.01%).

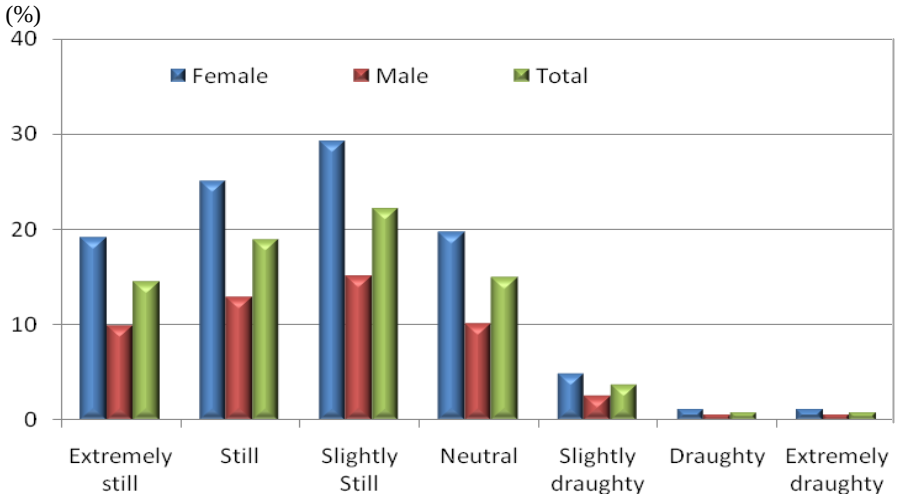

a) Air Movement

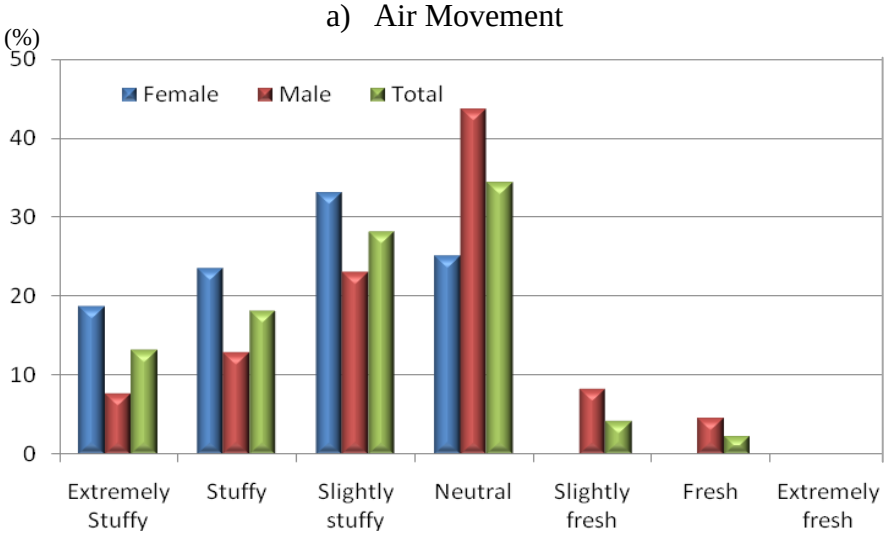

b) Air Freshness

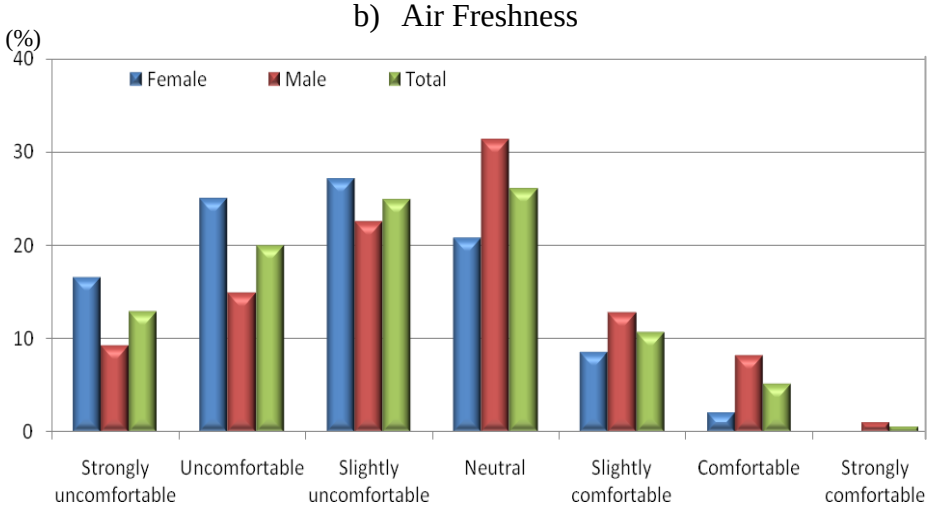

c) Air Quality Satisfactory

Figure 5.4 Internal air qualities

Figures 5.5(a) and 5.5(b) present the subjective responses to visual conditions. There was a slight bias towards 'slightly dark' at 26.01%; while 28.46% of respondents indicated 'neutral'. The majority of the visual comfort satisfaction vote was within the 'neutral' category at 27.15% and 'slightly uncomfortable' category at 26.37%.

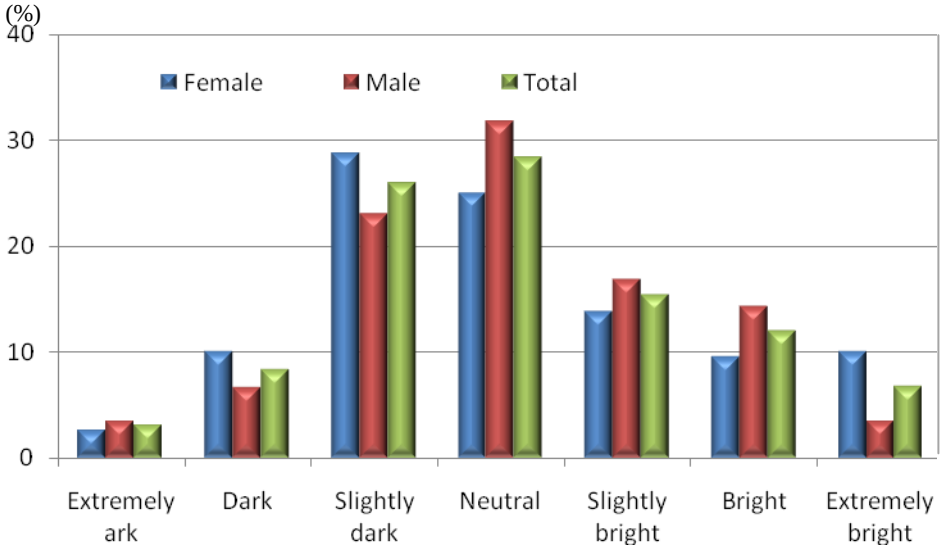

a) Visual condition

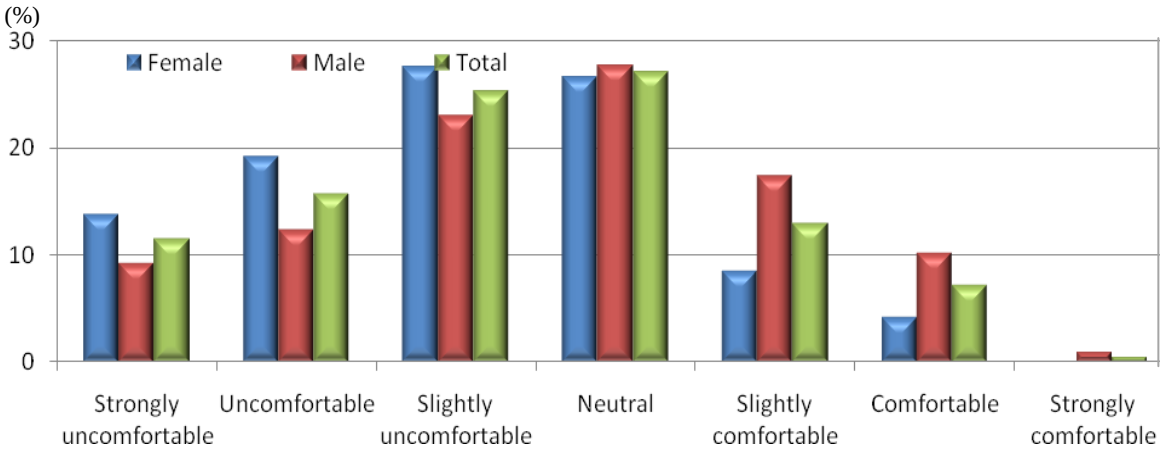

b) Visual comfort satisfaction

Figure 5.5 Visual comforts and visual condition

It was also found in this study that 184 respondents commented on the airport environment, reporting 311 problems which the researcher categorized into 10 groups as show in Figure 5.6. The most concern was for inefficient air-conditioning (20.90%) which led to temperature fluctuation directly in this terminal building. It was 'much too hot' at noon and summer and 'much too cold' at night. The second most common concern was sunlight penetrating into working areas, causing glare and too much heat, especially in summer (18.65%).

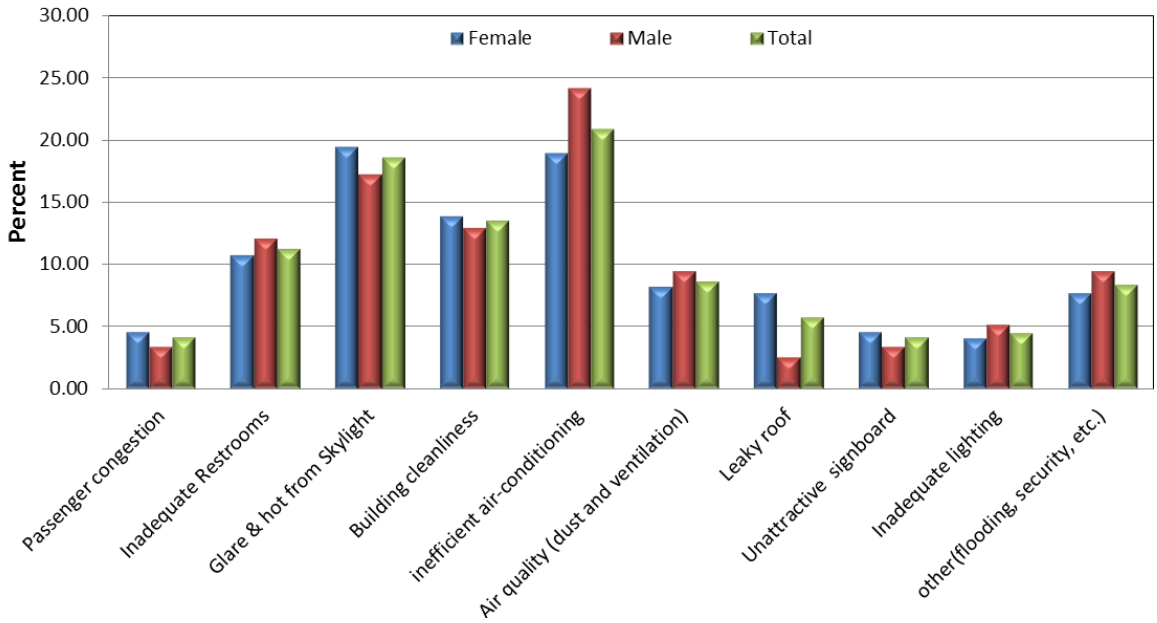

Figure 5.6 Comment of airport environment

5.6 Conclusion

This chapter described the post-occupancy evaluation fieldwork stage, using a questionnaire survey with representative quotes from the airport employees located in the main terminal building. The questionnaire survey was composed of three categories: respondents' demographics, the level of satisfaction in each season and the respondents' perceptions of the thermal sensation and impressions of comfort.

This survey was intended to obtain the airport officers' and staff groups' qualitative feedback on their experience with the existing internal environment through a questionnaire.

The total sample consisted of 383 employees. 50.9% of respondents were men and 49.1% of respondents were women. The majority of the respondents were under 30 years of age. The majority distribution in the dominant work period was for Thai Airways and Airports of Thailand (AOT) employees, on 6-12 hour day shifts.

The subjective assessments clearly show that the occupants perceived thermal discomfort in this passenger lounge of Suvarnabhumi Airport Terminal. In terms of the level of satisfaction in each season, the majority of respondents (54.05%) voted they were 'dissatisfied' in summer, 39.95% in winter and 46.21% in rainy weather. The thermal environment was also marginally unacceptable according to the respondents' vote.

Table 5.1 shows the percentage between positive and negative ratings. The responses on thermal sensation and impressions of comfort revealed that almost 50% of the respondents claimed that the temperature in the passenger lounge was 'hot', 'warm' and 'slightly warm', as well as the majority of employees perceiving the space to be slightly warm.

The results of the respondents' satisfaction with air quality were within a negative rating. Almost 60% had negative rating for 'air freshness' compared with a negative rating of almost 66% for 'air movement'.

The research also found that visual comfort had negative ratings when considering the 'visual condition' regarding the amount of light for working. This is somewhat surprising in that the majority of respondents were commenting on the inadequate lighting, even though this space was designed to take advantage of natural day lighting from the transparent roof. According to the field measurement in chapter 4, only 18.8 percent could be shown to have an adequate level of daylight as recommended by CIBSE (2009). The canopy shades over check-in counters could be the main cause of shadow over work surfaces. However no physical measures within the check-in area were taken of ambient conditions, so it is not possible to identify the problem with certainty.

Finally, a review of the open ended comments shows concern with inefficient air-conditioning within the researched space, leading to temperature fluctuations. Another problem was from sunlight penetrating through working areas, causing glare and too much heat, especially in summer.

Environmental Factor	(-3)-(-1)(%)	Neutral (%)	1-3(%)
Temperature	24.80(Cold)	25.33	49.87(Hot)
Humidity	44.91(Dry)	26.89	28.20(Humid)
Air quality comfort	57.44(Uncomforted)	26.11	16.45(Comforted)
Air freshness	59.53(Stuffy)	33.68	6.79(Fresh)
Air Movement	66.06(Still)	22.98	10.97(Draughty)
Visual comfort	37.34 (Uncomforted)	28.46	34.20(Comforted)
Visual condition	52.48(Dark)	27.15	20.37(Bright)

Table 5.1 Percentage of positive, neutral and negative Rating

From the above distribution of responses, it is possible to relate the votes of the various environment parameters to that of overall thermal comfort. The mean thermal comfort, humidity and air movement responses were under the categories of 'dissatisfied', 'slightly dry' and 'slightly still', respectively.

According to the field measurement discussed earlier in Chapter 4, the external air temperatures were between 24^{o}C and 35^{o}C, while the internal air temperature over the twenty days remained stable and marginally swung between 21.8^{o}C and 26.9^{o}C within the departure lounge floor. Slightly higher indoor air temperatures normally occurred between 1200h to about 1700h when the outdoor temperature gradually started to rise. The internal air temperatures considerably exceed the CIBSE (2006) standard at 24^{o}C; an event which occurred almost every day. This temperature rise confirms the idea that the majority of respondents were 'uncomfortable' in this passenger lounge.

Results from the parallel physical measurement were analyzed and compared with the predicted results from the dynamic thermal and lighting simulation. This was done to calibrate the capability and accuracy of the computer models to analyze the physical environment and energy performance within the large glazed pedestrian concourse, as set out in the next chapter.

CHAPTER 6–DYNAMIC THERMAL and LIGHTING SIMULATION MODELS

6.1 Introduction

Chapter 4 presents all the details of two field studies carried out by using data collection and filed measurements which will be used to build the dynamic thermal and lighting models and to calibrate the capacity of the dynamic thermal and lighting models. Chapter 5 presents the post-occupancy evaluation (POE) of the thermal and visual comfort in Suvarnabhumi Airport Terminal building. The purposes of the POE are to evaluate the actual performance of the case study in term of energy and internal environment performance and investigate the airport officers and staff groups' satisfaction with the existing environment including temperature, daylight and ventilation. This was accomplished through a survey questionnaire. Due to the complexity of the building geometries associated with a long-span glazed roof over large pedestrian concourse, together with the limited measurement period of the two case studies, dynamic thermal and lighting simulation models were thus used for overall assessment of the annual indoor physical environment and energy consumption of the two long-span glazed roofed case study buildings. The dynamic thermal and lighting models were created and run under the weather data files from the local meteorological stations over the same selected periods as the field measurements. In order to increase the accuracy of the thermal and lighting simulations, it is necessary to calibrate these models. Calibration of the thermal models were by comparisons with the measured results for two critical variables, the indoor temperatures and the total average cooling loads within the long-span glazed roof over the large pedestrian concourses on the hottest clear and overcast days. The calibrations of lighting models were by comparison with the daylight factors (DF) within the long-span glazed roof over large pedestrian concourse on the selected overcast days.

The representative models were also used to predict physical environment and energy performance using different shading configurations: high level and low level shadings and assessed by dynamic thermal and lighting simulation software. These will be later used to predict thermal and visual environment conditions for both case studies to find out the best shading in relating to the best thermal environment and energy performance

while maintaining adequate level of natural light. This will be discussed further in chapter 7.

This chapter is organised into four sections. Section 6.2 starts with discussion on methods to create representative dynamic thermal and lighting models. Section 6.3 discusses the dynamic thermal and lighting simulation model and focuses on the model calibration in the central glazed pedestrian concourse of the GITC building. Section 6.4 provides a discussion the dynamic thermal and lighting simulation model and also focuses on the model calibration in the glazed pedestrian concourse of the departure lounge of Suvarnabhumi Airport Terminal. Section 6.5 discusses limitations in the dynamic thermal and lighting simulation model. Finally, a conclusion is presented at the end of this chapter.

6.2 Methods

To create representative dynamic thermal and lighting simulation models, the study was carried out in three stages. It begins with creating long-span glazed roofs over large pedestrian concourse models using dynamic thermal and lighting modelling tools and assigning building elements and internal conditions in both cases. Then, the dynamic thermal and lighting models were divided into multi-zone and run under the weather data files from the local meteorological stations over the same selected periods as the field measurements. Finally, the predicted results were compared against the measured ones. For the dynamic thermal model calibrations, comparisons were made for two critical variables, the indoor temperatures and the total average cooling loads within the long-span glazed roofs over large pedestrian concourses on the hottest clear and on overcast days. For the lighting model calibration, comparisons were made for the DF within the long-span glazed roof over large pedestrian concourses on the selected overcast days.

6.2.1 Computer Simulation Modelling Tools

Recently, computer modelling has been popular due to increase in computer performance with both capacity and availability. Dynamic thermal modelling programs have been routinely used to model spaces in conventional building (Abdullah, 2007).

For large glazed pedestrian concourse buildings, assigning a large single zone or dividing each level into one zone may not be sufficient to correctly model the spaces. To provide a more accurate analysis, a multi-zonal model is recommended. They treat

each space within a building as a zone, calculate the heat and air movement among these zones through energy mass balance equations and predict dynamic thermal performance of a building. Hence they are often used for overall thermal performance and energy consumption of a specific design (Megri and Haghighat, 2007).

The long-span glazed roof over large pedestrian concourse spaces were divided both vertically and horizontally into a group of small zones in order to improve the spatial resolution for the solutions. The vertical division is essential for simulating stratification within the spaces (Voeltzel, Carrie and Guarracino, 2001). Each floor within the large glazed pedestrian concourse were further divided into horizontal zones to calculate the movement of heat and air flows, so that dynamic thermal models could correctly model the thermal behaviours within long-span glazed roof over large pedestrian concourses.

Creating dynamic thermal and lighting models are crucial to the achievement of objectives of the study. This is facilitated by a dynamic thermal and lighting software tools known as TAS, Ecotect and Dialux.

6.2.2 Model and Parameters Assignment

According to the field study presented earlier (see Chapter 4), the two case studies were created in both the dynamic thermal and lighting models. The building elements such as floor, wall, glazed roof and construction were specified from the software construction database with reference to architectural specifications from designers and contractors. In addition, internal conditions such as temperature in air-conditioned units were derived from the building mangers, while heat gains from occupants, lighting and equipment were set to the CIBSE Guide A (2006) value. In the thermal models each section of the building, large pedestrian concourse and central pedestrian concourse were divided into multi zones for each floor to capture the differences in thermal condition over the space. At the roof level, a separate zone was created between the transparent roof and the ceiling. Such division was intended to differentiate subtle changes in temperature from one place to another and to allow the predicted values of the models to be compared with those from field measurements at exactly the same positions in the calibration.

The dynamic thermal models were run under the weather data files from the local meteorological stations over the same selected periods as the field measurements. The

main tuned variables of both models were the solar transmittances of the glazed roofs and indoor heat gains.

6.2.3 Calibration Method

There are a few ways to evaluate the accuracy of the energy simulation software (Judkoff et al., 1983);

- *Empirical Calibration* - Calculated results from a program or software object are compared to monitored data from a real building or laboratory experiment;
- *Analytical Verification* - Outputs from a program, subroutine, algorithm, or software object are compared to results from a known analytical solution or a generally accepted numerical method for isolated heat transfer under very simple, highly constrained boundary conditions.
- *Comparative Testing* - A program is compared to itself or to other programs.

To evaluate whether the dynamic thermal models were suitable to investigate the proposed shadings in the next stage, dynamic thermal and lighting models calibrations in this study were carried out by using the Empirical Calibration method. Real buildings with similar form and features, and situated in a similar climatic condition was modeled and the predicted results were compared against the measured ones on the hottest clear and overcast days.

6.2.4 Variables for Calibration of Dynamic Thermal and Lighting Models

For dynamic thermal model calibration, comparisons were made to assess the accuracy of the thermal model in simulation as follow:

- The predicted average daily temperatures within the long-span glazed roof over large pedestrian concourse were compared against the measured ones for the whole selected period;
- The profiles of the predicted internal temperatures within the long-span glazed roof over large pedestrian concourse were compared against the measured ones on the representative hot clear and overcast days;
- The predicted total cooling loaded were compared against the survey mentioned in chapter 4 and also against the cooling load benchmark standard.

The main tuned inputs in representative dynamic thermal model were the solar transmittance of the glazed roofs and internal heat gains to allow the models to produce the indoor temperatures and cooling loads that were close to those derived from the measurements carried out in both case studies.

For lighting model calibration, comparisons were made for the DF within the long-span glazed roof over large pedestrian concourses on the selected overcast days. The calibration of the lighting model was simpler than that of the thermal model. Two of the inputs, namely the light transmittance of the transparent roof and light reflectance of the walls and floors of the long-span glazed roof over large pedestrian concourse buildings were tuned to allow the models to produce the DF that were close to those derived from the measurements carried out in both case studies.

Two different modelling approaches can be followed for accurate dynamic thermal and lighting simulations: the long-span glazed roof over large natural ventilated pedestrian concourse: Guangzhou International Textile City Building (GITC) and the long-span glazed roof over large air-conditioned pedestrian concourse: Suvarnabhumi Airport Terminal Building.

6.3 The Large Glazed Naturally Ventilated Pedestrian Concourse

The study was conducted in the central large glazed pedestrian concourse in Guangzhou International Textile City Building (GITC) in China. This city is located in Southern China at latitude of 23.13^{o} north and longitude of 113.23^{o} east. Average air temperature is 22.2^{o}C, while the average relative humidity is 77 percent. The highest average daily temperature is 29 °C during July and August and the coldest average is 14°C in January.

6.3.1 Dynamic Thermal and Lighting Models and Parameters Examined

The GITC building was created in both the thermal and lighting models including streets, corridors and atrium based on the architectural drawings. The thermal dynamic model was built using TAS and the lighting model by Ecotect (EDSL, Autodesk, 2011). The building was developed to contain the following elements (Figure 6.1a and 6.1b):

- The building is a seven storey blocks designs with a total floor area of nearly 140,000 square metres for all floors (1,506,960 sq ft). The 3-D model of the long-span glazed roof over large naturally ventilated pedestrian concourse

building was created based on the real building including the building elements specification and elongated along East-West axis;

- Each section of the street, the large glazed pedestrian concourse and the central large pedestrian concourse were divided into 35 zones over seven floors. The central large pedestrian concourse at the roof level was further divided between the transparent roof zone and the ceiling zone to capture the differences in thermal conditions over this space. Such division was intended to differentiate subtle changes in temperature from one place to another and to allow the predicted values of the models to be compared with those from field measurements at exactly the same positions in the calibration;
- 6.0 metres floor to floor height for the ground floor to first floor and 4.8 metres floor to floor height for all above.

The exact design details, material properties, and construction in the field needed to create the two computer models were incomplete. The dimensional construction data were created according to the designer and contractor. There was some uncertainty about building element inputs. Floor, glazed roof, internal wall and external glazed wall were all specified from software construction database with reference to the architectural specifications. The floor was simulated as being constructed with vinyl and concrete and it U-value was 2.88 $Wm^{-2o}C$. The glazed roof was simulated as being constructed with laminated glass and it U-value was 5.50 $Wm^{-2o}C$. The slab roof was simulated as being constructed with Bitumen and polystyrene on concrete and it U-value was 1.10 $Wm^{-2o}C$. The internal wall was simulated as being constructed with lightweight pastor and it U-value was 0.90 $Wm^{-2o}C$. The external wall was simulated as being constructed with tempered glass and it U-value was 5.50 $Wm^{-2o}C$ (Table 6.1).

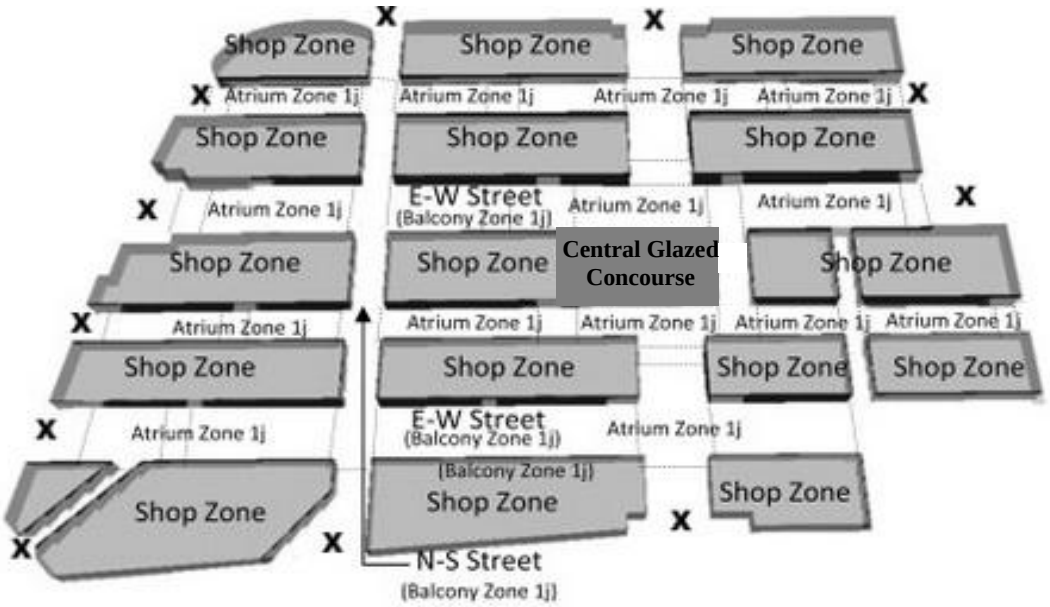

a) A ground floor plan of the building showing the central glazed spaces, indoor streets and model zoning i = location1, 2,…, 22 and j = floor1, 2,…,7

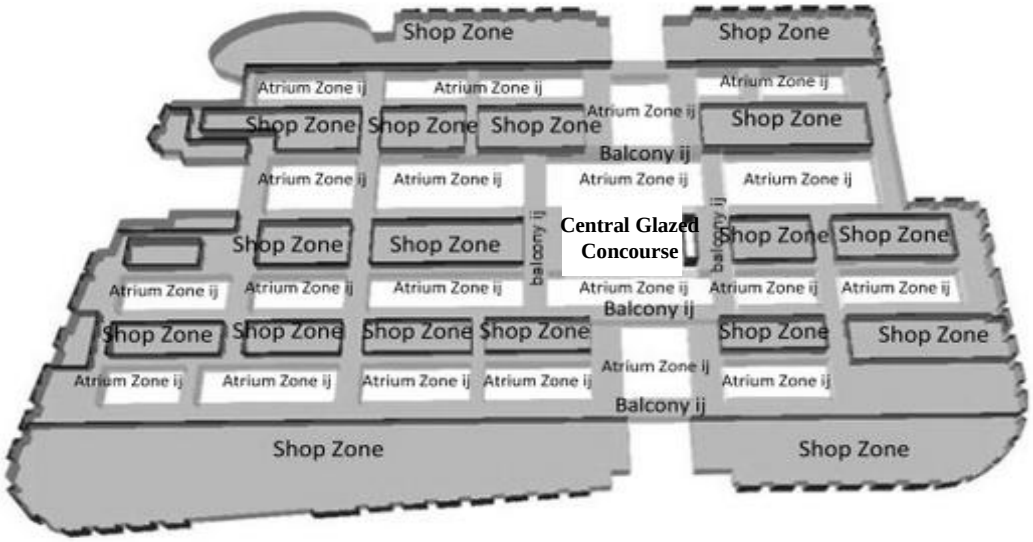

b) A typical floor plan showing zoning of the central glazed spaces, corridors, and units (i=2 – 7)

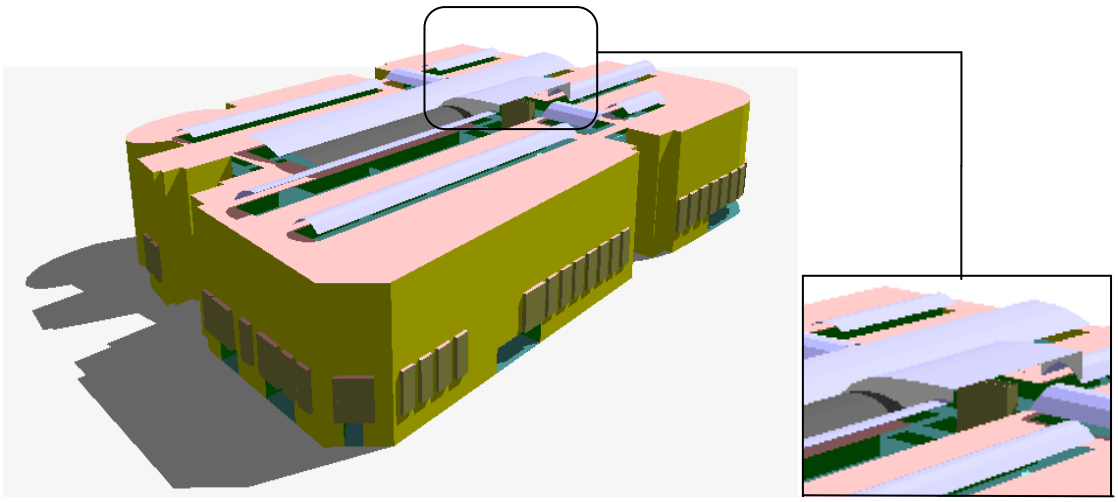

c) Top view of the computer model and the detail, showing the centre atrium

Figure 6.1 3D model by TAS

The lighting model had the same geometry as dynamic thermal model. The critical variables which affect simulation accuracy were reflectance of the internal surfaces and the transmittance of the external envelope. Base on the product datasheets, the reflectance was set to 20% for the floors, 60% for the internal walls and 70% for ceilings of the corridors (Zhu, 2012). Each of the open shop doors was assumed to have only 10% reflectance to the corridor space to represent the fully operating interior of each shop.

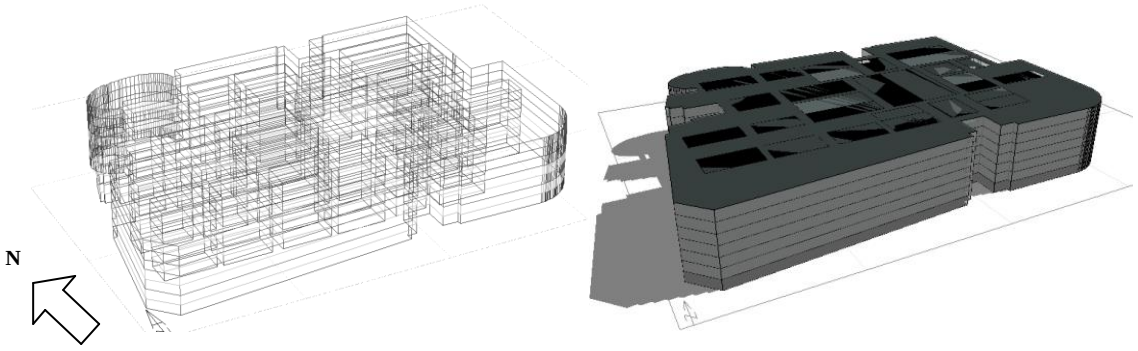

Figure 6.2 3-D Lighting model of GITC building by Ecotect (Zhu, 2012)

6.3.2 Weather and Internal Conditions

For dynamic thermal model, hourly weather data are required; the 2010 weather data file for Guangzhou meteorological weather data was used as the representative year data. The data set contains the hourly figures of the seven weather variables: the air temperature, relative humidity, global and diffuse solar radiations, cloudiness and wind

speed and direction for a whole year. In order to increase the accuracy of the thermal and lighting simulations, the calibration of the two models were carried out as follows:

- The representative dynamic thermal model was run for seven consecutive days from 30th July to 5th August 2011;
- Calibration of the thermal models were compared with the measured results for two critical variables, the indoor air temperatures and the total cooling loads within the long-span glazed roof over large pedestrian concourse on the hottest clear and overcast days. The calibration of lighting models were by comparison with the DF within the long-span glazed roof over large pedestrian concourse on the selected overcast days;
- For the average indoor air temperature comparison, the predicted indoor temperatures over the seven levels were compared against the measured ones;
- For the profiles of temperature comparison, 31st August 2011 was chosen to represent a summer clear day and on 1st September 2011 to represent a summer overcast day for use in the calibration;
- For the total cooling load comparison, the predicted total cooling load on a representative clear hot day was compared against the designed cooling load capacity. In addition, the predicted total cooling load per floor area during summer was compared against the cooling load benchmark in shopping mall;
- For simulating the lighting conditions, 1st September 2011 was chosen to represent a summer overcast day using in the calibration.

The building blocks were used as offices on the top three floors and retail units for the lower four floors. All these spaces were air-conditioned during operating hours of 0800h~2000h. In addition, the statistics of the building manager revealed that the temperatures in the offices on the top three floors were set to 25°C and the doors to the balconies were closed. The temperature in the typical retail units on the lower four floor were set to 28°C and the doors were open to the balconies to reflect the test conditions in the field measurement, while atria and corridor were defined as natural ventilation.

The heat gains from occupants, lighting and equipment were set to the CIBSE Guide A (2006) value. The occupancy was calculated to 4,166 persons around the whole

building, based on the average daily visits during operating hours of 0800h~2000h plus the members of staff and tenants (Appendix E).

Based on the typical floor plan of the model buildings (Figure 6.3), the central large glazed naturally ventilated pedestrian concourse zone was divided into four main categories according to the floor area namely Ground Floor Atrium Zone (7,008 m^2 floor area), corridor Zone (50,677 m^2 floor area), Retail Office and Office Zone (80,002 m^2 floor area) and Atrium Void Zone (7,008 m^2 floor area). The following general assumptions had been made to determine the internal conditions for these zones:

- Infiltration rate:

  According to Meyringer and Feustel, cited in Weber (2004), the value for infiltration can vary between 0.5 and 0.85 ach, so the infiltration rate of the parameter zones in this study was set as 0.5 ach.;

- Occupancy:

  Sensible and latent heat dissipation per person in light work in typical retail store was 75W and 55 W, respectively (CIBSE, 2006). It was assumed that the percentage presence for occupants for each zone was constant. There was 50,000 visitors cover the whole building of 140,000 m^2 during operating hours of 0800h ~2000h. It was assumed that only 5% of the total visitors (4,166 personal) were occupied while the remaining 35 % was used for corridor zone and the rest 60% was used for retail shop zone.

  Thus, occupancy sensible heat gains per ground floor atrium zone = (208x75W)/ 7,008 m^2 = 2.2 Wm^{-2};

  Occupancy latent heat gains per ground floor atrium zone = (208x55W)/ 7,008 m^2 = 1.6 Wm^{-2};

  Occupancy sensible heat gains per corridor zone = (1,460x75W)/ 50,677 m^2 = 2.1 Wm^{-2};

  Occupancy latent heat gains per corridor zone = (1,460x55W)/ 50,677 m^2= 1.6 Wm^{-2};

  Occupancy sensible heat gains per retail shop & office zone = (2,499x75W)/80,002 m^2= 2.3 Wm^{-2};

Occupancy latent heat gains per retail shop and office zone = (2,499x55W)/80,002 m^2= 1.7 Wm^{-2}.

The produced heat was transferred to the room partly by convection and partly by thermal radiation; the thermal radiation was homogeneously distributed over all surfaces facing the room;

- Lighting:

  The power, including the power of the ballast/starter was 12 Wm^{-2} over ground floor atrium zone, atrium void zone and corridor zone (CIBSE, 2006). It was assumed that switched-on percentage in atrium, void and corridor zone was constant at 50%, due to natural lighting benefits in this area.

  Thus, lighting heat gains per atrium, atrium void and corridor zone = 12×0.5 = 6 Wm^{-2}.

  The power, including the power of the ballast/starter, was 12 Wm^{-2} over office and retail shop zone. It was assumed that switched-on percentage in retail and office zone was constant at 100%.

  Thus, lighting heat gains per office zone = 12 Wm^{-2};

- Equipment:

  There were 400 retail shops on the lower four floors and 400 offices on the top three floors. Heat production from one PC was 55 W, medium monitor was 70 W and idle desktop printer was 70 W (CIBSE, 2006). It was assumed that there would be 2PC/ office in office zone and switched-on percentage was constant at 50%. It was assumed that there would be 1PC/ shop in retail shop zone and switched-on percentage was constant at 50%.

  Thus, equipment heat gains per retail shop and office zone = (No of PC in retail shops: 1600×195×0.5) + (No of PC in office: 2400×195×0.5)/80,002 m^2 = 5Wm^{-2}.

  The produced heat was 100% sensible heat and 0% latent heat. The heat was transferred to the room purely by convection (100%) and not by thermal radiation (0%).

Figure 6.3 TAS centre glazed pedestrian concourse model and the corresponding real photos

Specification	Material	Width (mm)	Solar Absorptance	Solar Reflectance	Conductivity (W/m^oC)	Specific Heat (J/kg^oC)	Density (Kg/m^3)	Vapour Diffusion Factor [g/(m.h.pal)]	Transmittance
Floor	Vinyl	2	0.48	0.5	N/A	N/A	N/A	N/A	-
	Concrete	120	0.65	0.2	1.74	0.92	2500	$1.58x10^{-5}$	-
Ceiling	Aluminium	4	N/A	N/A	N/A	N/A	N/A	N/A	-
Transparent Roof	Glass	6	0.08	0.08	0.76	0.84	2500	0	0.22
	Laminate	0.76/1.52	0.08	0.08	N/A	N/A	N/A	N/A	0.22
	Glass	6	0.08	0.08	0.76	0.84	2500	0	0.22
External wall	Glass	12	0.14	0.60	1.00	N/A	N/A	99999	0.85
Internal wall	Lightweight Plaster	150	0.40	N/A	1.05	N/A	1840	36.8	-
Slab Roof	Concrete	10	0.60	0.35	0.93	1.05	1800	$2.1x10^{-5}$	-
	Water Proof Coat	2.5	N/A	N/A	N/A	N/A	N/A	N/A	-
	Poly Styrene	10	N/A	N/A	N/A	N/A	N/A	N/A	-
	Concrete	120	0.65	0.2	1.74	0.92	2500	$1.58x10^{-5}$	-

Table 6.1 Properties of some key building elements used in the model

6.3.3 Results and Discussions

The calibration of the dynamic thermal model of the long-span glazed roof over large pedestrian concourse was by comparisons the two keys variables, the air temperatures over the seven floors and the total average cooling load. The comparison of the lighting model was by DF comparison.

6.3.3.1 Dynamic Thermal Model Calibration

Apart from the air temperatures comparison, the predicted average temperatures over the seven days and the temperature profile on the hot clear and overcast days were compared against the measured ones. As the cooling was concerned, the predicted total cooling load per floor area was compared with the cooling capacity calculated by the

designer. In addition, predicted cooling load were compared against the actual surveys and also against the cooling load benchmark standard.

(a) The Average Daily Air Temperature Calibration

Table 6.2 presents the average daily predicted temperatures over each floors are compared against the measured ones for the selected period. The listed are the maximum and average differences between the two set of the variable. The agreement between the two was generally good, the average differences were around $1^{o}C$ and the maximum difference was less than $1.6^{o}C$ over the examined period.

The average TAS predicted temperatures were smaller than the measured temperatures which could be due to underestimated thermal storage effect of the structure calculated by TAS which affected the air temperature of the simulation. However, these figures illustrate similar trend which indicated that the temperature stratification occurred at high level inside the atrium.

There were differences between predicted results by the TAS program and measured results. Comparison of the average differences of the predicted temperatures made by TAS and the measured temperatures were between 2.25 and 3.71 percent. This small error in the range of ±5.00 percent made by TAS was considered to be in the acceptable range.

Day	Floor	Avg. measured temp.(°C)	Avg. predicted temp.(°C)	Max. difference temp.(°C)	Avg. difference temp.(°C)
30th Aug 11	G.	34.3	33.3	1.2	1.0
	1st	34.3	33.0	1.2	1.3
	2nd	34.5	33.0	0.8	1.5
	3rd	34.6	34.0	1.1	0.6
	4t	35.4	34.0	1.0	1.3
	5th	35.3	35.0	1.3	0.2
	6th	35.2	33.6	1.0	1.6
31st Aug 11	G.	32.8	31.7	1.0	1.1
	1st	32.7	31.7	1.5	1.0
	2nd	32.7	31.7	1.3	1.0
	3rd	32.7	31.8	1.2	0.9
	4t	33.3	31.8	1.1	1.4
	5th	33.1	31.8	1.2	1.3
	6th	32.9	31.9	0.6	1.1
1st Sep 11	G.	28.9	28.2	0.7	0.7
	1st	28.8	28.1	0.3	0.6
	2nd	28.7	28.1	0.8	0.5
	3rd	28.6	28.2	1.4	0.5
	4t	28.9	28.2	1.2	0.7
	5th	28.8	28.2	1.0	0.6
	6th	28.6	28.2	1.1	0.4
2nd Sep 11	G.	29.2	28.5	0.8	0.7
	1st	29.1	28.6	0.8	0.5
	2nd	29.1	28.6	1.1	0.5
	3rd	29.1	28.6	1.5	0.5
	4t	29.5	28.6	1.6	0.9
	5th	29.5	28.6	1.0	0.8
	6th	29.4	28.6	1.0	0.7
3rd Sep 11	G.	29.5	28.5	1.1	0.9
	1st	29.4	28.6	1.2	0.8
	2nd	29.4	28.6	1.5	0.8
	3rd	29.4	28.6	1.0	0.9
	4t	29.9	28.6	1.1	1.3
	5th	29.8	28.6	1.3	1.2
	6th	29.7	28.6	1.0	1.2
4th Sep 11	G.	30.7	30.2	1.6	0.4
	1st	30.7	30.2	1.4	0.5
	2nd	30.7	30.3	1.0	0.5
	3rd	30.9	30.3	1.2	0.6
	4t	31.4	30.3	0.8	1.1
	5th	31.4	30.4	0.8	1.1
	6th	31.3	30.4	0.9	0.9

Table 6.2 Comparison between measured and predicted temperatures by the naturally ventilated model

(b) Calibration on Clear Hot Day and Overcast Hot Day

The profiles of the predicted were compared against the measured ones on both the hot clear and cloudy days over the ground floor and top floor (Figure 6.4). In general for both simulation days, the measured and predicted air temperatures on the ground floor and top floor agree considerably well. The average differences between the predicted and measured temperatures were around 1°C on the top floor during sunny hours, the hottest of the day and smaller for the rest. The differences on the ground level were smaller than those on the top. This suggests that the solar effect was difficult to be modelled accurately. These two sets of temperatures profiles were in a good agreement.

Over all the measured values were constantly higher than the predicted, especially on upper floors, which mean the modelling results could be slightly under estimated.

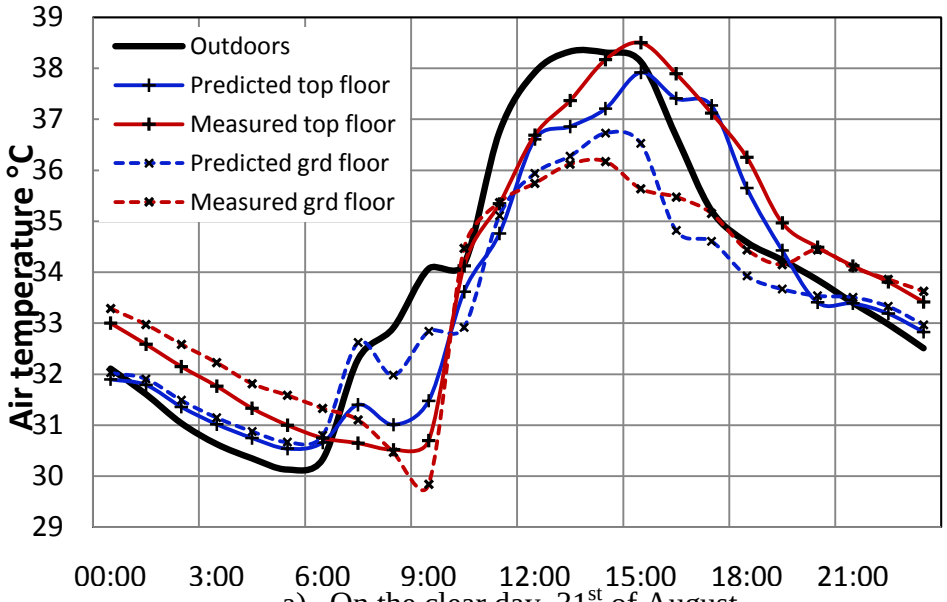

a) On the clear day, 31st of August

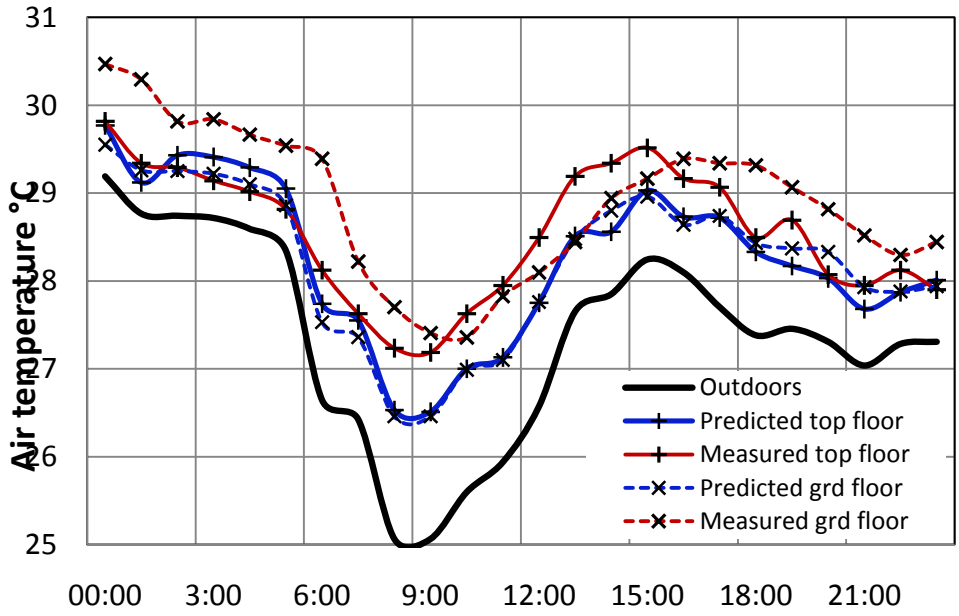

b) On the over cloudy day: 1st Sept

Figure 6.4 Comparison between the measurement and model prediction

(c) Cooling Load Calibration

- **Cooling Load Comparison against the Surveyed Data Collection**

As the cooling was concerned, the total cooling load predicted was 194,122 kWh in all the units over the air-conditioned area of 94,800 square metres during the clear

hot day, giving the cooling power of 171 Wm^{-2} (Figure 6.5). According to the actual cooling ratio 0.87 of the designed capacity obtained from the survey mentioned in chapter 4, the cooling capacity would be 197 Wm^{-2}. This was very close to the original design capacity 180 Wm^{-2}, with 8 percent relative differences. Hence the thermal model was considered accurate enough to assess the effects of the shading options on both the environmental and cooling aspects of the GITC building.

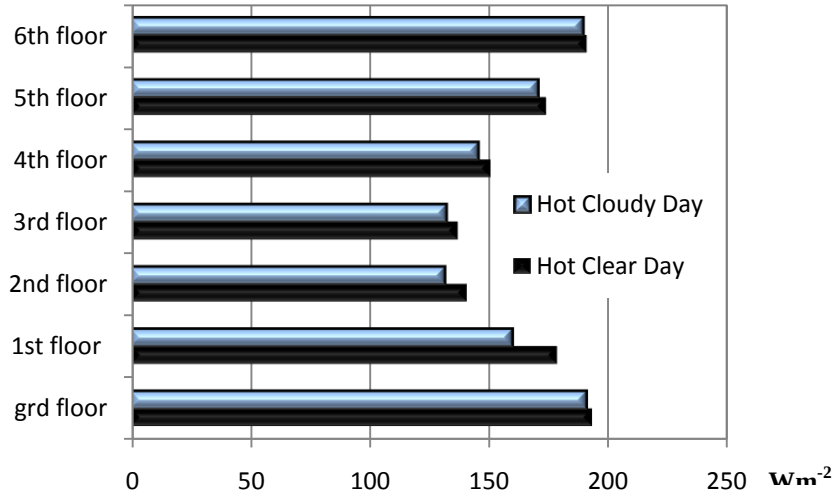

Figure 6.5 Predicted cooling load by TAS

- **Cooling Load Comparison against the Energy Benchmarking for Cooling System**

The energy performance of building can be identified by comparing with the building energy benchmarks. Energy utilization index (EUI) for large retail building is derived from national benchmarking for building in Singapore. The median EUI of large retail buildings is 405 $kWhm^{-2}$ including Heating Ventilation and Air Conditioning (HVAC), lighting and equipment operation (Building and Construction Authority, 2014).

Typically, the majority of commercial building electricity consumption is attributed to cooling (60%) and mechanical ventilation (10%). The remaining share goes to lighting (15%), lifts & escalators (10%) and other sources (5%) (Chua et al., 2013) (Figure 6.6). Therefore, the energy benchmarking for cooling system in large retail buildings would be 316 $kWhm^{-2}$.

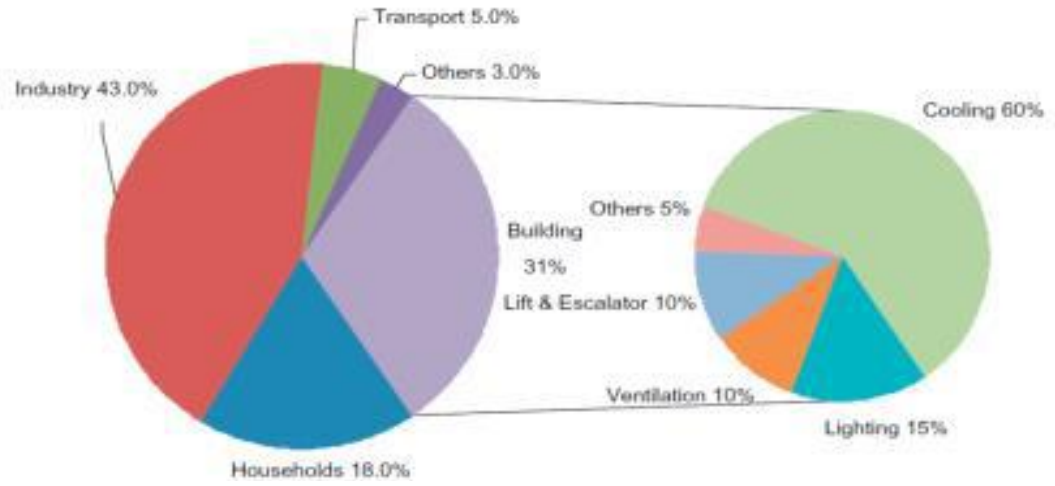

Figure 6.6 Typical electricity consumption by end-use in the building sector in Singapore (Chua et al., 2013)

Since there is no annual recorded energy consumption for air condition available in GITC building, the total energy consumption during summer period (153 days) thus was calculated by the original design capacity at 180 Wm^{-2}.

The total cooling load of GITC = 180 x 12h x 153

= 330 $kWhm^{-2}$

The total cooling load calculated by the original design capacity is 330 $kWhm^{-2}$ over GITC building of 140,000 square metres which is almost 10 percent higher than the benchmarking for cooling system standard at 316 $kWhm^{-2}$. This result reveals that this building has the overheating problem causing the expensive for cooling system to keep the space thermally comfortable.

6.3.2.2 Lighting Model Calibration

The lighting model from Ecotect was created and calibrated with the measured data. The central glazed pedestrian concourse on ground floor of the model, the corridors adjoining atrium on first floor and third floor were selected to analyse the nature daylight level in order to access the average daylight factor and daylight distribution compared with the measured ones.

The DF distribution predicted by the lighting model followed fairly well with the measured ones. An overall agreement between measured and simulated DF was good, even though there were a few points where the predictions were different from the

measured ones. The major discrepancy happened around the east and west escalators which could be not be modelled using the version of Ecotect (Figure 6.7). The average DF over each of the seven floors shows fairly good agreement. The lowest relative deviation, 3 percent was on the sixth floor and the poorest, 23 percent on the ground floor (Zhu, 2012). The daylight model was then accepted for shading assessment in this study (Figure 6.8).

Corridor

1.2%/ 1.1%	1.3%/ 1.3%	1.4%/ 1.7%	1.4%/ 1.8%	1.8%/ 1.5%	1.4%/ 1.7%	1.3%/ 1.5%	1.1%/ 0.9%
1.5%/ 1.4%	2.3%/ 1.6%	2.8%/ 2.0%	2.9%/ 2.1%	2.4%/ 2.2%	2.2%/ 2.0%	2.0%/ 1.7%	1.3%/ 1.1%
1.5%/ 1.6%	2.8%/ 1.9%	3.0%/ 2.2%	3.8%/ 2.4%	1.7%/ 2.4%	1.4%/ 2.2%	1.0%/ 2.0%	0.8%/ 1.2%
-	2.8%/ 2.1%	2.8%/ 2.3%	3.8%/ 2.6%	1.8%/ 2.5%	1.5%/ 2.6%	1.2%/ 2.0%	0.9%/ 1.3%
-	2.4%/ 2.1%	2.5%/ 2.4%	2.9%/ 2.6%	2.1%/ 2.8%	1.5%/ 2.4%	-	0.7%/ 1.3%
-	1.8%/ 2.0%	2.4%/ 2.7%	2.4%/ 2.49%	2.0%/ 2.6%	1.4%/ 2.3%	-	0.7%/ 1.3%
-	1.7%/ 1.9%	2.7%/ 2.2%	2.5%/ 2.6%	1.8%/ 2.4%	1.4%/ 2.2%	1.3%/ 2.0%	1.3%/ 1.2%
1.3%/ 1.4%	1.6%/ 1.8%	2.6%/ 2.1%	2.7%/ 2.0%	1.6%/ 2.2%	1.3%/ 2.0%	1.2%/ 1.7%	1.2%/ 1.1%
1.2%/ 1.2%	1.4%/ 1.4%	2.2%/ 1.6%	2.3%/ 1.8%	1.4%/ 1.7%	1.2%/ 1.6%	1.4%/ 1.5%	1.1%/ 0.9%

Corridor

(a) The ground floor (Measured/Simulated)

0.5%/ 0.8%	1.4%/ 1.2%	2.0%/ 1.4%	2.2%/ 1.5%	2.0%/ 1.6%	2.1%/ 1.5%	2.2%/ 1.6%	2.0% 1.4%	0.8%/ 1.2%	1.4%/ 1.1%	10
1	2	3	4	5	6	7	8	9	1.6%/ 1.2%	11
									1.3%/ 1.4%	12
									0.3%/ 1.4%	13
									0.3%/ 1.4%	14
Corridor				Atrium					0.3%/ 1.3%	15
									0.5%/ 1.4%	16
									1.4%/ 1.1%	17
									1.4%/ 1.1%	18

(b) The first floor corridor (Measured/Simulated)

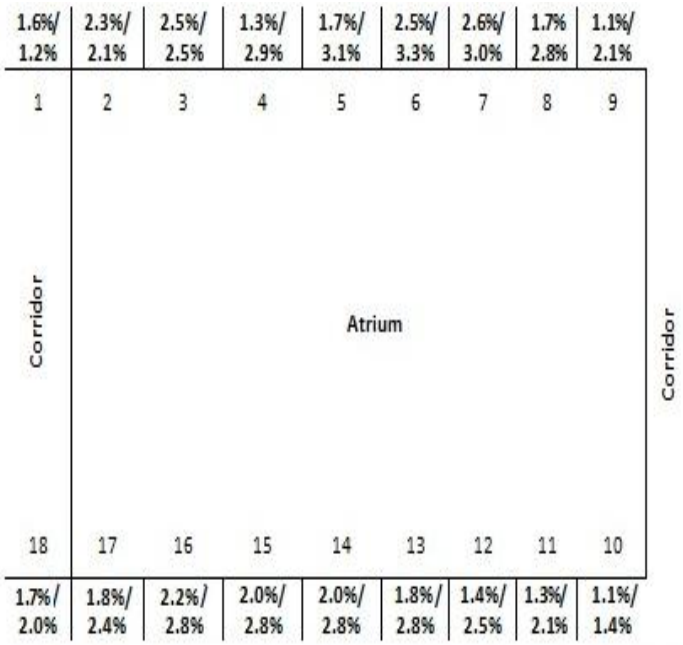

(c) The second floor corridor (Measured/Simulated)

Figure 6.7 Comparisons between the measured and simulated daylight factors ((Zhu, 2012)

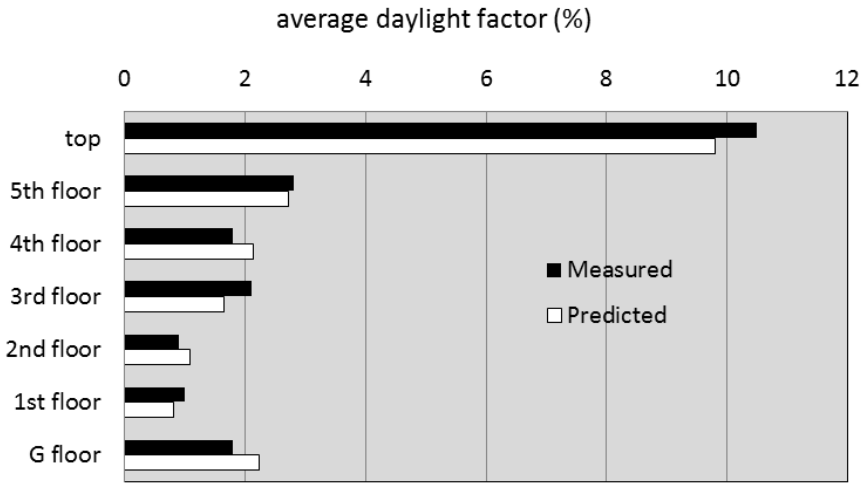

Figure 6.8 Comparison between the measured and predicted DF over 7 floors around the Centre pedestrian concourse

6.4 The Large Glazed Air-Conditioned Pedestrian Concourse

The study was conducted in the departure passenger lounge in Suvarnabhumi Airport Terminal Building, Thailand. This airport is located at 13°40’52” north latitude and 100° 44’50” east longitude.

6.4.1 Dynamic Thermal and Lighting Model and Parameters Examined

Suvarnabhumi Terminal building was created in both the thermal and lighting models based on the architectural drawings including the arrival lounge floor of buildings, departure lounge and long-span glazed roof over large air-conditioned pedestrian concourse. The thermal dynamic model was built using TAS and the lighting model by Dialux. The building was developed to contain the following elements (Figure 6.9a, 6.9b):

- The building is a six storey designs with a total floor area of nearly 140,000 square metres for all floors (1,506,960 sq ft). The 3-D model of the long-span glazed roof over large air-conditioned pedestrian concourse building was created based on the architectural drawings of Suvarnabhumi Airport Terminal building and the north angle was set to reflect the orientation of the real building;
- The long-span glazed roof over the large air-conditioned pedestrian concourse was divided into 17 zones over six floors to capture the differences in thermal condition over the space. The central large pedestrian concourse at the roof level was further divided between the transparent roof zone and the ceiling zone to capture the differences in thermal conditions over this space. Such division was intended to differentiate subtle changes in temperature from one place to another and to allow the predicted values of the models to be compared with those from field measurements at exactly the same positions in the calibration;
- 11.5 metres floor to floor height for the ground floor to first floor and 4.9 metres to floor height for all above.

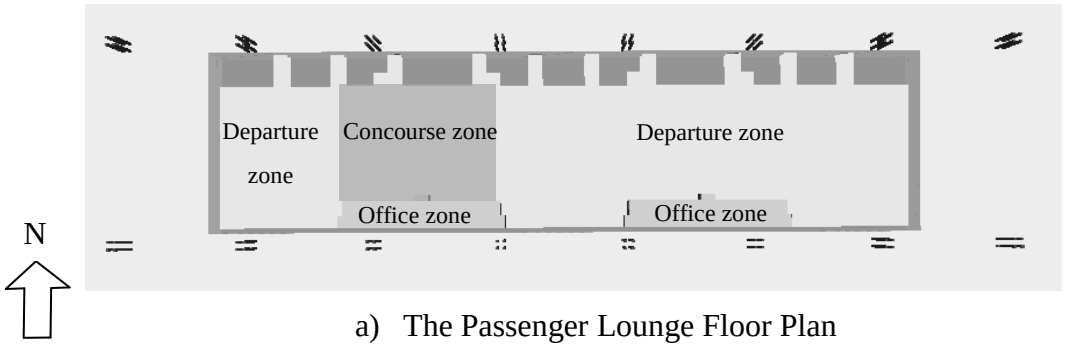

a) The Passenger Lounge Floor Plan

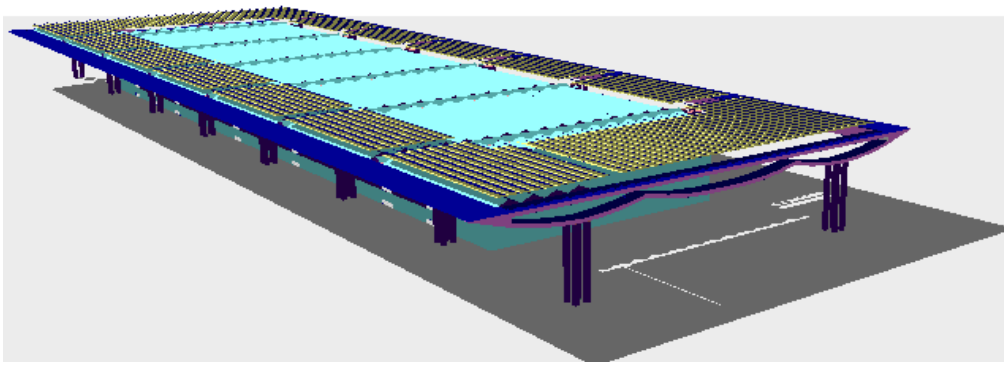

b) Computer Model

Figure 6.9 Suvarnabhumi International Airport Terminal configuration model

The exact design details, material properties, and construction in the field needed to create the two computer models were incomplete. The dimensional construction data were created according to the architectural drawing. There is some uncertainty about building element inputs. Floor, glazed roof, internal wall and external glazed wall were all specified from software construction database with reference to the architectural specifications. The floor was simulated as being constructed with terrazzo and concrete and it U-value was 2.22 $Wm^{-2o}C$. The glazed roof was simulated as being constructed with laminated glass and it U-value was 5.50 $Wm^{-2o}C$. The internal wall was simulated as being constructed with aluminium composite and it U-value was 0.50 $Wm^{-2o}C$. The external wall was simulated as being constructed with tempered glass and it U-value was 5.50 $Wm^{-2o}C$ (Table 6.3).

Specification	Material	Width (mm)	Solar Absorptances	Solar Reflectance	Conductivity (W/m^oC)	Specific Heat (J/kg^oC)	Density (Kg/m^3)	Vapour Diffusion Factor [g/(m.h.pal)]	Transmittance
Floor	Terrazzo tiles	3	0.65	0.35	1.75	850	2400	48	-
	Concrete screed	50	0.65	0.35	1.28	1000	2100	34	-
	Concrete 3%	200	0.65	0.35	0.87	920	1800	14	-
Ceiling	Acoustic tiles	15	0.50	0.50	0.058	586	288	14.0	-
External wall	Laminate Glass	12	0.22	0.04	0.16	0.20	0.45	5.6	0.15
Internal wall	A/L composite	5	0.53	0.47	43	500	7800	99999	-
	Mineral wool	90	0.53	0.40	0.048	1050	240	2.70	-
	A/L composite	5	0.53	0.47	43	500	7800	99999	-
Metal sheet roof	Insulated metal sandwich	2	0.53	0.47	43	500	7800	99999	-
		60	0.53	0.60	0.04	1210	16	21	-
		2	0.53	0.47	43	500	7800	99999	-
Transparent roof	Low E coated glass	10	0.2	0.20	0.12	0.16	0.15	4.5	0.22
External shading	Aluminium	5	0.50	0.50	204	896	2700	99999	-
Structure	Steel	50	0.53	0.47	43.0	500	7800	99999	-

Table 6.3 Properties of some key building elements used in the air-conditioned model

The lighting model had the same geometry as dynamic thermal model. The critical variables which affect simulation accuracy were reflectance of the internal surfaces and the transmittance of the external envelope. Base on the product datasheets, the reflectance was set to 20% for the floors, 60% for the internal walls and 50% for check in counters (Figure 6.10).

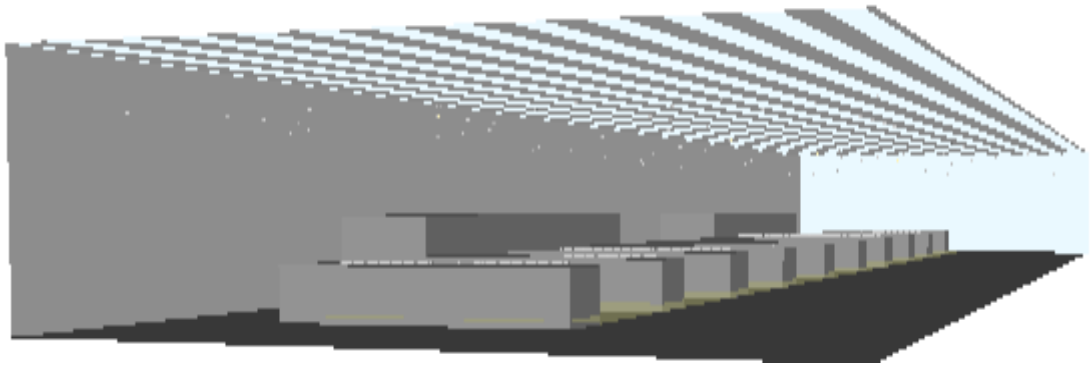

Figure 6.10 3-D model of the Departure Lounge, Suvarnabhumi Airport by Dialux (Anunnathapong, 2013)

6.4.2 Weather and Internal Conditions

For dynamic thermal model, hourly weather data is required; the 2012 weather data file for Bangkok meteorological weather data was used as the representative year data. The data set contains the hourly figures of the seven weather variables: the air temperature, relative humidity, global and diffuse solar radiations, cloudiness and wind speed and

direction for a whole year. In order to increase the accuracy of the thermal and lighting simulations, the calibration of the two models were carried out as follows:

- The representative dynamic thermal model was run for twenty consecutive days from 12th September to 1st October 2012;
- Calibration of the thermal models were compared with the measured results for two critical variables, the glazed roof surface temperatures and the total average cooling loads within the long-span glazed roof over large air-conditioned pedestrian concourse of Suvarnabhumi Airport Terminal on the hottest clear day and overcast day. Calibration of lighting models were compared with the DF within the long-span glazed roof over large pedestrian concourse on the selected overcast days;
- For the average indoor air temperature comparison, the average predicted glazed roof surface temperatures by date and by time were compared against the measured ones;
- For the profiles of temperature comparison, 12th September 2012 was chosen to represent a clear hot day and on 28th September 2012 to represent an overcast hot day to use in the calibration;
- For the total cooling load comparison, the predicted total cooling load was compared against the degree days predicted total cooling load. In addition, the predicted total cooling load per floor area was compared against the cooling load benchmark in airport building.

For simulating the lighting conditions, 28th September 2011 was chosen to represent an overcast hot day using in the calibration; the building blocks were used as domestic and international departure lounge. For the internal condition, the air temperature for all air-conditioned zones were set according to recommended comfort criteria for airport terminals by CIBSE (2006) between 21~25^{0}C for 24 hours.

The heat gains from occupants, lighting and equipment were set to the CIBSE Guide A (2006) value for standard offices and retail shops respectively. Since the usage of the airport was irregular, the occupancy was set to 145,211 persons around the whole building over the 24 hour period, based on the passenger statistics of the airport (AOT, 2012) (Appendix E).

Based on the typical floor plan of the model buildings (Figure 6.9), the large glazed air-conditioned pedestrian concourse zone was divided into three main categories according to the floor area, namely Departure Zone (40,500 m^2 floor area), Void Zone (40,500 m^2 floor area) and Office Zone (20,184 m^2 floor area). The following general assumptions had been made to determine the internal conditions for these zones:

- Infiltration rate:

  According to Meyringer and Feustel, cited in Weber (2004), the value for infiltration can vary between 0.5 and 0.85 ach, so the infiltration rate of the parameter zones in this study was set as 0.5 ach.

- Occupancy:

  Sensible and latent heat for light work and walking dissipation per person in airports (Refer to Chapter 5) was 75 W and 55 W, respectively (CIBSE, 2006). It was assumed that the percentage presence for occupants for each zone was constant. There was 145,211 visitors cover the whole building of 563,000 m^2 for 24 hours (AOT, 2012). The total visitors within the passenger lounge were 6050 visitors in each hour.

  According to the airport officers and staff groups' statistic in 2011, Suvarnabhumi Airport had a total number of 7,626 personnel and accommodated 100 scheduled airlines (AOT, 2012). It was assumed that each airline provides 10 employees for 24 hours service; the airlines would have an approximate total number of 1,000 personnel. In addition, there are other agencies' employees such as the Customs Department, Police and the Thailand Post Company, making up around 200 personnel. The total airport officers and staffs were 8,826 personal. Assuming that 25% of them were occupied within the passenger lounge zone (2206 personnel) and 10% of them were occupied within the office zone (883 personnel).

  Thus, occupancy sensible heat gains per departure zone = (No of passenger and staff: 6050+2206x75W)/40,500 m^2 = 15.3 Wm^{-2};

  Occupancy latent heat gains per departure zone = (No of passenger and staff: 6050+2206x55W)/40,500 m^2= 11.2 Wm^{-2};

  Occupancy sensible heat gains per office zone = (No of staff: 883x75W)/20,184 m^2= 3.2 Wm^{-2};

Occupancy latent heat gains per office zone = (No of staff: 883x55W)/20,184 m^2= 2.4 Wm^{-2}.

The produced heat was transferred to the room partly by convection and partly by thermal radiation; the thermal radiation was (homogeneously) distributed over all surfaces facing the room.

- Lighting:

  The power, including the power of the ballast/starter was 12 Wm^{-2} over ground floor atrium zone, atrium void zone and corridor zone (CIBSE, 2006). It was assumed that the lights switched-on percentage was constant at 100%.

- Equipment:

  There were 200 counters check in within departure lounge. Heat production from one PC was 55 W, medium monitor was 70 W and idle desktop printer was 70 W (CIBSE, 2006). It was assumed that there would be 2PC/ counter check in and switched-on percentage was constant at 50%. In addition, it was assumed that 1PC/ person per office zone and switched-on percentage was constant at 80%.

  Heat production from conveyor specification was 10 kW. There were 200 conveyors in departure lounge zone and switched-on percentage was constant at 80%.

  Thus, equipment heat gains per office zone = (No of PC: 883×195×0.5)/ 20,184 m^2 = 4.3Wm^{-2}.

  Equipment heat gains per departure lounge zone = (No of PC: 400×195×0.5) + (No of conveyor: 200×1000×0.8)/ 40,500 m^2= 5Wm^{-2}.

  The produced heat was 100% sensible heat and 0% latent heat. The heat was transferred to the room purely by convection (100%) and not by thermal radiation (0%).

6.4.3 Results and Discussions

The empirical calibration purpose was to establish the capability and accuracy of the created 3-D model by approaching in the internal surface temperature and cooling load distribution for the purpose of internal shading device in the next step. This test was

essential as it would provide a general picture of the expected thermal behaviour within the air-conditioned large concourse space.

6.4.3.1 Dynamic Thermal Model Calibration

Since this pedestrian concourse was air-conditioned, solar radiation had greatly influenced the transparent roof surface temperatures and the upper level air temperatures. The environment variable examined to calibrate the thermal model for this space was the inner surface temperatures of the transparent roof. Since the internal thermal condition within the air-conditioned large pedestrian concourse was contributed by the heat transfer in internal building material surfaces from convection and long-wave radiation exchange and solar heat gain from solar radiation from the transparent building components. Both the average inner transparent roof temperature and the inner transparent roof temperature profiles on hot clear and cloudy days of the predicted were also compared against the measured ones. In addition, predicted cooling load were compared against the actual surveys and also against the cooling load benchmark standard.

(a) The Average Surface Temperature by Date and Time Calibration

In order to calibrate the air-conditioned large space glazed concourse model, the inner transparent roof temperatures were the main outputs being measured from the model and compared with measured surface temperatures.

The main factor to contributed thermal condition in glazed pedestrian concourse is due to solar heat gain from solar radiation entering from the transparent component, especially the glazed roof. The high surface temperature that leads to high radiation heat to the space was considered to be the main cause for the negative effects on the thermal comfort resulting in more energy consumption from the air-conditioning system.

For average surface temperature by date and time, the TAS prediction results show a reasonably good agreement with the measured data as revealed by Figure 6.11 and 6.12. During the hottest hour of the day, the predicted and measured glazed roof surface temperatures increase dramatically. Both Predicted results and measured data show similar trend which indicates that the gazed roof surface temperature was exceed above the external air temperature, during the hottest hour of the day.

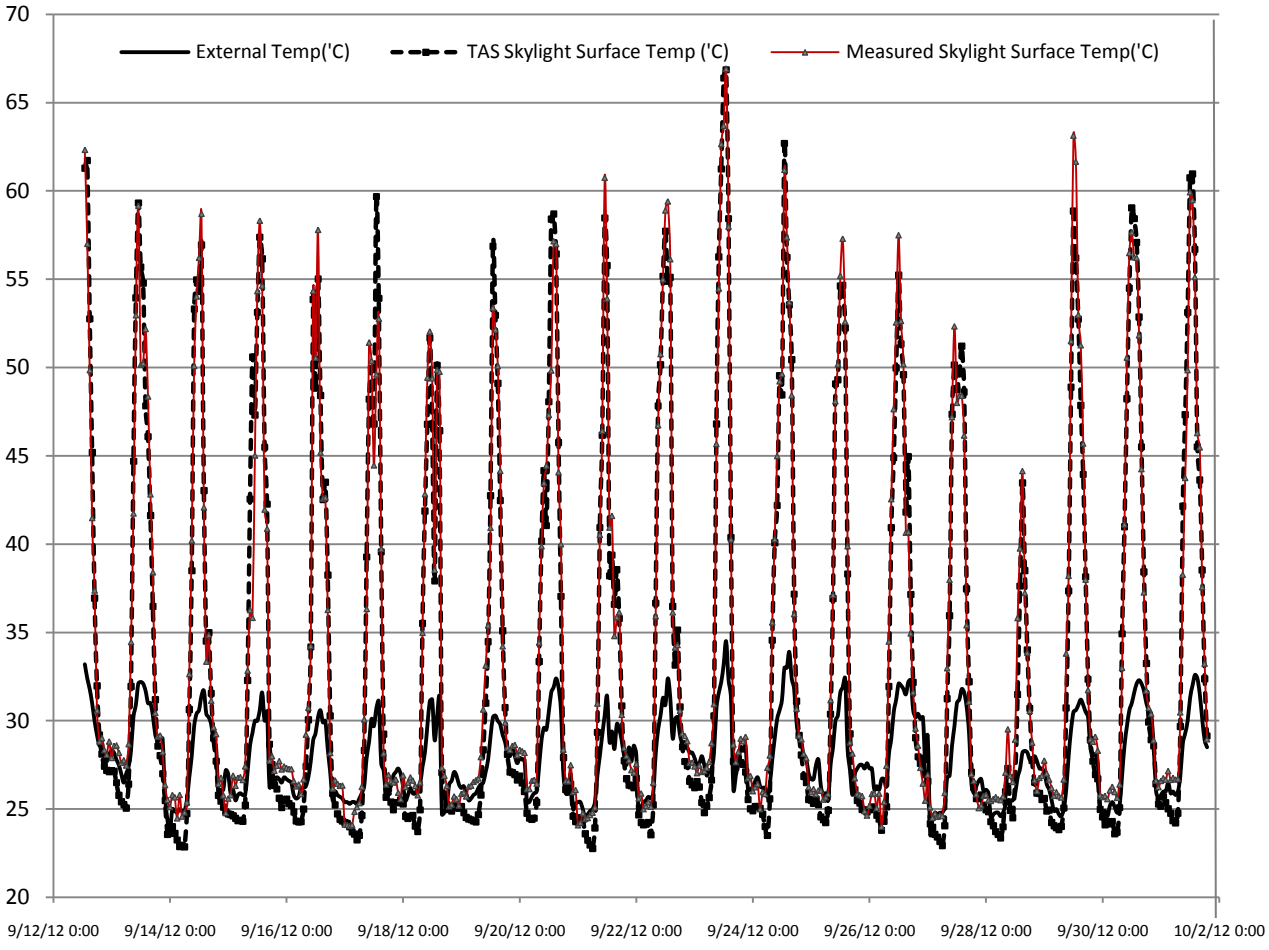

Figure 6.11 Transparent roof surface predicted temperatures by TAS vs. measurement by date

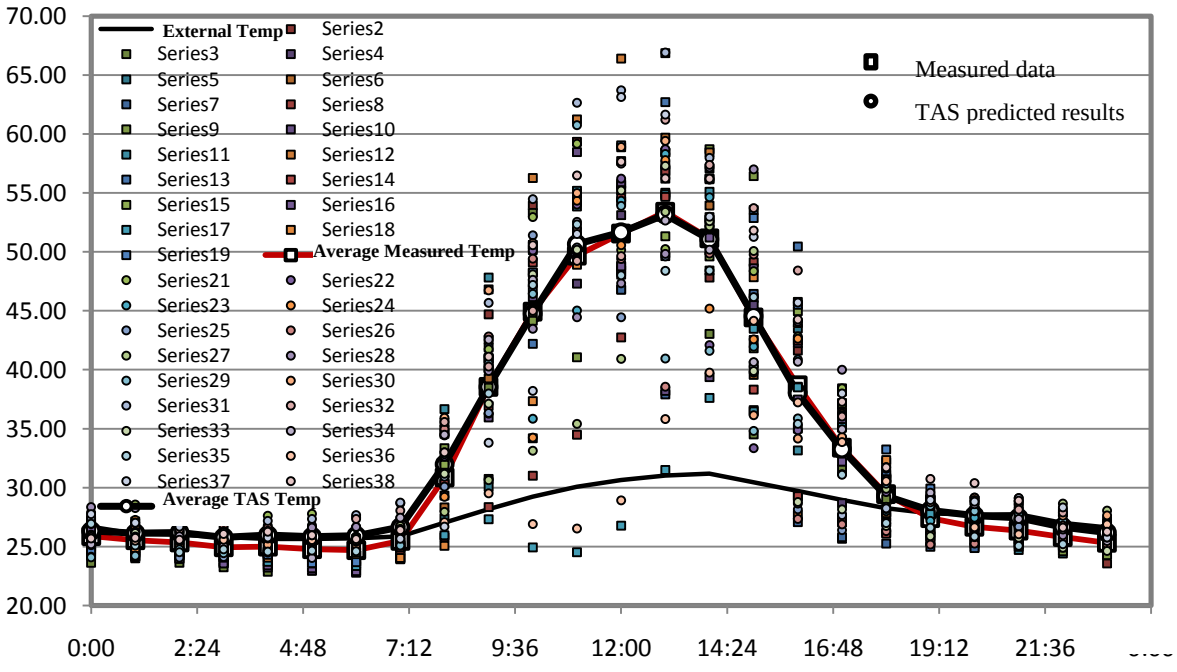

Figure 6.12 Transparent roof surface predicted temperatures by TAS vs. measurement by time

Table 6.4 showed the comparison between average measured temperature and average TAS predicted temperature by date. The average external temperature was 28.01^{o}C. The average measured glazed surface temperatures increased by 29.18^{o}C to 38.34^{o}C. Similarly the TAS predicted average glazed surface temperature increased by 27.90^{o}C to 38.99^{o}C. There were differences between predicted results by TAS and measured results. It was found that TAS calculations tend to be underestimated comparing to that of the measurement from 0.44 to 5.00 percent (Average 2.07 percent). The main reasons for these differences were due to the fixed internal conditions in the TAS model which were based on general assumptions, while the real internal conditions were irregular. Moreover, there were also numerous infiltration airflow paths which allowed the internal heat to be dissipated in the real building, while infiltration rates were fixed in the TAS model.

For average temperature by time, the average external temperature was 27.94^{o}C. The glazed surface average measured temperatures increased by 29.18^{o}C to 37.12^{o}C. Similarly the TAS predicted average temperature increased by 27.90^{o}C to 36.96^{o}C. TAS calculations tended to be underestimated compared to that of the measurement from 0.00 to 4.73 percent (Average 2.22 percent) (Table 6.5).

Comparison of the average differences of the predicted surface temperatures made by TAS and the measured surface temperatures were between 1.70 and 5.00 percent by date and 0.00 and 4.73 percent by time. This small error in the range of ±5.00 percent made by TAS is considered within the acceptable range.

This sensitivity test also confirms that the created 3D TAS model is capable of accurately modelling thermal stratification within the large glazed pedestrian concourse, and thus can be used to model shading in the next step.

Date	Average External Temp. (°C)	Average Measured Temp. (°C)	Average TAS Predicted Temp. (°C)	Average Difference Temp. (°C)	Average Difference Temp. (%)
12th Sep 2012	29.89	38.34	38.99	0.65	1.70
13th Sep 2012	28.99	36.01	35.21	0.80	2.23
14th Sep 2012	27.51	33.23	32.44	0.79	2.39
15th Sep 2012	27.60	33.55	33.70	0.15	0.45
16th Sep 2012	27.21	33.22	32.32	0.90	2.72
17th Sep 2012	27.08	31.90	31.85	0.05	0.13
18th Sep 2012	27.26	32.75	31.52	1.23	3.74
19th Sep 2012	27.61	32.67	31.75	0.92	2.82
20th Sep 2012	28.01	34.81	34.22	0.59	1.71
21st Sep 2012	27.55	32.81	32.21	0.60	1.82
22nd Sep 2012	28.36	35.28	34.44	0.84	2.39
23rd Sep 2012	28.83	36.15	35.37	0.78	2.16
24th Sep 2012	28.90	35.77	35.01	0.76	2.12
25th Sep 2012	27.92	32.89	32.22	0.67	2.03
26th Sep 2012	29.28	34.49	34.04	0.45	1.30
27th Sep 2012	27.38	32.69	32.50	0.19	0.58
28th Sep 2012	26.35	29.18	27.90	1.28	4.37
29th Sep 2012	27.70	35.13	33.46	1.67	5.00
30th Sep 2012	28.28	36.11	35.67	0.44	1.20
1st Oct 2012	28.51	37.12	36.96	0.16	0.44

Table 6.4 Average transparent roof surface temperatures comparison by date from 12th September to 1st October 2012

Time	Average External Temp. (°C)	Average Measured Temp. (°C)	Average TAS Predicted Temp. (°C)	Average Difference Temp.(°C)	Average Difference Temp.(%)
00:00	26.68	26.31	25.88	0.43	1.64
01:00	26.09	26.14	25.53	0.61	2.35
02:00	25.99	26.19	25.34	0.85	3.26
03:00	25.81	25.79	24.94	0.85	3.30
04:00	25.66	25.97	24.99	0.98	3.79
05:00	25.64	25.84	24.78	1.06	4.09
06:00	25.69	25.93	24.71	1.22	4.73
07:00	25.88	26.64	25.48	1.16	4.36
08:00	27.03	31.97	30.87	1.10	3.44
09:00	28.16	38.55	38.55	0.00	0.00
10:00	29.24	44.77	44.93	0.16	0.37
11:00	30.06	50.67	49.69	0.98	1.93
12:00	30.63	51.66	51.55	0.11	0.21
13:00	31.03	53.16	53.41	0.25	0.47
14:00	31.19	51.07	51.16	0.09	0.17
15:00	30.47	44.54	44.45	0.09	0.20
16:00	29.73	38.00	38.69	0.69	1.80
17:00	28.97	33.25	33.39	0.14	0.41
18:00	28.25	29.28	29.46	0.18	0.63
19:00	27.81	28.05	27.41	0.64	2.28
20:00	27.72	27.63	26.67	0.96	3.48
21:00	27.74	27.43	26.34	1.09	3.95
22:00	27.01	26.64	25.81	0.83	3.11
23:00	26.63	26.20	25.31	0.89	3.39

Table 6.5 Average transparent roof surface temperatures comparison by time from 12th September to 1st October 2012

(b) Calibration on Clear Hot Day and Overcast Hot Day

On a clear hot day, the average surface temperature difference between the predicted and measured was around 2.7°C. The average difference on a hot cloudy day was smaller. Over all the average measured temperatures are higher than the predicted,

which mean the modelling results could be slightly under estimated (Figure 6.13a and 6.13b).

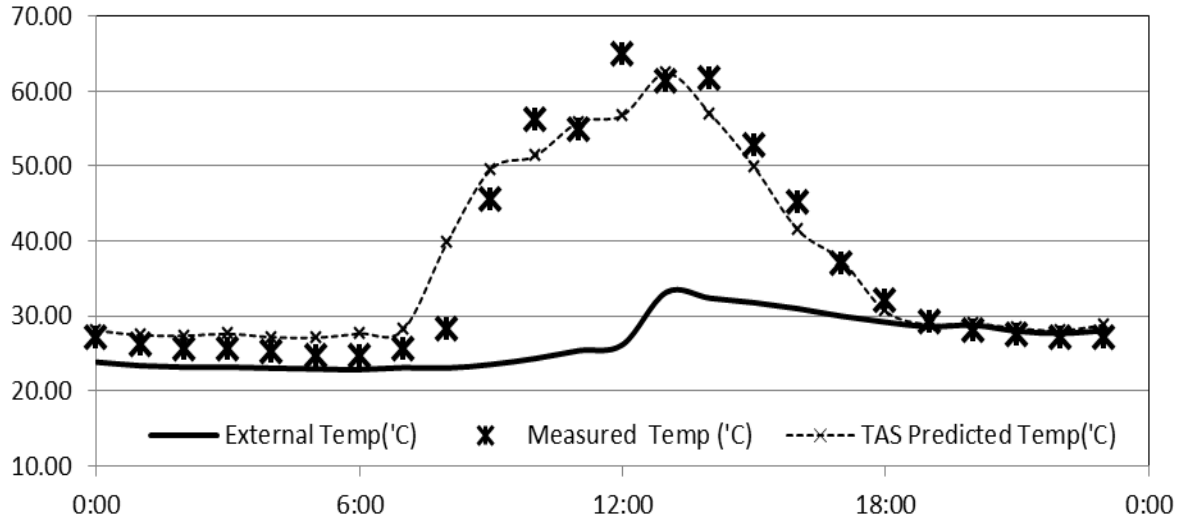

a) On the clear day, 12th of September

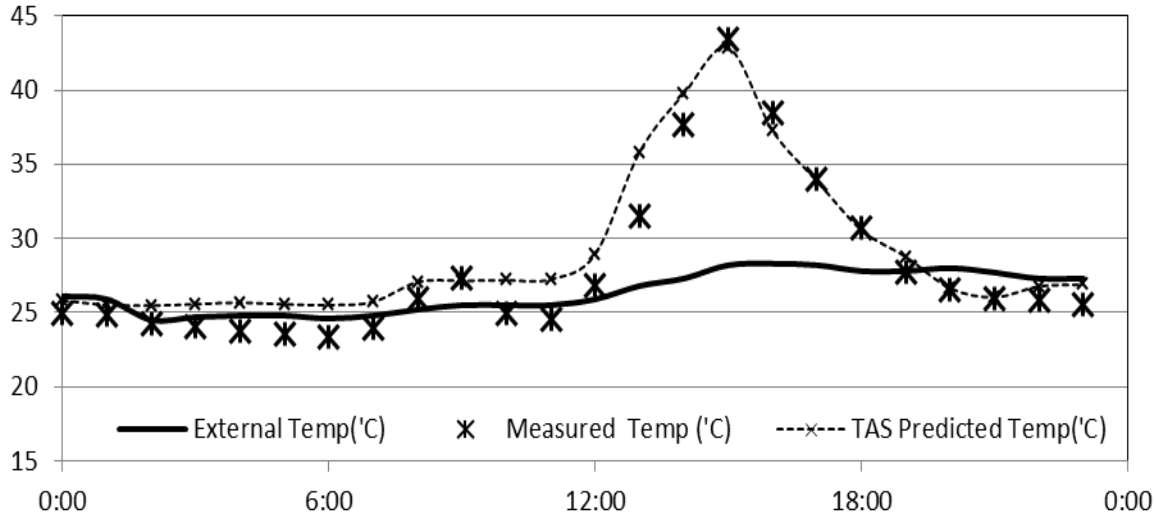

b) On the cloudy day, 28th of September

Figure 6.13 Comparison between the measurement and model prediction

(c) Cooling Load Calibration

- **Cooling Load Comparison against the Calculated Cooling Load by Cooling-Degree days**

  One of the key measures of building performance is the building energy consumption. Suvarnabhumi Airport Terminal is serving both domestic and international passenger. Total useable area is 563,000 square metres (6,060,081 sq ft). The internal temperatures in the airport would be maintained within the

range of 21°C to 25°C by using air conditioning for 24 hours; according to the comfort criteria for airport terminals by CIBSE guide A (2006).

Air-conditioning system of Suvarnabhumi Airport Terminal building is chilled water cooling system. According to the report of DCAP (2011), the amounts of chilled water to cooling coil for air-conditioning system in the airport are summarized in Table 6.6. The total cooling load of Suvarnabhumi Airport in 2010 was 1.06×10^9 MBTU.

Since cooling load data was derived to 2010 from DACP (2011). Thus cooling degree-days (CDD) are used for calculating energy used for air-conditioning for 2012. Calculation methods are simple and accurate. Equation 6.1 shows the general formula for this process for cooling degree-days (ASHRAE, 2001):

$$\mathrm{CDD} = (1\ \mathrm{day}) \sum_{\mathrm{days}} (T_m - T_b)^{+} \qquad (6.1)$$

Where T_b = the base temperature,

T_m = the daily mean outdoor temperature,

The annual heating or cooling requirements can be calculated using HDD and CDD, respectively as:

$$Q_c = \frac{K_{tot}}{\eta} \mathrm{CDD}\ \frac{24}{1000} \qquad (6.2)$$

where Q_h = the annual heating requirements (kWh),

Q_c = the annual cooling requirements (kWh),

K_{tot} = the total heat-transfer coefficient of the building in W/°C,

η = the efficiency of the heating or cooling system.

Traditionally, cooling degree-days are calculated at a base temperature of 18°C for a typical building (Kreider and Rabl, 1994).

YEAR	2006	2007	2008	2009	2010
Jan	-	7.43×10^7	8.00×10^7	6.73×10^7	8.12×10^7
Feb	-	7.78×10^7	7.84×10^7	7.88×10^7	8.23×10^7
Mar	2.91×10^7	1.01×10^8	9.34×10^7	9.47×10^7	9.35×10^7
Apr	1.99×10^7	9.71×10^7	9.69×10^7	9.49×10^7	9.70×10^7
May	2.09×10^7	9.73×10^7	9.67×10^7	9.32×10^7	9.89×10^7
Jun	2.40×10^7	9.76×10^7	9.33×10^7	9.25×10^7	9.12×10^7
Jul	5.68×10^7	9.63×10^7	9.30×10^7	9.04×10^7	9.36×10^7
Aug	5.82×10^7	9.60×10^7	9.33×10^7	9.05×10^7	9.09×10^7
Sep	6.85×10^7	9.05×10^7	8.53×10^7	8.29×10^7	8.84×10^7
Oct	9.57×10^7	8.87×10^7	9.06×10^7	8.54×10^7	8.73×10^7
Nov	9.01×10^7	7.56×10^7	7.22×10^7	7.90×10^7	7.73×10^7
Dec	7.73×10^7	8.21×10^7	6.56×10^7	7.83×10^7	8.16×10^7
MBTU	**5.40×10^8**	**1.07×10^9**	**1.04×10^9**	**1.03×10^9**	**1.06×10^9**
MBTU ft^{-2}	**89.21**	**177.23**	**171.40**	**169.63**	**175.43**
MJm^{-2}	**1,013.12**	**2,012.72**	**1,946.51**	**1,926.4**	**1992.28**
$kWhm^{-2}$	**281.42**	**559.10**	**540.70**	**535.11**	**553.41**

Table 6.6 Amounts of chilled water to cooling coil of Suvarnabhumi Airport (DCAP, 2011)

Cooling degree days relate the day's temperature to the energy demands of air-conditioning (Table 6.7). They can be used to calculate how much energy spent on air-conditioning using the linear regression analysis between energy consumption figures and degree days (Figure 6.14). R^2 indicates a reasonable correlation between energy consumption and degree days. The result is 0.87 likely an indication that the cooling control is quite good.

YEAR	2007	2008	2009	2010	2011	2012
Jan	510	519	371	508	428	467
Feb	525	502	549	565	490	194
Mar	713	644	638	667	488	703
Apr	681	646	648	728	582	736
May	645	631	614	716	625	720
Jun	643	593	596	648	578	644
Jul	605	603	590	618	580	619
Aug	616	611	626	577	586	616
Sep	583	569	584	567	548	564
Oct	589	596	571	532	522	642
Nov	485	418	492	512	503	608
Dec	569	378	502	498	513	618

Table 6.7 Thailand cooling degree days (Base 18^oC) (http://thai.wunderground.com, 2014)

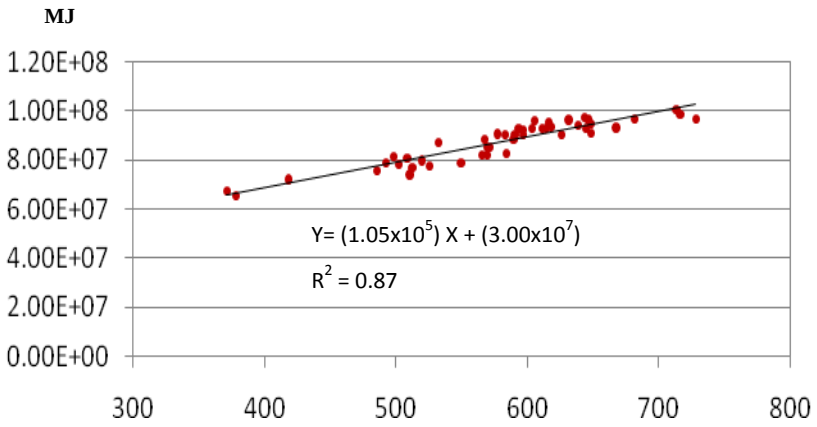

Figure 6.14 The Scatter Chart between energy consumption and degree days

From the linear regression analysis, the total calculated cooling load by degree-days of Suvarnabhumi Airport in 2012 was 1.17 x 10^9 MJ (3.25x10^8 kWh) over the whole building of 563,000 square metres giving cooling load of 2,078 MJm^{-2} (578 $kWhm^{-2}$) (Table 6.8).

	2011	2012
Jan	$7.49x10^7$	$7.88x10^7$
Feb	$8.15x10^7$	$5.03x10^7$
Mar	$8.12x10^7$	$1.03x10^8$
Apr	$9.11x10^7$	$1.07x10^8$
May	$9.56\ x10^7$	$1.05\ x10^8$
Jun	$9.07\ x10^7$	$9.73\ x10^7$
Jul	$9.09\ x10^7$	$9.47\ x10^7$
Aug	$9.15\ x10^7$	$9.44\ x10^7$
Sep	$8.75\ x10^7$	$8.90\ x10^7$
Oct	$8.48\ x10^7$	$9.71\ x10^7$
Nov	$8.28\ x10^7$	$9.36\ x10^7$
Dec	$8.39\ x10^7$	$9.46\ x10^7$
MBTU	**$1.04x10^9$**	**$1.11x10^9$**
MJ	**$1.10x10^9$**	**$1.17x10^9$**
kWh	**$3.06x10^8$**	**$3.25x10^8$**

Table 6.8 Calculated Chilled Water to Cooling Coil in 2012

From the simulated model by TAS, the total cooling load of Suvarnabhumi Airport Terminal building would be 2.83x10^8 MJ (7.86x10^7 kWh) over the terminal building of 140,000 square metres giving cooling load of 2,021.43 MJm^{-2} (562 $kWhm^{-2}$) (Figure 6.15). This is very close to the calculated cooling load by cooling degree-days, with 2.14 percent relative differences. Hence the computer model and the calculated results would be reliable enough to assess

the effects of the shading options on the internal environmental aspects of Suvarnabhumi Airport Terminal building.

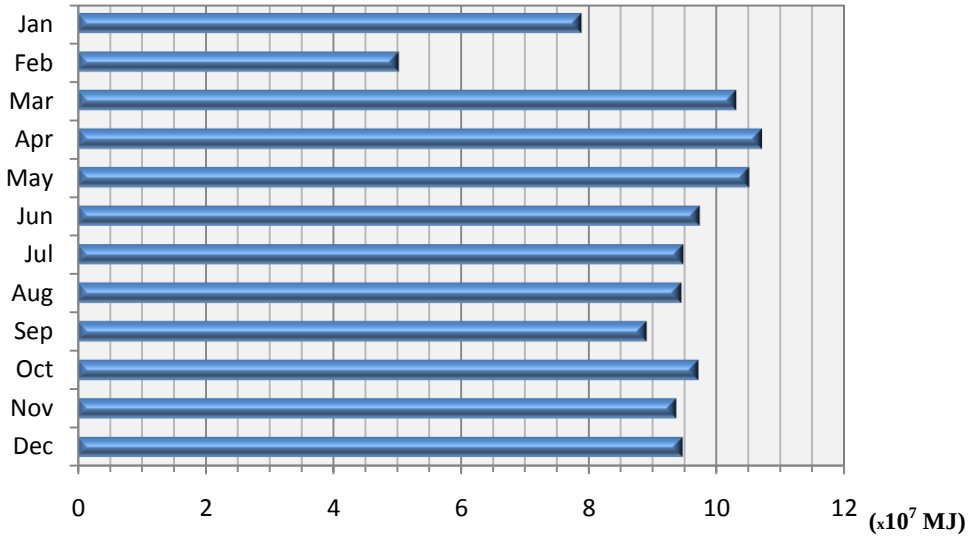

Figure 6.15 Predicted annual cooling loads by TAS

- **Cooling Load Comparison against the Energy Benchmarking for Cooling System**

In order to assess energy performance in airports, energy consumption was compared between the calculated and average energy intensity benchmark. However, energy consumption in airports can be difficult to measure, since airports are not routinely tracking energy use. Energy intensity benchmark for airport is derived from extensive worldwide research into available and appropriate case studies. The energy intensity per floor area benchmark for large airport is 2,085 MJm^{-2} (579.6 $kWhm^{-2}$), including Heating Ventilation and Air Conditioning (HVAC), lighting and equipment operation (Auckland International Airport, 2013).

A further breakdown of the energy used in Airport shows that the energy is used by HVAC 68 percent, lighting 17 percent, equipment operation 3 percent and concessionaries power 12 percent (BIA cited in ACI, 2014) (Figure 6.16). HVAC can be responsible for up to 80 percent of a facilities energy bill, due to poor design, operation and management (Costa et al., 2008), thereby contributing from 1,417 to 1,668 MJm^{-2} (393.1 – 467.7 $kWhm^{-2}$).

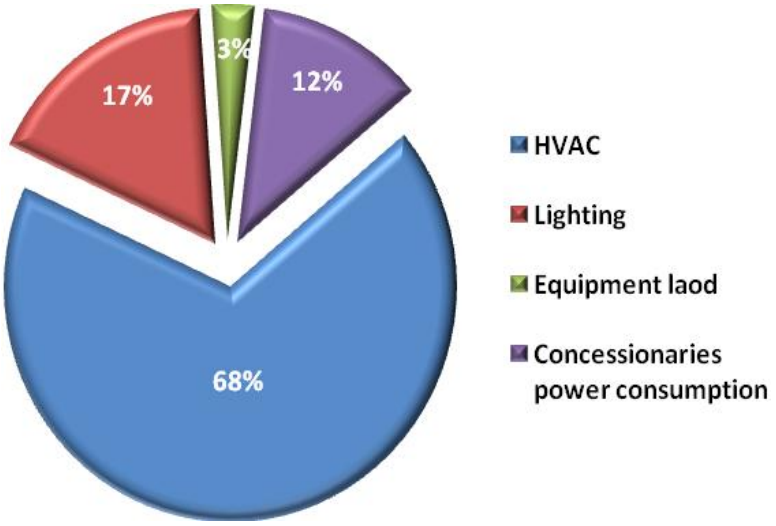

Figure 6.16 Typical energy consumption at terminal building (BIAL cited in ACI, 20014)

The total cooling load calculated by degree days was $2.83x10^{8}$ MJ over Suvarnabhumi Airport Terminal building of 140,000 square metres giving cooling load of 2,078 MJm^{-2} (578 $kWhm^{-2}$) which is very high compared with the benchmark due to the high solar altitude and ambient temperatures in the tropical climates. This clearly indicates that this passenger lounge has the overheating problem causing the excessive use of the cooling system to keep the space thermally comfortable.

6.4.3.2 Lighting Model Calibration

The internal lighting condition can be examined by using Dialux 4.11 which is the software that has been developed in order to simulate and analyse both indoor and outdoor lighting performance. The program is also suitable for lighting design and planning that is acceptable software for research work (Acosta et al., 2011).

The results of model calibration were calculated in the form of the daylight factor. Measured data was obtained in the check-in lounges between check-in counters on a cloudy day of 1st Oct 2012 at 1300h-1400h when the external illuminance was 5,000 lux. The measurement was carried out at 10 x 23 points and compared with computer simulation model results. The computer model was set in the same date at 14:00. The artificial lightings for the model was set according to the actual building: 637 sets of

halogen roof light (637x1000 W), 420 sets of check-in counter fluorescent light (420x58 W) and 220 sets of PLC canopy light (220x32 W) (Appendix F).

The DF distribution predicted by the lighting model followed fairly well with the measured ones. The minimum DF from measurement and simulation was 0.57 and 0.73 percent respectively. The maximum DF from measurement and simulation was 1.74 and 2.75 percent respectively (Figure 6.17). An overall agreement between the average measured and simulated DF was good, even though there were a few points where the predictions were different from the measured ones, especially points that were close to the glazed wall to the north (Anunnathapong, 2013).

Column1		Column 2		Column 3		Column 4		Column 5		Column 6		Column 7		Column 8		Column 9	
1.01%	1.73%		0.83%	1.53%		1.03%	1.51%		0.81%	1.50%		1.27%	1.50%		0.91%	1.50%		0.92%	1.50%		0.91%	1.53%		1.07%	1.74%
0.94%	1.64%		0.81%	1.47%		0.98%	1.45%		0.84%	1.45%		1.14%	1.45%		0.87%	1.45%		0.86%	1.45%		0.83%	1.47%		1.07%	1.64%
1.36%	1.55%		0.84%	1.42%		1.74%	1.41%		2.26%	1.41%		1.67%	1.41%		0.96%	1.41%		2.25%	1.41%		1.26%	1.43%		1.87%	1.57%
0.89%	1.36%		0.78%	1.33%		0.94%	1.33%		1.45%	1.34%		1.18%	1.34%		0.86%	1.34%		2.04%	1.33%		1.84%	1.35%		1.65%	1.41%
0.85%	1.25%		0.74%	1.28%		0.96%	1.30%		0.74%	1.31%		0.82%	1.31%		0.78%	1.31%		0.81%	1.30%		0.91%	1.30%		1.04%	1.31%
0.88%	1.18%		0.70%	1.23%		0.95%	1.24%		0.83%	1.26%		0.87%	1.26%		0.83%	1.26%		0.70%	1.25%		0.83%	1.25%		0.99%	1.24%
1.82%	1.12%		0.69%	1.16%		2.04%	1.19%		0.81%	1.21%		0.92%	1.21%		0.80%	1.21%		0.64%	1.20%		0.91%	1.19%		0.96%	1.18%
2.04%	1.08%		0.71%	1.13%		1.62%	1.15%		0.57%	1.17%		2.41%	1.17%		0.83%	1.17%		2.01%	1.15%		2.27%	1.15%		1.01%	1.13%
0.84%	1.06%		0.65%	1.09%		0.87%	1.12%		0.82%	1.14%		0.84%	1.15%		0.78%	1.14%		0.71%	1.13%		0.82%	1.12%		0.94%	1.11%
0.86%	1.03%		0.63%	1.06%		0.91%	1.08%		0.71%	1.11%		0.79%	1.11%		0.79%	1.11%		0.70%	1.10%		0.83%	1.09%		0.96%	1.08%
0.85%	1.00%	Counter Check in	0.68%	1.02%	Counter Check in	0.93%	1.04%	Counter Check in	0.75%	1.06%	Counter Check in	0.89%	1.07%	Counter Check in	0.75%	1.06%	Counter Check in	0.74%	1.05%	Counter Check in	0.82%	1.05%	Counter Check in	1.00%	1.04%
1.13%	0.98%		0.68%	1.00%		0.92%	1.02%		0.98%	1.04%		2.05%	1.05%		0.79%	1.04%		2.31%	1.03%		1.26%	1.03%		2.19%	1.03%
0.66%	0.96%		0.63%	0.97%		0.77%	0.99%		2.46%	1.01%		1.12%	1.02%		0.75%	1.02%		2.02%	1.00%		2.37%	1.00%		1.89%	1.01%
0.70%	0.94%		0.64%	0.96%		0.83%	0.98%		0.81%	0.99%		0.85%	1.00%		0.72%	1.00%		0.76%	0.98%		0.79%	0.98%		1.13%	0.99%
0.69%	0.93%		0.68%	0.95%		0.81%	0.96%		0.79%	0.98%		0.86%	0.99%		0.78%	0.98%		0.82%	0.96%		0.85%	0.96%		1.08%	0.97%
1.07%	0.92%		0.70%	0.93%		1.84%	0.94%		0.78%	0.96%		0.87%	0.97%		0.74%	0.96%		0.86%	0.95%		0.88%	0.95%		1.11%	0.96%
1.71%	0.91%		2.03%	0.92%		1.95%	0.93%		2.75%	0.95%		2.15%	0.96%		0.65%	0.95%		1.77%	0.94%		2.44%	0.94%		2.10%	0.95%
0.75%	0.90%		0.76%	0.90%		0.85%	0.90%		0.83%	0.92%		0.80%	0.94%		0.76%	0.92%		0.91%	0.90%		0.96%	0.90%		1.17%	0.94%
0.77%	0.88%		0.77%	0.88%		0.88%	0.89%		0.80%	0.91%		0.87%	0.93%		0.81%	0.91%		0.89%	0.89%		0.89%	0.89%		1.18%	0.92%
0.78%	0.86%		0.75%	0.86%		0.87%	0.86%		0.76%	0.88%		0.84%	0.90%		0.82%	0.88%		0.84%	0.87%		0.88%	0.87%		1.12%	0.90%
1.72%	0.87%		2.04%	0.84%		1.66%	0.85%		0.88%	0.87%		2.24%	0.90%		0.77%	0.87%		2.14%	0.86%		0.90%	0.86%			
0.79%	0.85%		0.73%	0.75%		0.88%	0.75%		2.58%	0.79%		1.25%	0.88%		1.37%	0.80%		2.16%	0.76%		2.56%	0.77%			
0.77%	0.88%		0.64%	0.73%		0.89%	0.73%		0.73%	0.77%		0.92%	0.87%		0.72%	0.77%		0.78%	0.74%		0.77%	0.75%			

Figure 6.17 Comparison between measurement and simulation daylight factors between check-in counters, Suvarnabhumi Airport Departure Lounge (Measured/Simulated) (Anunnathapong, 2013)

Figure 6.18 reveals that the average relative deviation on the departure lounge was less than 5 percent, while the poorest was closed to the glazed wall to the north. The daylight model was then accepted for shading assessment in this study.

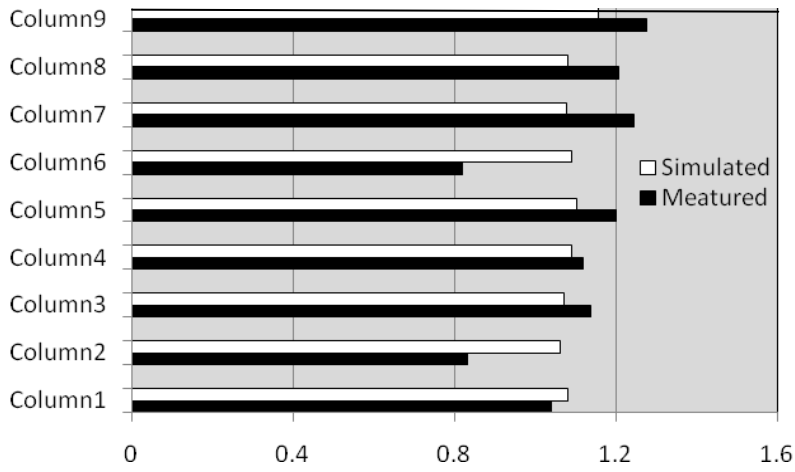

Figure 6.18 Comparison of maximum, minimum, and average daylight factor between measurement and simulation

6.5 Limitations in the Dynamic Thermal and Lighting Simulation Model

The dynamic thermal and lighting computer simulations were employed primarily for the prediction of the internal physical environment performance within the long-span glazed roofs over large naturally ventilated and air-conditioned pedestrian concourses. Therefore, it is important to carefully consider how the software simulates the heat transfer and lighting provision within the space. However, there were limitations during the computer simulation stages in this research project as follow:

- The accurate design details, material properties, and construction in the field needed to create the two computer models were incomplete. There was some uncertainty about building element inputs. They were all specified from software construction database with reference to the architectural specifications;
- They found significant variation between the results of the software tools in different version (Gado and Mohamed, 2012);
- The dynamic and lighting simulation stage, long simulation time consuming would be happened due to the large scale of these case studies;
- It was assumed that the percentage presence for occupants for each zone was constant, while there was very irregular behaviour of building users in reality.

Although these are not prohibitive problems in the computer simulation, they could play a very important role inaccurately determining for the internal physical environment performance results.

6.6 Conclusion

The GITC building was created in both the thermal and lighting models, including the nine blocks of buildings, streets, corridors and long-span glazed roof over large naturally ventilated pedestrian concourse. The thermal dynamic model was built using TAS and the lighting model by Ecotect.

In the thermal model each section of the spaces, large pedestrian concourse and the central large pedestrian concourse were divided into 35 zones over seven floors. The central large pedestrian concourse at the roof level was divided between the transparent roof zone and the ceiling zone to capture the differences in thermal conditions over this space. Such division was intended to differentiate subtle changes in temperature from one place to another and to allow the predicted values of the models to be compared with those from field measurements at exactly the same positions in the calibration.

Suvarnabhumi Airport Terminal building was created in both the thermal and lighting models, including the arrival lounge floor of buildings, departure lounge and long-span glazed roof over large air-conditioned pedestrian concourse. The thermal dynamic model was built using TAS and the lighting model by Dialux.

In the thermal model each section of the spaces, large pedestrian concourse and the central large pedestrian concourse were divided into 17 zones over six floors. The large pedestrian concourse at the roof level was further divided between the transparent roof zone and the ceiling zone to capture the differences in thermal conditions over this space. Such division was intended to differentiate subtle changes in temperature from one place to another and to allow the predicted values of the models to be compared with those from field measurements at exactly the same positions in the calibration.

Calibration of the thermal models were compared with the measured results in both case studies for two critical variables, the indoor temperatures and the total cooling loads within the long-span glazed roof over large pedestrian concourse on the hottest clear day and overcast day. Calibration of the lighting model in both case studies were by comparison with the DF within the long-span glazed roof over large pedestrian concourse on the selected overcast days.

From the dynamic thermal model calibration within the long-span glazed roof over large naturally ventilated pedestrian concourse, the measured indoor air temperatures

were compared with the simulated results. The average difference in air temperatures between measured and predicted was in the range of 2.25 and 3.71 percent. The average differences between the predicted and measured temperatures were around 1^{o}C on the top floor during sunny hours on the hottest of the day and smaller for the rest of the time. The calculated total cooling power from TAS was 171 Wm^{-2} which was very close to the original design capacity of 180 Wm^{-2}. Moreover, the cooling load comparison against the energy benchmarking for cooling system of large retail building reveals that this building has the overheating problem causing excessive use of the cooling system to keep the space thermally comfortable.

From the lighting model calibration within the long-span glazed roof over large naturally ventilated pedestrian concourse, the average DF over each of the seven floors shows fairly good agreement. The lowest relative deviation, 3 percent was on the sixth floor and the poorest, 23 percent on the ground floor.

From the dynamic thermal model calibration within the long-span glazed roof over large air-conditioned pedestrian concourse, the conditioned air was supplied to the whole area. Therefore internal air temperatures would not be able to reflect the thermo physical response of the model. The main heat contributors were the heat transfers in internal building element surfaces by convection and long-wave radiation exchange. In order to calibrate the long-span glazed roof over large air-conditioned pedestrian concourse model, the glazed roof surface temperatures were examined.

For average surface temperature by date and time, comparison of the average differences of the predicted surface temperatures made by TAS and the measured surface temperatures were between 1.70 and 5.00 percent by date and 0.00 and 4.73 percent by time. For the profile of glazed surface temperature comparison, the average difference surface temperature between the predicted and measured was around 2.7^{o}C on a clear hot day and was around 1.4^{o}C on an overcast hot day.

The predicted annual cooling load from TAS was 562 kWhm^{-2} which was very close to the calculated annual total cooling load by cooling degree-days of 578 kWhm^{-2}. Moreover, the predicted annual cooling load from TAS is very high compared against the energy benchmarking for airport cooling system of 467.7 kWhm^{-2}. This reveals

that this building has the overheating problem causing excessive use of the cooling system to keep the space thermally comfortable.

From the lighting model calibration within the long-span glazed roof over large air-conditioned pedestrian concourse, the average DF over the departure lounge shows fairly good agreement. The average relative deviation on the departure lounge was less than 5 percent, while the poorest was closest to the glazed wall to the north.

It was found that TAS calculations tend to be underestimated comparing to that of the measurement. These differences between the measured and predicted results might also be due to the following:

- As a results of uncertainties about the thermal properties of the existing construction material and specified building data editor by TAS. Inaccurate specifications of thermal property data had led to lower prediction of solar penetration in the model. The thermal property could not be matched with each other;
- The fixed internal conditions in TAS model were based on the general assumptions. There is a tendency for the heat gains from occupants, lighting and equipment to be underestimated in the model since the occupancy pattern and the use of lighting and equipment in the real conditions were somewhat irregular. Moreover, there is also a great possibility that the infiltration rates and conditioned air supply rates were underestimated due to the uncertainties of the actual flow rates and uncontrolled actions of the users in the real building.

Comparison of results from the site measurement and the prediction made by dynamic thermal and lighting model in both case studies has shown that the created models are suitable to model shading design with reasonably accurate results. Therefore both the dynamic thermal and lighting models were used in test and optimising the shading design- the ultimate purpose of this PhD project. The whole study is presented in the next chapter.

CHAPTER 7 – OPTIMIZING WEATHER RESPONSIVE SHADING SYSTEMS DESIGNED for LARGE GLAZED PEDESTRIAN CONCOURSES

7.1 Introduction

As mention in chapter one, long-span glazed roofs over large pedestrian concourses originated in temperate climates, but have since become very popular in other regions, including the hot countries which are less climatically appropriate for glazed atria. Heat gain through the transparent roof results in overheating risks which are exacerbated in the tropical climates due, to the high solar latitude and ambient temperatures in the equatorial regions. The poor thermal performance in these buildings also results in the constant use of large, expensive and maintenance intensive cooling systems. High running costs can be found after a couple years of occupancy. These were the problems in two high profile buildings: one in Guangzhou International Textile City (GITC), China, which has been the source of a number of thermal discomfort complaints reported by the tenants. The other is Suvarnabhumi airport; its cooling load in 2010 was very high, as compared to the energy intensity benchmark for cooling systems in large airports (discussed in chapter six).

The results of the measured data from the field experiments discussed in chapter four haves shown that long-span glazed roofs over large pedestrian concourses in the tropics would suffer high-temperature stratifications especially on the top, floor causing great discomfort to the occupants, regardless of the type of cooling system. In addition, it can be seen that daylighting tended not to be uniform within these buildings' interiors. The analysis of the post occupancy evaluation from the questionnaire survey in Suvarnabhumi airport terminal building (discussed in chapter five) has also shown that occupants perceived thermal discomfort in this passenger lounge.

To resolve the overheating problems, together with the extensive cost of operating their cooling systems, of the two case study buildings the proposed solution is to provide suitable sunshades, as described in both chapters one and two. Easy installation is considered crucial to minimise disruption to the already very busy occupants in the spaces. Most importantly, the light weight is considered vital as the large glazed pedestrian concourses spans (Wang et al., 2014). Thus the proposed solution for these buildings was an internal roof shading system.

Due to the complexity of the building geometries associated with a long-span glazed roof over a large pedestrian concourse, together with the limited measurement period of the two case studies, dynamic thermal and lighting simulation models were thus used for overall assessment of the annual indoor physical environment and energy consumption of the two long-span glazed roofed case study buildings. The dynamic thermal and lighting models were created and calibrated with the measured results, which have been discussed in chapter 6. The representative models were also used to predict physical environment and energy performance with differing designed shading configurations: high level and low level shadings in the next sage.

Therefore, this chapter 7 presents the details of the internal roof shading system developed in this research as a remedial solution to provide a better building-centric thermal environment and energy performance, while maintaining adequate levels of natural lighting within the existing long-span glazed roofs over large naturally ventilated and air-conditioned pedestrian concourses in the tropics. This chapter is structured into seven sections. It starts with a discussion on methods to optimise weather responsive shading system design. Second, fabric selection for the shading blind by conducting scale model experiment is presented. Third, the representative models are discussed. Fourth, the proposed shading positions are reviewed. Fifth, this chapter presents data from the assessed period selections used to examine thermal and lighting performance of the large glazed pedestrian concourses. Sixth, testing the performance of the proposed internal roof shading is presented by using the dynamic thermal and lighting model. Finally, a conclusion is presented at the end of this chapter.

7.2 Methods

In order to achieve the objective to examine the internal roof shading as remedial solutions of the problems described above, the shading blind fabrics were selected and examined. The fabrics were then tested under various simulated conditions.

Realistic light transmission was tested by scale model experiment in the artificial sky dome at Heriot-Watt University and also in an open-field context, under clear and overcast sky. The best fabric in terms of allowing visible light transmission to enter the building was tested in simulation as two design options and their effects were compared

with the thermal and lighting conditions in the large glazed pedestrian concourse against the base case.

Two shading arrangements were proposed: namely Model 1 (the low level shading or horizontal screen) and Model 2 (the high level shading or curved/sloped screen). The effects of the shading options were quantified and assessed using the defined variables to judge environmental and energy performance improvement. These assessments were based on comparisons between the Shading Cases and the Base Case on both clear summer and overcast days and clear winter and overcast days.

The environmental variables examined to assess the thermal conditions in the case studies were the solar gain, inner surface temperature of the ceiling, the mean radiant, air and operative temperatures and daylight factors over the existing long-span glazed roofs over large pedestrian concourses. The visual condition of these tested cases was assessed for illuminance and daylight factors. Then solar heat gain and cooling load variables were examined to assess the energy performance.

7.3 Fabric Selection for the Shading Blinds

The aims of the thesis are to propose design principles and guidelines for internal roof shading systems to provide a better building-centric thermal environment and energy performance, while maintaining adequate levels of natural lighting within the two case study buildings located in the tropics.

Internal shading blinds can contribute toward solar heat control by fabrics with a solar reflecting coating which could help reflect this solar heat and offer improved solar shading performance, when compared to conventional fabrics. Thus internal shading blinds that incorporate reflective materials usually have lower solar transmittances (CIBSE, 2006). In addition, to reduce the amount of solar radiation which leads to overheated indoor environments and high energy consumption associated with cooling systems; low solar transmittance material would be used in the internal shading device (Corrado, Serra and Vosilla, 2004).

The effectiveness of internal shading devices to block out the solar radiated heat depends on the devices' position with respect to glazed components, geometry, material properties, such as solar reflectance, solar transmittance and light transmittance, control options and colour (Unterpertinger, 2005). Light transmittance is also considered vital

in this thesis to allow the natural light stratification in the space. Ideally, properties for the shading fabrics should have the highest possible lighting transmittance and lowest possible solar transmittance in order to maximise light transmittance and minimise solar penetration into the large glazed pedestrian concourse.

The sample of fabrics was provided by the manufacturer 'Silent Gliss' for the thermal simulation and lighting simulation models. Thus five samples were selected from the best property of solar reflection, namely Alutex, Triscreen, Multiscreen, Skyscreen and Superscreen. The types of fabrics' purposes are as follows: (Silentgliss, 2011) (Table 7.1):

Parameter (%)	**Alutex** (Cream)	**Triscreen** (Light Gray)	**Multiscreen** (Light Gray)	**Skyscreen** (Light Gray)	**Superscreen** (Light Gray)
Visible Light Transmittance	6.00	10.14	N/A	N/A	N/A
Visible Light Reflectance	44.00	54.62	N/A	N/A	N/A
Visible Light Absorptance	50.00	35.24	N/A	N/A	N/A
UV transmittance	2.00	5.25	N/A	N/A	N/A
Solar transmittance	6.00	10.80	17.00	9.00	9.00
Solar Reflectance	45.00	47.10	35.00	37.00	40.00
Solar Absorptance	49.00	42.10	48.00	54.00	51.00
G-Value	0.46	0.45	N/A	N/A	N/A

Table 7.1 Manufacture data of fabric from Silent Gliss

Due to the fabric properties from the manufacturer being incomplete, the light transmittance properties from the selected fabrics for the proposed internal shading devices were examined by a scaled model tested under the artificial sky lab and also under actual sky (Zhu, 2012). In the next stage, the effectiveness of shading had to be assessed with dynamic thermal and lighting simulation models; in order to identify materials with the potential to minimise the possible overheating problems and to optimize day lighting on the large glazed concourses.

7.3.1 Lighting Transmittance Experiment

The general term *transmittance* refers to the proportion of radiation that passes through a sample. Lighting transmittance is the luminous flux entering the space divided by the luminous flux falling on the opener or window. It can be a single number, representing the overall performance of the window, or an array of values that are the transmittance

values at different directions (Tregenza, 2011). According to the Beer-Lambert law, transmittance is defined as:

$$T = \frac{I}{Io} \qquad (7.1)$$

where: I = the radiation intensity coming out of the sample;

I_o = the radiation intensity directed at the sample;

Transmittance (T) is sometimes calculated as a percentage by multiplying the above equation by one hundred (Garret, 2006).

A physical scaled model was used to investigate light transmittance within a large glazed concourse space. A scale model is a copy of an object, which is reduced from its actual size. Scale models have been used for centuries for evaluating building design under a real clear sky. The invention of artificial skies caused this method to become less dependent on various factors, especially weather, time and date. With artificial skies, the scale model showed the distribution of light within the room to be very accurate when compared with the one under the real sky (Bodart et al., 2005).

To obtain the light transmittances of these fabrics, the models were constructed to measure 35x 45x 25cm with an open void above of about 25x35 cm. No roof elements were used over the space in order to reduce the number of variables under consideration. The internal side of the model was given a black paint finish to minimize internal surface reflectance (2%). The floor of the model was given the same black paint finish for all of the experiments to avoid light being reflected from the model floor and affecting daylight factor values.

The experiments were conducted in a 2x2x1 m test environment with both an artificial sky capable of reproducing the luminance distribution of the overcast sky and the actual sky under both clear and overcast sky conditions. All illuminance measurements were made with illuminance (Lux) meters. In every measuring task, two photocells, one located inside the model at the middle and the second outside of the model, recorded the results. The outside illuminance values obtained in this model study were used for the systematically calculated daylight factor. According to the experiments' results, the best fabrics, which have the highest transmittance, can be chosen for further dynamic thermal and lighting simulation measurements, which will serve to identify the

appropriate internal shadings for large glazed concourse spaces in the next simulation stage.

7.3.2 Lighting Transmittance Experimentation Results

This exercise was undertaken to find out the best fabric to propose the appropriate internal shading to provide a better building-centric thermal environment and energy performance, while maintaining adequate levels of natural lighting within the existing large glazed pedestrian concourse. Under artificial sky condition, the average external illuminance of the model was 7,640 lux, while the average internal illuminance in the scale model without fabric was 3,117 lux. Then different kinds of fabric were added to the scale model. The results revealed that the internal illuminance decreased significantly. The illuminance from this experiment was also calculated; with the daylight factor and lighting transmittance compared with each other.

From the artificial sky dome experiment, the model with Triscreen and Multiscreen fabric had the highest lighting transmittance at 12.9% and 11.0%, respectively (Table 7.2).

The experiment under real sky was composed of clear sky and overcast sky experiments (Figure 7.1a and 7.1b). The models with Triscreen and Multiscreen still had the highest lighting transmittance at 11.3% and 11.1% on a clear sky day and 9.3% and 10.1% on an overcast sky day, respectively. Table 7.2 shows that Triscreen has the highest average lighting transmittance at 13.1%. This is followed by Multiscreen at 11.0%.

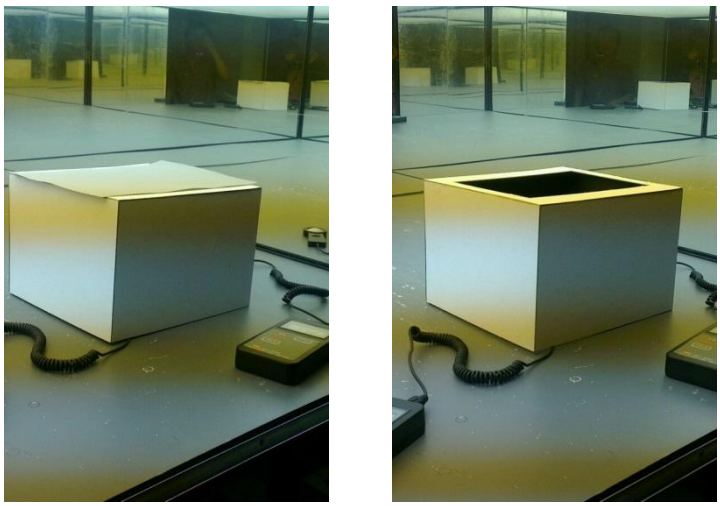

a) Scale model with and without fabric under artificial sky dome

b) Scale model with and without fabric under actual sky

Figure 7.1 Scale model experiment

According to the light transmittance experiment results, Triscreen is the best fabric in terms of allowing visible light transmission to enter the building (Table 7.2). Considering the solar transmittance properties from the manufacturer, Alutex is the best fabric in term of blocking solar energy transmission to space below, but it has a very low light transmittance (Table 7.1). Therefore, the fabric sheet finally selected for this study was the material with a light transmittance of 13.1%, solar reflectance at 47.0% and solar transmittance of 11.0% (Table 7.3).

	External Illuminance (lux)	**Internal Illuminance (lux)**	**Alutex**	**Triscreen**	**Multiscreen**	**Skyscreen**	**Superscreen**
Manufacture data	-	-	6.00%	10.14%	-	-	-
Artificial Sky	7,640	3,117	7.25%	12.92%	11.10%	9.35%	5.90%
Overcast Sky	23,800	11,135	7.90%	13.10%	11.93%	11.60%	7.20%
Clear sky	33,550	16,065	7.82%	13.21%	12.12%	10.92%	5.71%
Average	**-**	**-**	**7.65%**	**13.10%**	**11.70%**	**10.60%**	**6.20%**

Table 7.2 Comparison of lighting transmittance and manufacture data

	light transmittance	solar reflectance	solar transmittance
Selected for proposed shading	13.10%	47.0%	11.0%

Table 7.3 Selected for proposed shading properties

7.4 Representative Models

The detail roof cross-section of the naturally ventilated and air-conditioned representative models are illustrated in figure 7.2 (a) and (b), respectively. These two

models were initially used to investigate the effect of shading systems on both thermal and lighting environments of the two shading arrangements: low level shading (horizontal screen) and high level shading (curved/sloped screen). These representative models were tested under various conditions to provide base data for comparison purposes.

The environmental variables examined to assess the thermal and lighting conditions in the case studies were the solar gain, inner surface temperature of the ceiling, the mean radiant, air and operative temperatures and daylight factors over the existing long-span glazed roofs over large pedestrian concourses.

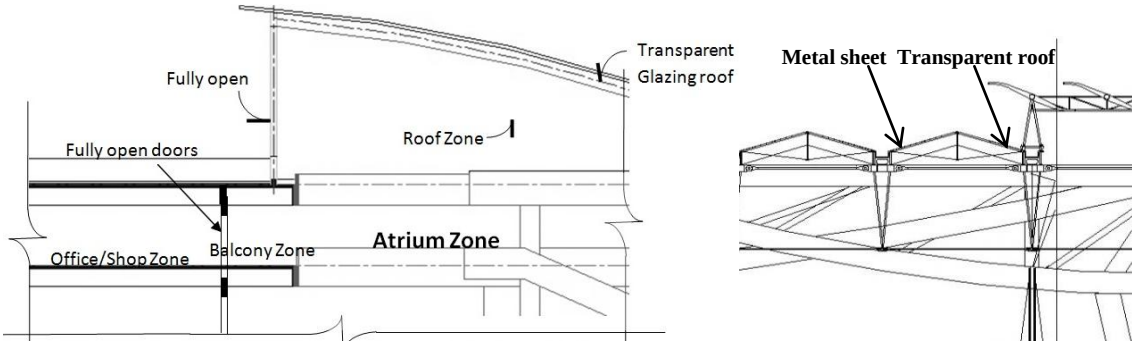

a) Large glazed naturally ventilated pedestrian concourse (Guangzhou International Textile City)

b) Large glazed air-conditioned pedestrian concourse (Suvarnabhumi Airport Terminal)

Figure 7.2 Detailed cross-sections showing the base models

7.5 Proposed Shading Position

Unterpertinger (2005) stated that the effectiveness of internal shading devices to block out the solar radiated heat depended on position with respect to glazed components, geometry, material properties, such as solar reflectance, solar transmittance, light transmittance, control options and colour. Abdullah et al., (2009) utilised a field study and reviewed that the effect of solar gain control using the sloped solar blind underneath the glazed roof over an atrium space would absorb solar energy from the top; its radiant temperature would rise due to the increase in surface temperature. With the contribution of radiant energy from other internal surfaces, the mean radiant temperature and the air temperature at high level would also increase and lead to greater stratification in the atrium. In addition, Energydesignresource (2014) recommended a horizontal shading to provide an additional layer of insulation to keep out hot air stratification into the atrium below.

These previous studies identified that the position of a shading device influences the effectiveness of internal shading devices to block out the solar radiated heat. Thus internal shading was proposed in the form of retractable internal fabric sheet blinds, in strips some 1 meter wide with 5-10 cm gaps between each fabric sheets. The two internal shading options: namely Model 1 (low level shading or horizontal screen) and Model 2 (high level shading or curved/sloped screen) were proposed and their effects compared on the thermal and lighting conditions in the two case study buildings (representative model without shading) (Figure 7.3 (a),(b), (c) and (d).

The environmental variables examined to assess the thermal and lighting conditions with the designed shading options were the solar gain, inner surface temperature of the ceiling, the mean radiant, air and operative temperatures and daylight factors over the existing long-span glazed roofs over large pedestrian concourses.

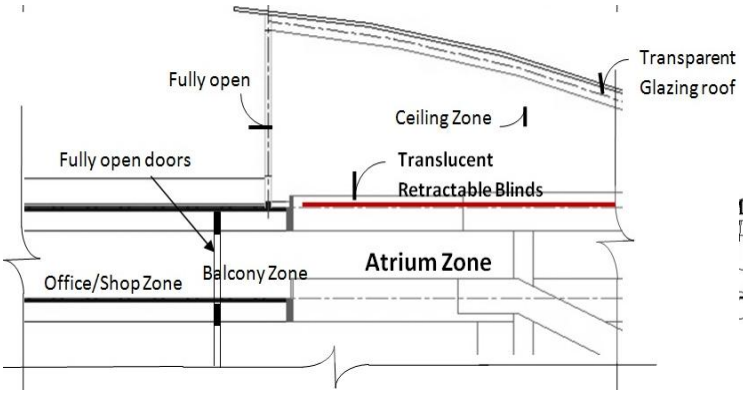

a) Large glazed naturally ventilated pedestrian concourse with low level shading (Guangzhou International Textile City)

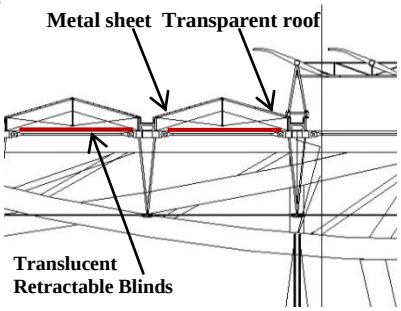

c) Large glazed air-conditioned pedestrian concourse with low level shading (Suvarnabhumi Airport Terminal)

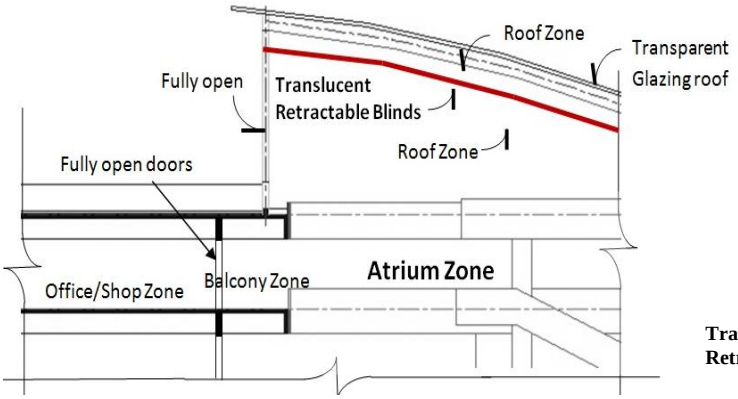

b) Large glazed naturally ventilated pedestrian concourse with high level shading (Guangzhou International Textile City)

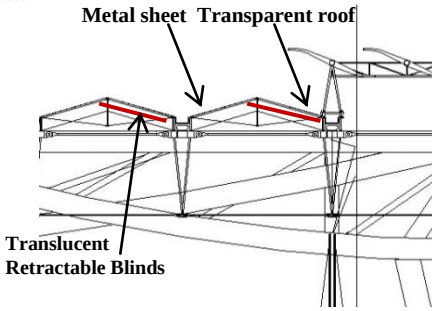

d) Large glazed air-conditioned pedestrian concourse with high level shading (Suvarnabhumi Airport Terminal)

Figure 7.3 Detailed across-section showing the roofs and shadings

7.6 Selected Weather Conditions for Assessment

When a designer performs a cooling load calculation, one of the first things that must be done is to select the worst weather condition in summer and winter to set the outdoor condition parameters. The periods were used to examine thermal and daylight performance of the large glazed concourses, together with the annual overview, as described below.

7.6.1 A Large Glazed Pedestrian Concourse with Natural Ventilation

A full year of weather data for 2010 was collected from the local Guangzhou, China weather station as the representative year's data, following the suggestion of the local meteorological office. The data set includes the hourly figures of the seven variables: the global and diffused solar radiation, air temperature, relative humidity, cloudiness and wind speed and direction.

Simulations were performed for the whole year for existing buildings without shading devices and with a combination of glazed roofs and shading devices. This would allow energy savings to be assessed for the shading designed options.

The set of weather data in the following periods were used in thermal modelling to predict the annual energy consumption for the base case and the shading cases, representing summer and winter seasons.

Representative Clear Summer and Overcast Days

According to the local data record, the weather data of the 30th August 2010, with very strong solar radiation at 874 wm^{-2} and high diurnal ambient temperature at 38.6^{o}C, were used in the thermal modelling tests of the shading design options to represent a clear summer day. While the weather data of the 1st September, which had very week solar radiation at 427 wm^{-2} and high diurnal ambient temperature at 28.3^{o}C, were used in the thermal modelling tests of the shading design options to represent an overcast summer day.

Representative Clear Winter and Overcast Days

In winter, the weather data of the 27th and 28th January 2010 had a low diurnal ambient temperature in range 7~15^{o}C. On 27th January, the solar radiation was at 210 Wm^{-2} and in 28th January, the solar radiation was at 432 Wm^{-2}. The outdoor temperature on both a

clear winter day and an overcast day were moderate. The shading screen would not be required in winter.

7.6.2 A Large Glazed Pedestrian Concourse with Air-Conditioning

This weather data for 2012 were gathered from the Meteorological Department of Thailand. The hourly climate data required for thermal and lighting simulation consisted of dry bulb temperatures, global solar radiation, cloud cover, wind speed and wind direction.

The following periods were used to examine thermal and visual performance of the building: a clear summer day and overcast summer day representing summer and a clear winter day and overcast winter day representing the winter season.

Representative Clear Summer and Overcast Summer Days:

According to the weather data of the 1st May 2012, the highest diurnal ambient temperature was at 38.0°C and the highest solar radiation was at 882 Wm^{-2}. These data were used in the thermal modelling tests of the shading design options to represent a clear summer day. The weather data of the 3rd May 2012 indicated the highest diurnal ambient temperature was 34.5°C and the highest solar radiation was 584 Wm^{-2}. These data were also used in the thermal modelling tests of the shading design options to represent an overcast summer day.

Representative Clear Winter and Overcast Days

The weather data of 26th December 2012 represents a clear winter day with the highest diurnal ambient temperature at 30.8°C and the highest solar radiation at 699 Wm^{-2}. The weather data of 7th December 2012 represents an overcast winter day with the highest diurnal ambient temperature at 32.3°C and the highest solar radiation at 466 Wm^{-2}.

The next section thus will discuss the thermal and lighting computer models of Guangzhou International Textile City and Suvarnabhumi Airport to investigate the effectiveness of internal shading for improvement of its environmental and energy performance.

7.7 Testing the Performance of the Proposed Internal Roof Shading

The effects of the shading device were qualified and assessed using the defined environment variables and energy performance improvements. The assessments were based on comparisons between the selected design options and the base case model, without shading.

The environmental performances were assessed by comparing their effects on internal ceiling surface temperatures, air temperatures, mean radiant temperatures and operative temperatures of both ground floor and surrounding space on the top level against the base case. The environmental aspects also included daylight provision, assessed by comparing the daylight factors and illuminance over the occupant space against the base model. Then the energy performances were assessed by comparing the solar heat gain and cooling loads against the base case.

In this study, the pedestrian concourse is used as a transitional space. The comfort requirement within this space is less stringent as most areas, particularly corridors, are normally used for short-term. Thus the internal operative temperatures of 23~26^{o}C are considered acceptable for the large naturally ventilated pedestrian concourse (ASHRAE, 1992). This thermal comfort limit was further extended to 31^{o}C in the transitional spaces, which are considered as short stay areas in this thesis. A wider range of temperature, 20~30^{o}C is redefined as the adaptive thermal comfort for naturally ventilated office space in such a climate (Brusch, 1992; Nicol and Humphrey, 2002). The internal operative temperatures of 22~24^{o}C are also considered acceptable for an airport departure lounge in summer (ASHRAE, 1992).

The solar penetration was also included as an environmental variable, as it can raise the air temperature in the glazed pedestrian concourse, as well as the surface temperature over the wall and floor surfaces, which were averaged as the mean radiant temperature (MRT). The effects of the two temperatures are combined by the operative temperature to take count of occupants' comfort. The reduction of these variables due to installation of a shading system was considered as an improvement to the thermal conditions in the atrium space (Topliss and Hurst, 2010). Other variables that also affect thermal comfort, such as air movement and relative humidity, were not included in this study but were previously recorded in the preliminary survey for this thesis.

The energy performance improvement from internal shading devices can be verified by estimating the saving amount of the cooling loading requirement, the reducing of solar heat gain and maintaining thermal comfort on operative temperatures, while the lighting performance can be verified by estimating the adequate daylight factors and illuminance.

7.7.1 Large Glazed Pedestrian Concourse with Natural Ventilation

Basically, the interest of this study was to examine the inner vertical temperatures within the large glazed pedestrian concourse well, served by natural ventilation. Therefore, the central glazed pedestrian concourse in the dynamic thermal model was further divided for each floor, in order to capture the different thermal conditions in this space. At the roof level, a separate zone was created between the transparent glazed roof and the proposed shadings. Such a division was intended to differentiate subtle changes in temperature from one place to another, which were used to compare with those from the base model at the same positions. The central glazed pedestrian concourse in the lighting model was divided for ground floor and upper floor corridors to capture the differences in lighting condition in this space.

7.7.1.1 Thermal Environment Aspect

a) Ceiling Surface Temperature

Both shading positions reduced a great amount of the ceiling's inner surface temperature, especially during the three hours around midday (Figure 7.4). The low position shading (Model 1) was better than the high position shading (Model 2) in terms of reduction of the ceiling inner surface temperature.

During the hottest period on a clear summer day, Model 1 predicted a drop of 8.6^{o}C (17.2%), whilst Model 2 predicted a drop of 4.4^{o}C (8.8%). The highest ceiling temperature, almost 50^{o}C, occurred at the inner surface of the transparent roof. This was reduced to 41.4^{o}C by the low position screening according the Model 1 and 47.3^{o}C by the high position screening according Model 2.

During the hottest period on an overcast summer day, the shadings still reduced this temperature, as they also block the scattered solar radiation. The reduction was slightly more than 2^{o}C by the low level shading (Model 1), and less than 1^{o}C by the high level shading (Model 2) around midday.

Hence the screening is considered very effective in reducing the inner surface temperature and the low position shading is more effective than the high position.

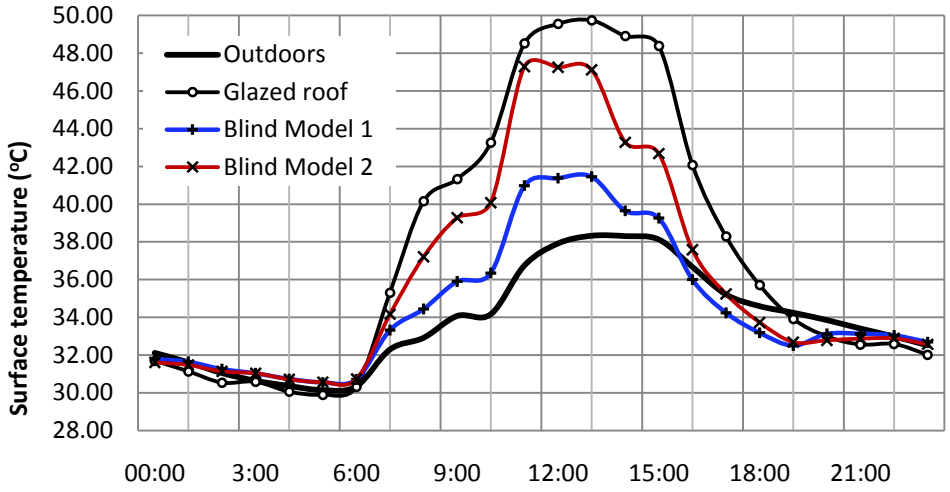

a) Clear summer day: 30th August 10

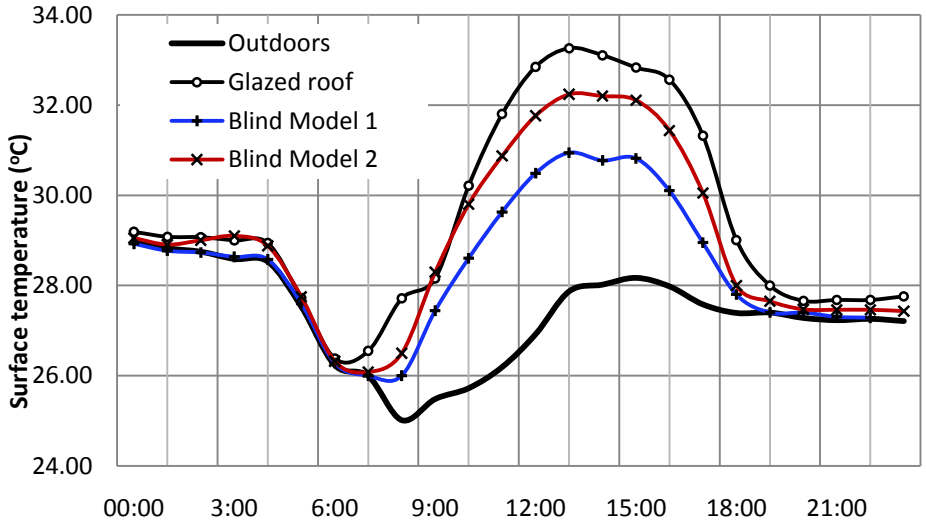

b) Overcast summer day: 1st September 10

Figure 7.4 Comparison of the internal surface temperature in the central concourse

b) Mean Radiant Temperature (MRT)

The MRT includes the surface temperatures of all visible surfaces including the ceiling; however the MRT at a specific location also takes into account the view factors of these surfaces. Two locations were considered; one on the top floor corridor and the other at the centre of the ground floor pedestrian concourse. Figure 7.5 illustrates that solar radiation greatly influenced the mean radiant temperatures (MRT) of the central pedestrian concourse, especially on the top floor corridor.

At the hottest hour on a clear summer day, at which the external temperature was 38.2°C, the MRT on the ground floor was nearly 48°C. The low level shading (Model 1) reduced this high MRT to 41.2°C, almost 7°C (14.6%) drop and the high level shading (Model 2) to 44°C, a 4°C reduction. The MRT on the top floor corridor was nearly 46°C. The low level shading (Model 1) reduced this high MRT by almost 7°C (15.2%) and the high level shading (Model 2) 4°C (8.7%).

At the hottest hour on an overcast summer day, the MRT on both the ground floor and the top floor corridor was nearly 34°C. The low level shading (Model 1) reduced the MRT by about 4°C (8.7%) on the ground floor centre concourse and 3°C (9.0%) on the top corridor. The high level shading (Model 2) achieved less than 3°C (9.0%) and 2°C (6.0%) drops for the two locations respectively. The low position shading is considered more effective for reducing the MRT for the entire concourse space.

The outdoor temperatures on both clear and overcast winter days were moderate. The highest predicted mean radiant temperatures within the typical floor walkways were 19.2°C on a clear day and 15.5°C on an overcast day. The internal shading was not needed and the concourse should be left open.

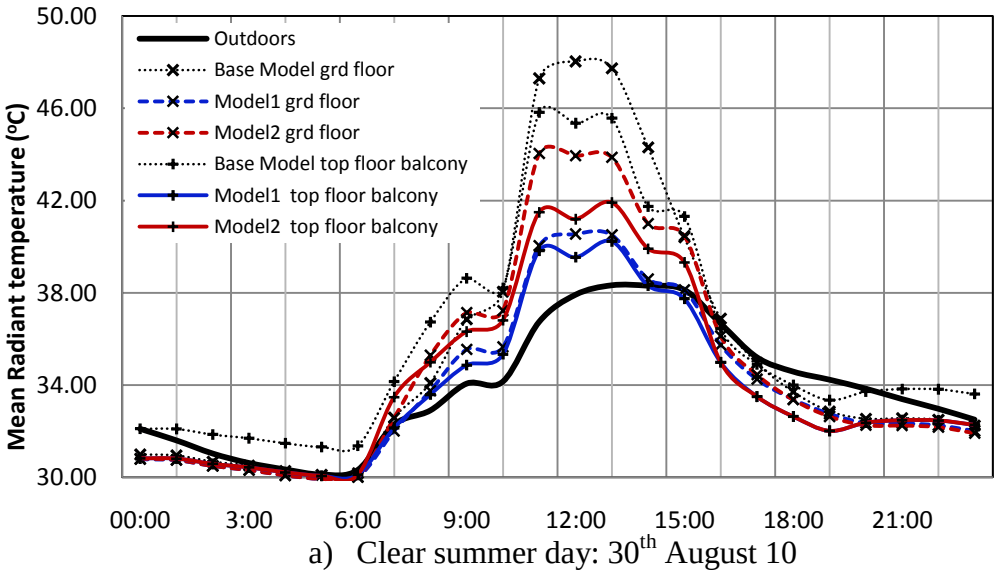

a) Clear summer day: 30th August 10

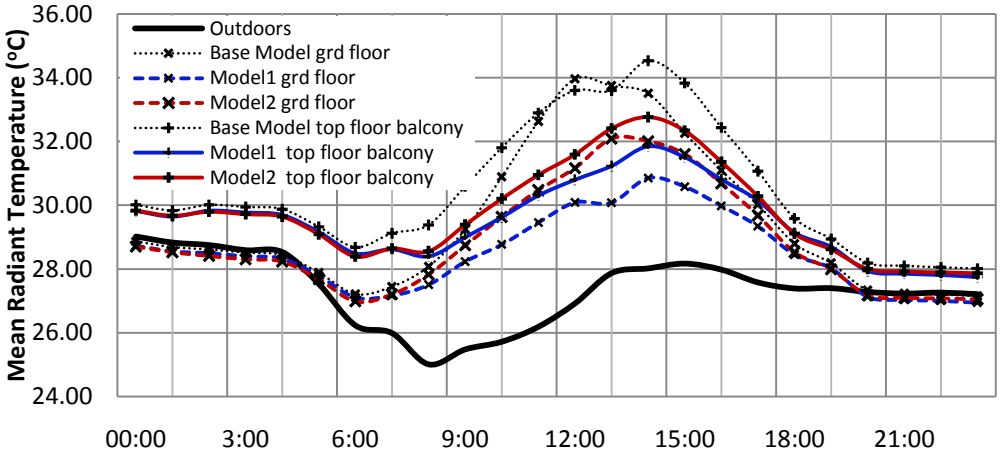

b) Overcast summer day: 1st September 10

Figure 7.5 Comparison of the mean radiant temperature in the central concourse

c) Air Temperature

During the hottest hour of the clear summer day, the outdoor air temperature reached a peak of 38.3°C, the predicted air temperature within the ground floor pedestrian concourse was 36.6°C and the top floor corridor was 37.8°C without the shading configuration (base model).

Figure 7.6 shows that, the predicted air temperature within the ground floor pedestrian concourse was decreased by the low level shading (Model 1) by 1.5°C (4.1%) on the ground floor pedestrian concourse and by 2.0°C (5.5%) at the top floor corridor. There was a reduction in the air temperature for the high level shading (Model 2) of around 1.0°C (2.7%) on both levels.

On an overcast summer day, the predicted hottest air temperature within the ground floor pedestrian concourse and top floor corridor was 29°C. This temperature was reduced by the low level shading (Model 1) by 0.7°C (2.4%) and by the high level shading (Model 2) by 0.6°C (2.0%). At the top floor corridor, the temperature reduction from the low level shading (Model 1) was 1.1°C (3.7%); and by the high level shading (Model 2) was 0.8°C (2.7%).

During winter, the outdoor air temperatures were low. The predicted indoor air temperatures within the ground floor pedestrian concourse were in range of 7.0-16.1°C on both clear and overcast days. The internal shading screen should be open for solar penetration for free heating and bright natural lighting.

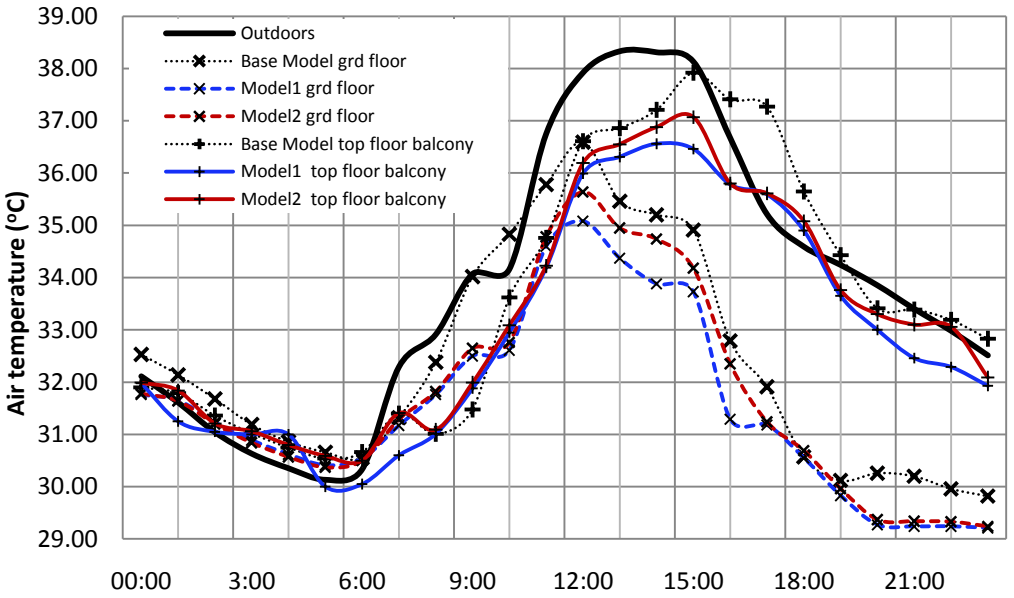

a) Clear summer day: 30th August 10

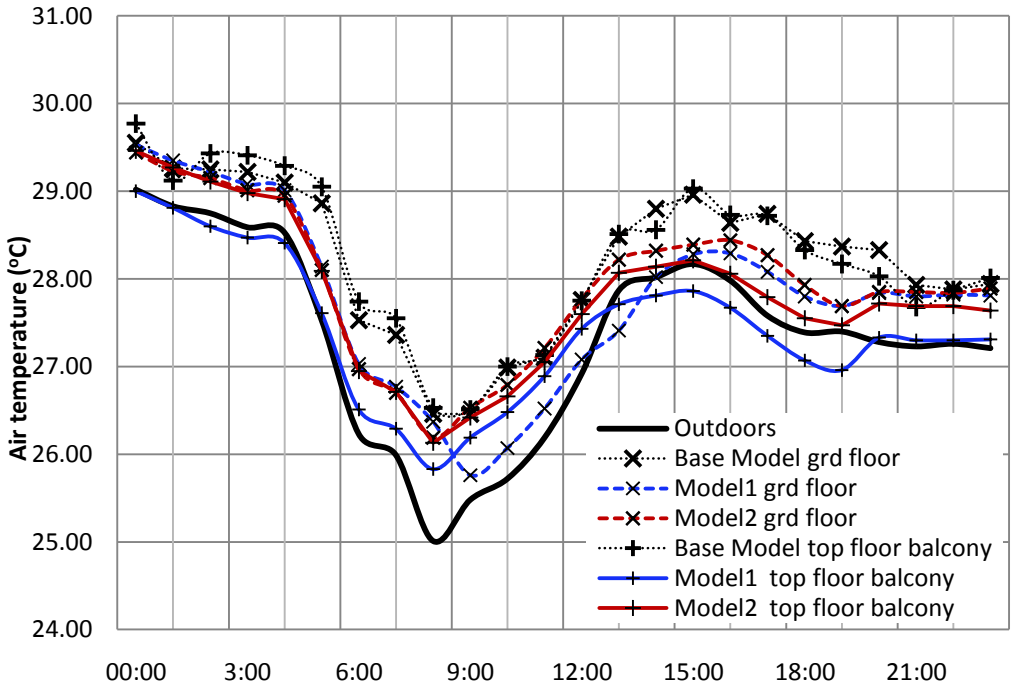

b) Overcast summer day: 1st September 10

Figure 7.6 Comparison of the air temperature in the central concourse

d) Operative Temperature

The concept of 'operative temperature' describes the average air temperature and means radiant temperature; it is the most useful indicator of thermal comfort in buildings.

The internal operative temperatures of 23-26°C are widely considered acceptable for naturally ventilated buildings, as recommended by ASHRAE (1992). This thermal comfort limit was further extended to 31°C in the transition space, which was

considered as a short stay area. A wider range of temperatures, 20-30^{o}C, is redefined as the adaptive thermal comfort for naturally ventilated office space in such a climate (Nicole, Humphrey and Roaf, 2012)

On a clear summer day, the predicted operative temperature of the base model peaked at 42.3^{o}C on the ground floor concourse and 41.2^{o}C in the top corridor (Figure 7.7). Both the two internal shading options could reduce the operative temperatures in the occupied areas, particularly the ground floor. The low level shading (Model 1) reduced this temperature by 4.2^{o}C (9.9%) on the ground floor pedestrian concourse and by 2.0^{o}C (4.8%) on the top corridor. The other option, the high level shading (Model 2) reduced this temperature by 0.4^{o}C (1.3%) on both the ground floor pedestrian concourse and top floor corridor.

On an overcast summer day, the Model 1 option reduced the temperature by 1.1^{o}C (3.5%) on the ground floor pedestrian concourse and 1.0^{o}C (3.2%) on the top level. The other option, the high level shading, reduced this temperature by 0.4^{o}C (1.0%) on both the ground floor pedestrian concourse and over the top floor corridor.

On both clear and overcast winter days, the highest predicted operative temperatures within the ground floor pedestrian concourse were in the range of 13.7~17.9^{o}C and on typical balconies were in the range of 13.6~17.9^{o}C. Therefore it was not necessary to shut the internal shading devices.

Figure 7.7 shows clearly the operative temperature went over 31^{o}C for more than 22 hours during this very hot day. This means both shading options could only ease to some degree thermal discomfort but could not improve the thermal condition; both shading models, particularly the low level screen, were able to significantly reduce the inner surface temperature and therefore ease significantly the radiation heat stress.

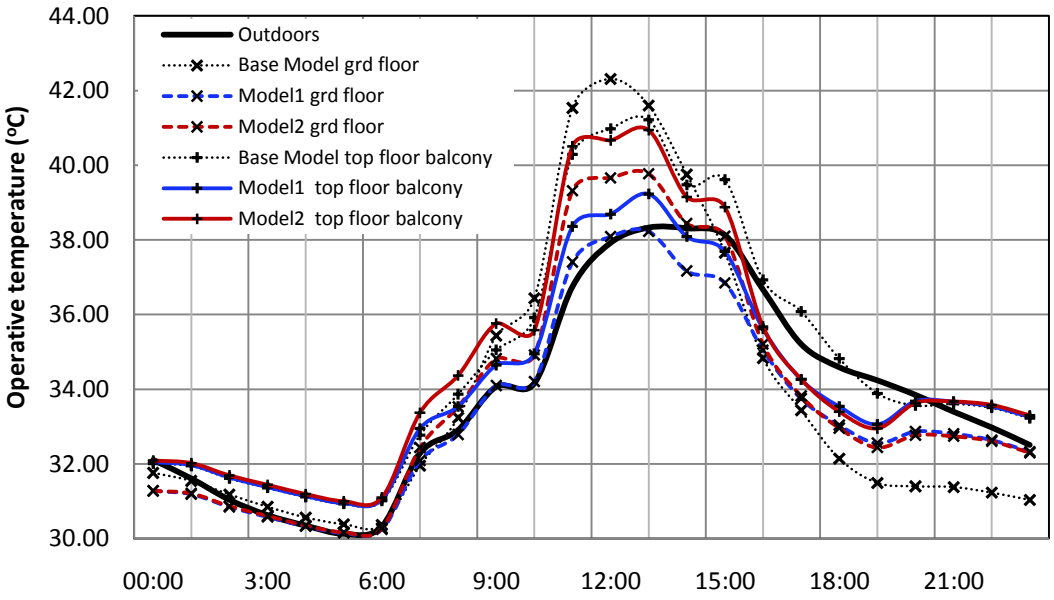

a) Clear summer day: 30th August 10

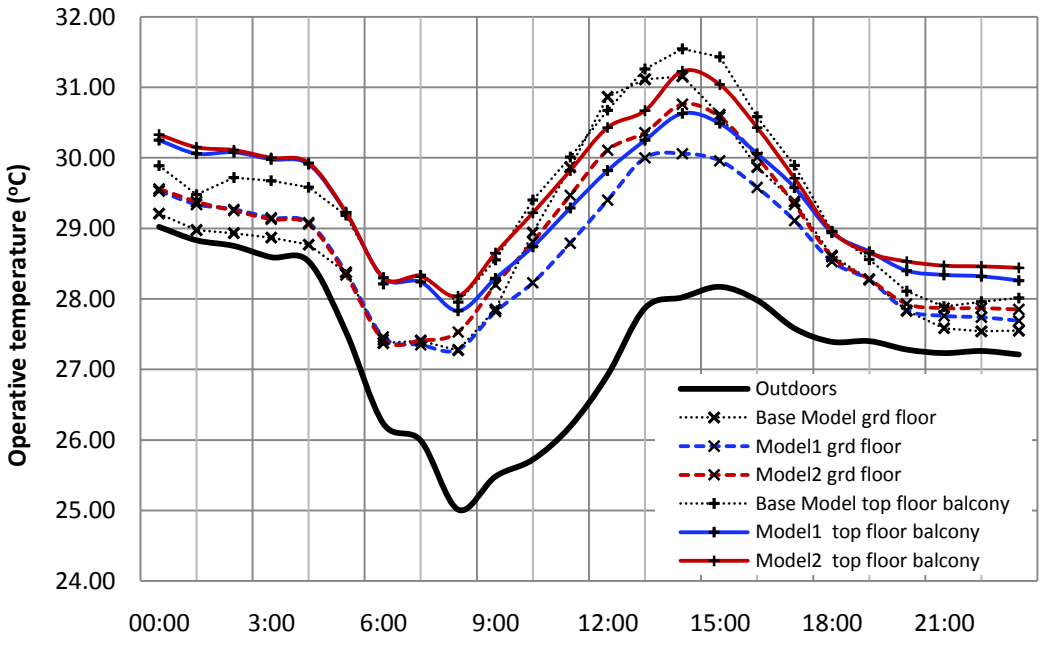

b) Overcast summer day: 1st September 10

Figure 7.7 Comparison of the operative temperature in the central concourse

7.7.1.2 Visual Environment Aspect

Tables 7.3 and 7.4 show the simulation results from the daylighting model on the ground floor centre pedestrian concourse and the first floor corridor. It can be seen that the internal shading devices not only cut solar heat but also reduced the daylight penetrating deeply through the lower levels. The daylight factors of the high level

shading (Model 2) were around one time higher than that with the low level shading (Model 1).

On the clear summer day, the lower level shading (Model 1) solutions reduced the lighting level to 423~543 lux, a level excitingly bright and appropriate according to the recommendation from CIBSE (1999) for foyers and entrance halls. During the overcast summer day, the illuminance of the centre ground floor pedestrian concourse with the high level shading was larger than 500 lux, an appropriate quality of light according to the CIBSE's recommendation. On the overcast summer day the blinds should not be needed, hence retractable blinds would be essential.

Generally the screening redistributed the natural light, and so it reduced the unevenness of the light distribution over the space, as without blinds there was a large difference between the illuminance on ground floor and the first floor, particularly during clear days. The diffusive nature of the screening reduced such differences.

On a clear winter day, the illuminance of the centre pedestrian concourse was 527 lux, so the blinds should remain fully opened, otherwise it would be too dark for the intended function of the building. Also the solar penetration in winter is weaker than summer and it is ideal energy for free heating when the inner air temperature was between 9~16^{o}C. The illuminance within the pedestrian concourse on a winter overcast day was just above 200 lux. Even with full open blinds, electric lighting can be added to achieve the occupants' requirement for lighting.

The lighting model also predicted a daylight factor over the centre pedestrian concourse and results show the daylight factor was between1~2% primarily on first floor corridor and the area underneath on the ground floor. Over the second floor, this variable increased, so that no artificial lighting would be needed. Although the natural light benefits most of the circulating areas within the concourse, the perimeter areas on the ground floor and the corridors on lower floors are lacking in natural lighting, according to the standard assessment of daylight quality.

Outside condition		The ground fl. concourse			The first fl. corridor		
		Base	Model1	Model2	Base	Model1	Model2
Summer	Overcast	855	358	496	586	262	280
	Clear	1844	494	543	1187	423	491
Winter	Overcast	301	139	160	212	142	152
	Clear	527	163	180	386	117	230

Table 7.4 The mean illuminance (lux) on the ground floor concourse and the first floor balconies

	Base model	**Low Level (Model 1)**	**High Level (Model 2)**
Ground floor concourse	1.9	1.04	1.74
First floor corridor	1.31	0.89	0.99
Third floor corridor	2.56	1.33	1.92

Table 7.5 The predicted average DF (%) in the concourse under overcast sky

7.7.1.3 Energy Efficiency Aspect

a) Solar Heat Gain

The solar heat gain depends on glazing types, shading devices, orientation, geometry of the spaces and specific heat storage capacity of the building material. Large panes of the glass roof introduce solar radiation into the inner space during day time; therefore the highest solar heat gain normally occurred between 1000h to 1700h, especially in the region near the ground floor pedestrian concourse and the highest floor (Reimer, 2009).

The total daily solar heat gain for the base model was 752 kWh on a clear summer day and 385 kWh on an overcast summer day. Figure 7.8 reviews the simulation results of total solar heat gain per floor area over the corridor areas of the base model, compared with the low level shading (Model 1) and the high level shading (Model 2).

On a clear summer day, the solar heat gain was reduced from 450 Whm^{-2} to 216 Whm^{-2} a 52.0% reduction on the top floor corridor; and from 465 Whm^{-2} to 220 Whm^{-2} , a 52.7% reduction, on the ground floor by the low level shading (Model 1). The result from the high level shading (Model 2) was a solar heat reduction to 407 Wm^{-2}, a 9.6% drop on the top floor corridor and to a 336 Whm^{-2} , 27.0% reduction on the ground floor. The reduction rates achieved were slightly lower over in the middle floor corridor.

On the overcast summer day, the shading could also reduce the scattered solar radiation. The results of Model 1 show that the lower level shading reduced the original figure without shading from 312 Whm^{-2} to 178 Wm^{-2}, a 43% reduction on the top corridor; and from 321Whm^{-2} to 171Whm^{-2}, a 47% reduction on the ground floor. The higher screenings again achieved less; a 3% reduction on the top corridor and less than 19% on the ground floor. The smaller shading effect of the higher screening system resulted from the scattered solar radiation still coming into the atrium via the large side openings of the atrium roof.

It can be clearly seen that the lower level shading (Model 1) reduces solar penetration more effectively than the high level shading (Model 2).

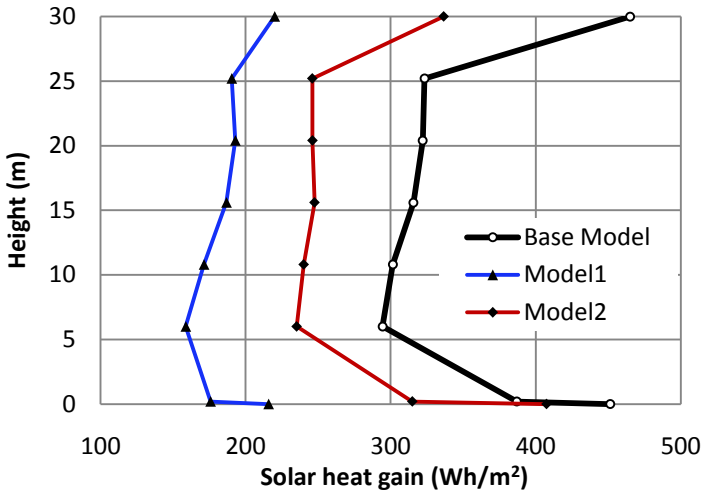

a) Clear summer clear day: 30th August 10

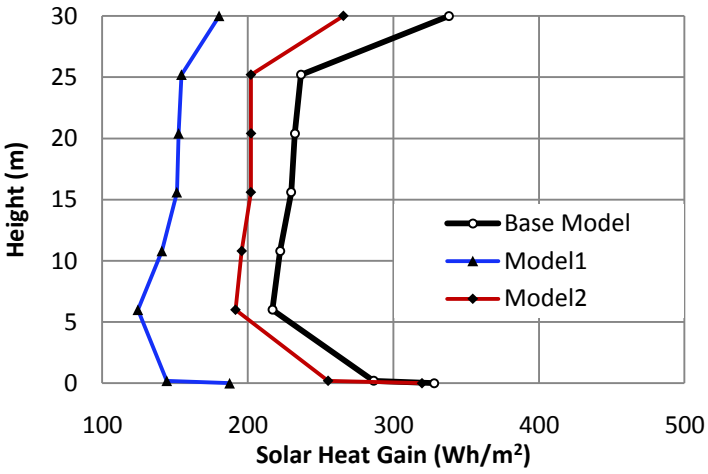

b) Overcast summer day: 1st September 10

Figure 7.8 The daily solar gain over the ground floor and balconies

b) Cooling Load

An important finding from chapter 6 was solar penetration greatly affects the cooling loads of the surrounding units, particularly those with open door retail units in this building. The total cooling load calculated by the original design capacity is 330 $kWhm^{-2}$ over the GITC building of 140,000 square metres, which is almost 10 percent higher than the benchmark for cooling system standards at 316 $kWhm^{-2}$.

Cooling load in the large glazed pedestrian concourse building is influenced by heat transfer through surfaces surrounding the pedestrian concourse space; the roof surfaces exposed to the external environment and also the side walls to the adjacent zone (Pan et al., 2010). For the purpose of this study, it was assumed that during the operating hours (0900h-2000h), all retail shops had a maintained temperature of 24~26^{o}C as a result of air-conditioning.

Thermal modelling software (TAS) predicted that the total cooling load for all retail units of the base model was 1.94×10^{5} kWh on the tested clear summer day and 1.87×10^{5} kWh on the tested overcast summer day. The difference between the loads during the clear day and overcast day is small. This was because the loads were for the retail units over seven stories in the whole building. Most of them did not receive direct solar heat and those that did were the few on the top floor and on the east and west sides.

Figure 7.9 shows that the low level shading (Model 1) performed better than the high level shading (Model 2) in terms of reducing the total cooling load. Model 1 saved 6.8% of the cooling load while the Model 2 saved only 4.7%.

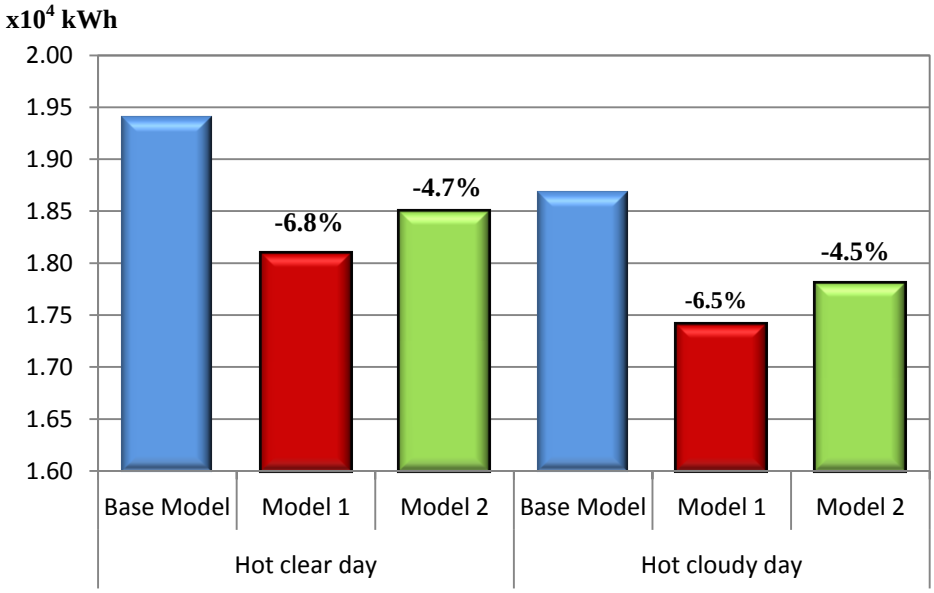

Figure 7.9 Daily total cooling loads in the retail units from the two shading options, compared against the base case

7.7.2 The Large Glazed Concourse with Air-Conditioning

Basically, the interest of this study was to examine the inner vertical temperatures within a large glazed pedestrian concourse well with air-conditioning. Therefore, the central glazed pedestrian concourse in the dynamic thermal model was further divided for each floor to capture the differences in thermal condition in this space. At the roof level, a separate zone was created between the transparent glazed roof and the proposed shadings. Such a division was intended to differentiate subtle changes in temperature from one place to another; data which was used to compare with those from the base model at the same positions. The central glazed pedestrian concourse in the lighting model was divided into 207 zones between check in counters for ground floor to capture the differences in lighting conditions in this space.

7.7.2.1 Thermal Environment Aspect

a) Inner Surface Temperature

Figure 7.10 shows that the high inner surface temperature could be alleviated by high position shading. In summer, the highest outdoor temperature was 38.0^{o}C on a clear day and 34.5^{o}C on an overcast day.

During the hottest period in summer, the internal glazed surface temperatures reached a peak of 55.7^{o}C on a clear day and 43.5^{o}C on an overcast day. The inner surface temperature of the high level shading (Model 2) increased dramatically to 58.7^{o}C

(+5.4%) on a clear day and to 47.8°C (+9.8%) on an overcast day. The inner surface temperature of the low level shading (Model 1) was reduced to 53.6°C (-3.7%) on a clear day and to 42.9°C (-1.5%) on an overcast day.

During the hottest period in winter, the highest outdoor temperature was 30.7°C on a clear day and 32.3°C on an overcast day. The internal glazed surface temperatures reached a peak of 38.6°C on a clear day and 39.3°C on an overcast day during the afternoon. The high level shading (Model 2) caused a significant increase of surface temperature to 42.3°C (+9.4%) on a clear day and to 41.8°C (+ 6.3%) on an overcast day. The low level shading (Model 1) reduced this temperature to 43.7°C (-2.5%) on a clear day and to 37.9°C (-1.9%) on an overcast day.

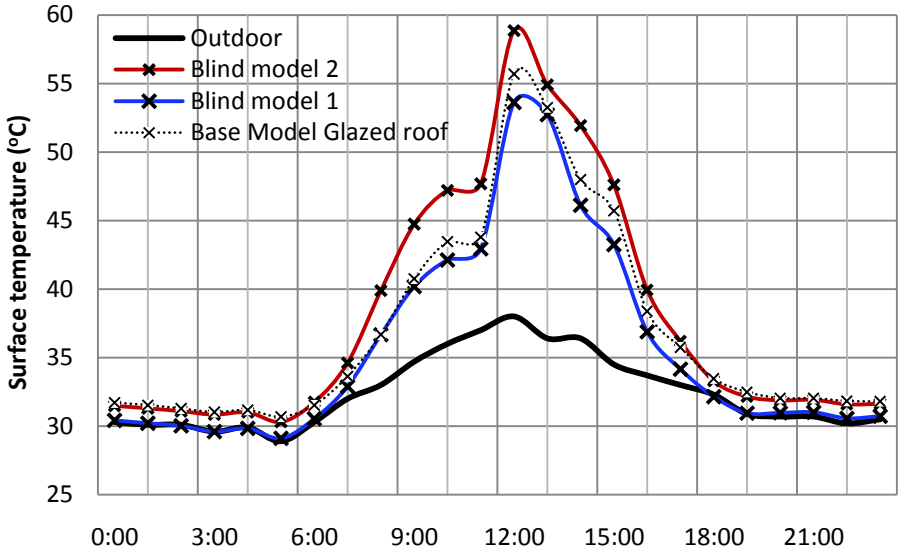

a) Clear summer day: 1st May 12

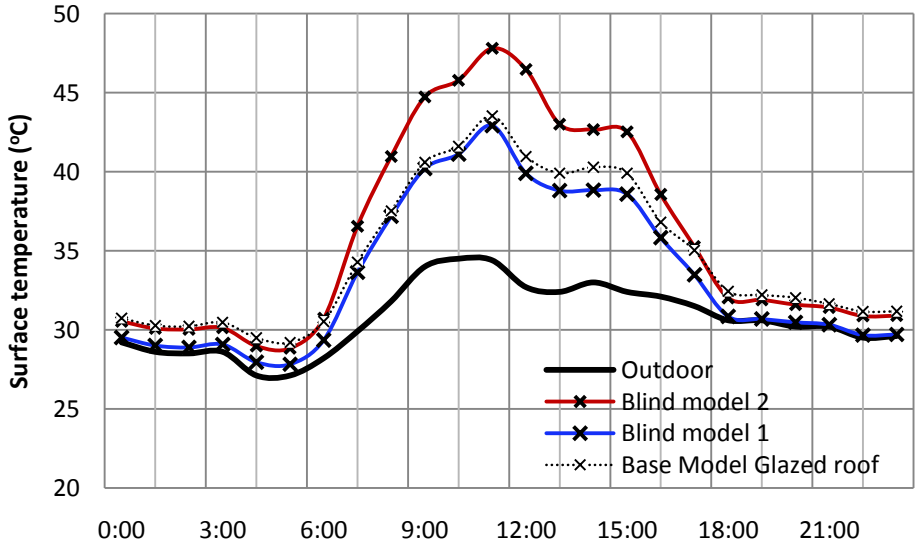

b) Overcast summer day: 3rd May 12

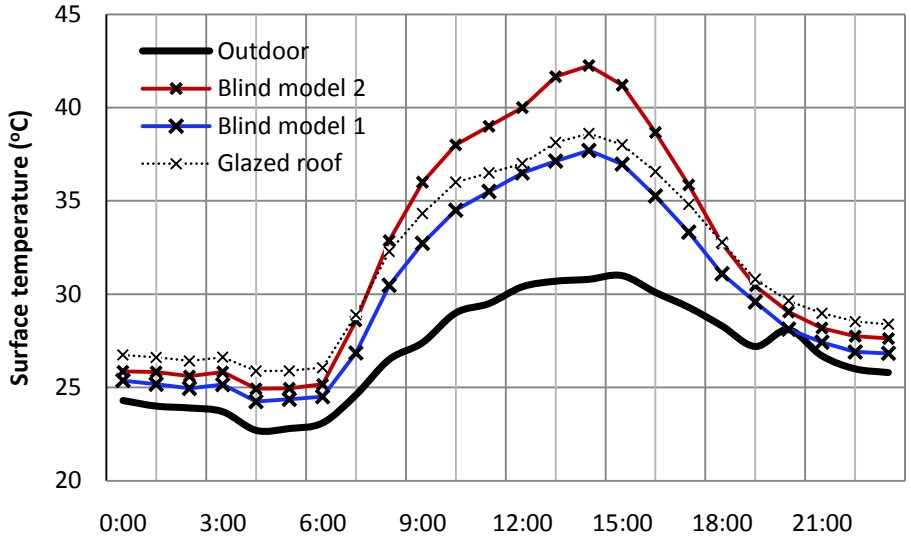

c) Clear winter clear day: 26th December 12

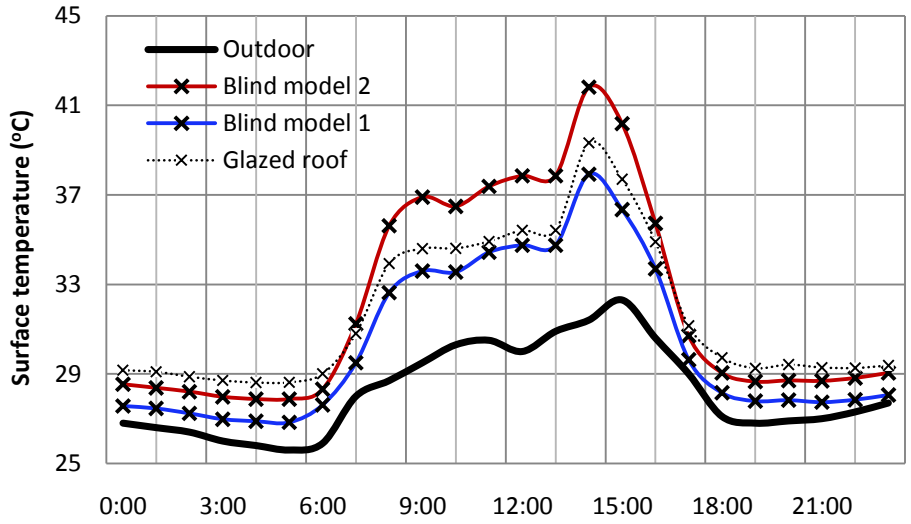

d) Overcast winter day: 7th December 12

Figure 7.10 Comparison of the internal surface temperature in the passenger lounge

b) Mean Radiant Temperature

The surface temperature greatly affected the mean radiant temperature (MRT) on both the ground floor pedestrian concourse and the top floor level. The MRT also took into account the view factors of these surfaces. Two locations were considered: one on the ground floor pedestrian concourse and the other on the top floor view point.

Around the midday of summer, solar energy penetrated through the surfaces of the passenger lounge and raised the MRT up to 32.0°C on a clear day and to 30.7°C on an overcast day. The high level shading (Model 2) increased this MRT to 33.3°C (+4.0%)

on a clear day and to 31.9oC (+ 3.9%) on an overcast day. The low level shading (Model 1) caused the MRT to decline to 31.2°C (-2.5%) on a clear day and to 30.0°C (-2.2%) on an overcast day (Figure 7.11).

On the top floor ceiling, the MRT reached a peak of 47.2°C on a clear day and 39.4°C on overcast day. The high level shading (Model 2) resulted in the increase of the MRT to 47.9°C (+1.4%) and to 40.6°C (+3.0%) on a clear day and an overcast day, respectively. The low level shading (Model 1) caused the decrease of MRT to 46.0°C (-2.5%) on a clear day and to 39.1°C (-0.8%) on an overcast day, respectively.

Around the midday of winter, solar energy penetrated through the surfaces of the passenger lounge, causing the MRT to rise to 29.1°C on both clear and overcast days. The high level shading (Model 2) increased the MRT to around 29.6°C (+1.7%) on both clear and overcast days; the low level shading (Model 1) decreased the MRT to 28.1°C (-3.4%) on clear days and to 28.2°C (-3.1%) on overcast days.

On the top floor ceiling, the highest MRT was 39.2°C on both clear and overcast days. The high level shading (Model 2) increased the MRT to 40.6°C (+3.6%) on a clear day and to 40.0°C (+2.0%) on an overcast day. The low level shading (Model 1) decreased the MRT to 38.2°C (-2.5%) on a clear day and to 39.0°C (-0.5%) on an overcast day.

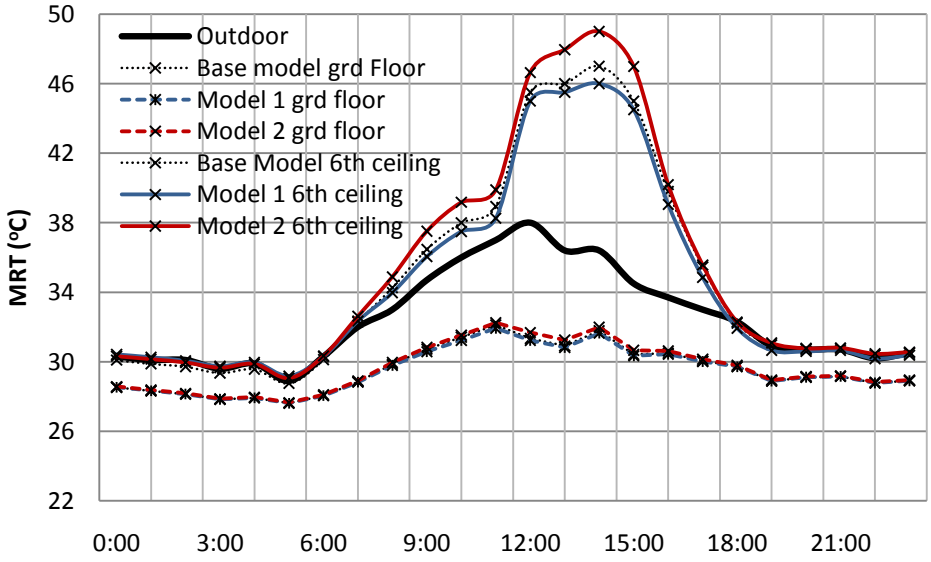

a) Clear summer day: 1st May 12

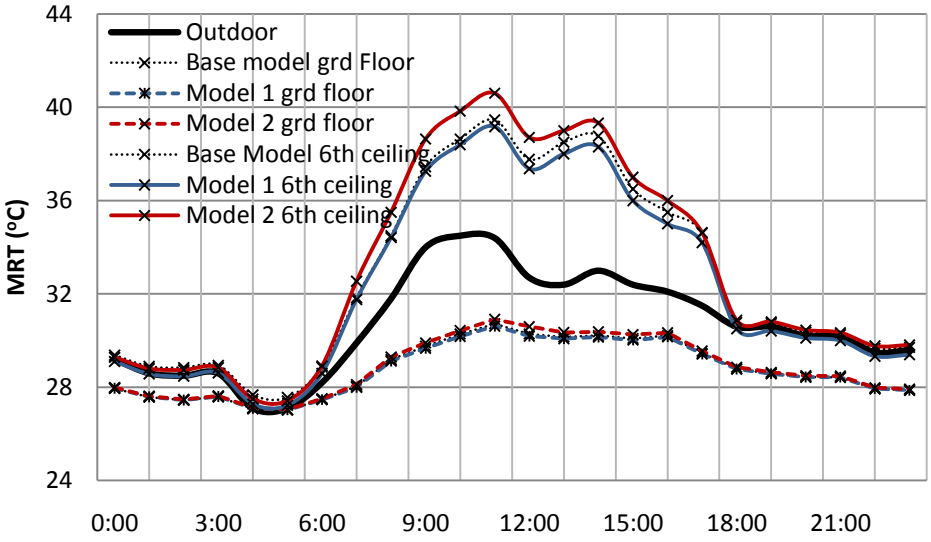

b) Overcast summer day: 3rd May 12

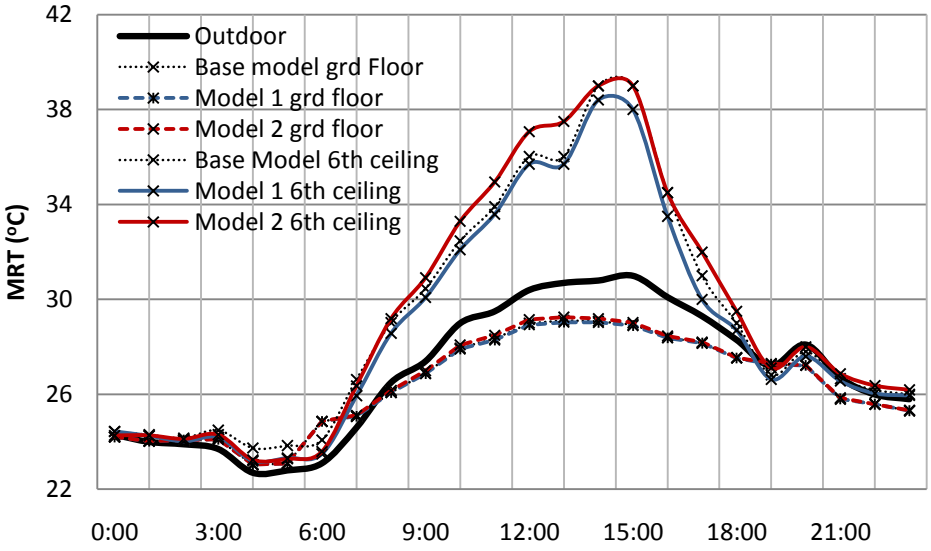

c) Clear winter day: 26th Dec 12

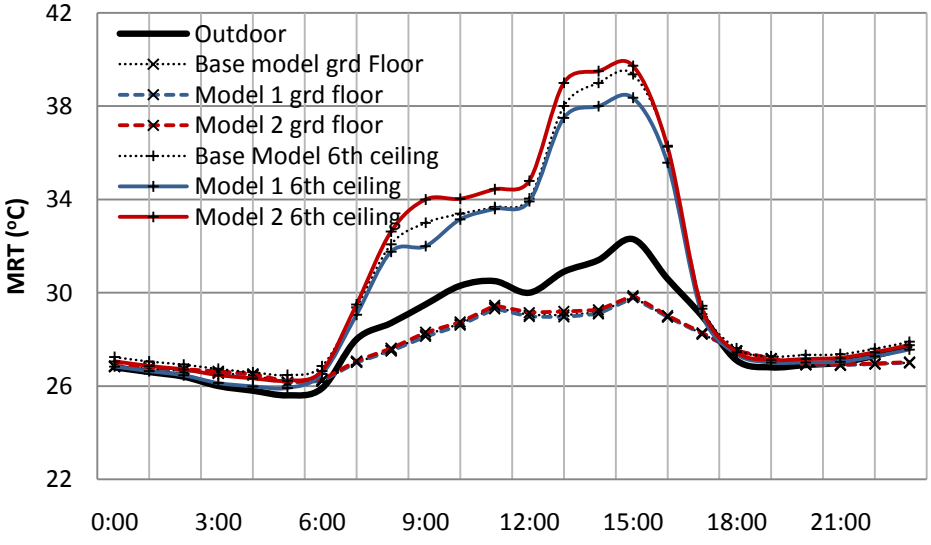

d) Overcast winter day: 7th Dec 12

Figure 7.11 Comparison of the MRT of the ground floor and the top floor ceiling

c) Air Temperature

Since the airport's pedestrian concourse was air-conditioned, the air temperature of this space had been only marginally affected by solar radiation. However, solar radiation had greatly influenced the air temperatures on the top floor ceiling, so this location received specific attention.

Figure 7.12 shows clearly that during the hottest hour in summer, the air temperature on the top floor ceiling peaked at 38.9°C on a clear day and 35.8°C on an overcast day. The high level shading (Model 2) increased the air temperature in this space to 39.3°C (+1.0%) on a clear day and to 36.3°C (+1.4%) on an overcast day. The low level shading (Model 1) reduced this temperature to 38.5°C (-1.0%) on a clear day and to 35.3°C (-1.4%) on an overcast day.

During the hottest hour in winter, the predicted highest air temperature on the top floor ceiling was 31.9°C on a clear day and 32.6°C on an overcast day. The high level shading (Model 2) raised the air to 32.2°C (+0.9%) on a clear and to 33.1°C (+1.5%) on an overcast day. The reduction by the low level shading (Model 1) was to 31.5°C (-1.3%) on a clear day and to 31.4°C (-3.7%) on an overcast day.

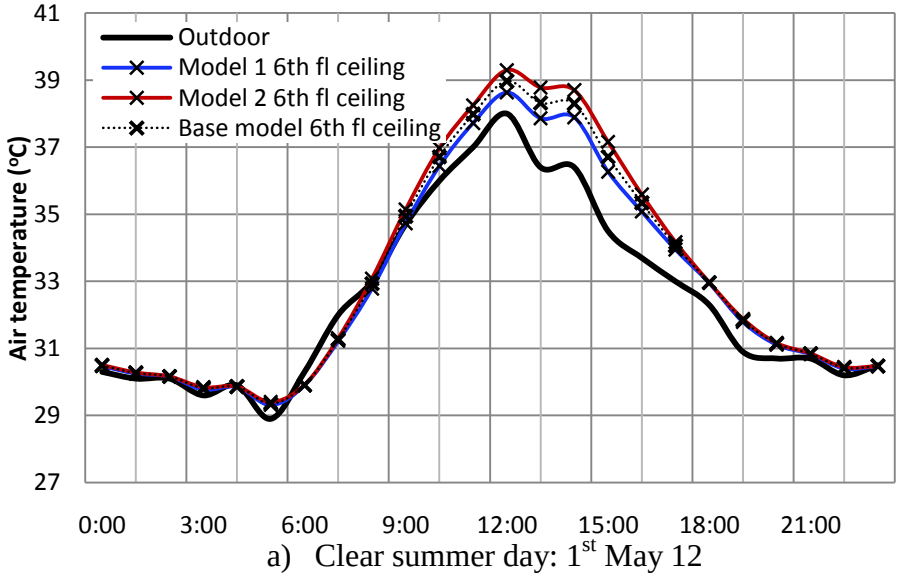

a) Clear summer day: 1st May 12

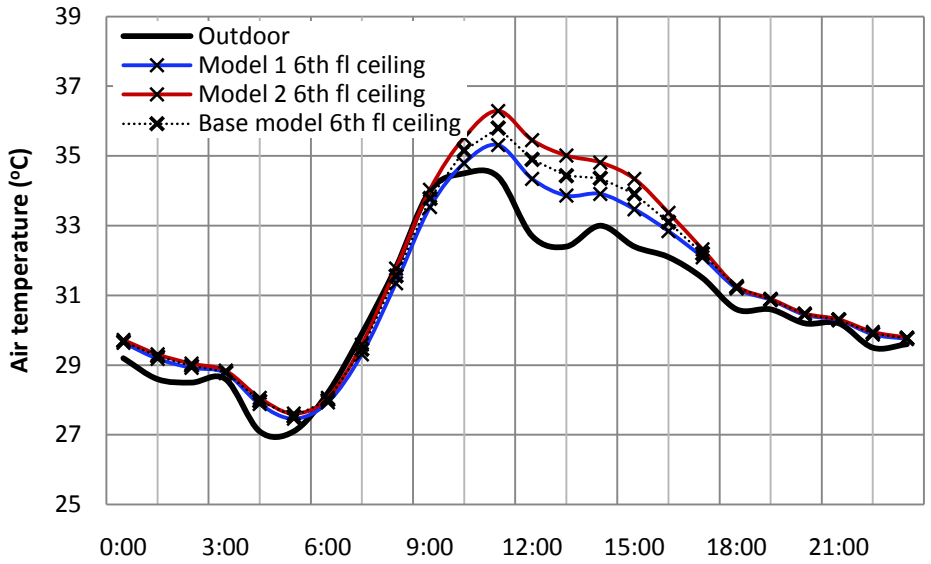

b) Overcast summer day: 3rd May 12

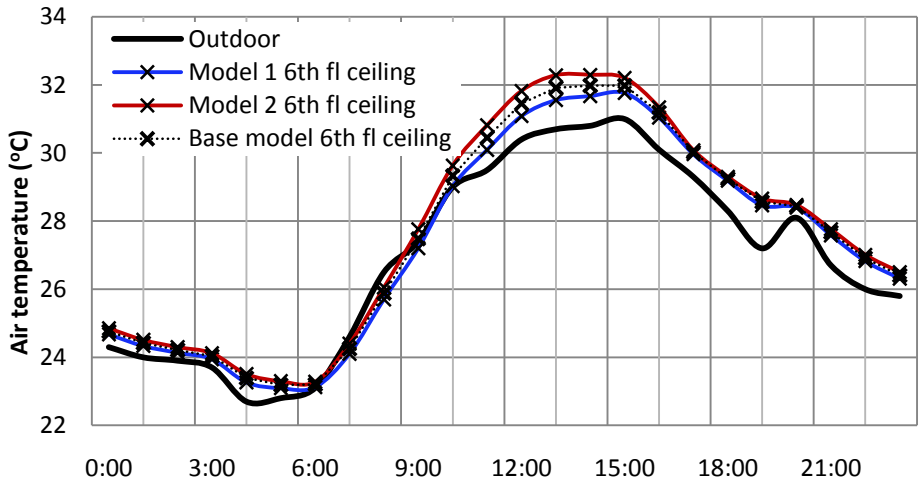

c) Clear winter day: 26th December 12

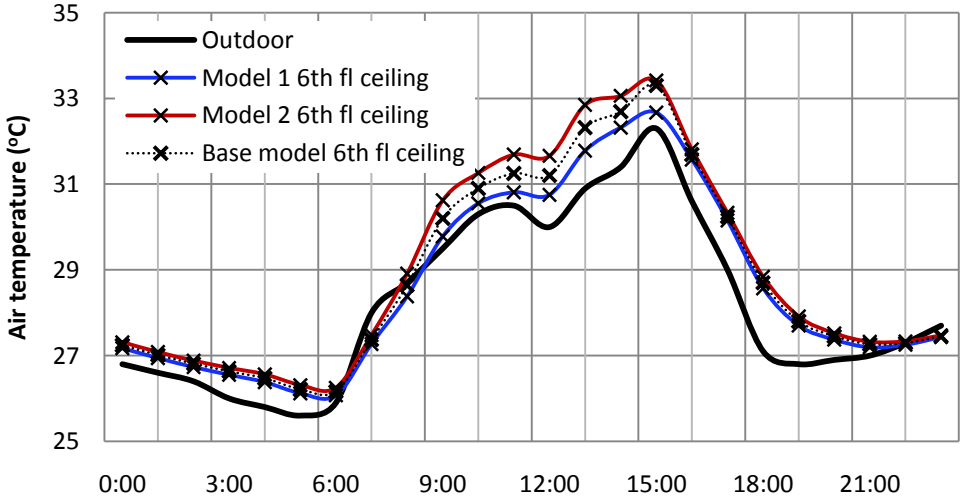

d) Overcast winter day: 7th December 12

Figure 7.12 Comparison of the air temperatures of the seventh floor ceiling and under glazed roof

d) Operative Temperature

Operative temperature describes the average of air temperature; mean radiant temperature (MRT) is the most useful indicator of thermal comfort in buildings. The internal operative temperatures of 22~24^{o}C are widely considered acceptable for an airport departure lounge, as recommended by ASHRAE (1992).

In summer midday, the highest operative temperature in the departure lounge was around 28.3^{o}C on both clear and overcast days. Figure 7.13 indicates that the predicted operative temperature was increased to 28.4^{o}C (+0.8%) on both a clear day and an overcast day by the high level shading (Model 2). However, the temperature was reduced to 27.9^{o}C (-1.1%) on a clear day and to 28.0^{o}C (-0.7%) on an overcast day by the low level shading (Model 1).

The highest operative temperature on the top floor was 29.7^{o}C on a clear day and 29.1^{o}C on an overcast day. The high level shading (Model 2) increased this temperature to 29.9^{o}C (+0.7%) on a clear day and to 29.3^{o}C (+0.5%) on an overcast day; the low level shading (Model 1) reduced this temperature to 29.3^{o}C (-1.3%) on a clear day and by 28.8^{o}C (-1.0%) on an overcast day.

In winter, the highest operative temperature in the departure lounge was around 27.5^{o}C on both clear and overcast days. The high level shading (Model 2) increased the operative temperature by 0.4^{o}C (+1.1%) on clear and overcast days. The low level shading (Model 1) reduced the temperature by 0.5^{o}C (-1.7%) on a clear day and 0.1^{o}C (-0.4%) on an overcast day. The highest operative temperature on the top floor was 28.8^{o}C on both clear and overcast days. Model 2 raised this temperature by 0.2^{o}C (+0.7%) on both clear and overcast days and Model 1 produced reductions of 0.3^{o}C (-1.0%) on a clear day and 0.2^{o}C (-0.7%) on an overcast day.

For the low level shading option (Model 1), the operative temperature went over 27^{o}C on the ground floor concourse and the top floor all day long, which identified that the shading option could not produce any great improvements in the thermal comfort conditions. On the other hand, the low level shading (Model 1) could reduce the internal surface temperature significantly which are the main causes of the radiation heat gain in the large glazed air-conditioned concourse.

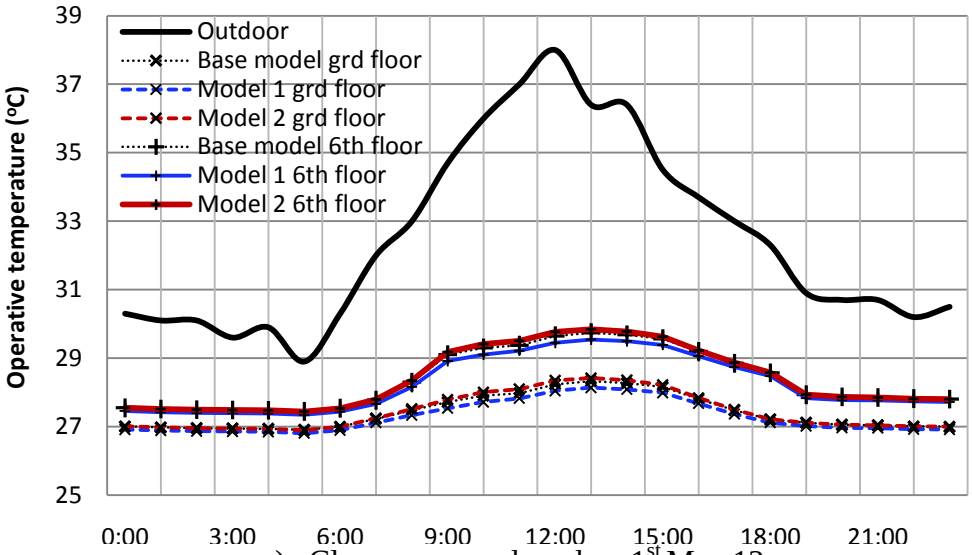

a) Clear summer clear day: 1st May 12

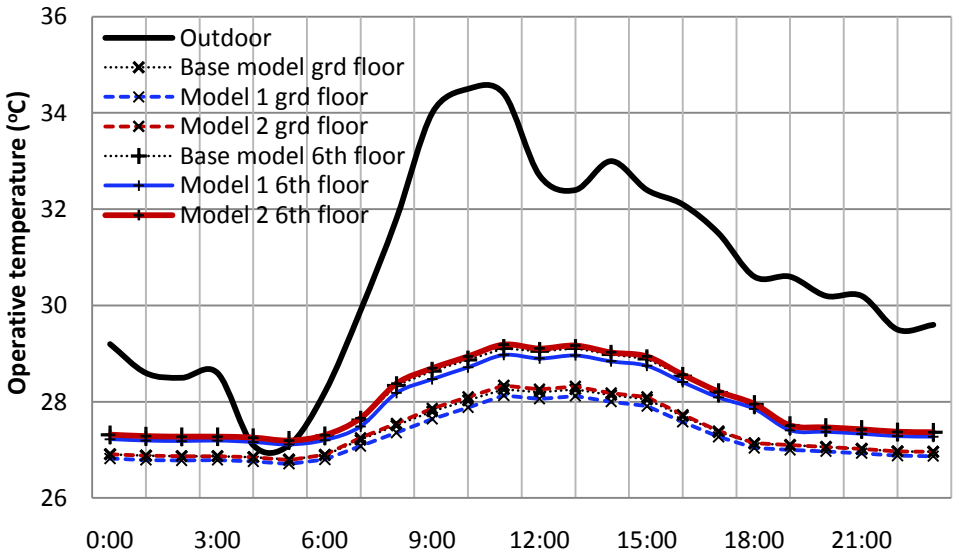

b) Overcast summer day: 3rd May 12

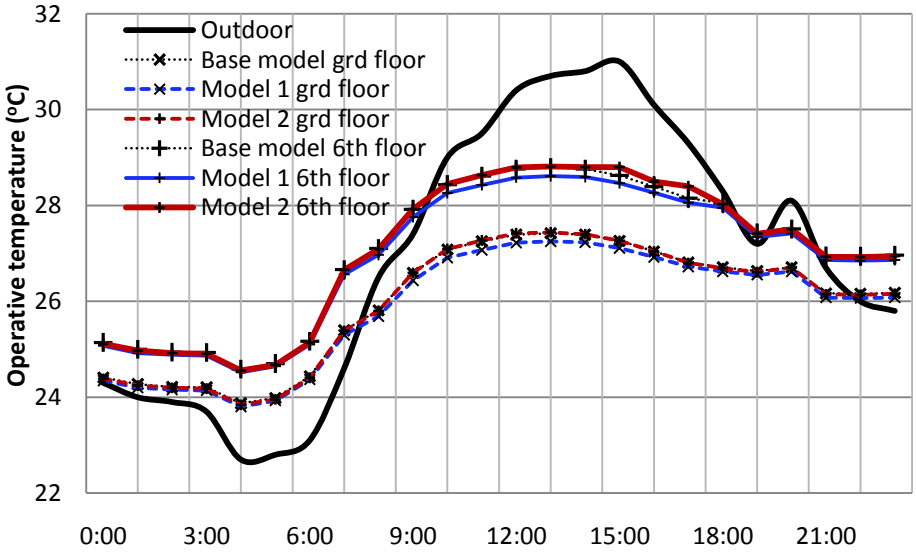

c) Clear winter day: 26th December 12

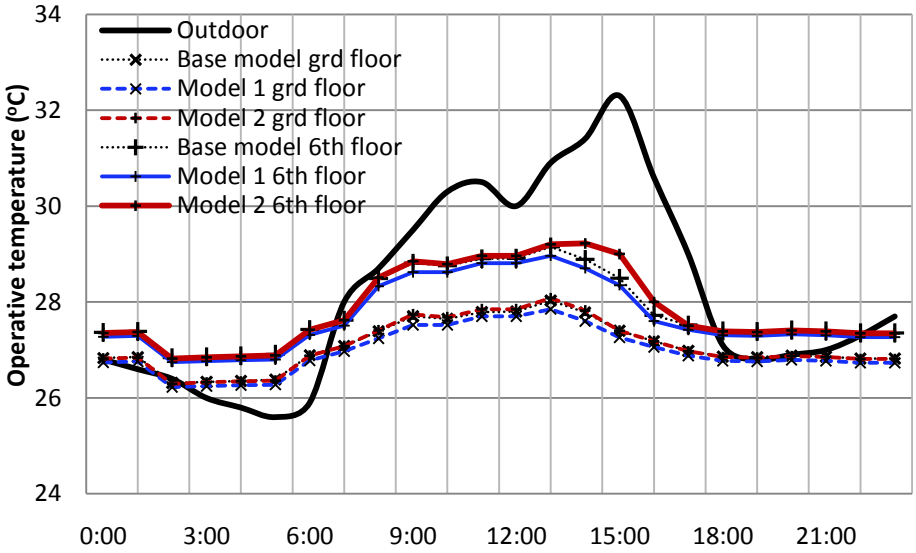

d) Overcast winter day: 7th December 12

Figure 7.13 Comparison of the operative temperature of the ground floor concourse and seventh floor view point

7.7.2.2 Visual Environment Aspect

In summer, the shading results reduced the illuminance level to 133~552 lux (Average 373.72 lux) on a clear day and to118~457 lux (Average 351.09) on an overcast day (Appendix G). Table 7.6 shows that the average illuminance of the base model was 301.35lux on a hot clear day and 274.83 lux on a hot overcast day. The average illuminance decreased by around 70 lux (-18.7%) on a hot clear day and 20 lux (-5.4%) on a hot overcast day by the low level shading (Model 1) (Anunnathapong, 2013).

In winter, the low level shading (Model 1) decreased the illuminance level to 117~496 lux (Average 341.08 lux) on a clear day and to113~445 lux (Average 338.43 lux) on an overcast day. The average illuminance was reduced by 60 lux (-17.6%) on a hot clear day and by 71.4 lux (-21.0%) by the low level shading (Model 1).

According to the CIBSE's recommendation for large office spaces (CIBSE, 1999), occupants can be satisfied with a lighting comfort of DF between 1-2%, when the shading screening is completely closed on a hot clear day (Table 7.6). On a hot overcast summer day and with both clear and overcast winter days, the shading would make the concourse a little too dark (DF lower than 21%), hence retractable shadings would be appropriate and artificial lighting would be needed.

Average illuminance (lux)	**Hot clear day**	**Hot overcast day**	**Cold clear day**	**Cold overcast day**
Base model	373.72	351.09	341.08	338.43
With Fabric	301.35	274.83	279.02	267
Maximum illuminance (lux)				
Without Fabric	613	569	567	552
With Fabric	535	485	496	474
Minimum illuminance (lux)				
Without Fabric	205	189	171	180
With Fabric	133	118	117	113

Table 7.6 Illuminance within the pedestrian concourse

		Base model	**Low Level (Model 1)**
Clear hot day	Passenger lounge	2.23	1.15
	Top floor view point	2.66	1.65
Overcast hot day	Passenger lounge	1.90	0.97
	Top floor view point	2.22	1.06
Clear cold day	Passenger lounge	1.87	0.77
	Top floor view point	2.02	0.93
Overcast cold day	Passenger lounge	1.65	0.76
	Top floor view point	1.89	0.89

Table 7.7 The predicted average DF (%) in the pedestrian concourse

7.7.2.3 Energy Efficiency Aspect

a) Solar Heat Gain

The total solar heat gain within the glazed pedestrian concourse for the base model was 1,047.1 Wh/m^2 on the clear summer day and 831.0 Wh/m^2 on the overcast summer day. Figure 7.14 illustrates that the presence of the low level shading (Model 1) cut direct solar radiations from deep penetration to lower levels, resulting in slightly lower solar heat gain on the passenger lounge floor to 1,000.0 Wh/m^2 (-5.9%) on the clear summer day and 775.5 Wh/m^2 (-9.5%) on the overcast summer day. However, the solar heat gain area tended to increase remarkably with the high level shading (Model 2); the levels rose to 1,171 Wh/m^2 (+3.3%) on the clear summer day and to 867.0 Wh/m^2 (+4.5%) on the overcast summer day.

The total solar heat gain within the glazed pedestrian concourse for the base model was 777.9 Wh/m^2 on the clear winter day and 598.2 Wh/m^2 on the overcast winter day. Only the low level shading (Model 1) prevented solar radiation from penetrating deeply to lower levels; by reducing solar heat gain to 746.2Wh/m^2 (-6.2%) on the clear winter day and 575.1 Wh/m^2 (-9.0%) on the overcast winter day. However, the solar heat gain area tended to increase remarkably with the high level shading (Model 2), which increased to 794.0 Wh/m^2 (+3.2%) on the clear winter day and to 632.0 Wh/m^2 (+6.0%) on the overcast winter day.

The difference between the solar heat reductions by the low level shading was very small. Since these terminal walls were glazed panels, the direct solar heat thus penetrates the external large glazed wall particularly the west-facing glazed wall during the hottest period of the day. For the higher level shading model (Model 2), the dramatic rise in solar heat gain in the below glazed roof area was due to the high surface solar gains of both the glazed roof and also the shading screen. The latter absorbed more solar energy from the top glazed roof leading to an increase in the temperature of the fabric and consequently releasing more heat into the air of the large glazed pedestrian concourse below.

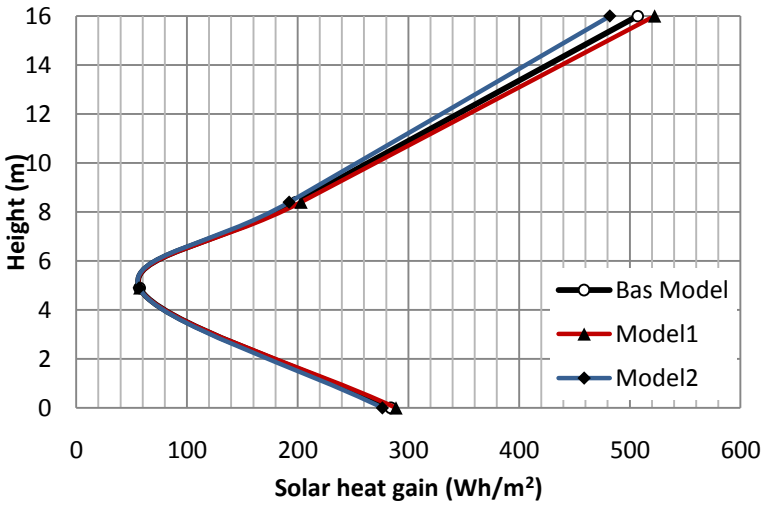

a) Clear summer day: 1st May 12

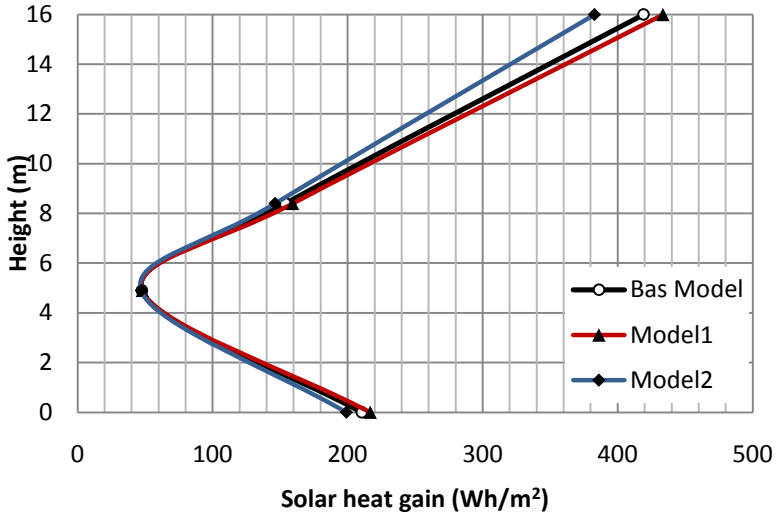

b) Overcast summer day: 3rd May 2012

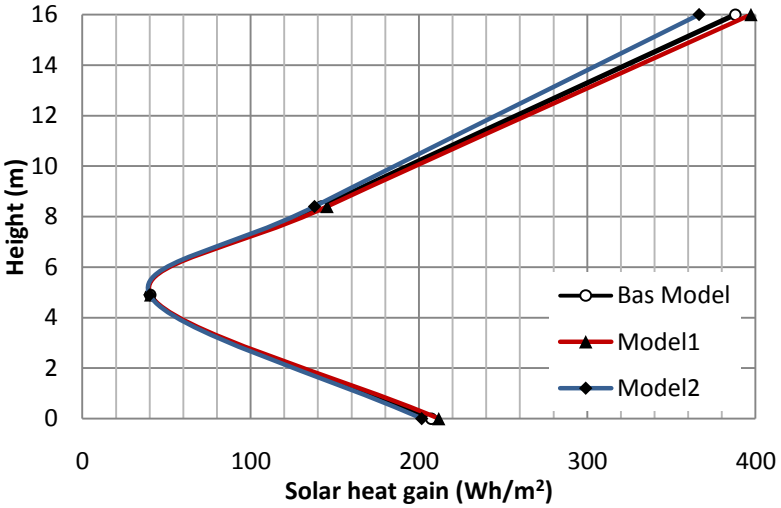

c) Clear winter day: 26th Dec 2012

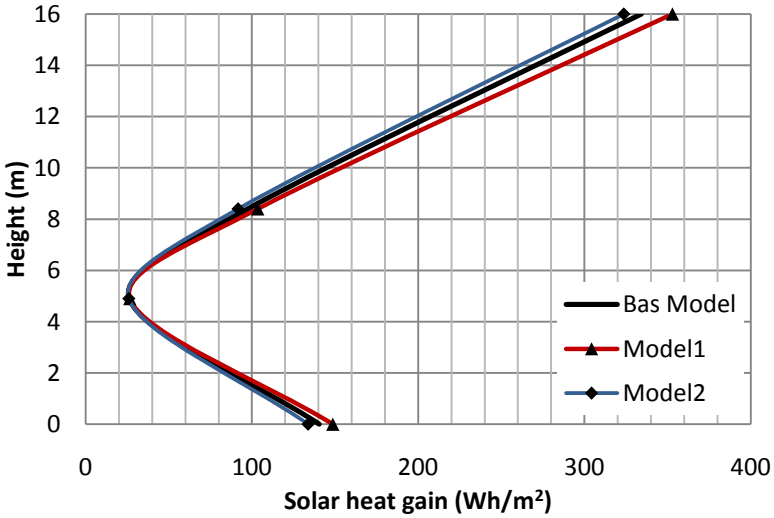

d) Overcast winter day: 7th Dec 2012

Figure 7.14 The total solar gain over the large glazed pedestrian concourse with air-conditioning

b) Cooling Load

The base model predicted that the total cooling for the whole terminal building was $2.83x10^8$ MJ ($7.86x10^7$ kWh). Figure 7.15 reveals that the low level shading (Model 1) reduced the total cooling load for the large air-conditioned glazed concourse of Suvarnabhumi airport terminal by 3.4% annually; while the high level shading (Model 2) increased the total cooling load by 11% annually.

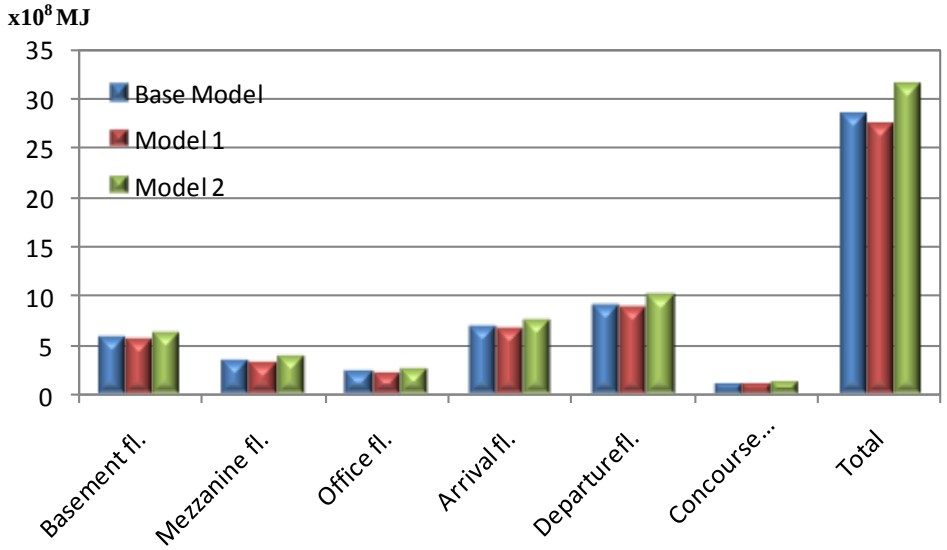

Figure 7.15 The total cooling load due the two shading options compared against the base case

7.8 Conclusion

In order to achieve the objective to examine the internal roof shading as a remedial solution relating to two case study buildings frequently described throughout the entirety of this thesis: one naturally ventilated and the other air-conditioned, the shading fabric was selected and examined. Their realistic light transmission performance was tested by scale model experiment in an artificial sky dome and also in an open-field context, under both clear and overcast skies.

Fabric samples tested in this thesis were provided by Silent Gliss Manufacturer (www.silentgliss.co.uk). Five reflective shade fabric samples were selected and examined for their realistic light transmittance. To obtain realistic light transmittance of these fabrics, a scale model box was made and each of the collected fabric samples was tested in the artificial sky at Heriot-Watt University and also in open field conditions under an overcast sky.

The highest light transmittance and lowest solar transmittance fabric sheet was finally selected for the proposed shading system. Two shading arrangements were proposed: the low level shading (horizontal screen) and the high level shading (curved/sloped screen). These were facilitated by dynamic thermal and lighting software tools known as TAS, Ecotect and Dialux. The effects of the shading options were quantified and assessed using the defined environmental variables to judge any environmental and energy performance improvements. These assessments were based on comparisons between the shading cases and the base case on both clear and overcast summer days; as well as clear and overcast winter days.

The environmental variables examined to assess the thermal conditions in the case studies were the inner surface temperature of the ceiling, the mean radiant, air and operative temperatures and daylight factors over the existing long-span glazed roofs over large pedestrian concourses. The visual condition of these tested cases was assessed for illuminance and daylight factors. Then solar heat gain and cooling load variables were examined to assess the energy performance.

The thermal simulated results of the large glazed pedestrian concourse with natural ventilation demonstrated that the internal shading devices were very effective in reducing inner surface temperatures in the space and consequently reducing radiant heat gain into the space; this also eased thermal discomfort particularly on the upper levels.

The low level shading was more effective than the high level shading in terms of providing better internal thermal and visual environments, as well as energy performance. The modelling indicates the low level shading goes a long way to alleviating summer thermal discomfort within the concourse, particularly on the high level corridors, by reducing significantly the surface temperature of the inner surface of the “ceiling”, the part that is thermally visible from those circulation areas. The shading reduced the air temperature by 4.1% and also the MRT by 8.7% within the ground floor pedestrian concourse on a clear hot day, respectively.

Apart from energy performance assessment within the large naturally ventilated glazed pedestrian concourse, the low level shading performed better than the high level shading in terms of reducing the total cooling load by saved 6.8%. The difference between the cooling load reductions was small because the cooling loads were for the

retail units over seven stories in the GITC. Most of them did not receive direct solar heat and those that did were the few on the top floor and on the east and west sides. In summer this configuration would reduce two thirds of the solar heat gain in the pedestrian concourse space significantly.

The larger spatial gap between the transparent roofs and the screen blinds could make a major contribution to all the temperature reductions. Due to the gap, the void space was well ventilated to avoid excessive heat building up. The gap for the high level shading was much smaller than the lower level shading. Hence less air movement leads to heat accumulating and increasing the temperature of the fabric; consequently releasing more heat to the air in the pedestrian concourse below.

These results showed that creating a ventilated naturally thermal buffer space is the design solution for an effective shading system for the large glazed naturally ventilated concourse. The large void space between the transparent roofs and the low shade shadings allows the free movement of the air to dissipate the heat at the high levels to the outside, before it can enter the concourse below. The buffer zone is a key reason that the lower blinds are more effective for shading than the higher blinds.

The thermal simulated results of the large glazed pedestrian concourse with air-conditioning have revealed that only the low level shading would improve the internal thermal and lighting performance by reducing inner surface temperatures and radiant heat gain within the large glazed air-conditioned concourse space. This configuration would reduce the internal surface temperature, which is the main cause of the radiation heat gain in the large glazed air-conditioned concourse. In summer this configuration would reduce the solar heat gain by 9.0% and the inner surface of the "ceiling" by 3.7% in the pedestrian concourse space. The shading also would reduce both the air temperature and the MRT by 1.0% within the passenger lounge on a clear hot day, respectively.

Low level shading manages to do this by trapping an insulating layer of hot air between the curtain and the transparent roof and also reduces ceiling surface temperatures. A larger volume of air between glazed roof and the low level shading leads more accumulation of heat as compared to a smaller volume of air between glazed roof and the high level shading. In addition, the high solar reflective property of the fabric

decreases the solar heat by reflecting a portion of the solar heat back out through the transparent roof, while some solar energy is also trapped within the air gap.

Interestingly, installing the high level internal shading does not improve the thermal environment in the large glazed air-conditioned concourse, since the glazed roofs and the internal blinds would be extremely hot. As the blinds absorb solar energy from the top, their radiant temperatures would rise due to the surface temperature. With the contribution of radiant energy from other internal surfaces, the mean radiant temperature and the air temperature at high level would also increase and lead to greater stratification throughout the lower occupied levels.

The visual conditions simulated results of the large glazed pedestrian concourse with natural ventilation demonstrated that the low level shading significantly reduced daylighting levels in the space. The average illuminance level over the ground floor concourse and the first floor balconies was maintained at over 500 lux by the low level shading on a clear day in summer in this building which would be acceptable by CIBSE standard for shopping malls. On overcast summer days and the winter days, the internal shading screenings should be opened to allow natural light in due to inadequate light by the shading. Therefore retractable shading blinds are recommended to provide sun screening only on clear summer days, on which the solar gain is likely to result in overheating, if not challenged in some way.

The visual conditions simulated results of the large glazed pedestrian concourse with air-conditioning demonstrated that the low level internal shadings also reduced the unevenness of the natural light distribution over the space. The average illuminance level at the ground floor concourse was at 373 lux on a clear summer day. The shading significantly reduced daylighting level to 301 lux, which would be acceptable by CIBSE's standard for foyer and entrance halls. The shading decreased the illuminance to less than 300 lux so that on overcast summer days, as well as both clear and overcast winter days, addition artificial lighting would be required.

Apart from energy performance assessment within the large air-conditioned glazed pedestrian concourse, the low level shading would reduce the total cooling load by 3.4%. In summer this configuration would reduce about 6% of the solar heat gain in the pedestrian concourse space. The difference between the solar heat reductions by the low

level shading was very small. Since these terminal walls were glazed panels, the direct solar heat thus penetrates the external large glazed wall particularly the west-facing glazed wall during the hottest period of the day.

Apart from considering internal thermal comfort by operative temperatures, proposed shading options for both glazed pedestrian concourses with natural ventilation and air-conditioning could only ease thermal discomfort to some degree. Shading could not improve the thermal comfort condition very much, although the shadings could reduce significantly the inner surface temperature.

The choice of electric motor or automatic control should be considered. Due to the limitations in this thesis, the shade control systems themselves were not a focal point in this study.

The next chapter will analyse the installation and operation costs of the shading system in terms of its economic benefits. In order to analyse those benefits, the energy savings and operating cost reduction were calculated over the entire life cycle of the system.

CHAPTER 8 – ECONOMIC ASSESSMENT

8. 1 Introduction

To achieve the objective of analysing the financial benefits from the remedial solutions applied in two cases of existing long-span glazed roofs over large pedestrian concourse buildings in the tropics, the naturally ventilated case (Guangzhou International Textile City) and the air-conditioned case (Suvarnabhumi Airport Terminal), the researcher used standard economic analysis methods to provide recommendations on the costs and payback periods.

The shading installation cost depends on the shade control system. Two primary types of internal shading systems may be used. Manual operated systems are suitable for small projects. Shade control systems are required for retractable internal fabric sheet blinds for these long-span glazed roofs over large pedestrian concourse spaces; such systems should be electric motor or automatically controlled. However shade control systems were not a focus in this thesis. Therefore, the cost analysis for installation covering the shade control system was directly calculated from the manufacturer's recommended price list.

It was assumed that the extended shading would not affect the lighting bill, as it would only be used on hot clear days when natural light is plentiful. Shading would affect the cooling load and, in turn, the ventilation and air-conditioning costs that normally account for the largest proportion of electricity used in commercial buildings in hot climates (National Instrument Co.Ltd).

In order to compare the economic profits, the initial investment for the internal shading devices was estimated under the material and installation price and compared with the energy saving by the air-conditioning system. Two cost scenarios were considered, one based on the UK prices, mainly from Silent Gliss Ltd., and the other on local prices.

The chapter contains four content specific sections. Section 8.2 presents standard economic analysis methods using in the thesis. Section 8.3 discusses the economic assessment of the long-span glazed roof over large pedestrian concourse with natural ventilation; while section 8.4 discusses the economic assessment of the long-span glazed roof over large pedestrian concourse with air-conditioning. Conclusions are presented at the end of this chapter.

8.2 Standard Economic Analysis Methods

The method used for calculating the economic profits of energy saving project alternatives are the net present value method (*NPV*), the internal rate of return method (*IRR*) and depreciated payback period (*DPP*) (Nikolaidis et al., 2009).

In finance, incoming and outgoing flows can also be described as benefit and cost cash flow respectively, which depends on the time value of money. Time value dictates that time has an impact on the value of cash flows. In other words, a cash flow today is more valuable than an identical cash flow in the future. Its effectiveness depends on interest rates for each period (Berk, DeMarzo, and Stangeland, 2011).

a) Net Present Value (*NPV*)

The NPV sums the discount cash flows over various time periods. The *NPV* is determined from the following equation:

$$NPV = -C_o + \sum_{t=1}^{n} \frac{F_t}{(1+n)^t} \quad \text{and} \quad F_t = B_t + C_t \tag{8.1}$$

where t is the time period (year); F_t the net cash flow at year t. B_t is the saved energy cost at year t; C_t the cost at year t. The value C_o is the initial investment; p the cost of capital, and n the number of years of the investment lifetime.

An investment of a project choice is profitable only if $NPV>0$, so the best choice would be the one with the highest *NPV*.

b) Internal Rate of Return (*IRR*)

The *IRR* evaluation method aims at the determination of the discount rate that renders the present value of future discounted net cash flows of an investment equal to the initial cash outflow (initial investment), for the total years of evaluation. The formula that is used for the determination of the *IRR* is:

$$IRR = -C_o + \sum_{t=1}^{n} \frac{F_t}{(1+n)^t} \tag{8.2}$$

where p is the interest rate, t is the number of year and F_t is the net cash flow

This method allows the investor to calculate *IRR* and identify the investment project that has the greatest value above the minimum acceptable interest rate. This is to ensure

the investment is profitable. The most attractive investment would be the one that has the highest *IRR*.

c) Depreciated Payback Period (*DPP*)

The Depreciated Payback Period method calculates the number of years (the duration of evaluation) that are needed to recover the initial outflow of an investment. This happens through net cash flows that are expected as a result of this investment. The formula that is used for the calculation of the *DPP* is:

$$DPP = \frac{-\ln\left(1 - \frac{pC_o}{F_t}\right)}{\ln(1+p)} \tag{8.3}$$

where C_o is the initial investment; p the cost of capital; and F_t the net cash flow which is assumed to be constant for every t.

8.3 The Long-Span Glazed Roof over Large Pedestrian Concourse with Natural Ventilation Economic Assessment

8.3.1 Costs of the Internal Shading System

In the UK scenario, the hardware for the electrically operated blind skylight system was about £112.60 m^{-2}. There was an additional cost for intermediate brackets for the skylight system at £10.00 m^{-2}. The fabric was about £131.5 m^{-2}. Hence the total cost for installation of the internal shading system would be c. £1.75 million for a transparent roof area of 6,900 m^2.

In the Chinese scenario, it was assumed the same quality could be bought at a lower cost, due to the lower costs of labour and materials in both manufacturing and installation. A quick survey showed that the same hardware for electrically operated skylight blinds would be reduced to £30.00 m^{-2}, based on current exchange rate of £0.1/Yuan. While installation costs and fabric costs would be reduced to £40.00 m^{-2}. The total cost for internal shading devices from Chinese manufacturers would be £435k.

8.3.2 Inflow of the Investment

The fuel prices in China have increased several times in recent years with significant impacts on the cost of power generation. In 2012, power prices in China increased by an average of 0.03 Yuan per kWh each year (4.6% increase) (Shenzhen Government Online).

Electricity prices vary in China and the average price in Guangdong Province was the highest, 0.68 Yuan per kWh (£0.07 per unit) at the time of this study.

The predicted cooling load from June to September of the Base model was 2.4 x 10^7 kWh. Assuming that the internal shading devices operated only for summer, the cooling load was 2.25x10^7 kWh, when the lower blinds were installed. The lower blinds would reduce the cooling load by at least 1.5x10^6 kWh throughout the summer season. This reduction of 6.8% means an equivalent saving at least, £105k annually at current electricity prices in China. This figure will be even higher as the energy prices rise.

8.3.3 Interest Rates in China

In China, interest rates decisions are taken by the People's Bank of China's Monetary Policy Committee. The interest rate in China was last recorded at 4.85 percent in 2015 (Figure 8.1). Interest rate in China averaged 6.37 percent from 2005 until 2015, reaching an all time high of 6.85 percent in 2008 and a record low of 4.85 percent in 2015 (PBC, 2015).

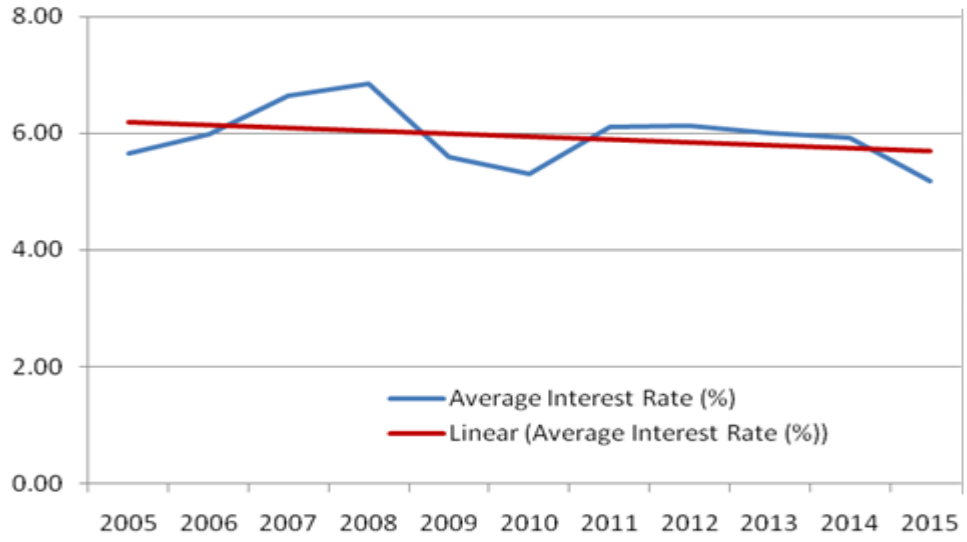

Figure 8.1 Average interest rate in China from 2005-2015 (PBC, 2015)

8.3.4 Economic Benefits

Figure 8.2 reveals the results of the economic evaluation; the energy cost savings over the years were calculated from the reduction of cooling loads predicted by the modelling and the economic benefit as calculated with an interest rate from 4.85 percent up to 6.85 percent (Appendix H).

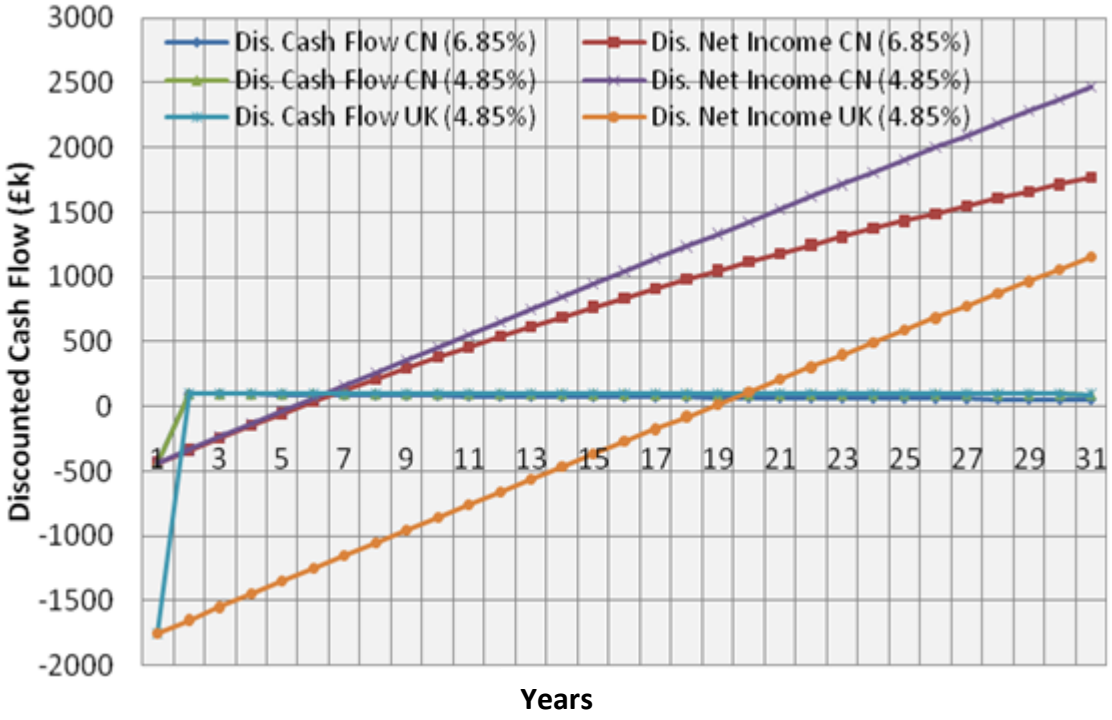

Figure 8.2 Cost analysis of the shading solution with UK and China price scenarios (*p*=4.8% and 6.85%)

In the UK scenario, the *NPV* would be £-224k with an interest rate at 4.85 percent. The result of *IRR* would be 4 percent. The recovery period of the investment would be approximately 20 years (*p*=4.85%).

In the Chinese scenario, the *NPV* would be £2,467k with an interest rate at 4.85 percent and £1,767k with an interest rate at 6.85 percent. The result of *IRR* would be 23 percent. The recovery period of the investment would be approximately 6 years (*p*=4.85%).

The Chinese price estimations of the paybacks are very reasonable, and seem very attractive by Chinese standards, particularly in relation to the major complaints from the tenants in the GITC building concerning rising energy costs and issues of heat stress and thermal discomfort. On the other hand, the application of any green solutions currently can be offset with other factors such as governmental incentives or impacts on the market perception of an organisation as 'green'. The less obvious environmental benefits, the carbon emission reductions, were not considered in this study. In China, where the carbon conversion rate is high and electricity generation done largely with polluting coal, an analysis of the environmental benefits of carbon reduction may well become increasingly attractive over time.

8.4 The Long-Span Glazed Roof over Large Pedestrian Concourses with Air-Conditioning Economic Assessment

8.4.1 Costs of the Internal Shading System

Considering the prices from Silent Gliss Ltd., the hardware for electrically operated blind skylight system costs about £112.60/ m^2. There is an additional cost for intermediate brackets for the skylight system at £10.00/m^2. The fabric costs about £131.5/ m^2. It comes out that total investment for internal shading devices for the whole roof area 48,000 m^2 is £12.196m.

In the Thailand scenario, it was assumed the same quality could be bought at a lower cost, due to the lower costs of labour and materials in both manufacturing and installation. A quick survey showed that the same hardware for electrically operated skylight blinds, installation cost and fabric costs would be reduced to 30.00 percent, based on the current exchange rate of £0.02/Baht. The total cost for internal shading screens from Thai manufacturers would be £8.537m.

8.4.2 Inflow of the Investment

The global fuel price, inflation rate and international exchange rate have had a significant impact on Thailand's electricity prices in recent years, so the prices have increased several times. In 2011, basic power prices in Thailand were set at 3.02 baht per kWh in peak period (9.00-22.00) and 2.02 baht per kWh in peak period (22.00-9.00) excluding 10% VAT. In 2012, power prices in Thailand increased 0.30 baht per kWh (9.8% increase annually) (EGAT, 2014). The average electricity price in Thailand was 3.07 baht per kWh (£0.06 per unit) at the time of this study.

The predicted annual cooling load from 2012 of the Base model was $1.86x10^8$kWh. The cooling load was reduced to $1.79x10^8$ kWh, when the blinds were installed. These blinds would reduce the cooling load by at least $7.0x10^6$ kWh throughout the whole year. This reduction of 3.4% means an equivalent saving of at least £420k annually at current electricity prices in Thailand.

8.4.3 Interest Rates in Thailand

In 2015, the interest rate in Thailand was last recorded at 1.50 percent (Figure 8.3). Interest rates in Thailand averaged 2.75 percent from 2005 until 2015, reaching an all

time high of 4.80 percent in 2006 and a record low of 1.35 percent in 2009 (BOT, 2015).

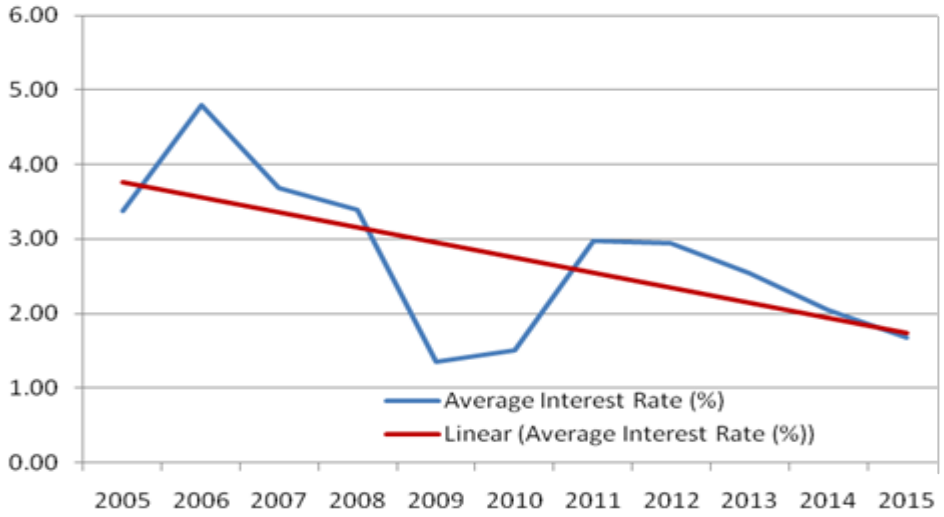

Figure 8.3 Average interest rate in Thailand from 2005-2015 (BOT, 2015)

8.4.4 Economic Benefits

Figure 8.4 shows the results of the economic evaluation. The annual energy cost savings were calculated from the predicted reduction of cooling loads by the modelling and the economic benefit as calculated with an interest rate from 1.35 percent up to 4.80 percent (Appendix I).

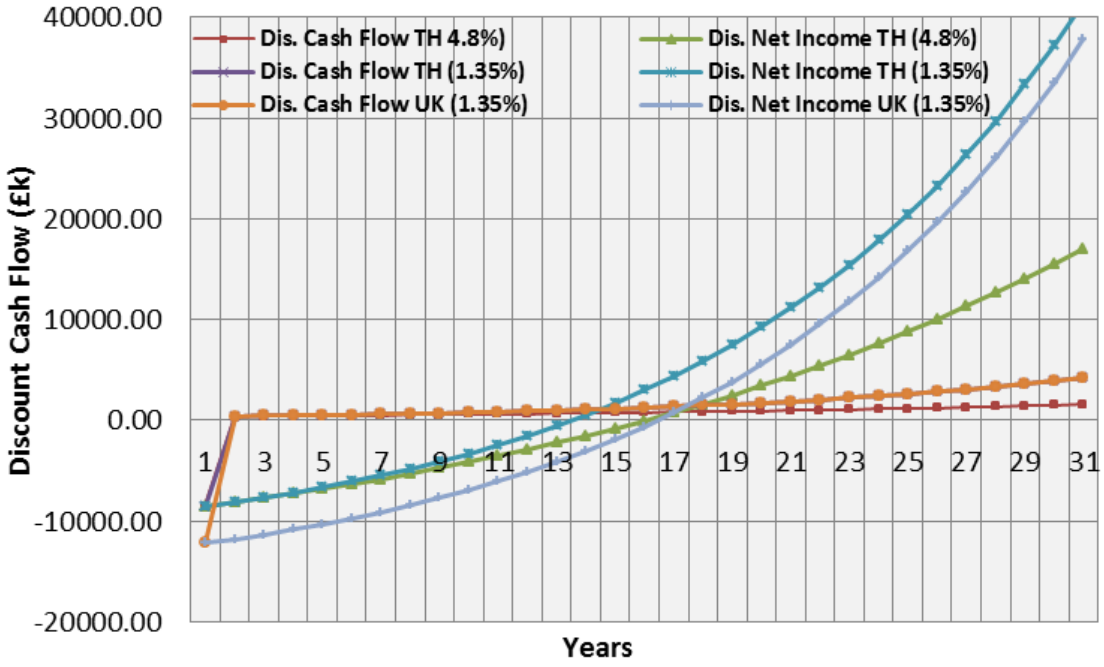

Figure 8.4 Cost analysis of the shading solution with UK and Thailand price scenarios (p=4.8% and 1.35%)

In the UK scenario, the *NPV* would be £37.756m with an interest rate at 1.35 percent. The result of *IRR* would be 8 percent. The recovery period of the investment would be approximately 15.5 years (*p*=1.35%).

In the Thailand scenario, the *NPV* would be £41.415m with an interest rate at 1.35% and £17.065m with an interest rate at 4.80 percent. The result of *IRR* would be 11percent. The recovery period of the investment would be approximately 12.5 years (*p*=1.35%).

The long-span glazed roof over large pedestrian concourse with air-conditioning of Suvarnabhumi Airport Terminal building, in which internal condition needed to be maintained within the range of 21°C to 25°C on a seasonal basis, the use of internal shading screenings is economic enough and profitable. The advantage of these screens is not only to save energy, thereby reducing the large annual net cash flow, but will also support the reduction of greenhouse gas and CO_2 emissions, which should be considered in further studies.

8.5 Conclusions

The standard economic analysis methods were employed to provide recommendations on the solutions' costs and payback periods.

A cost analysis was carried out taking into consideration both the installation and the running costs of the shading options. There is a need for studies to evaluate the relative, long term performance of common capital budgeting decision procedures, when used in practice.

As mentioned in the scope of this thesis, micro details of the recommended shade control systems were not focused on. Therefore, the cost analysis for installation of the shade control system was directly calculated from the manufacturer's recommended price list.

The shading devices that have the greatest potential for reducing energy consumption and achieve better physical environment will be assessed financially by using the following concepts: Internal Rate of Return (*IRR*), Net Present Value (*NPV*) and Discount Payback Period (*DPP*).

With an interest rate of 4.85 percent in China, the investment of the shading system in the atrium with the long-span glazed roof over a large pedestrian concourse with natural ventilation, could be financially beneficial due to the *NPV*>0 and the *IRR* was greater than the investment opportunity rate at 23 percent, over a life time of 30 years. By examining *DPP*, the investment of low level blinds in Guangzhou International Textile City Building would be recovered after the period of 4.4 years at the Chinese prices (Table 8.1).

With an interest rate of 1.35 percent in Thailand, the investment of the low level blinds in the long-span glazed roof over a large pedestrian concourse with air-conditioning, could be financially beneficial due to the *NPV*>0 and the *IRR* was greater than interest rate at 11 percent, over a life time of 30 years and could be recovered after a period of 12.5 years at Thai prices. Even though *DPP* was quite long, it was not over than the maximum acceptable *DPP* of 15 years (Table 8.1).

China	**P=6.85%**	**P=5.85%**	**P=4.85%**
NPV	1,767	2,083	2,467
IRR	20%	22%	23%
***DPP* (years)**	4.5	4.5	4.4
Thailand	**P=4.80%**	**P=2.75%**	**P=1.35%**
NPV	17,065	29,124	41,415
IRR	7%	9%	11%
***DPP* (years)**	15.04	13.4	12.5

Table 8.1 Economic analysis of the shading solution

The next chapter recommends certain internal roof shading design principles and guidelines for long-span glazed roofs over large pedestrian concourses with natural ventilation and air-conditioning in the tropics, based on the data gathered in field trials and/ or simulation from this research. All the important findings in the previous chapters will be presented as a remedial solution to provide a better building-centric thermal environment and energy performance, while maintaining adequate levels of natural lighting, within existing long-span glazed roofs over naturally ventilated and air-conditioned large pedestrian concourses in the tropics.

CHAPTER 9 –DESIGN PRINCIPLES and RECOMMENDATIONS

9. 1 Introduction

This chapter presents the internal shading design principles and guidelines based on and informed by the results of the work described in detail in the previous chapters. These recommendations are steps towards creating internal shadings with an environment-friendly performance. They are based on the thermal and lighting measurements and the simulated models carried out using dynamic thermal and lighting simulation software and some supporting literature. It is proposed that the thermal comfort assessment, which can provide a better physical environment, should be followed up.

The effectiveness of any shading device in blocking out the solar radiated heat depends not only on the form and position of the shading device, but also on its materials and colour. The different materials also obtain the different shading effects (Corrado, Serra and Vosilla, 2004; Unterpertinger, 2005).

The chapter contains two content specific sections. In section 9.2, it presents design principles and recommendations regarding internal roof shading for existing long-span glazed roofs over one large naturally ventilated and one large air-conditioned pedestrian concourse in the tropics; the former in China and the latter in Thailand. A brief conclusion is presented at the end of this chapter.

9.2 Design Principles and Recommendations Concerning Internal Roof Shadings for Long-Span Glazed Roofs over Large Naturally Ventilated and Air-Conditioned Pedestrian Concourses in the Tropics

The design principles and recommendations are based on the size of the project in excess of 100,000 m^2 and designed with long-span glazed roofs over large pedestrian concourses, with mainly external glazed walls and transparent roofs in the tropics. The construction of the outside façade of the case studies is mainly 12 mm. thick laminated glasses with a *U*-value of 5.5 W/m^2K. Hence these case studies are applicable to many other long-span glazed roofs over large pedestrian concourse buildings with the similar construction.

This study deals with existing long-span glazed roofs over large pedestrian concourses and shading devices in the form of retractable internal fabric sheet blinds; in particular

how they could be used to reduce temperatures while maintaining adequate levels of natural lighting for the occupants. Three mains factors play a significant role in designing an internal roof shading device: internal roof sheet blinds materials, form and positions. Some general guidelines for designing internal shading devices that can contribute to better thermal and visual environments in the two case-study buildings are summarised as follows:

9.2.1 Internal Shading Fabrics

According to summarizing the data analysis of the site measurements and computer simulation, internal shading fabrics would be used base on the following criteria:

- The materials used should be highly reflectance to bounce much of the unwanted direct solar radiation back to the exterior.
- Low solar transmittance fabrics would be used in the internal shading device, in order to reduce the amount of solar radiation;
- In order to maximize daylight environment by internal shading, the selected fabrics for the shading blinds should have the highest possible lighting transmittance;
- The lighter colour would be selected to obtain the better shading results by reducing heat gain and reflecting more light into internal spaces.

Once these criteria are met, these properties are furfures recommended from manufactures for safety and environment (Creston, 2013):

- Fabrics which could prevent or resist the spreading of fire;
- Fabrics which are tested and certificated to be safe and healthy for use in internal environment;
- Use no fabrics that contain polyvinyl chloride (PVC), which is known to be an environmental and health hazard.

9.2.2 Internal Shading Form and Position

Figure 9.1 presents the air temperature increases gradually along with the height and the temperature gradient becomes fairy large in the region near the top large glazed pedestrian concourses. In naturally ventilated case, low level shading are used as a buffer zone, hot air is blocked by the blinds and escape through high-level openings by the stack effect. While, in air-conditioned case, low level shading traps an insulating

layer of hot air between the shading and roof and also reduces the ceiling surface temperature. A larger volume of air at the low level shading leads to more accumulation of heat. The lower blind reduce the volume of cooling space which causes the reduction of the cooling load.

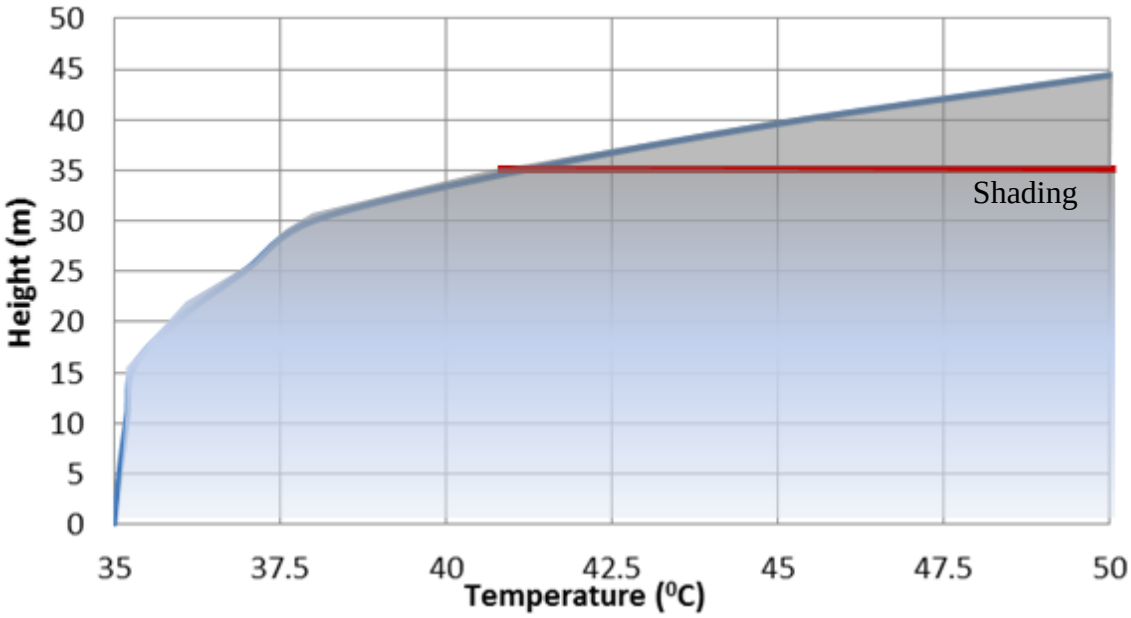

Figure 9.1 Temperature stratification in the large glazed pedestrian concourse space

Selecting the correct form and position of internal roof shading is considered vital. Energy performance improvement and cost savings can be less than expected, since some fixed shading systems can obstruct incoming daylight and increasing the use of electric lighting. Thus internal roof shading from and position are recommended as follow:

A. The Long-Span Glazed Roof over a Large Naturally Ventilated Pedestrian Concourse in the Tropics

- Internal solar blind installation has improved the thermal environment within the naturally ventilated pedestrian concourse in the tropics for both representative forms; the lower level shadings (horizontal screenings) and the high level shadings (curved roof screenings). The lower level shading blind was generally more effective in terms of providing better internal thermal conditions than the other form.

- The key to good thermal performance lies in the location of the shadings. They would be located at low level away from the glazed roofs. Apparently, the large void space between the glazed roofs and the lower shading shadings allows the free movement of air to dissipate to the outside at a high level before entering the spaces below. The high surface temperature of the glazed roofs led to the rise of the air and the air temperature in the area below, which was blocked by internal blinds; warm or hot air is able to escape through high-level openings by the stack effect (Figure 9.2).

- Apart from glazed roof buildings that experience heat gain from surroundings, solar radiation represents the major influence on the cooling load in buildings. The direct solar radiation impacts on cooling load when it reaches the transparent roofs and transmits directly to the building's interior. The effectiveness of internal shading in preventing heat gain can also reduce the need for a cooling load, which can be around 6.8% for the lower blinds and 4.7% for the higher blinds.

- The low level shading reduced the lighting level more than the high level shadings. The shading systems reduced the lighting level appropriate for occupants' visual comfort on clear summer days, while the blinds would make the space too dark on cloudy summer days and in winter. Hence retractable blinds would be essential.

- Both shading options could only ease thermal discomfort to a limited degree but could not greatly improve the building's thermal condition, due to the operative temperature being over 31^{o}C for more than 22 hours on the hottest day.

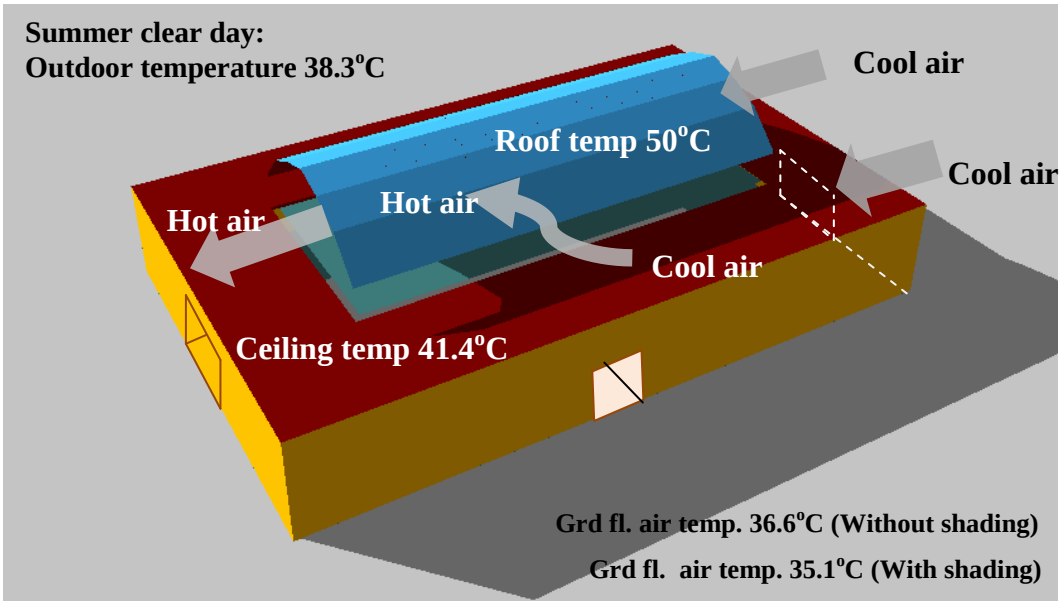

Figure 9.2 Free air movement of air dissipates to the external diagram in the large naturally ventilated glazed pedestrian concourse

B. The Long-Span Glazed Roof over a Large Pedestrian Concourse with Air-Conditioning in the Tropics

- Only the low level shading (horizontal screen) improved the physical environment and energy performance within the glazed pedestrian concourse with air-conditioning. Low level shading traps an insulating layer of hot air between the curtain and the transparent roof and also reduces the ceiling surface temperature. A larger volume of air at the low level shading leads to more accumulation of heat, as compared to a smaller volume of air of the high level shading (sloped roof screen) (Figure 9.3).

- The direct solar radiation impacts on the cooling load when it reaches the transparent roof and transmits directly to the building's interior. The effectiveness of low level internal shading in preventing heat gain can also reduce the need for cooling load, which can be around 3.4%.

- The shading systems reduced the lighting to a level appropriate for occupants' visual comfort on only clear summer days; the blinds made the space too dark on cloudy summer days and in winter. Hence retractable blinds would be essential.

- Operative temperatures for the glass roofed building with air-conditioning would be maintained within the range of 21°C to 25°C by using that air

conditioning for 24 hours out of 24. The low level shading could not meaningfully improve the thermal comfort condition for the building's occupants. The operative temperature reached the peak at 29.1°C within the ground floor concourse, while that temperature was reduced by 0.7-1.0% by the low level shading.

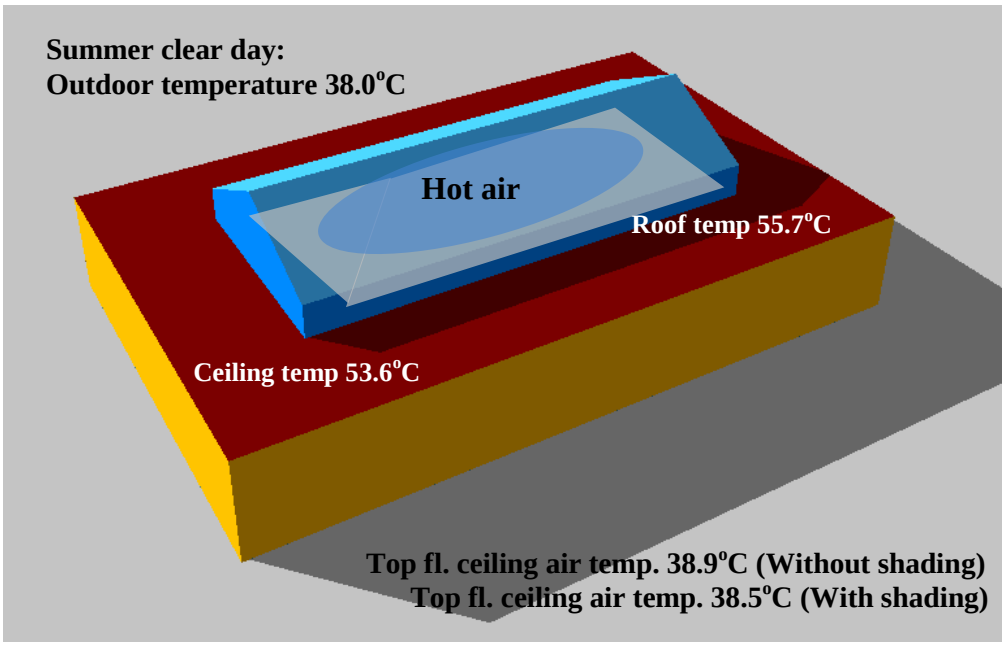

Figure 9.3 Insulting layer of hot air diagram in the large air-conditioned glazed pedestrian concourse

Once these criteria are met, these properties are furfures recommended:

- The operating mechanisms of shading device should be easily accessible to maintenance personnel and replacement parts easily obtained.

9.3 Conclusion

This chapter has presented the design principles and recommendations regarding internal shading fabrics and the internal shading form and position for long-span glazed roofs over large pedestrian concourses in the tropics for buildings with either natural ventilation or air-conditioning. These recommendations are based on the thermal and lighting measurements and the simulated models carried out using dynamic thermal and lighting simulation software and some supporting literature. These internal roof shading recommendations are not only applicable in malls or airport terminals but also in any similar construction of long-span glazed roofs over large pedestrian concourses in

tropical climates. The next chapter addresses the final stages of the two case studies; concluding the research work and recommending some future research.

CHAPTER 10 – CONCLUSIONS

10. 1 Introduction

The ultimate aims of this research are to optimize weather responsive internal roof shading design systems and to recommend some design principles and guidelines for internal roof shading systems. Such systems would then provide a better building-centric thermal environment and energy performance, while maintaining adequate levels of natural lighting within the existing long-span glazed roofs over large naturally ventilated and air-conditioned pedestrian concourse in the tropics. The two case studies in this research are Guangzhou International Textile City (GITC), China and Suvarnabhumi Airport Terminal. They were selected to gain a better understanding of the thermal and lighting conditions within large glazed pedestrian concourse buildings in the tropics and to obtain measured data for calibrating the capacity of dynamic thermal and lighting models to propose and optimise internal roof shadings.

The chapter contains four content specific sections. Section 10.2 presents the summary of research development. Section 10.3 discusses the summary the overall findings. Section 10.4 discusses the originality of the proposed solution and contribution to knowledge. The last section provides some recommendations, including future research related to this thesis.

10. 2 Summary of Research Development

The use of highly glazed spaces, either an atrium or pedestrian concourse, allows the benefit of natural light to penetrate through the centre spaces of buildings in every region, including hot climates. Covering impressive spaces with glazed roof leads not only to more daylight penetration, but also to more heat gain, which could affect the severity of thermal and visual problems within the occupied areas. In order to provide comfort for the occupants, these spaces require fully air-conditioned. This demand results in high energy costs for cooling and complicate cooling system to keep people thermally comfortable. The poor thermal performance in many of these buildings may also necessitate remedial improvements to increase comfort and lower operating cost after a couple year of occupancy.

One of the techniques that can possibly reduce solar heat gains within these spaces is by the installation of various shading devices. External shading is the most effective at

preventing the build-up of internal solar heat gain by intercepting solar radiation before it reaches the building. Hence it is often considered at the design stage for better integration with a new building. Internal shading with a reflective coating can reflect solar radiation to the outside of the building but can also transfer some of the heat gains to internal space by convection. Shading blinds are not only light and hence impose less loading on existing structures, but are also easier and cheaper to install and to operate. These points are considered vital if such systems are to be used in buildings with existing long-span glazed roofs over large pedestrian concourses.

Two case studies were selected: a naturally ventilated case in China (Mall) and an air-conditioned case in Thailand (Airport Terminal). The effects of the shading systems on the physical indoor environments and their implications were also analysed. To achieve the aims of this study, the research work was carried out in six stages.

To begin with the study attempted to achieve the objective of investigating the conditions and overall indoor physical behaviours within the two selected buildings with long-span glazed roofs over large pedestrian concourses. Studies were carried out by using data collection and field measurements within the large naturally ventilated concourse building (Mall) in Guangzhou, China and the existing concourse building (Airport) in Samut Prakarn, Thailand. The method of data collection combines the two common sources, namely primary and secondary. The primary sources include site measurement using mechanical equipment and building simulation using building modelling software. Meanwhile the secondary sources are obtained from field measurement data from a colleague team in China; as well as publications and earlier researches. The field measurement results were used to calibrate the thermal and lighting computer model. Questionnaire survey was future explore occupancy satisfaction levels and the existing indoor environment qualities in Suvarnabhumi Airport Terminal While a naturally ventilated case study in China, the air flow speed was further monitored at the building's entrances and the roof openings.

In order to achieve the objective to create dynamic thermal and lighting models of the existing long-span glazed roof over large naturally ventilated or air-conditioned pedestrian concourse buildings in the tropics, the case study buildings were created in both thermal and lighting models in the second stage. The purpose of this exercise was to develop confidence in creating a correct model, by comparing it with the measured

data. The thermal, energy and lighting performance of the case studies were also tested using the building simulation software running under the same conditions as those that informed the site measurements over the same period. The performance of these tested cases was assessed using the key variables: solar gain, cooling loads, internal surface temperatures, air temperatures and operative temperatures of both ground floor and surrounding spaces on various levels within the existing pedestrian concourse.

In order to achieve the objective to examine the internal roof shading as remedial solutions relating to two cases of existing long-span glazed roofs over large pedestrian concourse buildings in the tropics with two cases: natural ventilation and air-conditioning, the shading blind fabric was selected and examined. Their realistic light transmission was tested by scale model experiment in the artificial sky dome at Heriot-Watt University and also in an open-field context, under clear and overcast sky. Shading blind fabric was selected using scale model experiments ranging from the highest possible lighting transmittance and lowest solar transmittance in order to reduce heat gain and reflect more light back into internal space below in the third stage. Then two screening positions for the internal blinds were tested in simulation as two design options to compare their effects on the thermal and daylight condition in the two case-study buildings against the base case in the fourth stage.

In order to achieve the objective to analyse the potential financial benefits from the proposed remedial shading solutions a standard economic analysis method was employed to provide recommendations on the costs and payback periods in the fifth stage.

Based on the thermal and lighting measurements and the simulated models carried out using dynamic thermal and lighting simulation software, as well as information from some supporting literature, the proposed design principles and guidelines for internal roof shading systems applicable to the two case study buildings were recommended. These recommendations are presented in the last stage.

10.3 Summary of Findings

This section presents a brief summary of this study's findings, with particular focus on the five research objectives. First, the study investigated the existing conditions and overall indoor physical behaviour within two sample buildings with long-span glazed

roofs over large pedestrian concourses in the tropics. Second, the study created dynamic thermal and lighting models for the two sample buildings; one which was naturally ventilated and the other air-conditioned, for the purpose of comparison. Third, the study explored options regarding the internal roof shadings in the form of retractable internal fabric sheet blinds to reduce the discomfort of the buildings' occupants and the cooling focused high energy consumption. Fourth, the study analysed the financial benefits from the remedial solutions suggested for the two buildings with their long-span glazed roofs over large pedestrian concourses. Finally, the study made recommendations concerning internal roof shading design principles and guidelines in order to reduce discomfort and energy consumption, as well as enhance energy performance, while maintaining adequate levels of natural lighting in two atria in the tropics.

10.3.1 Objective 1: to investigate the existing conditions and overall indoor physical behaviours within the existing long-span glazed roof over large pedestrian concourse buildings in the tropics.

In order to achieve this objective, studies were carried out by using data collection; field measurements and a questionnaire survey

The main points with regard to the field study are:

- In order to obtain more reliable measured data, the measuring and monitoring should be carried out in summer.
- It was found from the field study that in the existing long-span glazed roof over large pedestrian concourse with natural ventilation; the building was fairly well ventilated through the purposefully designed building layout which directly affected heat removal from within the space. When air movement is weak heat removal also becomes slower causing internal air temperature to rise higher than the external temperature. This field measurement of the key indoor environment variables also calibrated the thermal and lighting computer models.
- It was found from the field study that in the existing long-span glazed roof over large pedestrian concourse with air-conditioning, the internal air temperature on the ground floor concourse was not significantly affected by the external weather conditions. The indoor air temperature on the ground

remained stable. The indoor thermal environment on the ceiling over the top floor was affected by the outside conditions. The air temperature would rise as high as those externals during the hottest period, even though it was cooled down by air-conditioning. Moreover, solar radiation had greatly influenced the transparent roof surface temperatures. These glazed roof surface temperatures would be two times higher than those externals.

- The results of the measured data from the field experiment confirmed that the long-span glazed roof over large pedestrian concourses with both natural ventilation and air-conditioning in the tropics would suffer high-temperature stratifications, especially on the top floor, causing great discomfort to the occupants. In addition, it can be seen that daylighting tended not to be uniform within these building interiors.

- In addition, the analysis of the post occupancy evaluation from the questionnaire survey in Suvarnabhumi Airport Terminal building has also shown that occupants perceived thermal discomfort in the passenger lounge.

10.3.2 Objective 2: to create dynamic thermal and lighting models of the existing long-span glazed roof over large pedestrian concourse buildings in the tropics with two cases: natural ventilation and air-conditioning for the purpose of comparison.

In order to achieve this objective, the entire case study buildings were created in both dynamic thermal and lighting models and run under the weather data files from the local meteorological stations over the same selected periods as the field measurements. These simulations were facilitated by dynamic thermal and lighting software tools known as TAS, Ecotect and Dialux.

The main points with regard to the dynamic thermal modelling have been observed as follows:

- The accuracy of the simulation results in both the existing long-span glazed roof over large pedestrian concourse with natural ventilation and air-conditioning were largely associated with the similarity of the weather, the geometry of the buildings, the heat gain properties and internal conditions. Although accurate modelling for such a complex buildings were very challenging, the carefully calibrated and implemented models were able to

reveal changes to the key physical variables with the designed options and made quantitative comparisons possible.

- The accuracy of the simulation results is dependent on both the correct representation of the dynamic thermal and lighting model and the quality of input data.
    - The building's geometry of the dynamic thermal and lighting model should closely match the real building(s).
    - Correct specifications of weather parameters, building elements' materials and their thermal properties, and internal conditions are the most important factors affecting the accuracy of the prediction results.
- In order to increase the accuracy of the thermal and lighting simulations, it is necessary to calibrate these models. Calibration of the thermal models was by comparison with the measured results for two critical variables, the indoor temperatures and the total average cooling loads within the long-span glazed roofs on the hottest clear and overcast days, while calibration of lighting models was by comparison with the daylight factors (DF) within the long-span glazed roofs on the selected overcast days. The representative models were also used to predict the physical environment with differing shading configurations and were assessed by dynamic thermal and lighting simulation software.
- For large glazed pedestrian concourse buildings, assigning a large single zone or dividing each level into one zone may not be sufficient to correctly model the spaces. To provide a more accurate analysis, a multi-zonal model is recommended. This model would treat each space within a building as a zone, calculate the heat and air movement among these zones through energy mass balance equations and predict dynamic thermal performance of a building. Thus the central large pedestrian concourse at the roof level was further separated into zones between the transparent roof and the ceiling zone to capture the differences in thermal conditions throughout this space. Such divisions were intended to differentiate subtle changes in temperature from one place to another and to allow the predicted values of the models to

be compared with those from field measurements at exactly the same positions in the calibration.

- In the dynamic thermal modelling exercise, the TAS calculations tended to be underestimated, compared to that of the measurement. These differences between the measured and predicted results might also be due to the following:
    - As a results of uncertainties about the thermal properties of the existing construction material and specified building data editor by TAS. Inaccurate specifications of thermal property data had led to lower predictions of solar penetration in the model. The thermal properties could not be matched with each other.
    - The fixed internal conditions in the TAS model were based on general assumptions. There is a tendency for the heat gains from occupants, lighting and equipment to be underestimated in the model since the occupancy patterns and the use of lighting and equipment in the real conditions were somewhat irregular. Moreover, there is also a possibility that the infiltration rates and conditioned air supply rates were underestimated due to the uncertainties of the actual flow rates and uncontrolled actions of the users in the real buildings.

- **The Existing Long-Span Glazed Roof over Large Pedestrian Concourse with Natural Ventilation:**

  It was found from the dynamic thermal modelling exercise that in the existing long-span glazed roof over large pedestrian concourse with natural ventilation, the measured indoor air temperatures were compared with the simulated results.
    - The average difference in air temperatures, between measured and predicted, was in the range of 2.25 and 3.71 percent. The average differences between the predicted and measured temperatures were around $1^{o}C$ on the top floor during sunny hours, the hottest of the day and smaller for the rest. The calculated total cooling power from TAS was 171 Wm^{-2} which was very close to the original design capacity of 180 Wm^{-2}. Moreover, the cooling load comparison

against the energy benchmarking for cooling systems of large retail buildings reveals that this building has an overheating problem causing the expensive cooling system to keep the space thermally comfortable.

- It was found from the lighting modelling exercise that in the existing long-span glazed roof over large naturally ventilated pedestrian concourse, the average DF over each of the seven floors showed fairly good agreement. The lowest relative deviation, 3 percent, was on the sixth floor and the poorest, 23 percent on the ground floor.

- **The Existing Long-Span Glazed Roof over Large Air-Conditioned Pedestrian Concourse**:

  It was found from the dynamic thermal modelling exercise that in the long-span glazed roof over large air-conditioned pedestrian concourse, the conditioned air was supplied to the whole area. Therefore internal air temperatures would not be able to reflect the thermo physical response of the model. The main heat contributors were the heat transfers in internal building element surfaces by convection and long-wave radiation exchange. In order to calibrate the long-span glazed roof over large air-conditioned pedestrian concourse model, the glazed roof surface temperatures were examined.

  - For average surface temperature by date and time comparison, the average differences of the predicted surface temperatures made by TAS and the measured surface temperatures were between 1.70 and 5.00 percent by date and 0.00 and 4.73 percent by time. For the profile of glazed surface temperature comparison, the average difference surface temperature between the predicted and measured was around 2.7^{o}C on a hot clear day and was around 1.4^{o}C on a hot overcast day.
  - The predicted annual cooling load from TAS was 562 kWhm^{-2} which was very close to the calculated annual total cooling load by cooling degree-days of 578 kWhm^{-2}. Moreover, the predicted annual cooling load from TAS is very high compared against the energy benchmarking for airport cooling system of 467.7 kWhm^{-2}. This

reveals that this building has an overheating problem causing the expensive cooling system to be operated in order to keep the space thermally comfortable.

- It was found from the lighting modelling exercise that in the long-span glazed roof over large air-conditioned pedestrian concourse, the average DF over the departure lounge shows fairly good agreement. The average relative deviation on the departure lounge was less than 5 percent, while the poorest was close to the glazed wall to the north.

10.3.3 Objective 3: to examine the internal roof shadings in the form of retractable internal fabric sheet blinds to reduce discomfort and high energy consumption for the existing long-span glazed roofs over large pedestrian concourse buildings in the tropics with two cases; naturally ventilated case and air-conditioned case.

In order to achieve this objective, the shading blind fabric was selected, proposed and tested with the simulation under various conditions.

The effectiveness of internal shading devices to block out the solar radiated heat depends on the position with respect to glazed components, geometry, material properties (solar reflectance, solar transmittance and light transmittance), control options and colour (Unterpertinger, 2005). Easy installation is considered crucial to minimise disruption to the already very busy occupants in the adjacent businesses. Most importantly, light weight is considered vital as the large atria pedestrian concourses are spanned by glass roofs spanning over 40 meters in both directions (Wang et al., 2013).

Ideally the selected material for the shading blinds should have the highest possible lighting transmittance and lowest solar transmittance in order to maximise light transmission and minimise solar penetration into the atrium. To find such a material, five samples from Silent Gliss manufacturers were examined; their realistic light transmission by scale model experiment was tested in the artificial sky dome at Heriot-Watt University and also in open-field context, under an overcast sky. The highest lighting transmission and lowest solar transmission material was selected for proposed shadings.

The main points with regard to the internal roof shading examination have been observed as follows

- The highest light transmittance and lowest solar transmittance fabric sheet was finally selected for the proposed shading system. Two shading arrangements were proposed: the low level shading (horizontal screen) and the high level shading (curved/sloped screen). These were facilitated by dynamic thermal and lighting software tools known as TAS, Ecotect and Dialux.

- The environmental variables examined to assess the thermal conditions in the case studies were the inner surface temperature of the ceiling, the mean radiant, air and operative temperatures and daylight factors over the existing long-span glazed roofs over large pedestrian concourses. The visual condition of these tested cases was assessed for illuminance and daylight factors. Then solar heat gain and cooling load variables were examined to assess the energy performance.

- **The Existing Long-Span Glazed Roof over Large Pedestrian Concourse with Natural Ventilation**:

  It was found from the dynamic thermal modelling exercise that, the internal roof shading device was very effective in reducing inner surface temperatures and consequently reducing radiant heat gain into the space.

    - The low level shading is more effective than the high level shadings in terms of providing better energy, internal thermal and lighting performance. The modelling indicates the low level shading goes a long way to alleviating summer thermal discomfort within the concourse, particularly on the high level corridors, by reducing significantly the surface temperature of the inner surface of the "ceiling", the part that is thermally visible from those circulation areas. The shading reduced the air temperature by 4.1% and also the MRT by 8.7% within the ground floor pedestrian concourse on a clear hot day, respectively.

    - The modelling also indicates the low level shading go a long way to alleviating summer thermal discomfort within the atrium,

particularly on the top floor balcony by significantly reducing the inner ceiling surface temperature in the part that is thermally visible from those circulation areas. Apart from considering internal thermal comfort by operative temperatures, proposed shading options for glazed pedestrian concourses with natural ventilation could only ease thermal discomfort to some degree. Shading could not improve the thermal comfort condition very much, although the shadings could reduce significantly the inner surface temperature.

- Apart from energy performance assessment, the low level shading performed better than the high level shading in terms of reducing the total cooling load by saved 6.8%. The difference between the cooling load reductions was small because the cooling loads were for the retail units over seven stories in the building. Most of them did not receive direct solar heat and those that did were the few on the top floor and on the east and west sides. Moreover, this configuration would reduce two thirds of the solar heat gain in the pedestrian concourse space in summer significantly.

- The low level roof shading significantly reduced daylighting levels in the existing long-span glazed roof over a naturally ventilated large pedestrian concourse. When the internal roof shadings were fully extended on a clear summer day, the average illuminance level over the ground floor and the first floor was maintained at over 500 lux. On the other hand, the outdoor temperature on both a clear winter day and cloudy day were moderate, so the internal roof shadings should be opened to allow natural light in on overcast summer days or on winter days. Therefore retractable shading devices are recommended to provide sun screening only when required, such as on clear summer days when solar gain is likely to result in overheating.

- The buffer zone is a key reason that the low level screening performs better than the high level screening. Creating a naturally ventilated thermal buffer space is critical to the design of an effective internal roof screening system. The large void space between the glazed roof and the low level screening allows the free movement of the hot air to dissipate to the outdoors at a high level before it can enter the spaces below.

- **The Existing Long-span Glazed Roof over Large Air-conditioned Pedestrian Concourse**:

  It was found from the dynamic thermal modelling exercise that, only the low level screening can improve the physical environment in terms of energy, thermal and lighting conditions.

  - This configuration would reduce the internal surface temperature, which is the main cause of the radiation heat gain in the large glazed air-conditioned concourse. In summer this configuration would reduce the solar heat gain by 9.0% and the inner surface of the "ceiling" by 3.7% in the pedestrian concourse space. The shading also would reduce both the air temperature and the MRT by 1.0% within the passenger lounge on a clear hot day, respectively.

  - The low level screening traps an insulating layer of hot air between the curtain and the transparent roof and also reduces the ceiling surface temperature. A larger volume of air of the low level screening led to more accumulation of heat, as compared to a smaller volume of air with the high screening. In addition, the high solar reflective property of the fabric decreases the solar heat by reflecting a portion of the solar heat back out through the transparent roof, while some solar energy is also trapped within the air gap.

  - Interestingly, installing the high internal solar blinds cannot improve the thermal environment in the air-conditioned atrium, due to the high surface temperatures of both the glazed roof and the internal blinds. As the blinds absorbed solar energy from the top, the radiant

temperatures would rise due to the surface temperature. With the contribution of radiant energy from other internal surface, the mean radiant temperature and the air temperature at high level would also increase and lead to greater stratification throughout the lower occupied levels.

- Apart from energy performance assessment, the low level shading would reduce the total cooling load by 3.4%. In summer this configuration would reduce about 6% of the solar heat gain in the pedestrian concourse space. The difference between the solar heat reductions by the low level shading was very small. Since these terminal walls were glazed panels, the direct solar heat thus penetrates the external large glazed wall particularly the west-facing glazed wall during the hottest period of the day.

- The study reveals that the internal roof shading significantly reduced daylighting levels in the air-conditioned pedestrian concourse. When the internal roof shadings were fully extended on the clear summer day, the average illuminance level over the passenger lounge was maintained at over 300 lux. The shading decreased the illuminance to less than 300 lux on cloudy summer days as well as both clear and cloudy winter days; therefore in those conditions additional artificial lighting would be required.

10.3.4 Objective 4: to analyse the financial benefits from the remedial solutions of the existing long-span glazed roof over large pedestrian concourse buildings in the tropics with the two cases.

In order to achieve this objective, standard economic analysis methods were employed to provide recommendations on their costs and payback periods.

The main points with regard to the financial benefit assessment have been observed as follows:

- With an interest rate at 4.85% over a life time of 30 years in China, the investment of the shading system could be financially beneficial due to the *NPV*>0 and the *IRR* being greater than interest rates at 23%. By examining

DPP, the investment of low level blinds in the GITC Building would be recovered after the period of 6 years based on the Chinese price

- With an interest rate at 1.35% over a life time of 30 years in Thailand, the investment of the shading system could be financially beneficial due to the *NPV*>0 and the *IRR* being greater than interest rates at 7%. By examining *DPP*, and the investment of low level blinds in Suvarnabhumi Airport Terminal Building would be recovered after the period of 13 years based on the Thailand price.

10.3.5 Objective 5: to recommend internal roof shading design principles and guidelines applicable to the existing long-span glazed roof over large pedestrian concourses with natural ventilation and air-conditioning to reduce discomfort and energy consumption in the tropics:

In order to achieve this objective, design principles and guidelines were recommended. These recommendations are based on the thermal and lighting measurements and the simulated modelling carried out using dynamic thermal and lighting simulation software and some supporting literature. In order to maximize the daylight environment by internal shading, the selected material for the shading blinds should have the highest possible lighting transmittance. Low solar transmittance fabrics would be used in the internal shading device; in order to reduce the amount of solar radiation high solar reflectance fabrics were very effective, because the fabrics perform well at reflecting solar energy, as they are designed to do. These internal roof shading recommendations are not only applicable in malls or airport terminals but also in any similar existing atria in the tropics.

10.4 Originality of the Proposed Solution and Contribution to Knowledge

Much research has concentrated on identification of the solar heat stratification behaviour and on the daylight distribution in large atria. Currently there appears to be no specific research into remedial solution of this problem through the use of internal roof shadings. Original contributions to consultants, architects, facility managers and owners on energy use for internal roof shading installation within existing long-span glazed roofs over large pedestrian concourses, resulting from and based upon this research, are as follows:

- The number of shading systems available today on the market is huge and it is not always easy to choose the best solution for a building. Many parameters influence the choice of the system and of the control strategy itself. The building's energy performance using different shading designs and internal shadings has been studied already. But none of these studies investigated both thermal and lighting environment affected by the internal roof shading systems.

- The different materials also create different shading effects, when it comes to the same kind of material; the lighter colour material obtains the better shading results. The selected internal roof blinds should have high lighting transmittance in order to maximise light transmission and low solar transmittance in order to minimise solar penetration into the space below. Thus the research attempted to examine the effectiveness of any shading device in blocking out the solar radiate heat with the form and position of the shading device.

- This research has also revealed possible financial benefits from the proposed solutions. Thus, it allows consultants, architects, facility managers and owners to make better decisions.

10.5 Recommendations for Future Research

Recommendations for future research and investigation have been identified during the progress of this research as follows:

- The glazing characteristics and shading fabric properties are particularly important for buildings with large glazed pedestrian concourse. Therefore, extensive investigation should be conducted to identify the type of glazing and fabric properties most suitable for the tropics, which can provide not only optimum daylighting level but also better thermal and energy performance.

- Further investigations using both field study and computer modelling should be carried out to better qualify and evaluate the effect of the internal thermal and visual environment by other methods, such as evaporative water spray on the outer transparent roof or external plant shading for existing long-span glazed roof over large pedestrian concourse in tropical climates.

- This study assumed that the extended shading would not affect lighting bills in the context of the financial assessment. However, more studies need to take account of the increase of lighting bills resulting from this remedial solution in order to achieve a thorough financial assessment of the suggested shading solution.